UNIVERSITY OF SOUTHAMPTON

FACULTY OF MEDICINE

CANCER SCIENCES

The Role of the Pro-survival Molecule Bfl-1 in Melanoma

By

Charlotte Hind

Thesis for the degree of Doctor of Philosophy

2012

UNIVERSITY OF SOUTHAMPTON

ABSTRACT

FACULTY OF MEDICINE
CANCER SCIENCES

Doctor of Philosophy

THE ROLE OF THE PRO-SURVIVAL MOLECULE BFL-1 IN MELANOMA

By Charlotte Katherine Hind

Melanoma, the cancer derived from the melanocytes of the skin, is becoming an ever more common cancer in the ageing population of the developed world and displays an intrinsic resistance to current therapies. This chemo resistance makes metastatic melanoma an extremely difficult cancer to treat leading to a 5 year survival rate of just 20%. As such, it is important to unearth new potential drug targets to increase the prospects for melanoma patients.

Bfl-1 is a pro-survival protein of the Bcl-2 family of apoptosis regulating proteins. It has been found to be over-expressed in a small subset of chemo resistant tumours, including melanoma. Accordingly, I characterised the molecule in melanoma cells and determined its role in protecting these cells from chemotherapy-induced apoptosis. I elucidated the expression profile and half-lives of the protein and mRNA across a panel of melanoma cell-lines and healthy melanocytes. I also confirmed, using pathway specific inhibitors, that Bfl-1 was transcriptionally regulated by the NFκB pathway and concluded through pulse-chase experiments that Bfl-1 protein was degraded, at least in part, by the proteasome. Subcellular fractionation and indirect immunofluorescence techniques elucidated that Bfl-1 was located mostly at the mitochondria in both resting and apoptotic cells, with a diffuse level present throughout the cytoplasm. As well as characterising the protein in both melanoma cells and healthy primary melanocytes, I determined its role in the resistance of these cells to apoptosis. Over-expressed Bfl-1 was found to protect melanoma cells from apoptosis caused by a range of chemotherapeutic agents in A375 melanoma cells, which naturally expressed very low levels of Bfl-1. Further, knock down of Bfl-1 using siRNA technology in melanoma cells revealed the dependence of these cells on Bfl-1 for their resistance to certain chemotherapeutic agents currently used in melanoma treatment, including the MEK inhibitor PD901. All together, this research contributes to our understanding of Bfl-1 and highlights it as a potentially important therapeutic target in metastatic melanoma.

List of Contents

LIST OF FIGURES

CHAPTER 1

CHAPTER 3

CHAPTER 4

CHAPTER 5

CHAPTER 6

APPENDIX

LIST OF TABLES

CHAPTER 2

CHAPTER 3

CHAPTER 4

CHAPTER 6

DECLARATION OF AUTHORSHIP

I, **Charlotte Hind,** declare that the thesis entitled

The Role of the Pro-Survival Molecule Bfl-1 in Melanoma

and the work presented in the thesis are both my own, and have been generated as a result of my own original research. I confirm that:

- This work was done wholly or mainly while in candidature for a research degree at this University;
- Where any part of this thesis has previously been submitted for a degree or any other qualification at this University or any other institution, this has been clearly stated;
- Where I have consulted the published work of others, this is always clearly attributed;
- Where I have quoted from the work of others, the source is always given. With the exception of such quotations, this thesis is entirely my own work;
- I have acknowledged all main sources of help;
- Where the thesis is based on work done by myself jointly with others, I have made clear exactly what was done by others and what I have contributed myself;
- None of this work has been published before submission

Signed: .....

Date: .....

ACKNOWLEDGMENTS

Many, many, many thanks must go to my supervisor Prof. Mark Cragg for his help and support over the last 3 years. I'm also very grateful to the members of the Tenovus laboratory who have provided a friendly and helpful working environment. In particular, Dr. Claire Harris and Dr. Emily Williams for both the scientific and writing-up support. Also thanks to the members of the lab who went out of their way to assist me in their specialist fields, Dr. Claude Chan, Dr. Sonja James, Sandie Dixon and David Johnson. Also the continued encouragement from Prof. Paul Townsend has been brilliant.

In addition, the support of my friends and family have been invaluable and have kept me sane throughout the process, especially Dr. Breeze Cavell, soon-to-be-Dr. Franky Lock and soon-to-be-professor, Dr. Charlie Birts. Thanks guys!

LIST OF ABBREVIATIONS

2-ME	2-Mercaptoethanol
A1	BCL2-related protein A1
APAF1	Apoptotic Protease-Activating Factor-1
ARF	Alternate Reading Frame
ATP	Adenosine TriPhosphate
B2M	Beta-2-microglobulin
Bad	Bcl-2 associated death promoter
Bak	Bcl-2 homologous antagonist/killer
Bax	Bcl-2 associated X protein
Bcl-2	B-cell lymphoma-2
BCL2A1	Bcl-2-related protein A1
Bcl-w	B-cell leukemia w
Bcl-xl	B-cell leukemia xl
Bfl-1	Bcl-2-like family protein-1
BH domain	Bcl-2 Homology domain
Bid	Bcl-2 interacting domain
t-Bid	truncated-Bid
Bik	Bcl-2 interacting killer
Bim	Bcl-2 interacting mediator of cell death
Bmf	Bcl-2 modifying factor
B-Raf	v-raf murine sarcoma viral oncogene homolog B1
Bok	Bcl-2-related ovarian killer
BSA	Bovine Serum Albumin
$CaCl_2$	Calcium Chloride
c-MYC	Myelocytomatosis Oncogene
CDK4	Cyclin-D Dependent Kinase 4
CDKN2A	Cyclin-Dependent Kinase Inhibitor 2A
cDNA	copy-DNA
CEBPα	CCAAT/Enhancer-Binding Protein alpha
dATP	Deoxyadenosine triphosphate
dCTP	Deoxycytosine Triphosphate
dGTP	Deoxyguanine Triphosphate
dH2O	Distilled Water
DNA	Deoxyribonuclease
dNTP	Deoxynucleotide Triphosphate
DTT	Dithiothreitol
dTTP	Deoxythymidine Triphosphate
dUTP	Deoxyuracil Triphosphate
ECL	Enhanced Chemiluminescence
EDTA	Ethylenediamine Tetra-acetic Acid
EGFR	Epidermal Growth Factor Receptor
EGTA	Ethylene Glycol Tetraacetic Acid
ELISA	Enzyme-Linked Immunosorbent Assay
ER	Endoplasmic Reticulum
ERK1/2	Extracellular signal-Regulated Kinases 1/2
FADD	Fas-Associated Death Domain
FACS	Fluorescence Activated Cell Sorting

FCS	Foetal Calf Serum
FLICE	FADD-like Interleukin-1 beta-Converting Enzyme
FLIP	FLICE Inhibitory Protein
FOXO3A	class O Forkhead box transcription factor-3A
G	Gram
GAPDH	Glyceraldehyde 3-Phosphate Dehydrogenase
GDP	Guanosine Diphosphate
GF	Growth Factor
GFP	Green Flourescent Protein
GTP	Guanosine-5'-triphosphate
HALI	Hyperoxic Acute Lung Injury
HCl	Hydrochloric Acid
Hrk	Harakiri
HRP	Horse Radish Peroxidase
IAP	Inhibitor of Apoptosis Protein
Ig	Immunoglobulin
IκBα	I kappa B alpha protein
IKK	IκB Kinase
IL	Interleukin
JNK	c-Jun N-terminal Kinase
Kb	Kilo base
KCl	Potassium Chloride
L	Litre
LB broth	Lunia Bertani
MADD	MAPK-Activating Death Domain
MAPK	Mitogen Activated Protein Kinase
MAPKK	Mitogen Activated Protein Kinase Kinase
Mcl-1	Myeloid Cell Leukemia 1
MC1R	Melanocortin 1 Receptor
MDM2	Murine Double Minute 2
MEK	MAP kinase/Erk kinase Kinase
MEKi	MEK inhibitor
Mg	Milligram
$MgCl_2$	Magnesium Chloride
Mg SO_4	Magnesium Sulphate
Ml	Millilitre
mM	milli-molar
mMol	milli-Mole
MOMP	Mitochondrial Outer Membrane Permeabilisation
MOPS	3-(N-morpholino)propanesulfonic acid
MORT1	Mediator Of Receptor-induced Toxicity-1
mRNA	messenger-RNA
MSH	Melanocyte Stimulating Hormone
mTOR	Mammalian Target of Rapamycin
NaCl	Sodium Chloride
NaF	Sodium Fluoride
Na_3VO_4	Sodium Orthovanadate
NFκB	Necrosis factor kappa b
NIK	NFκB-Inducing Kinase

Nmol	nano-mole
N-RAS	Neuroblastoma RAS viral oncogene
Noxa	Phorbol-12-myristate-13-acetate-induced protein 1
OMM	Outer Mitochondrial Membrane
PBS	Phosphate Buffered Saline
PCD	Programmed Cell Death
PCR	Polymerase Chain Reaction
PI	Propidium Iodide
PI3K	Phosphoinositide-3-kinase
PIP3	Phosphatidylinositol (3,4,5) Trisphosphate
PKB	Protein Kinase B
Pmol	pico-mol
PTEN	Protein Tyrosine Phosphatase
Puma	p53 upregulated modulator of apoptosis
PVDF	Polyvinylidene Fluoride
qPCR	quantitative Polymerase Chain Reaction
Rb	Retinoblastoma
pRb	Retinoblastoma protein
c-Rel	Reticuloendotheliosis viral oncogene homolog
RIP	Receptor Interacting Protein
RNA	Ribonucleic acid
ROS	Reactive Oxygen Species
RSV	Rous's Sarcoma Virus
RT	Room Temperature
RT	Reverse Transcriptase
RTK	Receptor Tyrosine Kinases
RT-PCR	Real Time PCR
SDS	Sodium Dodecyl Sulphate
shRNA	Small Hairpin RNA
siRNA	Small Interfering RNA
smac/DIABLO	second mitochondria-derived activator of caspases/Direct IAP-Binding protein with Low pI
Src	Sarcoma
TB	Transfer Buffer
TBS	Tris Buffered Saline
TF	Transcription Factor
TNF	Tumour Necrosis Factor
TNFR1	TNF Receptor-1
TRADD	TNF Receptor-Associated Death Domain
TRAF2	TNFR-Associated Factor-2
UDG	uracil DNA glycosylase
µg	micro-gram
µl	micro-litre
µM	micro-Molar
µMol	micro-Mole
UPR	Unfolded Protein Response
UV	Ultra-Violet
VEGF	Vascular Endothelial Growth Factor
YFP	Yellow Fluorescent Protein

1: INTRODUCTION

1.1 Cancer

Cancer can be defined as a group of cells undergoing uncontrolled proliferation with the ability to spread throughout the body from the original site. It is not a single disease, but a collective term for over 100 different disorders which are becoming ever more common in an ageing population. With 60% of cancers diagnosed in patients over sixty-five, it is a relatively new player among the biggest killers in the western world given that until recently, the population died younger of infectious diseases, malnutrition or accidents.

The first documented case of cancer was recorded on papyrus in ancient Egypt in 1500BC, and was believed to be caused by the gods. However, the most famous early diagnosis of cancer as a disease as we understand it today, was in 1775 when Percivall Pott first described scrotal cancers in men who had worked as chimney sweeps in their youth [1, 2]. This was the first time a link between the development of cancer and the exposure to an external chemical, a carcinogen, had been recorded. Even with such advances in the understanding of the disease, it was the late 19th century before the German scientist Rudolph Virchow realised that cancer cells derive from normal cells rather than from black bile or lymph fluid, as had previously been believed. After the discovery of the 'cancer-causing' sarcoma virus by Rous in 1909 [3,4] research into genetics continued and the hypothetical gene thought to be responsible for a cell becoming cancerous was named an oncogene [5]. In the 1960s the *src* (sarcoma) oncogene was discovered in Rous's sarcoma virus (RSV) [6] and in 1975 this oncogene was found in not only cancerous cells [7], but also in normal healthy cells [8]. This led researchers to hypothesize that the *src* oncogene was triggered to become cancerous by the introduction of the virus into the cells. Hence, the *src* oncogene in healthy cells was renamed a proto-oncogene [9]. Through further research it became clear that proto-oncogenes underwent mutations to become oncogenes and that these mutations were caused by a variety of factors, both internal and external to the cell.

By looking at hereditary cancers, the first tumour suppressor genes such as retinoblastoma (Rb) [10,11] and p53 [12] were discovered in the 1970s. Tumour suppressor genes have the ability to prevent healthy cells from becoming cancerous and are often found mutated and inactive in cancer cells. For example, when potentially damaging mutations occur in the cell, levels of the transcription factor p53 rise to slow the transition of the cell through the cell cycle to allow high fidelity DNA repair which if unsuccessful triggers cell death, preventing potentially oncogenic mutations from becoming incorporated into the genome [13,14]. As a result, it is perhaps no surprise that a large proportion of cancers have mutated

p53 genes, which disrupts the cell death pathway and permits propagation of mutation. As mutation and loss of genome integrity promotes tumour progression, loss or mutation of p53 contributes to the uncontrolled growth and division of cells leading to tumour formation and progression [15].

In addition to activating an oncogene or inactivating a tumour suppressor gene, healthy cells have other hurdles to jump before they become cancerous (Figure 1.1) (reviewed by Hanahan and Weinberg [16,17]). Cells must become self sufficient for growth signals, for example by overexpressing growth receptors or switching the types of extracellular matrix receptors expressed [18,19]. Cells must also become insensitive to anti-growth signals, for example by disrupting the tumour suppressors Rb and p53 [20], in order to achieve unchecked proliferation. When mutations are not repaired by DNA repair mechanisms, cells will usually undergo cell suicide; however cancer cells can avoid this programmed cell death by dysregulating this pathway, for example through the over-expression of pro-survival proteins or the downregulation of pro-apoptotic proteins, as discussed later.

Cells can also become immortalized by upregulating the enzyme telomerase (reviewed by Shay et al., 2001 [21]). Telomerase prevents the shortening of telomere DNA which occurs every time a cell is replicated. In normal somatic cells telomerase is downregulated. As such, telomere shortening limits the proliferative potential of a cell to a certain number of replication cycles and denotes cell ageing, or senescence. The cell can proliferate until the telomeres are shortened to the degree that there is not enough protection from DNA end-to-end fusions between chromosomes and the cell remains viable, but cannot proliferate. At this stage, the cell enters replicative senescence or cell death.

To grow extensively, tumours also support their expansion by growing their own blood supply through the formation of small capillaries (angiogenesis) which can be initiated by growth factors such as vascular endothelial growth factor (VEGF) [22]. This increases the volume that a tumour can reach before nutrients become inaccessible to cells which are far from the original blood supply and is therefore a key factor in tumour growth.

Most tumours are associated with inflammation, which was initially believed to be the immune systems attempt to rid the body of the tumour. However, studies have determined that inflammation can in fact provide a mutagenic environment, cultivating the initiation and progression of tumours. In fact, it has been suggested that when inflammation is not the trigger for the initiation of the cancer, most cancers will trigger inflammation

themselves [23]. For example, necrotic cells in the centre of solid tumours release pro-inflammatory mediators and certain oncogenes can initiate inflammation through the expression of cytokines and the recruitment of tumour associated macrophages (TAMs) [24]. Inflammatory cells can help tumour progression by providing bioactive molecules for many of the other hallmarks of cancer that derive from the tumour microenvironment. For example, they can provide factors for angiogenesis, enhance invasive capabilities, provide pro-survival molecules to inhibit cell death and suppress anti-tumour immunity [25,26].

There are also two emerging hallmarks of cancer, which are currently less well understood in their role in tumourigenesis; deregulation of cellular energetics and avoiding immune destruction. The reprogramming of energy metabolism occurs in tumour masses to avoid nutrient deficiency in hypoxic conditions. Typically, cancer cells switch their energy metabolism to glycolysis and upregulate glucose transporters through a phenomenon termed the Warburg effect [27]. Additionally, tumours must avoid detection by the immune system which destroys cells presenting foreign antigens, as might be expected in cancer cells expressing mutant proteins. One way tumour cells subvert immune cells is by secreting immunosuppressive factors [28].

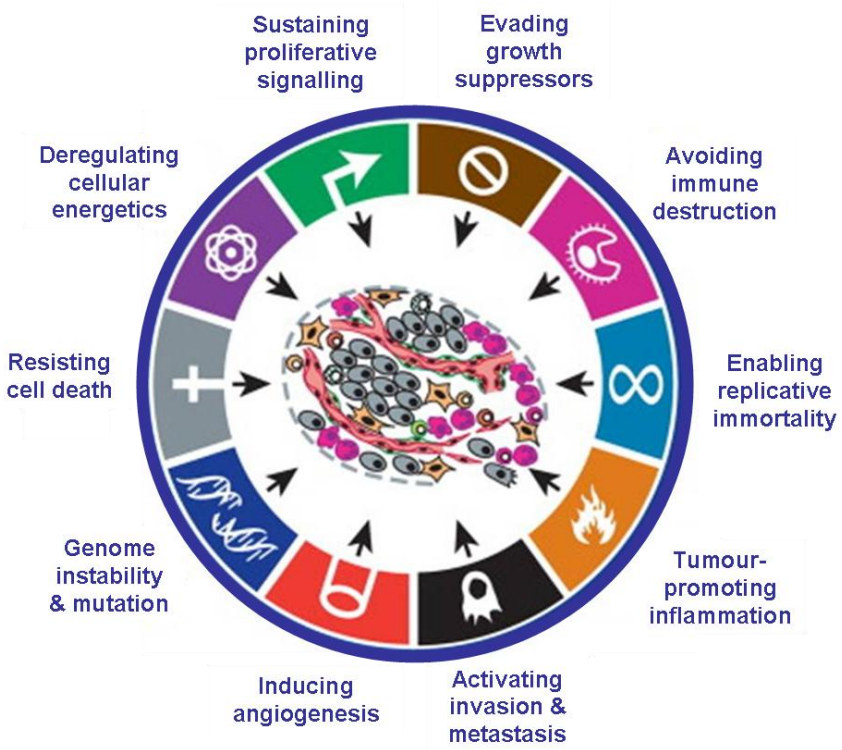

Figure 1.1: The hallmarks of cancer.
These hallmarks represent the multiple steps through which cells must pass to become cancerous. Taken from Hanahen and Weinberg 2011 [17].

Following the establishment of the initial tumour, malignant tumours can metastasize to other sites in the body by travelling through the blood and lymph systems. Solid tumours, such as melanoma, can form discrete masses in any tissue of the body, whilst cancers of the blood, such as lymphomas and leukemias, can infiltrate a tissue without forming a mass. A single cancer cell can break away from the initial tumour mass due to a lack of cell-adhesion molecules such as E-cadherin [29]. Such separation from the extracellular matrix would typically result in apoptosis and highlights the requirement for the tumour cells to subvert the cell death programme. In fact, cell death would, in a healthy cell, be activated in response to almost every step in the transformation of a healthy cell to a cancerous cell, so inactivation of the cell death machinery through the mutations detailed above is extremely important in the successful tumourigenesis of a cell.

Many of these ten hallmarks have been targeted for the development of new drug treatments, and as a consequence, a myriad of different treatments and drugs exist. But the success of most drugs depends on the physiology and genetics of the individual tumour, which leads to the concept of stratified medicine where each patient and tumour is assessed before deciding on a course of treatment. A common way of identifying a new drug target is to focus on an individual hallmark, e.g. the ability to evade cell suicide, or on one type of cancer, e.g. melanoma. This allows researchers to determine if there are any common patterns or mutations within a given step or type of cancer which can be targeted for drug development.

1.2 Melanoma

The term skin cancer covers three different forms of cancer, squamous cell carcinoma, basal cell carcinoma and melanoma. Melanoma may not be the most common type (90% of diagnosed skin cancers in the UK are basal cell or squamous), but it is by far the most dangerous. Unlike non-melanoma skin cancers, melanomas can grow very quickly and metastasize to anywhere in the body. In contrast, squamous cell carcinoma is capable of metastasis, but only if it has been left untreated for a very long time [30].

Malignant melanoma is also by far the most difficult type of skin cancer to treat and cure. Simple techniques, such as surgery, have high curative rates with non-melanoma skin cancers, but metastatic melanoma displays an intrinsic resistance to chemotherapeutic agents currently in use in the clinic.

1.2.1 Melanocytes and Melanin

Melanoma is a solid cancer that originates from pigmented melanocyte cells in the skin and, less commonly, from noncutaneous melanocytes in the eye or gastro-intestinal (GI) mucosal surfaces. Melanocytes form between 1-10% of the cells in the skin with the majority of the remainder made up of keratinocytes which produce a family of strong protective proteins called keratins (Figure 1.2). These proteins, together with actin, make up the majority of the skin, hair and nails [31].

Melanocytes originate in the neural crest and migrate towards the inner layer of the epidermis, the stratum basal, as well as the hair matrices, the inner ear, the eye and the leptomeninges, the membranes that surround the brain and spinal cord [32]. These melanocytes produce a protein called melanin, derived from tyrosine [33,34], to protect cells in the skin from hazardous UV radiation [35].

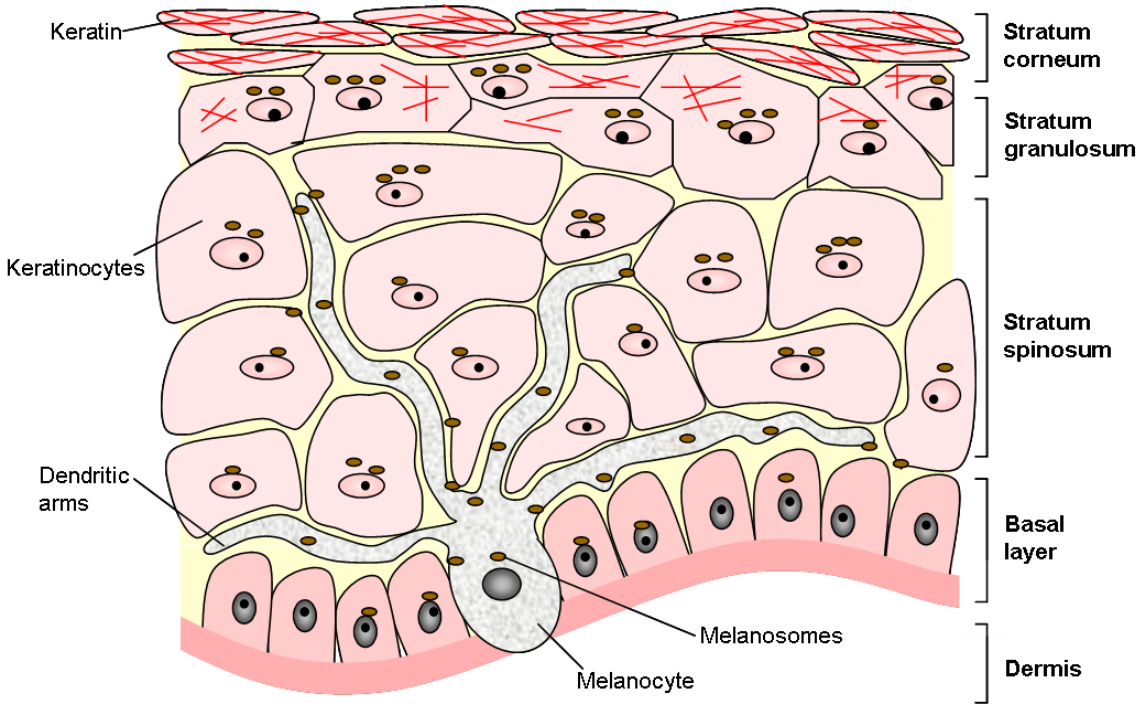

Figure 1.2: Melanocytes provide surrounding cells with protection from UV radiation.
Melanin protein produced in melanocytes is packaged into vesicles called melanosomes which are transported along the dendritic arms of the melanocytes to the other cells of the skin. The melanosomes collect over the nucleus of the cell to form a protective cap for the cellular DNA. Keratinocytes produce keratin which hardens as cells approach the stratum corneum and provides structure to the skin.

Melanin exists in two forms, the brown/black eumelanin which is the cause of tanning and the yellow/red pheomelanin. It is the balance between these two forms of melanin which determines skin colour, not the activity of the melanocytes. The production of melanin

depends on the interaction between melanocortin 1 receptor (MC1R) with either melanocyte stimulating hormone (MSH) (producing eumelanin) or the agouti signalling protein (producing pheomelanin) [36-38]. MSH and agouti are coded for by the *extension* and *agouti* loci, respectively. The melanin is packaged into small vesicles called melanosomes which, after external stimulation (or mutations in their transport system), are transported rapidly along microtubules from the centre of the melanocyte towards the dendritic arms and trafficked to other cells. The transfer of melanosomes from melanocytes to keratinocytes is not completely understood, but it is suggested that it occurs via a form of phagocytosis [39].

One melanocyte typically supplies melanin to over 30 keratinocytes (Figure 1.2) and one Langerhans cell. In the cells, melanosomes collect over the nucleus to protect the cellular DNA from radiation damage [40,41]. The mechanism behind this protection by melanin relies upon chemical reactions involved in photoprotection which cause efficient internal conversion of harmful UV into a harmless level of heat energy rather than harmful reactive species such as free radicals. However, under extreme conditions, for example harmful levels of UVA radiation, melanin can also have deleterious effects. These include toxicity [42,43], the ability to produce reactive oxygen species (ROS) [44] and photodegradation leading to hydrogen peroxide production [45]. Pheomelanin may also have a carcinogenic effect that contributes to malignant melanoma formation as one study found that albinos with melanocytes incapable of producing melanin had a very low incidence of melanoma, with only 27 cases reported in the literature [46]. A high concentration of melanocytes can form highly pigmented nevi, or moles, which unless they acquire the ability for uncontrolled proliferation, are benign.

1.2.2 The Incidence and Treatment of Malignant Melanoma

Over the last 40 years, the incidence of melanoma has increased more than any other cancer in the developed world [47]. If diagnosed early as a primary tumour, melanoma is easily removed by surgery and survival rates are high [48], however once melanoma has metastasized, it is extremely difficult to treat as it displays an inherent resistance to conventional therapies. As such, prognosis is poor, with a 5-year survival rate of just 20% for patients with extra-cutaneous metastases [49] and a 3-year survival rate of just 10-15% for patients with dissemination to distant sites or visceral organs [50]. In fact a meta-analysis looking at phase II trials from 1975 to 2005 in 2,100 patients found a median overall survival rate of just 6.2 months and a median progression free survival rate of just 1.7 months [51]. These intimidating statistics have led to a plethora of studies on the causes of

the intrinsic chemo resistance observed in melanoma, with the identification of numerous potential drug targets.

1.2.3 Chemoresistance and Treatment in Malignant Melanoma

Some of the more obvious targets for developing new drugs are the frequent carcinogenic mutations that occur in the cell. An activating mutation of v-raf murine sarcoma viral oncogene homolog B1 (BRaf) (mutation: V600E, also less commonly: V600K) [52], which encodes for a protein kinase that regulates cell growth, is present in 50-70% of melanomas [53]. It is thought that mutant BRaf becomes locked into an activated mode, sending a continuous proliferative signal to the cell through the mitogen activated protein kinase (MAPK) pathway, which also serves to lower the levels of the pro-apoptotic protein Bcl-2 interacting mediator (Bim) which is targeted for degradation by the MAPK pathway [54,55]. The presence of this mutation is associated with poorer prognosis in metastatic melanoma than when it is absent [56]. Another activating mutation observed in melanoma, albeit to a lesser extent, is the neuroblastoma RAS viral oncogene (NRAS) (mutation: Q61R) [57], which also upregulates the MAPK pathway and can cause upregulation of the pro-survival proteins of the B-cell lymphoma-2 (Bcl-2) family such as myeloid cell leukemia-1 (Mcl-1) and B-cell leukemia-xl (Bcl-xL) through the Akt signalling pathway [58] and Bcl-2-related gene expressed in fetal liver (Bfl-1) through the nuclear factor kappa B (NFκB) pathway [59]. Intriguingly this mutation tends to be mutually exclusive with the B-Raf mutation and occurs predominantly in malignant cells that lack a B-Raf mutation [60]. As a result of these mutations, 80% of melanomas have upregulated MAPK signalling.

An activating mutation of the proto-oncogene tyrosine kinase receptor Kit, or CD117, is often observed in acral and mucosal melanomas, which although only account for 20% of melanomas diagnosed in the western world, account for 70% of melanomas in Asia. c-Kit mutations are also observed in chronically sun-damaged skin. Furthermore, c-Kit plays a critical role in the growth of melanocytes and mutations of the proto-oncogene has been shown to lead to malignancy [61,62].

Other oncogenes such as the myelocytomatosis oncogene (c-Myc) and Dek are also critical for the carcinogenesis of melanocytes. c-Myc has been shown to suppress the inherent senescence seen in melanoma cells when BRaf or NRAS mutations are present [63]. The chromatin remodelling factor Dek, which promotes proliferation and down-regulates the p53 pathway, has been seen to transcriptionally activate the pro-survival molecule Mcl-1 [64]. Similarly, apoptotic protease-activating factor-1 (APAF1), a protein involved in the

construction of the apoptosome during p53-induced apoptosis has been observed to be lacking in typically chemo-resistant, malignant melanoma [65]. Tumour suppressor genes such as phosphatase and tensin homologue deleted on chromosome 10 (PTEN)/MMAC1 have also been identified as being mutated or expressed at a reduced level in 10-15% of melanomas [66].

Proteins involved in the inhibition of apoptosis are often observed to be over expressed in cancer and can also provide viable drug targets, for example Bcl-2 in follicular lymphoma. In respect to the expression patterns of the apoptosis regulating Bcl-2 family in melanoma, there are disagreements in the literature, which are discussed later (section 1.5). Elevated levels of microphthalmia associated transcription factor (MITF) which directly upregulates Bcl-2 expression has been linked to melanoma progression [67]. The inhibitor of Fas-associated apoptosis, FLIP (FLICE (FADD-like interleukin-1 beta-converting enzyme) inhibitory protein), has also been seen to be upregulated in human melanoma [68] and a high expression level of the inhibitor of apoptosis protein (IAP), survivin, has been linked to poor prognosis for patients with metastatic melanoma and a decreased response to immunotherapy [69].

Interestingly, the tumour suppressor gene for TP53 is mutated in a high proportion of cancers, but very few melanomas [70]. The inactivation of p53 through the deletion or mutation of TP53 leads to a reduced level of apoptotic cell death, providing the cell with increased survival potential. Cyclin-dependent kinase inhibitor 2A (CDKN2A) is a gene that can be alternatively spliced to encode two structurally related proteins, $p16^{INK4A}$ and the alternative reading frame (ARF), and is often mutated in melanoma instead of TP53 [71] (). Germ-line mutations within CDKN2A result in the expression of inactive forms of its two gene products [72], both of which are important cell cycle regulators. Inactivation of $p16^{INK4A}$ leads to the degradation of protein Rb (pRb). This occurs through a mechanism by which mutated $p16^{INK4A}$ is less efficient at inhibiting the activity of cyclin-D dependent kinase 4 (CDK4), resulting in the hyperphosphorylation and subsequent degradation of pRb [73]. Mutations of ARF can result in a loss of cellular p53, as it is no longer able to bind murine double minute 2 (MDM2), a negative regulator of p53. Thus, MDM2 is free to target p53 for ubiquitination leading to increased p53 degradation [74, 75]. With little pRb and p53 present in the cell, the G1 cell cycle checkpoint is lost and uncontrollable cell growth can occur. Studies have determined that dual loss of the pRb and p53 pathways are present in up to 80% of melanoma cell-lines [76], and that this concomitant dysregulation of both pathways could be important in the transformation of human melanocytes.

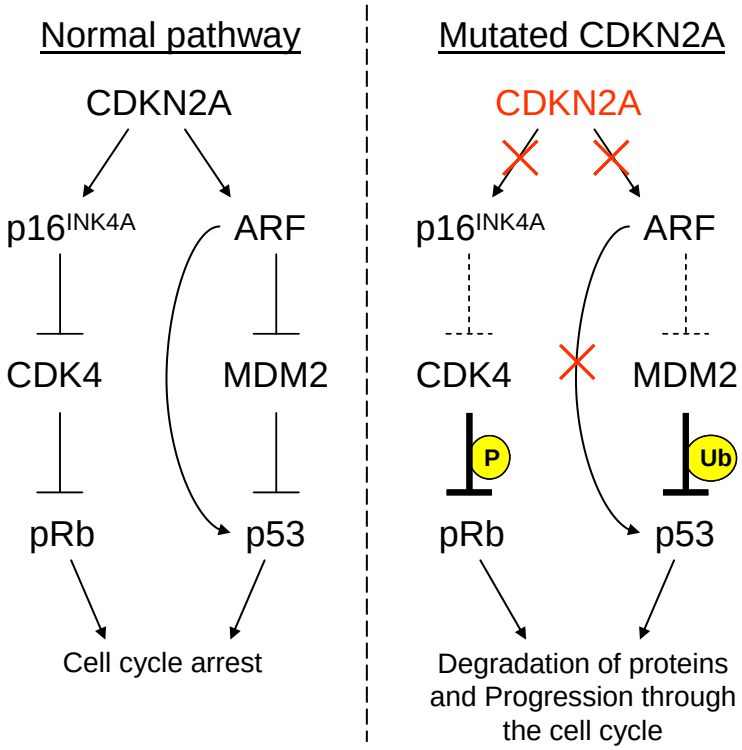

Figure 1.3: The pRb and p53 pathways are functionally impaired in a high percentage of melanomas.
This simplified schematic depicts how the mutation of CDKN2A leads to an absence of p53 and pRb in the cell and therefore the loss of the ability to inhibit growth through cell cycle arrest. When CDKN2A is mutated, $p16^{INK4A}$ and ARF are functionally inhibited and therefore unable to block the activity of CDK4 and MDM2 which cause degradation of pRb and p53 through phosphorylation or ubiquitination.

After the initiation of carcinogenesis through the acquisition of mutations and deregulation of the pathways described above, melanoma typically progresses through secondary events such as adapting to endoplasmic reticulum (ER) stress (reviewed by Hercey and Zhang, 2008 [77]) which unless it is relieved by the unfolded protein response (UPR) usually leads to ER stress-mediated apoptosis or senescence.

As has been detailed in this section there are many possible causes for the intrinsic drug resistance observed in melanoma. Drugs are being developed to target many of these deregulated pathways, and the outlook seems promising, but until very recently, the standard treatment for metastatic melanoma (Decarbazine) was strikingly ineffective.

1.2.4 Current Therapies in the Treatment of Metastatic Melanoma

Whereas new treatments for many cancers have improved survival rates significantly, advancement in the treatment for metastatic melanoma has been completely lacking for the past 40 years. Decarbazine (DTIC), an alkyating agent which prevents DNA replication and therefore blocks proliferation, has remained as the standard, but relatively ineffective, treatment since its introduction in 1975 (except in the United States, where the cytokine interleukin-2 was approved by the FDA as an alternative treatment in 1992 [78]). However in recent years, as research has improved our understanding of the carcinogenic mutations involved in melanoma, a number of exciting new drugs have been developed and tested in clinical trials with promising results in the overall survival and progression free survival rates of patients with advanced metastatic melanoma.

The highly publicised and celebrated new drug from Roche, Vemurafenib, or PLX4032/RG7204, is a BRaf specific inhibitor which blocks the continuous growth signal transmitted by the activating mutation of BRaf observed in 50-70% of melanomas [79]. This targeted drug therapy showed such success in phase III trials that at the first interim assessment, the trial was un-blinded and patients on the control drug arm of the trial receiving DTIC standard of care, were transferred to Vemurafenib [80]. This led to the approval of Vemurafenib by the FDA in August 2011. Roche have also developed an assay for determining if the patient has the BRaf mutation, the Cobas 4800 BRaf V600E Mutation assay, which was approved at the same time [80]. Furthermore, as this inhibitor is only effective on cells transformed by this V600E mutation, another BRaf-specific inhibitor, GSK2118436, which targets the V600K mutation, is also in a small phase III trial having shown great potential in patients with brain metastases [81]. However some caution remains as the inhibition of the BRaf mutation V600E (and also V600K by GSK2118436) with these BRaf inhibitors has been shown in some patients to reactivate the MAPK pathway through CRaf [82,83], and developing resistance to BRaf inhibitors is a problem. Additionally, loss of PTEN activity in BRaf mutant cells can lead to lower levels of pro-apoptotic Bim through hyperactivated Akt, which can result in resistance to BRaf inhibitors [84].

As an alternative to BRaf inibitors, MEK inhibitors have caused some excitement, and the inhibitor GSK1120212 has been shown to have response rates of about 40% [85]. Hence, trials combining a BRaf inhibitor and a MEK inhibitor are ongoing and show promise with

additive, or even synergistic, effects expected. Drugs targeting other mutations such as c-Kit (imatinib) are also showing promise in trials [86].

However for the 30-50% of patients without the BRaf mutation, other treatments are being developed. One strategy being explored in metastatic melanoma treatment is through boosting the immune response. The IgG1 monoclonal antibody, ipilumumab, targets cytotoxic T-lymphocyte-associated antigen 4 (CTLA4) [87]. This encourages the activation and proliferation of T-cells in a response against the tumour by removing the negative signals typically transduced by CTLA4 [87]. Ipilumumab was approved for single-agent treatment in March 2011 by the FDA, and results in patients at very high risk of relapse (with high-risk lymph-node-positive disease) have been so positive that a large phase III trial is currently underway to establish the efficacy of ipilumumab as an adjuvant therapy [88]. Other immunomodulatory antibodies are also in development and in early clinical trials and showing great promise in augmenting T-cell responses [89,90].

In a similar fashion, pegylated interferon-α2b, a drug originally approved for the treatment of hepatitis c, was also approved for use in advanced metastatic melanoma in March 2011 as an adjuvant therapy based on a phase III trial which indicated improvement in relapse-free survival rates [91]. The PEG protects the interferon protein from proteolysis, thereby increasing its half-life which acts as an immunoregulatory cytokine and induces apoptosis in malignant cells [92].

There are still gaps in our understanding relating to the mechanisms through which melanoma resists treatment with chemotherapeutics, and the discovery of other possible targets will increase the possibility of finding drugs that work for an increasing majority of these patients. The ability of melanoma cells to avoid the cell death usually caused by drugs in other cancer types is obviously important and worthy of further exploration.

1.3 Cell Death

In 2009, the Nomenclature Committee on Cell Death recommended at least eleven different definitions of cell death classified by morphological changes and biochemical mechanisms [93]. The most studied and commonly accepted types of cell death within these are ‘accidental cell death’, termed necrosis, and ‘programmed cell death’ (PCD), a term which encompasses both apoptosis and autophagy. These pathways overlap both in function and characterization and a simplified explanation of current understanding is covered below.

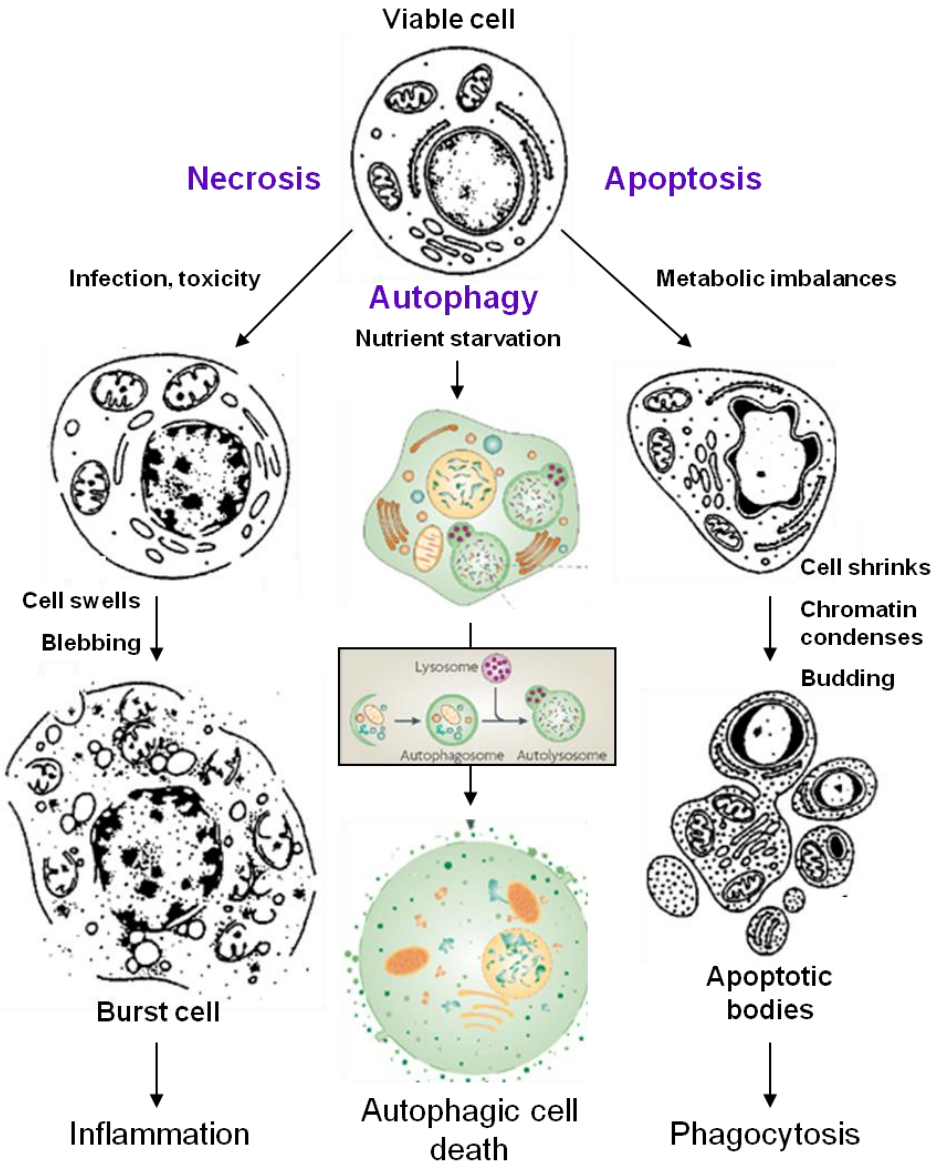

Figure 1.4: The morphological changes associated with necrosis, autophagy and apoptosis.
The representation of the autophagic pathway includes a diagram of the formation of the autophagosome and goes to completion, therefore resulting in cell death. Adapted from Van Cruchten *et al.*, 2002 [94] and Kroemer & Levine, 2008 [95].

1.3.1 Necrosis

Necrosis refers to the irreversible and premature death of cells caused by external factors such as toxins, reactive oxygen species, infarction, infection and inflammation [96,97]. Necrotic cells undergo morphological changes including cellular swelling (oncosis), disruption of organelle and plasma membranes and chromatin degradation, leading to the breakdown of organelles and resulting in the bursting of the cell [98,99] (Figure 1.4). However clear definitive biochemical changes for the absolute identification of necrosis have not yet been determined and necrosis is often identified in cells only when there is a lack of autophagic or apoptotic markers. Unlike during other types of cell death, a necrotic cell is

not always detected or disposed of by the body's immune system before the cell has disintegrated, allowing the contents of the necrotic cells to spread to surrounding cells. This leakage of cell contents attracts the attention of immune cells such as macrophages and results in an inflammatory response. For example, the chromatin bound protein high mobility group box 1 (HMGB1) is passively released from necrotic cells and can bind to Toll-like receptors and receptor for advanced glycation end products (RAGE) on macrophages and enhance the release of pro-inflammatory cytokines [100-102].

Necrosis has traditionally been termed as accidental uncontrolled cell death; however there is mounting evidence which suggests that certain forms of necrosis may actually be finely executed events occurring through death receptors and signal transduction pathways such as the receptor interacting protein (RIP) kinase and tumour necrosis factor (TNF) pathways [103-105]. This has led to the adoption by some authors of the term 'necroptosis' as a description of regulated necrosis which can be blocked by inhibiting RIP [106,107].

1.3.1.1 Necrosis in Cancer

Necrosis and its associated inflammation are commonly associated with a poor prognosis in cancer and it has been suggested that the inflammation caused by necrosis can accelerate the formation of tumours (reviewed by Vakkila and Lotze, 2004 [108]). This may come about from the association of macrophages which, once activated, can produce angiogenic and growth factors, promoting survival and proliferation in the surrounding cancer cells [109,110]. Conversely, in more established tumours, the release of cytokines such as HMGB1 from necrotic cells may alert the immune system to the presence of tumour cells [111]. If these necrotic cells carry tumour-specific antigens, the immune system may be able to detect and attack the associated cancer cells. The inhibition of other cell death mechanisms, such as autophagy, has also been seen to stimulate necrosis in cancer cells [112].

1.3.2 Autophagy

Autophagy (or more precisely, macroautophagy) refers to the self-digestion of a cell through the formation of vesicles around the components of the cell which need degrading [113]. These vesicles, termed autophagosomes, then fuse to lysosomes, forming autolysosomes, which break down the contents of the vesicle (Figure 1.4). Autophagy can be induced under a range of situations and stimuli, including growth factor withdrawal [114], inhibition of degradation by the ubiquitin-proteasome system [115], increases in cytosolic calcium [116] and endoplasmic reticulum stress [117]. Morphologically, autophagy can be

identified by electron microscopy where cytoplasmic vacuolation without chromatin condensation is observed. This process, if allowed to go to completion, is a means of achieving cell death; however it does not always lead to cell death and in fact can be involved in maintaining the survival of a damaged or nutrient deprived cell [118]. For example, a cell starved of nutrients can employ autophagy to recycle nutrients from non-vital structures and processes ensuring they are available for more essential processes, thereby ensuring cell survival [119-121]. In fact, when essential components of the autophagic pathway are genetically deleted, cells undergo accelerated cell death compared to cells with normal amounts of autophagy after apoptotic stimulation (reviewed by Galluzzi *et al*, 2008 [122]). This suggests that autophagy predominantly plays an important role as a cell survival mechanism. Thus, it is advisable to take the term 'autophagic cell death' to mean cell death occurring with associated autophagy rather than as a result of autophagy. The role of autophagy in disease is not well understood; it appears to play a protective role in the progression of neurodegenerative diseases and muscular disorders and provide protection from infections [123-125], but contributes to the pathology of other diseases such as Alzheimer's disease [126].

1.3.2.1 Autophagy in Cancer

The role of autophagy in cancer is complicated, with the activation of autophagy seen to be both beneficial and detrimental to tumour progression depending on the model. On one hand, autophagy has been presented as a tumour suppressor pathway in human cancers. The activation of autophagy in early tumour formation limits genomic instability by maintaining the metabolism of the cell, thereby reducing DNA damage and gene amplification, and thereby, tumourigenesis [127]. Autophagy has also been shown to trigger non-apoptotic cell death in tumours and hence, prevent malignancy [128,129]. In some cancers, the autophagy machinery has been seen to be inhibitory to the early stages of tumour growth through the deletion of the autophagic gene beclin 1, a gene essential for the formation of autophagosomes [130-132]. To add further complication, Förster resonance energy transfer (FRET) analysis and coimmunoprecipitation experiments have shown the interaction of the pro-survival molecule Bcl-2 and beclin 1 [133,134]. Through this interaction, Bcl-2 inhibits beclin 1, therefore preventing autophagy from occurring and providing an additional link and level of complexity between autophagy and apoptosis [134].

MAPK/extracellular signalling kinase (ERK) upregulation in cancer (seen in 80% of melanomas) can also disrupt the maturation of autophagosomes, preventing autophagy, and allowing the progression of the cancer [135,136]. In theory, this inactivation of autophagy in

early cancer cells could allow protein synthesis to occur at a much faster rate than protein degradation, giving the cell the building blocks required for unlimited cell growth. However, on the other hand, established tumours have been seen to activate autophagy as a means of cell survival against tumour stresses. Stress-induced autophagy can protect cancer cells from necrosis caused by a lack of nutrients [112], as occurs at the necrotic centre of a tumour. In fact most therapies currently used in cancer treatment have been shown to induce autophagy. This includes radiation [137,138], kinase inhibitors (e.g. the tyrosine kinase inhibitor imatinib [139]), inhibition of growth factor signalling (e.g. inhibition of PDGF signalling [140]), cytotoxic chemotherapy (e.g. vinblastine [141]) and hormonal therapy [142]. On this basis, investigations are currently ongoing to assess the combination of these autophagy inducing therapies with autophagy inhibitors such as tumour necrosis factor-related apoptosis-inducing ligand (TRAIL) and hydroxychloroquine in the treatment of established tumours [143].

Another form of PCD, which is extremely important in cancer and probably the most common form of physiological cell death, is apoptosis.

1.3.3 Apoptosis

Between fifty and seventy billion cells die by apoptosis in the average adult body every day. These cells may be infected, redundant or irreparably damaged and as such, are invoked to undergo cell suicide through a highly regulated form of programmed cell death known as apoptosis. Apoptosis is also crucial during development, for example, apoptosis is the mechanism through which webbing (redundant cells) between the fingers and toes is removed in the womb to give digit definition. Apoptosis was first recognised as a form of cell death over 100 years ago, but the term apoptosis was only coined in 1972 in histological studies of ischeamic liver injury by Kerr et al [144].

1.3.3.1 Morphology of Apoptosis

Apoptosis can be initiated by a wide variety of stimuli, from the smallest metabolic imbalances or inappropriate growth signalling to severe genotoxic stress. Once triggered, the cell undergoes several hallmark morphological changes; the nucleus shrinks, chromatin condenses and the chromosomal DNA is fragmented into small pieces. Subsequently, the cell is broken up into vesicles by cytoplasmic blebbing, and engulfed by surrounding cells, typically in under an hour [98,145,146] (Figure 1.4). Unlike in necrotic cells, an inflammatory response is generally avoided because the plasma membrane remains intact until the final

stages of the process. The vesicles, or apoptotic bodies, contain the dismantled components of the cells and are quickly engulfed by surrounding cells before the contents of the cell are released [147]. If the apoptotic bodies are not cleared quickly, the vesicles can undergo a form of necrosis termed secondary necrosis, which elicits an inflammatory response. Hence, when large numbers of apoptotic cells are generated, professional phagocytic cells such as macrophages and primary monocytes are recruited to clean up the numerous apoptotic bodies. Apoptotic cells have been shown to attract professional phagocytic cells to their locality through the secretion of 'eat me' signals. These include the release of chemotactic signals, such as the phospholipid lysophosphatidylcholine and the specific monocyte chemoattractant chemokine MCP-1 [148,149]. The apoptotic cells are recognised by the phagocytic cells through the presentation of phagocytic molecules early on in the process of apoptosis. These phagocytic molecules, such as phosphatidylserine and annexin I, are normally found on the cytosolic surface of the plasma membrane, but are flipped to the external surface during apoptosis [150-152]. Many receptors on macrophages have been implicated with a role in either the tethering of apoptotic bodies to macrophages or their engulfment, but elucidating individual roles of receptors and ligands has proven difficult [153].

1.3.3.2 Apoptosis in Cancer

Apoptosis can quickly and efficiently clear the body of cells exhibiting the classic hallmarks of tumourigenesis; Hallmarks such as irreparable DNA damage, genetic mutations, inappropriate growth signalling and oncogene expression (e.g. *myc*). All these faults can lead to a cell becoming cancerous and therefore trigger apoptosis. Defective apoptosis is hence generally crucial in the carcinogenesis of a cell. For example, the introduction of the growth-promoting *myc* oncogene into a cell can cause imbalances which trigger most cells to undergo apoptosis [154, 155]. This was shown in rat-1 fibroblasts, where the induction of *myc* lead to higher proliferation levels, but no relative increase in cell numbers due to the equivalent levels of apoptosis induced [156]. However in cancer, a secondary mutation, such as an activated apoptosis-inhibiting *Bcl-2* oncogene, or secretion of a pro-survival growth factor, can cause the cell to avoid apoptosis, allowing a relative increase in cell number and progression of the tumour [157,158]. Not only is defective apoptosis critical in carcinogenesis, but it can also contribute to the long term survival of tumours by lending a resistance to the apoptosis caused by chemotherapeutic agents. Defective apoptosis can also assist in the metastasis of a tumour, by preventing the death of cells that detach and escape from the primary tumour mass, as discussed earlier (section 1.1).

Defective apoptosis can occur as a result of mutations in the apoptotic machinery (e.g. mutated Bcl-2 associated X protein (Bax)), lack of upstream initiators of apoptosis (e.g. p53 loss), or the over-expression of an apoptosis inhibitor (e.g. IAPs or the pro-survival members of the Bcl-2 family). Defective apoptosis can prevent the killing of a cell and when cells survive apoptotic stimuli and go on to multiply again (enhanced clonogenicity) they can expand to repopulate the space left by cells that were killed by apoptosis in the last round of chemotherapy. In this manner, rounds of chemotherapy treatment can actually drive the selection of apoptosis resistant populations.

An imbalance of the proteins of the Bcl-2 family of apoptosis regulating proteins is often seen to influence the ability of cancerous cells to avoid the activation of their apoptotic machinery. This is due to the tight regulatory control that these proteins exhibit in the intrinsic and extrinsic pathways to apoptosis.

1.3.3.3 The Two Pathways to Apoptosis

There are two main routes through which apoptosis is thought to occur, the intrinsic and extrinsic pathways, both of which converge upon the terminal caspase cascade (Figure 1.5)

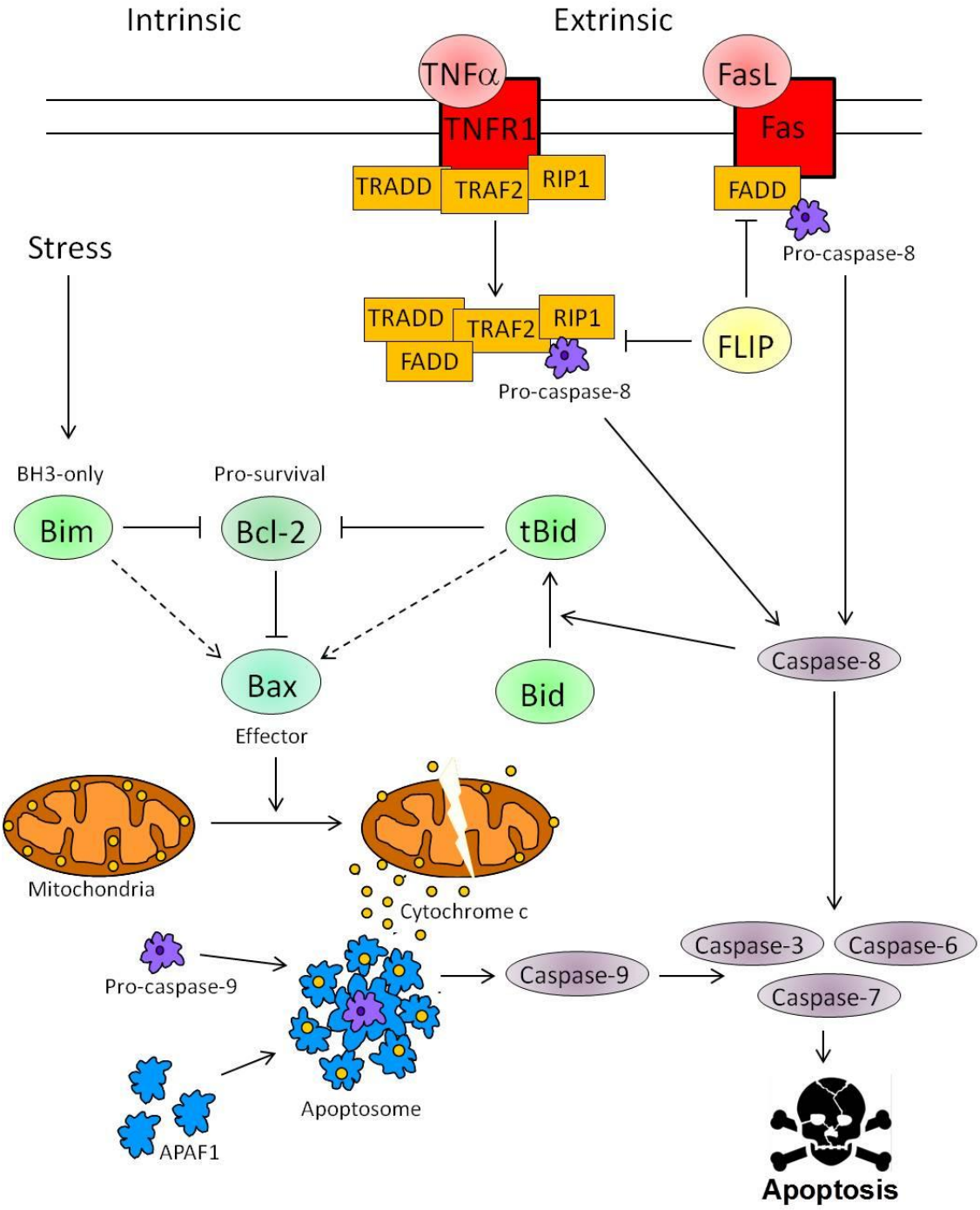

Figure 1.5: The intrinsic and extrinsic pathways that lead to apoptosis.
The intrinsic pathway is initiated by stress signals in the cell which activate the first sub-group of the Bcl-2 family, the pro-apoptotic BH3-only proteins. The BH3-only proteins bind to and cause the second sub-group, the pro-survival proteins, to release the third sub-group, the Bax/Bak-like pro-apoptotic proteins. Bax/Bak then form pores in the outer mitochondrial membrane causing release of cytochrome c which then binds with apoptotic protease-activating factor-1 (APAF1) and pro-caspase 9 to form the apoptosome. Pro-caspase 9 is cleaved into caspase 9 and then the caspase cascade is initiated. The alternate pathway is the extrinsic pathway which involves members of the tumour necrosis factor (TNF) family of receptors. Through binding to a death domain in the receptor, molecules such as Fas-associated death domain (FADD) activate the caspase cascade through caspase 8. Caspase 8 can also interact with the pro-apoptotic BH3-only protein Bid causing Bid cleavage. Bid can then link to the intrinsic pathway which can inhibit the apoptosis blocking abilities of the pro-survival proteins.

1.3.3.3.1 Caspases and the Apoptosome

Caspases belong to a group of enzymes called cysteinyl aspartate–specific proteases and are one of the main executioners of apoptosis, being the final step of both the intrinsic and extrinsic pathways (reviewed by Shi, 2002 [159]). There are 12 known caspases, although not all of them are involved in cell death. In a healthy cell, caspases exist as relatively inactive pro-forms or zymogens which are activated by cleavage following the induction of apoptosis. There are 2 tiers of caspases involved in apoptosis, the initiator caspases, -2, -8, -9 and -10 and the executioner caspases -3, -6 and -7 (Figure 1.6). The initiator caspases contain long pro-domains, not present in the executioner caspases, which are essential for their activation through interactions with other molecules. These interactions consist of the formation of multiprotein complexes through caspase recruitment domains (CARDs) in the intrinsic pathway (Figure 1.7), or the interaction with a specific scaffold protein through death effector domains (DEDs) in the extrinsic pathway (Figure 1.8). The resulting cleavage events and conformational change activates the initiator caspases, leading to an increased activation of executioner caspases such as caspase-3, -6 and -7.

Caspases cleave hundreds of key substrates in the cell by proteolysis and by freeing the caspase activated DNAse (CAD) from its inhibitor (ICAD), leading to the cleavage of chromosomal DNA, a morphological hallmark of apoptosis [160-162]. Furthermore, the activated executioner caspases can also create a positive feedback loop resulting in an amplification of activated executioner and initiator caspases in an activation cascade (Figure 1.6).

Caspases can be negatively regulated by the binding of the IAPs; c-IAP, XIAP, NIAP, livin and survivin. Some of these IAPS, such as survivin, are often observed to be overexpressed in human tumours, potentially resulting in resistance to caspase-dependent apoptosis [163]. Indeed, the activity of IAPs in humans is complex, with many members containing RING domains through which they catalyse the transfer of ubiquitin from E2 ligases to the target protein [164].

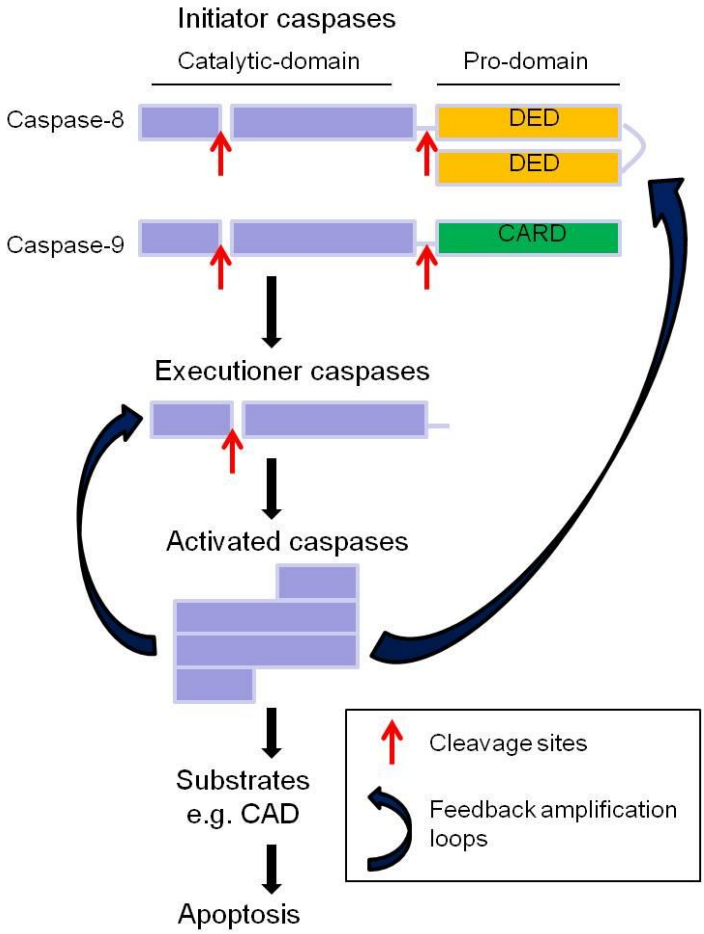

Figure 1.6: The caspase cascade in apoptosis.
The initiator caspases consist of a catalytic domain and a variable pro-domain containing death effector domains (DED) or caspase recruitment domains (CARDS). The pro-domain is removed after an apoptotic trigger causes them to form multidomain complexes. The catalytic domain is then cleaved to form the active caspase which, in turn, causes the activation of the executioner caspases through cleavage events in their catalytic domains. Activated caspases form positive feedback amplification loops to cause an amplification cascade for caspases which results in apoptosis through interactions with caspase substrates such as caspase activated DNAse (CAD).

1.3.3.3.2 The Intrinsic Pathway

The intrinsic, indirect, Bcl-2 regulated or mitochondrial pathway occurs when apoptosis signals from within the cell, for example stress, viral infection, oncogenes or direct DNA damage, activate the pro-apoptotic BH3-only members of the Bcl-2 family. The tumour suppressor p53 is a critical activator of the intrinsic pathway. It acts to transcriptionally upregulate the BH3-only proteins Noxa, p53 upregulated modulator of apoptosis (Puma) and Bcl-2 interacting domain (Bid) and also the pro-apoptotic protein Bax [165-167]. The pro-apoptotic and pro-survival members of the Bcl-2 family regulate the intrinsic pathway through their interactions with each other. The Bcl-2 family interactions are very complicated and so are discussed in detail later (section 1.5) with a simple overview given here.

Upon apoptotic stimulus, activated Bax and Bcl-2 homologous antagonist/killer (Bak) undergo conformational changes (potentially by forming pores in the outer mitochondrial membrane (OMM), although the details of this process have yet to be resolved) and cause mitochondrial outer membrane permeabilization (MOMP) [168]. This can be prevented by the pro-survival proteins, which are in turn regulated by the pro-apoptotic BH3-only proteins. After MOMP, the mitochondria release mitochondrial proteins such as cytochrome c and Smac/DIABLO (second mitochondria-derived activator of caspases/direct IAP-binding protein with low pI) into the cytosol before undergoing fragmentation dependent upon Bak/Bax [169].

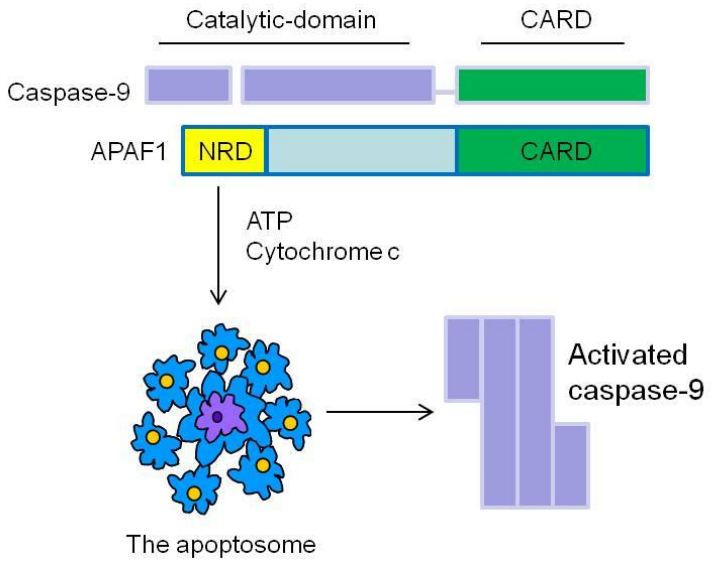

Figure 1.7: Caspase-9 is activated through the formation of the apoptosome.
Pro-caspase-9 is recruited by apoptotic protease-activating factor 1 (APAF1), in the presence of ATP and cytochrome c, through their homologous caspase recruitment domains (CARD). APAF1 also contains a negative regulatory domain (NRD) which is blocked by cytochrome c. These interactions form the apoptosome, which causes the cleavage of caspase-9 to its active form.

Cytochrome c released from the mitochondria binds to the adapter molecule APAF1 in the presence of ATP to form a heptameric protein ring called an apoptosome (Figure 1.7). Cytochrome c is essential for blocking the negative regulatory domain (NRD) in APAF1. APAF1 is then able to recruit pro-caspase-9 into the structure via the homologous CARDs [170]. The apoptosome, although originally believed to be essential for Bcl-2-regulated apoptosis [171,172], has more recently been defined as merely an amplifier of caspase activation. This was determined through studies which showed that in the absence of APAF1, or pro-caspase 9, cells could still die through Bcl-2 family driven apoptosis in lymphocytes and post mitotic neurones [173,174]. The apoptosome therefore appears to have

more impact on apoptosis occurring in some cell types, such as lymphocytes, than in others, for example neuronal precursors [173].

Smac, and its homologous murine protein DIABLO, are also released from the mitochondria after MOMP and interact with the IAP proteins to inhibit them, thereby preventing the blockade of activated caspases. Smac/DIABLO are nuclear encoded proteins containing a mitochondrial localisation sequence which is cleaved upon their import into the mitochondria to produce the mature protein which displays a newly exposed IAP-binding domain, critical for its function [175,176].

In cancers, typically the most common mechanisms for avoiding intrinsic cell death are through inactivated p53, or the overexpression of the pro-survival molecules of the Bcl-2 family and the IAP proteins, although inactivating mutations have also been observed in the terminal regulator Bax in some cancers [177]. The majority of cancer therapies directed at defective apoptosis target the intrinsic pathway but mutations in this pathway are often seen to correlate with treatment resistance.

1.3.3.3.3 The Extrinsic Pathway

The extrinsic, direct or death receptor pathway is the second pathway leading to apoptosis. Here, apoptosis can be induced by extracellular ligands which activate death receptors on the cell surface. These death receptors, such as tumour necrosis factor receptor-1 (TNFR1) and Fas, belong to the TNFR superfamily of receptors which have carefully regulated and discrete expression patterns among cell types. The receptors are present on the cell surface and contain cysteine rich extracellular domains and an intracellular domain termed the death domain [178]. The receptors activate the downstream apoptotic machinery through adapter molecules such as Fas-associated death domain (FADD) or TNF receptor-1-associated death domain (TRADD) which contain death domains and death effector domains [179,180].

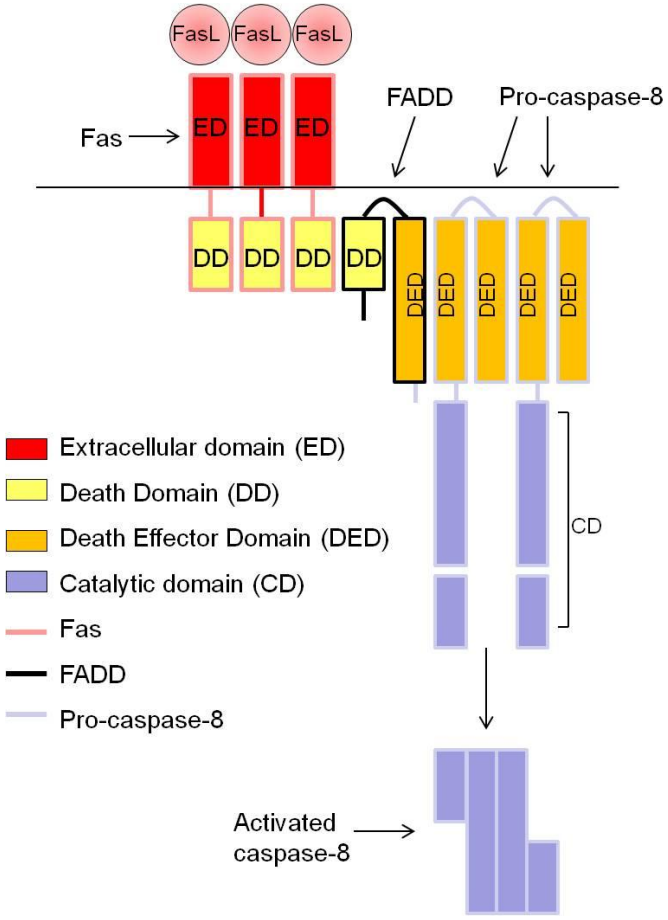

Figure 1.8: Fas receptor signalling in the extrinsic pathway to apoptosis.
Upon activation by Fas ligand (FasL), the Fas receptor oligomerises, bringing together its death domains (DD), which recruit the adaptor protein fas-associated death domain (FADD) through its DD. FADD then recruits pro-caspase-8 to the complex through interactions through the death effector domains (DED). Pro-caspase-8 undergoes a cleavage event to form active caspase-8.

The binding of the Fas ligand (FasL) encourages the oligomerisation of the Fas receptor (also known as CD95 or Apo1) and the bringing together of the death domains [181] (Figure 1.8). This also occurs when the TRAIL (also called Apo2) receptor is activated by its ligand. The adapter molecule FADD binds to the receptor and recruits pro-caspase-8 via its DED motif [182]. This complex of Fas, FADD and pro-caspase-8 is referred to as the death inducing signalling complex (DISC) [183]. The activity of the adapter molecule FADD can be inhibited by the presence of the anti-apoptotic molecule, FLIP, which is also important in the regulation of TNFR1 activated apoptosis [68]. There is evidence that in addition to blocking Fas-induced apoptosis, FLIP can also upregulate the NFκB pathway through the recruitment of TNF receptor activating factor 1/2 (TRAF1/2) at the DISC [184]. There are also other proteins capable of interacting with Fas which can transduce signals for proliferation and differentiation such as RIP1 and Fas associated phosphatase (FAP1) [185].

TNFR1-dependent initiation of apoptosis involves various death domain containing proteins which are capable of binding to the activated receptor. Two distinct complexes lead to completely different outcomes from activated TNFR1. Complex I involves the binding of TRADD, and the 2 adapter proteins TRAF2 and receptor interacting protein 1 (RIP1) to the activated receptor [186]. This complex initiates the NFκB pathway through the recruitment of I-kappaB-alpha-kinase (IKK) leading to cell survival and proliferation [187]. However when complex I dissociates from the receptor another complex, complex II, can be formed. Complex II in the cytosol recruits FADD and pro-caspase-8, possibly through the now available death domain in TRADD, and leads to apoptosis [188]. This recruitment of new molecules in complex II may occur as a result of post-translational modifications, such as ubiquitination, in some of the components of complex I [189]. The caspase-8 inhibitor FLIP can competitively bind into complex II to block the activation of caspase-8 [190]. As it is complex I that activates the NFκB pathway, leading to the upregulation of FLIP, apoptosis can only occur efficiently when complex I is not activated sufficiently to produce enough FLIP to block the caspase-8 in complex II. This dual complex formation explains the delay in the activation of the apoptotic machinery in TNF signalling compared to the extremely quick activation through Fas signalling. The formation of two different complexes and the range of proteins and ligands that can bind to Fas also explains the pleiotropic actions of the TNFR family [191].

Irrespective of the above, after the formation of the DISC, there are 2 directions the extrinsic pathway can take, type I or type II CD95/Fas signalling [192]. The direction it takes seems to be cell specific. In so-called Type I cells, pro-caspase-8 undergoes a self-cleavage event to form the active caspase-8 molecule which can activate sufficient levels of caspase-3 directly, to cause cell death. In Type II cell death, caspase-8 alone is not sufficient to potently induce the caspase cascade. Instead, caspase-8 cleaves the BH3 only pro-apoptotic protein Bid to form tBid, a truncated form which is translocated to the mitochondria [193]. tBid amplifies death signalling by promoting further caspase activation and acting on Bax and Bak, either directly or by blocking the Bcl-2 family pro-survival molecules, causing the mitochondria to release cytochrome c, AIF and Smac/DIABLO in a similar manner to that seen in the intrinsic pathway [194]. As such, Bid serves as a conduit between the extrinsic and intrinsic pathways to amplify terminal caspase activation and cause cell death. Curiously, this dependence on Bid for amplification of the cell death signal has been shown to be necessary in some cell types, such as hepatocytes [195,196], but not in others [197].

Cancer cells have been shown to adapt the receptors they express on the surface in order to evade apoptosis caused by extrinsic signals. For example, a mutated form of Fas has been shown to be expressed in many solid tumours and haematological malignancies [198]. Cancer cells can also express decoy receptors (DRs), which competitively bind death receptor ligands such as FasL and interfere with Fas-induced apoptosis [199]. Alternatively, anti-apoptotic proteins such as FLIP can be overexpressed, as has been observed in metastatic melanoma [68]. It is attractive to target death receptors for cancer therapy as they are involved in a death pathway which is independent of the tumour suppressor p53, but the practicalities have proved challenging. The use of death receptor ligands has had very toxic side effects, with the exception of TRAIL which has shown synergistic effects with conventional chemotherapeutic agents [200] and is being explored as a therapy in ongoing clinical trials (Amgen, clinicaltrials.gov identifier: NCT00508625).

Additional to death signalling pathways, the cell also has a myriad of cell survival signalling pathways which are also under tight regulation and often seen to be over-active in cancer cells, frequently as a result of a mutation in a protein involved in the signal transduction pathway.

1.4 Cell Survival

1.4.1 Signalling pathways

External factors can also influence cell growth through interactions with a different set of receptors on the cell surface. The activation of the receptor tyrosine kinases (RTKs), and indeed the TNFR, can initiate signalling pathways which can trigger the transcription of many downstream targets. The pathways involved in cell survival include a vast number of proteins which overlap at many points giving a complex web of interconnected pathways which have been simplified in the following section into three distinct pathways.

All three pathways include protein kinases. These proteins are responsible for the addition of covalently bound phosphate groups to a threonine, serine or tyrosine on specific downstream target molecules within cells. The phosphate group comes from the donor molecule adenosine triphosphate (ATP) which is a product of respiration and becomes adenosine diphosphate (ADP) after the loss of one of its phosphate groups. This post-translational modification, phosphorylation, can target the protein for degradation, change its localisation within the cell, alter its enzymatic activity or regulate its interaction with other proteins. The phosphate groups can be removed by protein phosphatases. Often, but

not always, in the case of signalling pathways, kinase-induced phosphorylation can be the switch between inactivated and activated proteins, with phosphatases having the opposing function.

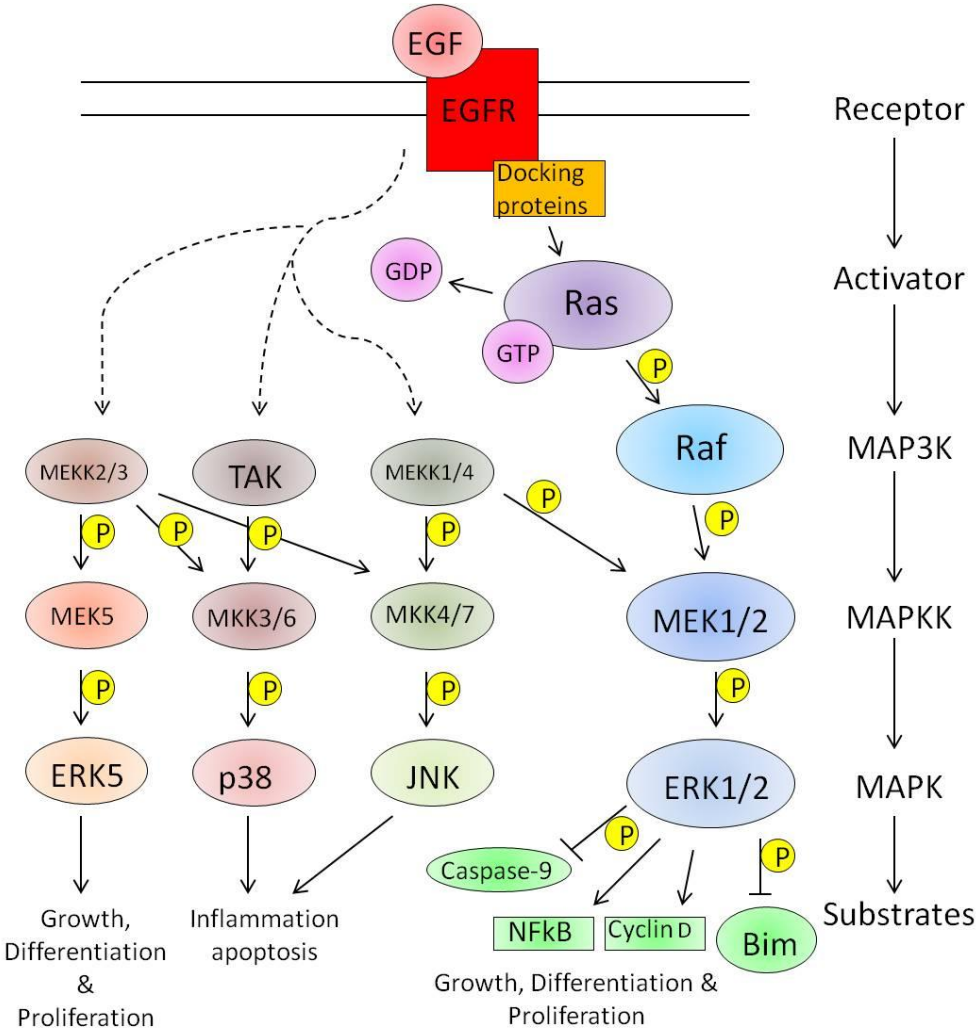

Figure 1.9: The mitogen activated protein kinase (MAPK) pathway.
This pathway is activated by ligands bound to receptor tyrosine kinases (RTKs) such as the epidermal growth factor receptor (EGFR) on the cell surface. This initiates a cascade of phosphorylation events through three tiers of kinases, the MAP three kinases (MAP3K), MAP kinase kinases (MAPKK) and MAPK. If the ligand is a growth factor, these phosphorylation events can lead to the inactivation of the pro-apoptotic molecule Bim though the MAPK extracellular signal-regulated kinases (ERK1/2) and hence can lead to cell survival. If the pathway is initiated by stress signals, different MAPKs such as c-Jun N-terminal kinases (JNK) and p38 become activated and lead to apoptosis or inflammation. Alternatively, stress can induce growth, differentiation and proliferation through MEK5/ERK5. Note the extensive cross-talk between pathways that allow convergence between signalling from other receptors.

1.4.1.1 The MAPK Pathway

The MAPK pathway (Figure 1.9) has been widely investigated in cancer research. The binding of ligands to a variety of receptors, including growth factor receptors or cytokine receptors, on the cell surface sets off a signalling cascade involving the activation, through kinase-driven phosphorylation, of three successive tiers of MAP kinases. MAP kinases are serine/threonine kinases which require double phosphorylation on the serine and threonine residues for activation. There are several distinct proteins which belong to the top tier of MAPKs, the MAPK kinase kinases (MAP3K). These proteins can be uniquely activated by specific ligands and matched with particular MAPK pathways to result in individual outcomes.

Generally, this pathway is initiated by the binding of mitogens to receptors which recruit docking proteins and activate an 'activator' molecule. The activator molecule initiates a MAP3K which in turn phosphorylates a MAPK kinase (MAPKK) which then activates a MAPK. The most well understood MAPK pathway which leads to cell survival and proliferation is activated through the binding of growth factors, such as epidermal growth factor (EGF), to receptors such as the EGF receptor (EGFR). Docking proteins activated by the EGFR remove guanosine diphosphate (GDP) from the GTPase Ras, the 'activator' molecule, allowing GTP (Guanosine-5'-triphosphate) to bind. Activated Ras triggers the protein kinase activity of Raf (the MAP3K) which then phosphorylates and activates the MAPKKs MAP and ERK Kinase 1 and 2 (MEK1/2). MEK1/2 then phosphorylate the MAP kinases ERK1 and ERK2 (also known as p42/p44), increasing their ability to activate their own substrates. It is emerging that the kinase suppressor of Ras-1 (KSR) acts as a scaffold protein through which Raf, MEK and ERK recognise and interact with each other [201,202]. KSR was observed to block oncogenic ras transformation when mutated and appears to have no inherent enzymatic activity [203].

The activation of ERK1/2 can happen in response to growth signals, hormones and viral infection. But within cancers, the over-activation of this MAPK pathway often results from mutations in the proto-oncogene Ras, or the activating mutation of B-Raf [204]. As discussed earlier, the MAPK pathway is observed to be hyperactivated in melanoma, but not in melanocytes [205]. The activation of ERK1/2 by oncogenic Ras or B-Raf contributes to the increased proliferation rate seen in tumours and as such is an attractive target for cancer therapies. In addition to phosphorylating Bim, there is also evidence ERK1/2 can target other pro-apoptotic Bcl-2 family members such as Bcl-2 associated death promoter (Bad)

for phosphorylation [206] and decrease expression levels of Bmf [207]. ERK1/2 can also inhibit caspase-9 by direct phosphorylation on Thr125, preventing the processing of caspase-9 and the subsequent activation of caspase-3 [208]. ERK1/2 can also have positive cell proliferation effects, for example through the regulation of the transcription of cyclin D, giving enhanced cell cycle entry [209]. ERKs may also be involved in cytoskeletal reorganisation during mitosis, as a proportion of ERKs in the cell are found bound to the microtubule cytoskeleton [210].

The other MAP kinases c-Jun N-terminal Kinases (JNK) and p38 are activated through a different selection of upstream MAPKK and MAP3Ks triggered by different mitogenic signals interacting with the tyrosine kinase receptors and result in outcomes typically varying from inflammation to apoptosis. Stimuli for these pathways include stress, growth factors and inflammatory cytokines. Targets for these protein kinases include p53 and c-Jun, and JNK can activate the pro-apoptotic function of Bax in response to stress [211].

The MEK5/ERK5 pathway has also recently emerged as an important MAPK signalling pathway which is often overactive in human cancers [212]. This alternative MAPK pathway is activated by stress, growth factors and mitogens and results in growth, proliferation, and differentiation. There is evidence which suggests this pathway as a promising emerging target for drug therapies to overcome chemoresistance with minimal side-effects, as ERK5 has a significantly different structure from the other ERK kinases [213].

Although delineated above as separate pathways, it is clear that these distinct MAPK pathways sometimes interconnect which blurs the clarity of the separate MAPK pathways and functions. The MAPK pathway also overlaps with other signalling pathways, such as the Akt pathway.

1.4.1.2 The Akt Pathway

The Akt pathway (Figure 1.10) is involved in protein synthesis, glucose metabolism, angiogenesis, proliferation and cell survival and is another pathway which is often deregulated in cancer. The serine/threonine protein kinase Akt, also known as protein kinase B (PKB) is encoded for by the proto-oncogene *akt* [214]. There are three Akt isoforms, Akt1, 2 and 3, which share a common structure and similar regulation and functions. Akt1 null mice displayed decreased body weight and growth retardation [215]. In contrast, Akt2 null mice display defects in the regulation of blood glucose level [216]. Perhaps surprisingly, both $Akt1^{-/-}$ and $Akt2^{-/-}$ mice were viable, and even the double knockout $Akt1/2^{-/-}$ mice

developed normally through embryogenesis, suggesting the three isoforms can substitute for each other in cellular processes, at least during development [217]. In transgenic mice expressing constitutively activated Akt, increased resistance to apoptosis and increased tumour formation were observed [218].

Akt (Akt1) is a downstream target of the lipid kinase phosphoinositide-3-kinase (PI3K) which is activated by cell RTKs and G protein-coupled receptors in response to growth signals. PI3K specifically phosphorylates serine and threonine residues as well as phosphoinositides such as phosphatidylinositol (3,4,5) trisphosphate (PIP3) and phosphatidylinositol-3,4-bisphosphate (PI-3,4-P2). These phosphorylated phosphoinositides bind to the pleckstrin homology (PH) domain of Akt, activating the enzymatic function of the protein [219]. The PH domain in other molecules has been shown to specifically bind PIP3, whereas the Akt PH domain can bind both phosphoinositides, although with higher affinity to PI-3,4-P2, which may be an important factor in the hyper-activation of Akt observed in cancer cells [219]. The binding of Akt to the membrane bound phosphoinositides results in the translocation of Akt to the plasma membrane. However to become fully activated, Akt must also be phosphorylated on the threonine-308 and serine-473 residues, through phosphoinositide-dependent kinase 1 (PDK1), which is also activated by PI3K phosphoinositide targets [220].

The tumour suppressor PTEN can dephosphorylate the PI3K lipid products [221]. Hence, PTEN can counteract the pro-oncogenic over-expression of PI3K by reducing its lipid substrates to normal levels and preventing the hyper-activation of Akt. Over-expression of PTEN has been shown to arrest the cell cycle in the G1 phase in multiple cancer types [221], however loss of function of PTEN is common in these cancers.

Akt acts on many downstream molecules including mTORC1, NFκB, mdm2, forkhead-related transcription factors and caspase 9. The first Akt substrate to be defined was glycogen synthase kinase 3 (GSK3), which is involved in regulating proliferative and anti-apoptotic pathways and phosphorylates cyclin D1, regulating cell cycle progression [222]. Akt has also been shown to phosphorylate the pro-apoptotic protein Bim [223,224], allowing the release of pro-survival proteins and targeting Bim for degradation. Akt can also block the transcription of Bim by targeting the forkhead transcription factor FOXO3A for phosphorylation leading to its association with the 14-3-3 proteins and targeting it for degradation [225,226]. These mechanisms are thought to be secondary mechanisms for Bim neutralisation if it has escaped phosphorylation by ERK1/2. Another Bcl-2 family member

regulated by Akt is the BH3-only protein Bad. Bad is phosphorylated by Akt to reveal binding sites for 14-3-3 molecules, thereby localising the protein to the cytosol and preventing the inhibition of the pro-survival molecules of the Bcl-2 family [227].

In cancers, Akt activity and the downstream Akt signalling cascade is frequently upregulated to dangerous levels through multiple potential causes. As seen in the MAPK pathway, extrinsic signals such as growth factors may increase, key receptors may become hyper-activated through mutations or be present at higher levels. Intrinsic events such as the activating mutation of the proto-oncogene Ras, increases expression of PI3K and inactivating mutations in PTEN can also lead to increases in Akt activity [228]. All these events can lead to the hyper-activation of Akt and the uncontrolled growth of the cell. The Akt pathway has been targeted for cancer therapy through the development of Akt inhibitors to be used in conjunction with apoptosis-causing chemotherapeutics. However, Akt is endogenously expressed at high levels uniformly over most tissue types, so side effects would be potentially be severe [229]. Among the substrates for activated Akt is NFκB, a transcription factor which has an important role in cell survival.

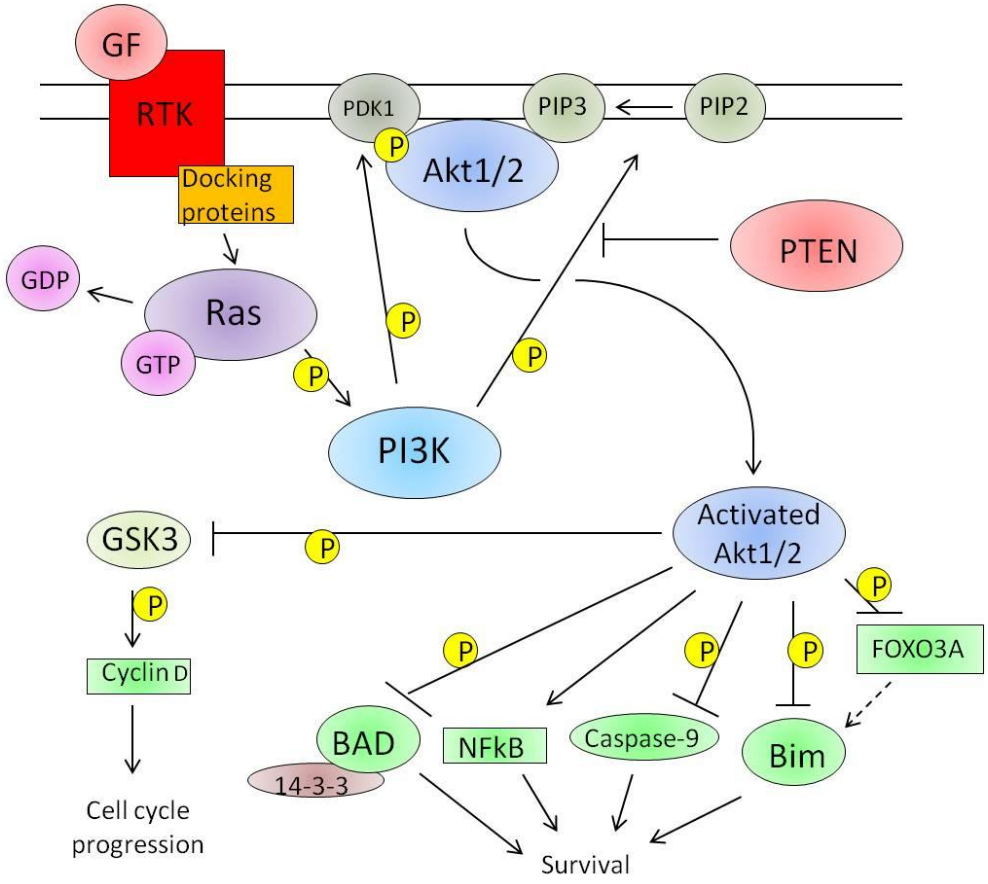

Figure 1.10: The Akt pathway.
Growth factors bind to the receptor tyrosine kinase (RTK) on the cell surface which activates phosphoinositide-3-kinase (PI3K) through the G-protein Ras. PI3K causes the phosphorylation of its lipid products such as phosphatidylinositol diphosphate (PIP2) and phosphoinositide-dependent kinase-1 (PDK1) which act to translocate Akt from the cytosol to the plasma membrane. Activated Akt is present at the plasma membrane, but is shown here as separate for convenience. Akt can act on downstream molecules such as the pro-apoptotic proteins Bim and BAD, the forkhead transcription factor FOXO3A which induces transcription of Bim, and glycogen synthase kinase-3 (GSK3) to promote cell survival. The tumour suppressor phosphatase and tensin homologue deleted on chromosome 10 (PTEN) can de-phosphorylate PI3K lipid products and inhibit the activation of Akt.

1.4.1.3 The NFκB Pathway

NFκB was first discovered in 1986 and is responsible for the regulation of over 150 genes [230]. The activity of this transcription factor can contribute to the decision between cell survival and apoptosis and can play a crucial role in carcinogenesis. NFκB upregulation has been shown to be an important factor in the progression of many inflammatory diseases and cancers [231]. However, these relationships are not always simple. For example, in the early stages of melanoma progression, NFκB can induce apoptosis through TNFR1, TRAIL and the Fas receptor pathways [232,233], whereas in later stages, NFκB blocks these pro-apoptotic pathways through the upregulation of TRAF2, TRAIL decoy receptor and Fas associated phosphatase-1 (FAP-1) [234]. Indeed in late stage metastatic melanoma NFκB

also upregulates pro-survival molecules such as FLIP, survivin and some pro-survival Bcl-2 family members [68,69,235]. The switch between the pro-apoptotic and pro-survival functions of NFκB comes from the result of other chemokines and growth factors activating the pathways and the expression levels of various proteins involved in the pathways. For example, at higher expression levels of IKK, the survival pathway dominates and levels of activated caspase 3 decrease [236]. Higher levels of NFκB regulated chemokines have been observed in melanoma and appear to accelerate the progression and metastasis of the tumour [237,238]. Indeed NFκB becomes constitutively upregulated in melanoma through the development of an autocrine loop where NFκB upregulates the same chemokines which are responsible for initiating its activation [239].

In mammals, NFκB is made up of five structurally related subunits, c-Rel, p65/RelA, RelB, p50/NFκB1 and p52/NFκB2 (reviewed by Grilli et al. [240] and Kopp et al. [241]). These subunits interact to form the homo or heterodimers which make up the NFκB complex. All the subunits contain conserved nuclear localisation sequences, dimerisation sequences and DNA-binding domains in a region termed the Rel homology domain (RHD) on the N-terminus [240,241]. However the Rel (reticuloendotheliosis viral oncogene homolog) proteins, RelA, RelB and c-Rel, also contain transactivation domains (TDs) for the activation of transcription, which are not present in p50 or p52.

The NFκB subunits p50 and p52 form after the proteolytic cleavage of the inactive precursors p105 (IKKβ) and p100 (IKKα), respectively [242]. These exist in the cytoplasm until the cleavage and proteasomal degradation of the inhibitory C-terminal domain allows them to translocate to the nucleus where they can form homodimers with each other or heterodimers with the Rel subunits [243]. The heterodimers, which contain a TD, act as transcription factors for genes containing a κB sequence in the promoter or enhancer region [244]. Conversely, the homodimers, which lack a TD, have been observed to repress κB site activated transcription, possibly because they competitively bind to the same DNA sites as the heterodimers [245].

NFκB activity is tightly regulated through the functions of the inhibitor of κB (IκB) proteins. This is a family of proteins which interact with NFκB dimers containing the p65/RelA subunit, preventing them from translocating to the nucleus [246]. IκB proteins can be removed from the dimers, and targeted for degradation by the proteasome, through phosphorylation events mediated by IKK (IκB kinase) proteins themselves, activated

through the NFκB pathway [247]. Furthermore, IκBα is transcriptionally upregulated through activated NFκB, providing a negative feedback loop for NFκB activation which can only be overcome through persistent activation signals [248].

There are two pathways through which NFκB can be directly regulated, the canonical (or classic) and non-canonical (or alternate) pathways (). Common to both pathways is the activation of an IKK complex. In the canonical pathway, the activation of surface receptors, (such as TNFR, IL-1 receptor and Toll-like receptors) by external ligands (TNFα, IL-1 and LPS) and the recruitment of the adapter proteins activate the IKK complex. The adapter protein complex is the same as complex I discussed in the extrinsic death pathway (section 1.3.3.3.3). The binding of TRADD to TNFR1 would normally initiate a caspase-8 dependent apoptotic pathway, but the recruitment of TRAF2 prevents this and instead promotes activation of NFκB through the IKK complex. The IKK complex is made up of the IKKα (p100), IKKβ (p105) and IKKγ (NEMO) (NFκB essential modulator) subunits and is responsible for targeting IκB for degradation by the proteasome [247]. IKKα and IKKβ are the catalytic kinase subunits whereas NEMO acts as a non-catalytic scaffold protein in this complex [249]. The removal of IκB from the Rel NFκB subunits frees the NFκB dimers for translocation to the nucleus where they can act as a transcription factor [250]. TNF belongs to the TNF superfamily of cytokines and is an initiator of the canonical NFκB pathway. TNFα is produced in response to infection or inflammation by the white blood cells of the immune system and initiates the NFκB pathway by binding to the TNFR on the cell surface.

In the non-canonical pathway, activated receptors recruit NIK (NFκB inducing kinase) which causes the phosphorylation of IKKα (p100) subunits, which exist as homodimers in the cytosol [251]. The phosphorylation event leads to the degradation of the inhibitory C-terminus to produce the p52 NFκB subunit which can form heterodimers with RelB subunits, translocate to the nucleus and act as a transcription factor. Fewer ligands have been elucidated that activate this pathway, but include important immunological biomolecules such as B cell activating factor (BAFF), CD40 and lymphotoxin B [252].

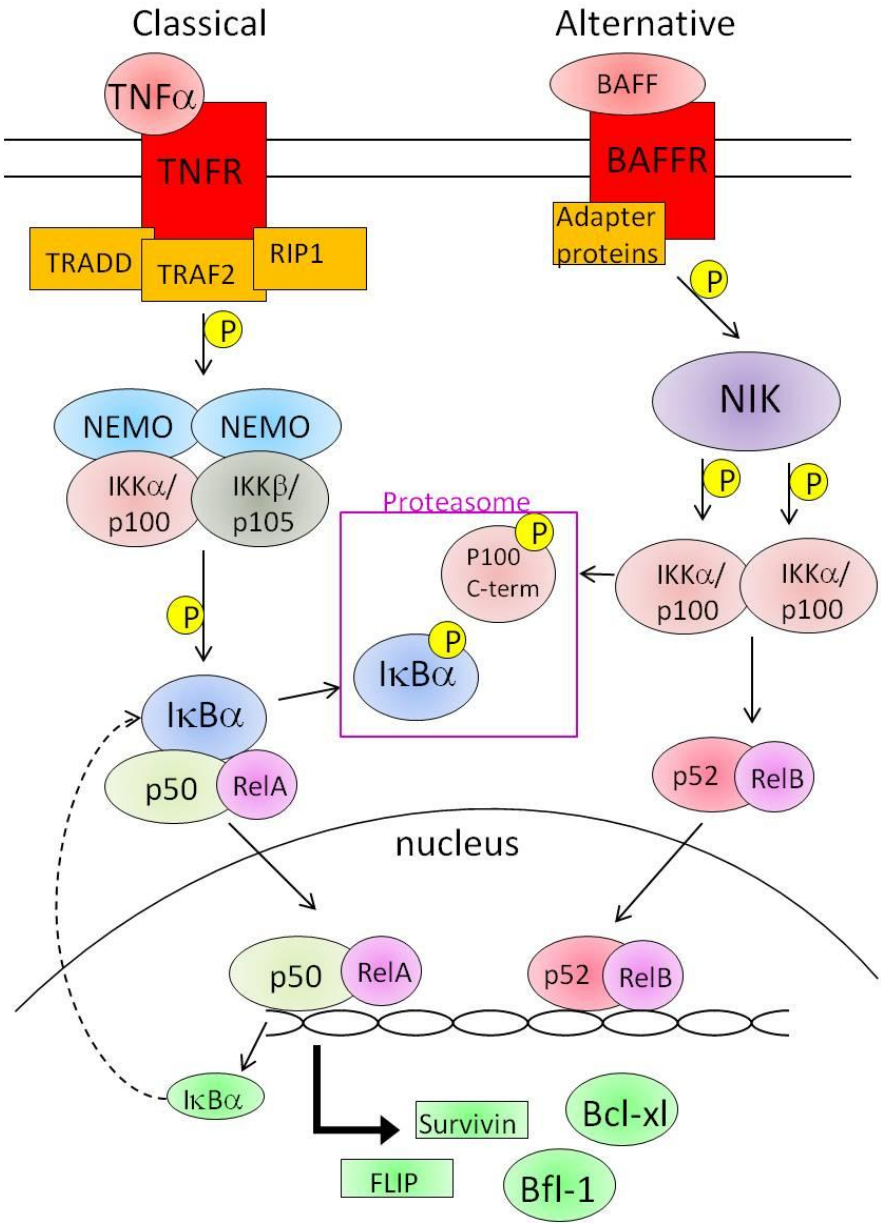

Figure 1.11: The NFκB pathways.
The classical NFκB pathway is initiated by the binding of TNFα to the TNF receptor (TNFR1) which recruits a complex of adapter proteins including TRAF2 (TNFR-associated factor 2), RIP1 (receptor interacting protein 1) and TRADD (TNFR associated death domain). These activate the IKK (IκB kinase) complex containing 2 NEMO (NFκB essential modulator) subunits and IKKα and IKKβ subunits. This IKK complex causes the phosphorylation of IκBα, removing it from the NFκB dimer and targeting it for degradation by the proteasome. The NFκB dimer is now free to translocate to the nucleus and act as a transcription factor for many targets including IκBα, forming a negative feedback loop for further NFκB activation. The alternate pathway is activated through the binding of ligands such as BAFF to cell surface receptors which through adapter proteins activate NIK (NFκB inducing kinase). NIK causes the phosphorylation of IKKα subunits, targeting their inhibitory C-terminal domains for degradation by the proteasome and freeing the p52 fraction to form NFκB heterodimers which translocate to the nucleus and act as transcription factors on a variety of target genes.

There are several mutations often observed in melanoma which have been associated with an increase in NFκB activation. Loss of p53 through mutated ARF (present in 20-40% of

melanomas) leads to the activation of NFκB through the upregulation of IKKα; When p53 is present, it inhibits the transcription of IKKα through binding to the p53 binding site in the promoter of IKKα [253]. The wild type form of $p16^{INK4A}$ strongly inhibits NFκB dependent transcription, and mutations or loss of $p16^{INK4A}$ (seen in 10-30% of melanomas) can increase NFκB activation, possibly through its decreased binding affinity to the NFκB subunit p65 compared with wild-type $p16^{INK4A}$ [254].

The hyperactivating mutations in BRaf (present in 50-70% of melanomas) and NRas (present in 20-40% of melanomas) can both lead to an upregulation in ERK1/2 activity through the MAPK pathway (as discussed ealier, section 1.4.1.1) [204]. ERK1/2 has not been shown to directly activate NFκB, but it does upregulate the transcription of various inflammatory cytokines known to activate the NFκB pathway [255]. Hence constitutive ERK1/2 activation may indirectly upregulate NFκB activity.

PTEN is also sometimes mutated or deleted in melanoma (10-15%) and therefore cannot block Akt activity. Akt has been shown to directly upregulate NFκB activity by causing the phosphorylation of the NFκB subunit p65, increasing the binding efficiency of the NFκB dimer to DNA [256]. Furthermore, NFκB acts as a transcription factor for several members of the Bcl-2 family, which are often seen overexpressed in human cancers.

1.5 The Bcl-2 Family

As discussed briefly earlier, the Bcl-2 family are key regulators of apoptosis. In fact, one of the first apoptosis regulators to be defined was Bcl-2, a pro-survival protein encoded by the *Bcl-2* oncogene. The *Bcl-2* oncogene was discovered at the t(14;18) chromosome translocation breakpoint present in almost all human follicular lymphomas where the Bcl-2 gene is translocated to the heavy chain enhancer on chromosome 14 [257]. Later, functional studies determined that expression of the *Bcl-2* oncogene products increased the survival rates of cells [258,259]. It is now known that Bcl-2 belongs to a family of apoptosis regulators named the Bcl-2 family, which contains three sub-groups. The pro-survival proteins (Bcl-2, Bcl-w, Bcl-xL, Mcl-1, Bcl-b and Bfl-1/A1) form one sub-group and the pro-apoptotic proteins are split into 2 groups by structure; the effector proteins (Bax, Bak and Bok) and the BH3-only proteins (Bim, Bid, Bik, Bad, Noxa, Puma, Bmf and Hrk). The proteins of the Bcl-2 family are involved in apoptosis, tissue turnover and defence against pathogens, and are linked by their regulatory function and Bcl-2 homology (BH) domains. Each member of the Bcl-2 family contains the BH3-domain which is necessary for their

interactions with each other (discussed in more detail later). The balance of the pro-survival and pro-apoptotic proteins, and their post translational modifications, has been shown to determine whether a cell lives or dies and hence, the Bcl-2 family is extremely important in the survival of cancer cells.

The complex interactions that occur between the BH3-only proteins and the pro-survival proteins during the regulation of apoptosis have not been completely elucidated. However, it is widely accepted that the pro-apoptotic proteins Bim, tBid and Puma bind all the pro-survival proteins in a promiscuous manner, whereas Noxa and Bad display more selective binding [260] (Figure 1.12). Mcl-1 has been shown, using four separate techniques (pull-down, yeast hybrid screens, surface plasmon resonance and BH3 profiling), to be unable to bind Bad but to be bound tightly to Noxa [260-263]. Bfl-1 has been identified as being able to bind to Noxa by surface plasmon resonance [260]. However, BH3 profiling, a technique which measures mitochondrial activation as a marker of the interaction between the pro-survival proteins and BH3 peptides isolated from BH3-only proteins, has shown a lack of binding between Noxa and Bfl-1 [262]. As a result of the inconsistencies observed with Bfl-1 and Noxa binding using different techniques, it is thought that they do bind each other, but only weakly. The promiscuous proteins Bim and Puma have been shown to induce apoptosis more potently in mouse embryonic fibroblasts (MEFs) than Noxa, Bad, Bcl-2 modifying factor (Bmf), Bcl-2 interacting killer (Bik) or Harakiri (Hrk) [260]. But in the same study, the combination of Noxa and Bad was shown to be extremely potent, as between them they bind all the pro-survival proteins, which is necessary for the efficient progression of apoptosis [260].

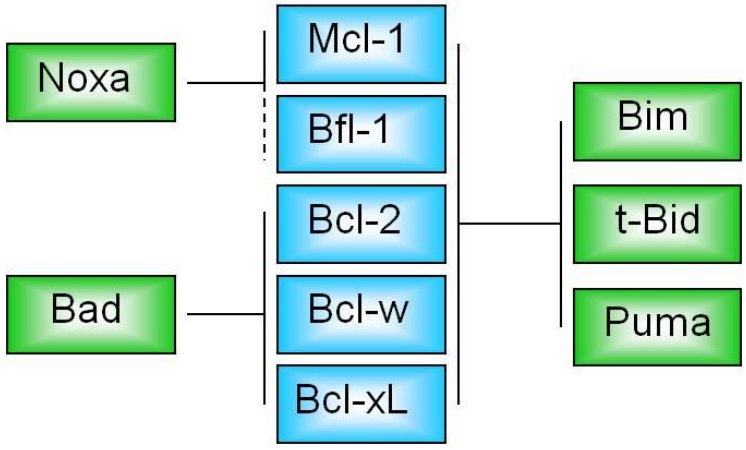

Figure 1.12: The binding profile of the members of the Bcl-2 family.
The BH3-only proteins are represented in green and the pro-survival proteins are blue. Bim, t-Bid and Puma are promiscuous proteins which can bind all the members of the pro-survival sub family, whereas Noxa and Bad can only bind select members.

The interaction of the pro-survival and BH3-only proteins with the multidomain effector proteins, Bax and Bak, is a more controversial topic. The conflicting evidence in the literature has lead to the development of two theories describing these interactions (Figure.1.13). The indirect binding theory holds that the effector proteins are spontaneously activated and as such, binding of all the pro-survival proteins by the BH3-only proteins is sufficient to induce apoptosis [264,265]. The direct theory separates the BH3-only proteins into two groups, the sensitizers and the activators. Within this model, the sensitizers bind to and inhibit the pro-survival proteins, releasing the activators from the pro-survival proteins, so that the activators can bind directly to the effector proteins [266,267].

Evidence supporting the indirect theory relies on the observation that apoptosis can ensue without the BH3-only proteins binding to the effector proteins [264]. Mice lacking Bim and Bid, both essential activators in the direct model, grow normally and display normal developmental apoptosis [264], whereas mice lacking Bax and Bak usually die as neonates [268]. If Bid and Bim were essential for apoptosis initiation, the same developmental failure would be expected in mice lacking these BH3-only proteins. The indirect theory also indicates that the effector proteins must always be bound by the pro-survival proteins to prevent their pro-apoptotic function and can only cause MOMP when they are displaced from the pro-survival molecules by the BH3-only proteins [264,265,269].

However, BH3-only protein binding to the effectors has also been observed to be necessary for the initiation of apoptosis and certain BH3-only proteins have been observed bound to the activated forms of Bax and Bak, supporting the direct theory [270]. Within the BH3-only proteins, Bim and tBid are termed activators, as they have been observed to directly bind to Bax and Bak [267], whereas Noxa and Bad are referred to as sensitizers as they have only been found to bind the pro-survival proteins [266]. There is debate as to whether Puma acts as an activator or sensitizer protein, as it has been found to bind weakly with the effector proteins [271], as has the Bmf BH3-peptide [272]. The Bmf and Puma peptides bound weakly to the effector proteins, but were apparently sufficient such that in the absence of Bid and Bim, they could initiate cytochrome c release [272]. In the direct model, the activators are essential for the activation of MOMP, however $Bid^{-/-}Bim^{-/-}$ mice display normal apoptosis. The reason for this has been postulated to be that other activators exist which initiate apoptosis through Bax and Bak including other BH3-only proteins and cytosolic p53 [271]. Cytosolic p53 has been shown to activate Bax in the absence of a nucleus, suggesting that p53 is not activating Bax through its role as a transcription factor, as synthesis of new proteins is not necessary [273]. p53 has also been shown to possess the ability to remove

BH3-only and effector pro-apoptotic proteins from the pro-survival molecule Bcl-xL [274]. Additionally, BH3 peptides other than Bid and Bim, including Bmf and Puma, have been observed to bind weakly to Bax and Bak but at sufficient levels to induce MOMP [272]. The level of MOMP caused by these peptides correlated with the levels of apoptosis induced by the full-length proteins.

In reality, a combination of the two models probably occurs as neither model can explain all the results presented. For example, a model termed the 'embedded together model' has been proposed by Leber et al. which holds that the pro-survival proteins bind to the activator BH3-only and effector proteins in a dominant-negative manner in the OMM to prevent apoptosis [275-277]. As such, Bcl-xl acts as a dominant-negative Bax. This helps to explain the similar structures, yet opposing functions, of Bax and Bcl-xL.

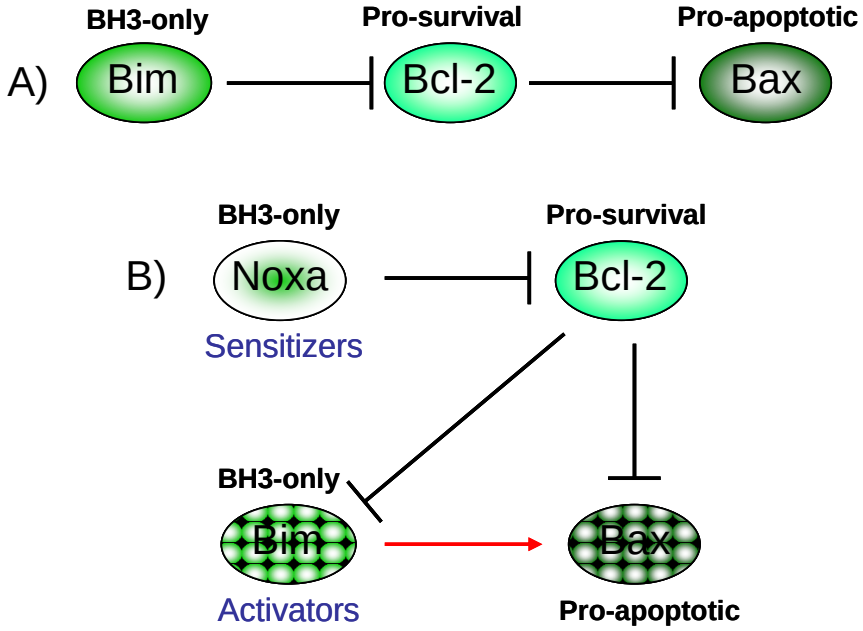

Figure.1.13: The two models for the interactions between the Bcl-2 family proteins.
A) The indirect binding model relies on the removal of the pro-survival proteins by the BH3-only proteins for the release of the effector proteins which can then homodimerise and form pores in the mitochondrial membrane. B) The direct binding model suggests that activator BH3-only proteins can interact directly to the effector proteins causing them to form pores in the mitochondrial membrane. There are also sensitizer BH3-only proteins which bind to the pro-survival proteins, releasing the activator proteins and preventing the pro-survival proteins from blocking the actions of the effector proteins.

1.5.1 The Pro-Apoptotic BH3-only Proteins

The BH3-only sub-family detect cell damage, and appear to induce apoptosis primarily by inhibition of the pro-survival members of the Bcl-2 family or by activation of the effector molecules Bax and Bak, as discussed above. Apart from the BH3 domain, which was first

identified as the binding site for Bcl-xL on Bak [278], the BH3-only sub-family are structurally unrelated to the rest of the Bcl-2 family. In fact there is evidence that the BH3 domain in these proteins developed via convergent evolution [279]. BH3-only proteins are also unrelated in structure to each other, both in 3D shape and predicted secondary structure, except for the BH3 domain which is essential for their pro-apoptotic function (Figure 1.14). A defined solution structure (i.e. the structure of the soluble form of the protein) has been determined for Bid which is surprisingly similar to that of Bcl-xL, despite the fact that they only share homology in the 16-amino acid BH3 domain [280].

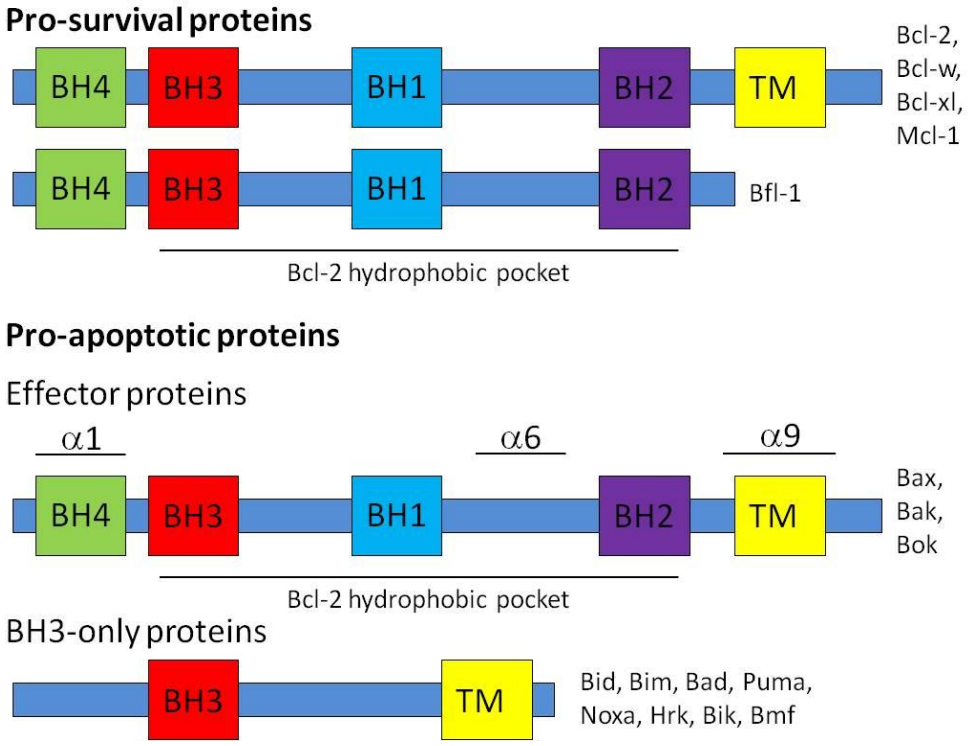

Figure 1.14: The Bcl-2 family. The Bcl-2 family are related by function and the presence of Bcl-2 homology (BH) domains.
BH1, BH2 and BH3 fold into a hydrophobic groove on the surface of the protein which interacts with the BH3 domain of other family members. All the Bcl-2 family proteins, except for Bfl-1, contain a transmembrane (TM) domain at the C-terminus. Note that the putative BH4 domain in Bax is based on homology to the BH4 domain in Bcl-xL, not function.

BH3-only single protein knockout mice are all viable, with a range of relatively mild physiological faults due to defective apoptosis which presumably highlights the functional redundancy within the BH3-only sub-family. Specific defects in certain cell types can also be seen, the most profound of which are observed $Bim^{-/-}$ mice, resulting in 50% death of mice through splenomegaly, kidney defects and increased levels of blood leukocytes [281]. $Puma^{-/-}$ lymphocytes are resistant to genotoxic stress [282] and $Bid^{-/-}$ thymocytes have increased resistance to death-receptor initiated apoptosis, but ultimately die [196].

1.5.1.1 Regulation of the BH3-only proteins

The BH3-only proteins are induced in response to a range of stress stimuli including loss of adhesion to the extracellular matrix, DNA damage and oncogene activation. As mentioned earlier, Noxa (the latin word for damage) and Puma both contain p53 response elements and are therefore induced by DNA damage via the p53 tumour suppressor [283, 284], although Noxa can also undergo p53 independent induction [285]. Post-translational modifications of these two proteins have not yet been described, but they are both understood to translocate to the mitochondria when they are activated. Puma$^{-/-}$ and Noxa$^{-/-}$ mice display no obvious developmental abnormalities however Puma$^{-/-}$ mice cells display resistance to p53-induced apoptosis [286].

Bim upregulation is induced by a host of stimuli, including growth factor deprivation via FOXO3A [287] and ER stress via CEBPα [288]. Bim can be sequestered to microtubules where it is kept inactive until it is activated and translocates to the mitochondria [289]. Bim can be further phosphorylated by ERK at a number of residues, with phosphorylation on serine 69 targeting it for degradation by the proteasome [290]. Bmf is also associated with the cytoskeleton until activation causes it to translocate to the mitochondria [291].

Other BH3-only proteins are activated by post-translational modifications, for example, loss of phosphorylation on Bad due to growth factor deprivation allows translocation from the cytosol, where it is bound to 14-3-3 proteins, to the mitochondria [227]. Bad is inactivated by phosphorylation through the MAPK pathway, with ERK phosphorylating p90Rsk, which in turn phosphorylates Bad at amino acid (aa) 75 (aa112 in mice) [292]. Akt can also phosphorylate Bad at aa999 (aa136 nin mice) [293] and PKA can phosphorylate it at aa118 (aa155 in mice) [294]. Caspase-8 mediated proteolysis of Bid results in active truncated Bid (t-Bid) which acts as the bridge between the extrinsic and intrinsic apoptotic pathways (Figure 1.5) [295]. Bid can also be activated through cleavage by calpains and lysosomal enzymes meaning it is not limited to activation through the extrinsic pathway [296,297]. Bik expression is induced through the E1A oncogene and p53 and is also activated via phosphorylation events [298].

1.5.1.2 The Role of BH3-only Proteins in Melanoma

BH3-only proteins have potential tumour suppressor roles through their ability to induce apoptosis in malignant cells. In melanoma, a microarray analysis showed a decrease in

Puma expression between non-malignant nevi and metastatic melanoma and these lower Puma expression levels correlated with poorer 5-year survival rates [299]. Although Puma loss has not been shown to cause cancer, knockdown of Puma expression mimics loss of p53 function in that it causes transformation of MEFs which already have activated E1A and Ras oncogenes [300]. Noxa has been shown to be upregulated in melanoma in response to proteasome inhibition resulting in cells becoming re-sensitized to apoptosis [301], although again there is no evidence that loss of Noxa causes carcinogenesis. Interestingly, Bid appears to play an important role in cisplatin induced apoptosis in melanoma [302], however in general it appears that Bid expression does not correlate with sensitivity to chemotherapy in many cancers [303].

Bim regulates apoptosis caused by the microtubule disrupter, paclitaxel, and loss of Bim sensitizes tumour-prone cells to carcinogenesis [304]. In melanoma, Bim downregulation has been reported in TRAIL-resistant cells, possibly as a result of the associated high levels of ERK1/2 activation [305]. Bad is also downregulated in melanoma cells which display hyperactivated MAPK pathways and the dephosphorylation of this protein is the key step in MEK inhibitor induced apoptosis in melanoma cells [306], as is the translocation of Bmf [307]. However there is no evidence suggesting Bad inactivation, mutation or dysregulation contributes to the development of melanoma. One study has shown that Bik expression mildly increases in melanoma cells compared to nevi and that Bik over-expression sensitized cells to various chemotherapeutics and induced growth inhibition, although the mechanisms behind these effects were not elucidated [308]. There are as yet no studies of the roles or expression of Hrk in melanoma.

Although the distinct roles of BH3-only proteins in carcinogenesis are poorly understood, it is clear that higher levels of these proteins in cancerous cells prime the cells for apoptosis. Hence, drugs which mimic BH3-only proteins (BH3 mimetics) could re-sensitize cancer cells to apoptosis, by overcoming the typically high levels of pro-survival proteins present. ABT-737, and the bio-available version ABT-263, bind to and block the functions of the pro-survival proteins Bcl-2, Bcl-w and Bcl-xL by mimicking the BH3-only protein Bad [309].

1.5.2 The Pro-Survival Proteins

There are six known related pro-survival proteins in the Bcl-2 family; Bcl-2, Bcl-xL, Bcl-w, Mcl-1 and Bfl-1/A1 (Figure 1.14) and the lesser understood Bcl-b. The four BH domains are conserved throughout the Bcl-2 pro-survival proteins and fold into globular

motifs with a hydrophobic groove on the surface, as determined by exploring the solution structures of Bcl-2, Bcl-xL and Bcl-w [310-312]. This groove is where the BH3 domain can bind to an amphipathic α-helix of about 24 residues contained in Bax and Bak, as observed in solution structures of Bcl-x:Bak/Bax complexes [313,314]. This coupling blocks the pro-apoptotic function of Bax and Bak and results in evasion of apoptosis [315]. The solution structure for Mcl-1 has also been elucidated and shown to have a structurally different hydrophobic groove explaining the different binding pattern for this protein compared to Bcl-x [316]. The structure of Bfl-1 has only been recorded when it is bound to peptides as it appears to display structural plasticity (discussed in more detail below). The pro-survival proteins, with the exception of Bfl-1, contain a transmembrane domain which localises them to the outer mitochondrial membrane or other intracellular membranes such as the endoplasmic reticulum. However, structures of the proteins have only been determined in their soluble or crystallised forms. There is a lack of information on the structures these proteins adopt when they are in a lipid environment other than their reported ability to form pores in lipid membranes, and whether these pores actually form in physiological situations remains to be determined [317,318].

Additional to their roles as apoptosis regulators, the Bcl-2 pro-survival proteins have been shown to have further functions. Bcl-2 and Bcl-xL have roles in blocking autophagy through their interaction with a BH3-like domain in beclin-1 [319]. Knock-out mice for the pro-survival proteins have the most severe phenotypes of all single knock-outs of the Bcl-2 family and reveal the physiological importance of each protein.

In contrast to the BH3-only proteins, the knockout mice of the pro-survival proteins display specific defects, indicating a lack of compensation and redundancy between this subfamily. Mcl-1 is seen to be essential for development, as Mcl-$1^{-/-}$ mice result in pre-implantation lethality due to a defect in the trophoectoderm [320]. Bcl-$xL^{-/-}$ mice display embryonic lethality due to increased apoptosis in neuronal and haematopoietic cells [321]. Bcl-$2^{-/-}$ mice are viable, but 50% die within 6 weeks due to a rapid loss of immune cells, while the survivors are smaller than expected, prone to polycystic renal disease and their haematopoietic cells show increased sensitivity to apoptotic stimuli [322]. Bcl-$w^{-/-}$ mice are viable but display sterility due to impeded spermatogenesis and testicular degeneration [323] and $A1^{-/-}$ (the murine homologue to Bfl-1) mice are also viable but display increased neutrophil apoptosis [324].

1.5.2.1 Regulation of the Pro-Survival Proteins

Levels of the pro-survival proteins can be controlled through a variety of stimuli and pathways. For example, Bcl-2 has been seen to be upregulated transcriptionally through NFκB and MITF [325]. Activated NFκB can also result in the upregulation of Bcl-xL and Bfl-1 [326]. External factors such as growth factors (e.g. VEGF for Mcl-1, Bcl-2 and Bcl-xL [327]), hormones (e.g. estrogen for Bcl-xL [328]) and cytokines (e.g. IL6 for Bcl-xL and Mcl-1 [329]) have been shown to increase the expression levels of the pro-survival proteins. These levels can also be further regulated through intrinsic events such as proteasomal degradation and p53-induced downregulation [330,331].

The regulation of Mcl-1 has been most widely studied as it has been shown to be the main cause of resistance to BH3 mimetic drugs which do not inhibit it [332]. Mcl-1 is targeted for degradation by ubiquitination through the E3 ligase MULE after genotoxic stress [333]. GSK3 can also target Mcl-1 for degradation through the E3 ligase βTrCP [334]. Removal of the ubiquitin groups by a deubiquitinase has been shown to rescue Mcl-1 from degradation and hence give cells increased survival potential [335].

1.5.2.2 The Role of the Pro-Survival Proteins in Melanoma

Melanocytes appear to depend on Bcl-2 for survival, as when Bcl-2 expression is knocked down, melanocytes die. As such, Bcl-2 knock-out mice display a loss of hair colour due to the diminished survival of melanocytes to provide the melanin pigments [164]. The levels of various pro-survival proteins have been shown to increase, decrease or remain the same during melanoma progression. For example, the pro-survival proteins Mcl-1 and Bcl-xL have been shown to be upregulated in malignant cells in comparison with nevi [336], however Bcl-xL and Bcl-2 levels have also been shown to be comparable between malignant and nevi cells [337,338] and levels of Bcl-2 were found not to correlate with disease progression in a large series of uveal melanomas [339].

Treatment with DTIC, the standard regimen of care for metastatic melanoma causes upregulation of the pro-apoptotic proteins in several cellular models of melanoma, but appears to have no effect on the levels of pro-survival proteins [340,341]. This inability to downregulate the high levels of pro-survival proteins seen in metastatic melanoma is potentially an important factor in the ineffectiveness of DTIC treatment. Bcl-2 antisense (Oblimersin sodium) therapy appeared to decrease apoptosis resistance in xenograft models [342] and has been trialled in melanoma treatment, although combination with DITC

was disappointing in clinical trials (trials conducted by Genta Inc.). BH3-mimetics, which target the pro-survival proteins, have shown promise in the clinic. ABT-737 has been shown to synergise with many chemotherapeutic drugs, such as DTIC, MG132 and MEK and p38 inhibitors [341,343,344]. However, ABT-737 has no effect against Mcl-1 or Bfl-1 function, and as such, resistance to this drug has been shown to be an issue in various cancers with high levels of these proteins [332,345]. Other BH3-mimetics are being developed to overcome this resistance by targeting different arrays of pro-survival proteins, such as TW-37, which targets Bcl-2, Bcl-xL and Mcl-1 [346].

1.5.3 The Pro-Apoptotic Effector Proteins

Bax, Bak and Bcl-2 related ovarian killer (Bok) are the three members of the Bax-like effector sub-family, which act downstream of the other Bcl-2 proteins in the apoptosis pathway. Bax and Bak are essential for the stimulation of apoptosis whereas Bok is seen as the more redundant member of the effector proteins. There is functional redundancy between Bax and Bak as is apparent from single knock-out mice for Bax or Bak which display normal apoptosis and have very limited defects, while the double knock-out mice are unable to accomplish physiological apoptosis and most die perinatally [268]. The effector proteins exhibit similar structures to the pro-survival molecules, retaining the BH domains and a transmembrane domain, with the hydrophobic pocket which can accept a BH3 domain (Figure 1.14 and Figure 1.15).

Bax and Bak have also been observed to regulate mitochondrial dynamics with roles in the fission and fusion of mitochondria [347]. The mitochondrial network is constantly rearranging through fission and fusion events in order to repair damaged mitochondria and ensure correct distribution of mitochondria to daughter cells [348]. Bax-induced mitochondrial fission has been shown to be independent of the mitochondrial fragmentation which occurs as a result of apoptosis, as the addition of Bcl-xL blocked apoptosis but not fission [349].

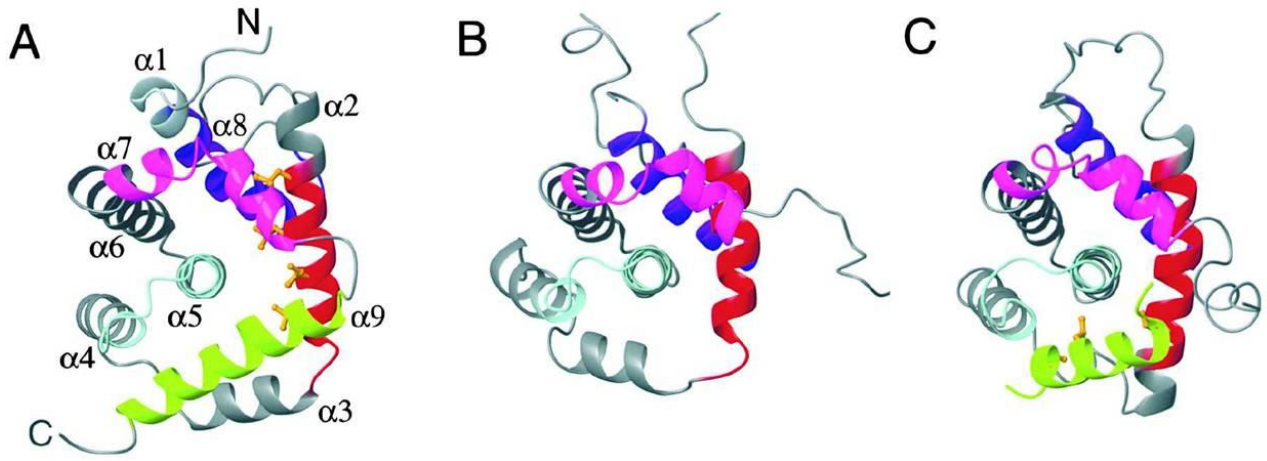

Figure 1.15: Ribbon structures of (A) Bax, (B) Bcl-xL and (C) Bcl-xL complexed with Bak BH3-peptide.
The BH domains are colour coded; BH1 (cyan), BH2 (magenta), BH3 (red) and BH4 (blue). The C-terminal α9 helix and the Bak BH3-peptide are coloured lime green. The BH1, BH2 and BH3 domains form a hydrophobic pocket, which is inhabited by the C-terminus of Bax in its inactive form, and is where the BH3 domain from other members of the family bind. Taken from *Suzuki et al.* (2000) [350].

1.5.3.1 Activation of the Effector Proteins

An essential step in the progress of apoptosis is the activation of Bax and Bak which exist in inactive, soluble forms in most healthy cells. Bax undergoes a conformational change and translocates from the cytosol to the OMM upon activation [351], whereas Bak exists at the mitochondria even before it is activated [267]. A small amount of Bax and Bak have been observed at the ER, although their role there is not clear [352]. The activation, conformational change and pore formation by the effector proteins are poorly understood events which are being heavily researched. Presented in this section are outlines of the current theories relating to the mechanisms of action and structures of the effector proteins.

The activation of the effector proteins involves a conformational change which exposes epitopes which are hidden in the inactive state, allowing peptide-specific antibodies, such as 6A7 for Bax, to visualise the activated form [353]. During the conformational change of Bax, the α9 helix formed by the C-terminus of Bax, which resides in the hydrophobic pocket in the inactive form, is released [350]. This exposes the previously blocked BH3 domain and the transmembrane domain of α9, allowing activation by BH3-only proteins, insertion into the OMM, and Bax homo-oligomerisation and pore formation (Figure 1.16). In Bak, the α9 helix is missing, and the hydrophobic groove is narrower and blocked by surrounding side-chains [354]. Upon activation, it is predicted that Bak undergoes a conformational change which exposes the hydrophobic groove; however structures of the

activated or oligomerised forms of Bax or Bak have not been elucidated to date, so our understanding of the conformational changes are limited.

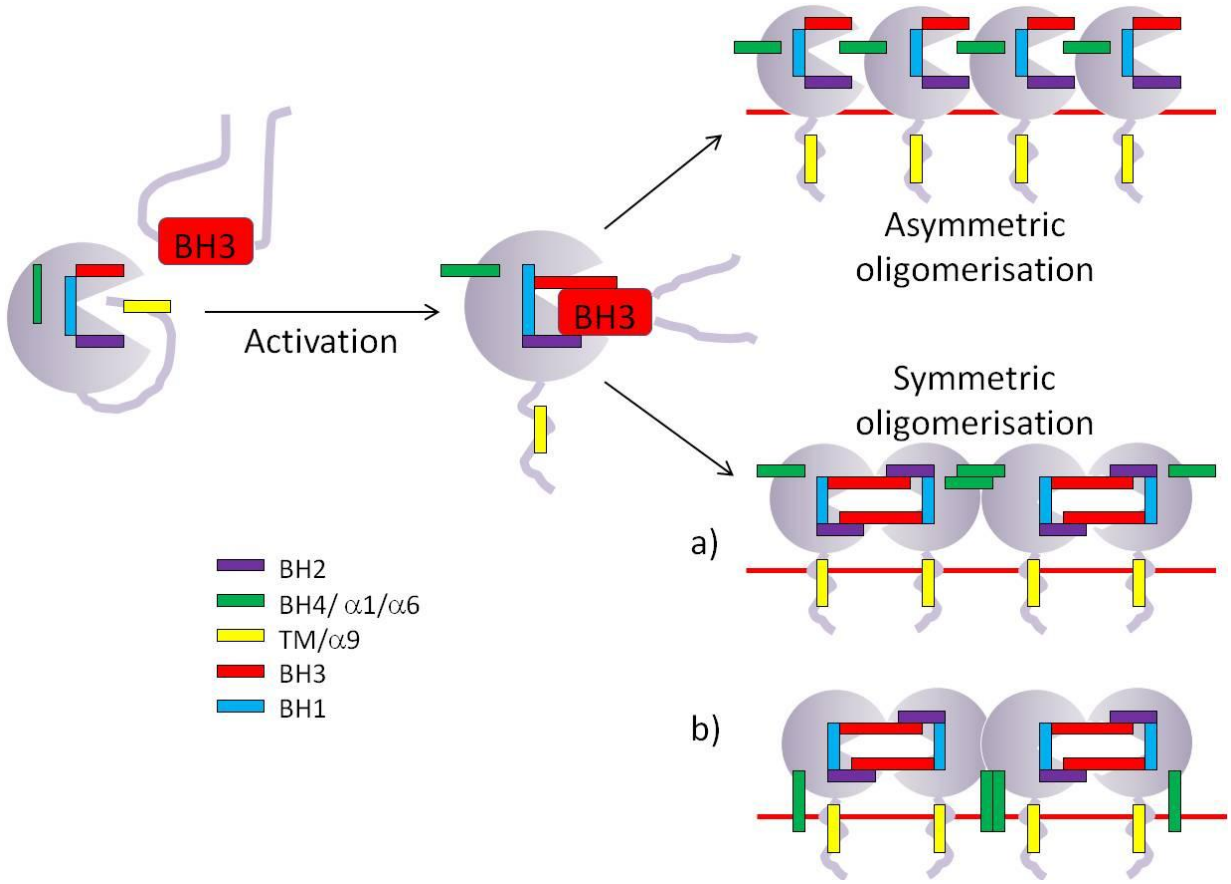

Figure 1.16: Bax activation involves a conformational change and insertion into the outer mitochondrial membrane (OMM).
Activation by BH3-only proteins causes a conformational change in Bax which results in the removal of the C-terminal α9 helix from the hydrophobic groove, the exposure of the BH3 domain and the exposure of the N-terminal α1/α6 helices. Activated Bax inserts into the OMM and forms homo-oligomers. This was originally thought to happen asymmetrically, but current evidence suggests it is in fact a symmetrical oligomerisation around the BH3:hydrophobic groove and the α6 helix on the backbone. There is debate whether the α6 interaction occurs on the cytoplasmic face of Bax (a) or whether the helices are inserted into the membrane where they interact (b).

There is evidence that the BH3-only proteins are not solely responsible for the activation of Bax, but that interaction with lipids is also necessary to bring about the loosening of the soluble structure to prime the protein for activation [355]. Changes in pH, addition of detergents and mild heat shock have also been observed to cause a conformational change in Bax, but not insertion into membranes [356,357]. The BH3-only proteins can displace the loosened α9 helix from the hydrophobic pocket, and Bax can insert into the OMM. However, there is debate about where in Bax/Bak the BH3-only proteins interact, be it the hydrophobic pocket or the backbone pocket formed by α1, on the N-terminus, and α6 [270,350,358]. This debate is difficult to resolve due to the seemingly transient nature of the

effector:BH3-only interaction. This has been termed 'hit and run' activation and would explain why Bax bound to BH3-only proteins is not observed during late stage apoptosis. This transient nature may be explained by the loss of affinity of the effector proteins for the BH3-only proteins once the effector proteins are in their active conformation.

After insertion into the OMM, Bax either homo-oligomerises with itself to form pores, or it interacts with pro-survival molecules also present in the OMM. These interactions are again poorly understood, with early evidence suggesting that Bax forms asymmetric homo-oligomers in a 'daisy-chain' structure [359]. However, more recent evidence seems to suggest that both Bak and Bax form symmetrical homo-oligomers around the BH3 domain and the hydrophobic pocket, which then go on to form higher order oligomers through interactions between the α6 helices on the backbone of the molecule [360,361]. The formation of pores is also poorly understood. Initial theories speculated that Bax targeted the 'permeability transition' pore, a pore that already exists in the OMM, to cause the swelling and bursting of the mitochondria [362]. However, genetic studies have apparently disproved this model [363]. It is currently believed that the effector proteins mimic bacterial toxins in forming pores which are wide enough for apoptosis proteins such as cytochrome c to escape through. This is based on structural studies which show similarities between the helical fold of the Bcl-2 proteins and pore forming domains of diphtheria toxin and colicins [311]. In support of this, a pore termed the mitochondrial apoptosis-induced channel (MAC) made up of Bax oligomers was elucidated from mitochondria by patch clamp analysis, and either Bax or Bak were required for this pore to form [364].

The pro-survival molecules can prevent homo-oligomerisation through interactions between the effector proteins hydrophobic pockets and their own BH3 domains [315,365]. These interactions are also transient, but due to the concentration and orientation of the proteins caused by their anchorage in the membrane, the interactions continually break apart and reform. Hence, high expression levels of pro-survival proteins can block apoptosis at this final step. There is also evidence supporting a theory that the effector and pro-survival proteins do not just sit in the OMM, but are continually translocating back to the cytosol, and that this event is accelerated by the interaction of these proteins in the OMM [366].

1.5.3.2 The Effector proteins in Melanoma

The roles of the effector proteins within melanoma have not been studied to the extent of the pro-survival or BH3-only proteins. However there does appear to be a correlation

between lower levels of Bax/Bak and increased melanoma progression [367]. There is no evidence that these proteins are specifically downregulated in melanoma, but the downregulation of the BH3-only proteins and upregulation of the pro-survival proteins may determine the levels of activated effector proteins present. One of the pro-survival proteins observed to be upregulated in metastatic melanoma is Bfl-1 [368].

1.6 The Pro-Survival Molecule Bfl-1

The pro-survival murine protein A1, or the homologous human protein Bfl-1, or Bcl2A1, is one of the lesser understood members of the Bcl-2 family. The gene was originally discovered through data bank searches for expressed sequence tags [369] and identical cDNA was later found after induction with TNF [370]. Bfl-1 belongs to the pro-survival group of the Bcl-2 family through its structure and function and is often compared within that group to Mcl-1. As such, Bfl-1 is thought to employ similar means to repress apoptosis as Mcl-1 [371,372], as they appear to have similar binding profiles (Figure 1.12), but the sequence of the two proteins is different and as they have become more understood, they are increasingly represented as unique proteins.

Bfl-1 is attracting attention as a potential drug target as it has been observed to be highly expressed in a small selection of infamously chemo resistant malignancies, such as B-cell chronic lymphocytic leukemia [373], large B-cell lymphomas [374] and acute myeloid leukemia [375], whereas the other pro-survival proteins are more broadly overexpressed in a wider range of cancers.

1.6.1 The Role of Bfl-1 in Healthy Tissues

Bfl-1 appears to play an important role in the protection of cells from apoptosis in a number of environments, including inflammation, allergic reactions and malignancies. As such, high levels of Bfl-1 expression invariably correlate with an ability to evade apoptosis and an intrinsic resistance to chemotherapeutic agents [59].

The first cDNA clones of A1 were identified from mouse bone marrow as a granulocyte macrophage-colony stimulating factor-inducible Bcl-2 related gene [376] and were later cloned in fetal liver [369], activated endothelial cells after cytokine treatment [370], and myeloid leukaemia [377]. There is some confliction in the literature as to the expression pattern of Bfl-1, possibly through a difference in murine and human expression patterns. However, Bfl-1 has been shown to have preferential expression in haematopoietic, myeloid and endothelial

cells and Bfl-1 mRNA has been seen in bone marrow, lymphoid organs, peripheral blood leukocytes and in the lung [370, 369].

Physiologically, Bfl-1 appears to play an important role in the immune system. In mice, activation of the IgE receptor has been shown to upregulate Bfl-1 expression in mast cells after allergens challenge [378], suggesting that Bfl-1 has an important role in the survival of mast cells during an allergic reaction. This proposal has been supported by the fact that Bfl-1 null mice have less mast cells after an allergic reaction compared with normal mice [379]. Bfl-1 is the only known Bcl-2 pro-survival protein to be induced by inflammatory cytokines, such as TNFα and IL-1β, to give protection to cells in an inflammatory environment [379, 370]. Additionally, the level of Bfl-1 protein in long-lived mature B-cells was found to be ten times the expression in immature B-cells, suggesting a role for Bfl-1 in maintaining the long life of mature B-cells [380]. T-cells also express Bfl-1 in a developmentally regulated manner [381], and Bfl-1 is induced during macrophage and lymphocyte activation [376,382] and in human coronary artery smooth muscle cells under high glucose conditions [383]. Bfl-1 has also been observed to bind beclin-1, and was hence seen to play a role in the inhibition of autophagy in mycobacterium infected macrophages [384].

1.6.2 The Role of Bfl-1 in Cancer

Bfl-1 over-expression has also been shown to be a key factor in certain malignancies. Bfl-1 was observed to be essential for the survival of malignant B-cells [385]. It has also been seen to be overexpressed in acute lymphoblastic and chronic lymphocytic leukemia (CLL) [386], mantle cell lymphoma [386], and large B-cell lymphoma [387]. Indeed, high Bfl-1 expression was seen to correlate with the more severe cases of CLL [373]. It has also been seen to protect against growth factor withdrawal-induced apoptosis in myeloid precursor cells, and surprisingly to allow differentiation of these cells, whereas Bcl-2 had an anti-proliferative function [388]. Bfl-1 is also seen overexpressed in solid tumours, such as stomach cancer [369], breast cancer [389], and metastatic melanoma [368]. It also appears to regulate hypoxia-induced apoptosis and oxidant-induced necrosis of epithelial cells in culture [390], presenting an opportunity for drug studies targeting Bfl-1 in hyperoxic acute lung injury (HALI) in addition to haematological malignancies and solid tumours. However, the limitation of these studies is that most look at mRNA expression levels rather than the protein expression levels, probably because of the lack of high quality commercially available antibodies for the protein.

There appears to be a possible tumourigenic role for Bfl-1 in cancer, as several of these studies have observed higher Bfl-1 expression levels in later stage cancers. As such, although overexpression of Bfl-1 alone was not tumorigenic in mice [391], Bfl-1 overexpression led to increased E1A-induced transformation [392], and enhanced *myc*-induced leukemogenesis [393]. It has also been suggested that Bfl-1 contributes to the transformation of pre-T-cells when T-cell receptor signalling is deregulated [394] and that, along with CEBP, Bfl-1 is essential for anaplastic lymphoma kinase (ALK)-driven transformation to anaplastic large cell lymphoma [387].

Importantly, Bfl-1 has been linked to chemo-resistance in a number of malignancies, as mentioned above. In cell-lines, Bfl-1 overexpression protected cells from treatment with cisplatin [395], etoposide [59], and staurosporin (STS) [396]. Fortunately, knocking down Bfl-1 expression re-sensitised malignant B-cells to chemotherapy [385]. In the clinic, Bfl-1 overexpression has also been noted to correlate with chemoresistance, for example in CLL and breast cancers [397]. It is because of its ability to protect cancer cells from chemotherapy induced apoptosis that makes it, or the molecules that regulate it, interesting new drug targets.

1.6.3 The Regulation of Bfl-1

Bfl-1 has been shown to be up-regulated in response to a range of apoptotic stimuli through the NFκB pathway [59,235,398,399]. It has been determined to be a direct transcriptional target of NFκB with an NFκB binding site in the promoter region of the gene, which is also found in the Bcl-x promoter [400]. In addition to NFκB, other transcription factors have been implicated in the transcriptional regulation of Bfl-1. These include all-trans retinoic acids in leukemia cells [401], retinoic X receptor agonists in naïve T lymphocytes [402], and the transcription factors WT-1 [403] and PU.1 [404]. On the other hand, Bfl-1 transcription has also been observed to be blocked by the transcription factor Blimp-1 in plasma cells [405].

Post-translational modification of Bfl-1 has also been observed to regulate the activity of the protein. Although no E3-ligase has yet been identified for the protein, Bfl-1 was shown in pro-B cells to have two modes of post-translational regulation that controlled its pro-death activities; protein turnover by ubiquitin/proteasome degradation and cleavage by μ-calpain or a calpain-like activity induced by TNF receptor activation, the latter of which apparently changed the Bfl-1 protein into a pro-death factor [406]. The polyubiquitination and proteasomal turnover of Bfl-1 have been shown to be mediated by the C-terminus of the

protein [407] and this post-translational control results in a short half-life for the protein. The control of the proteasomal regulation of Bfl-1 by pro- or anti-apoptotic stimuli has not yet been investigated, but insights into its binding partners are emerging.

1.6.4 The Binding Profile of Bfl-1

As a pro-survival molecule, Bfl-1's expected mode of action is through binding the effector proteins Bax and Bak, thereby blocking apoptosis. However there are conflicting reports as to Bfl-1's association with Bax and Bak. Bfl-1 has been shown to interact with both Bax and Bak in yeast two-hybrid assays [408,409]. Both the murine and human proteins have been seen to bind Bak but not Bax [371,410]. But, conversely, others report no interaction between Bfl-1 and either of the effector proteins [269,411]. The conclusion from these results would suggest that Bfl-1 binds preferentially with Bak rather than Bax, and the experimental variation may be explained by the different techniques, expression systems and assay sensitivities used.

Bfl-1 has also been determined to bind to a selection of BH3-only proteins, previously touched upon in section 1.5. The literature shows that Bfl-1 associates with tBid, Bim and Puma, with suggestions that it may also bind other BH3-only proteins. Werner et al. (2002) [411] found that Bfl-1 directly associated with both Bid and tBid via the Bid BH3 domain. Although Bfl-1 had no inhibitory affect on full length Bid, the complex Bfl-1 formed with tBid was strong enough to block apoptosis as tBid could not interact with Bax or Bak despite retaining the ability to translocate to the mitochondria. However Simmons et al. (2008) [371] found that while Bfl-1 interacts with tBid it had no interaction with Bid in living cells and the interaction with tBid was not strong enough to block apoptosis regulated by tBid. As mentioned previously, there is some debate as to whether Bfl-1 binds Noxa. BH3-profiling suggests that Bfl-1 binds Bim, Bid and Puma, but has no interaction with Noxa whereas other studies have seen Bfl-1 bound to Noxa [260,262,412]. Hence, in regards to BH3-only protein interactions, Bfl-1 is grouped with Mcl-1 within the pro-survival proteins. It is anticipated that the binding profile of Bfl-1 will be more conclusively elucidated as more detailed structures of the protein are uncovered.

1.6.5 The Structure of Bfl-1

Bfl-1 is a small protein of 175 amino acids, transcribed from the gene located on chromosome 15 at position q24.3 [413]. The BH1 and BH2 domains are conserved with the other pro-survival family members, with a less conserved BH3 domain, and a very limited

homology in the BH4 domain [414]. Bfl-1 contains nine α-helices which fold up to create a hydrophobic pocket similar to the one found in Bcl-xL where Bak binds [415]. This was observed through crystal structures of the protein bound to BH3 peptides [414] (Figure 1.17), which is the only way the protein can be visualised as Bfl-1 displays conformational plasticity which probably allows it to bind to a range of ligands with different sequences in the BH3 domain [416].

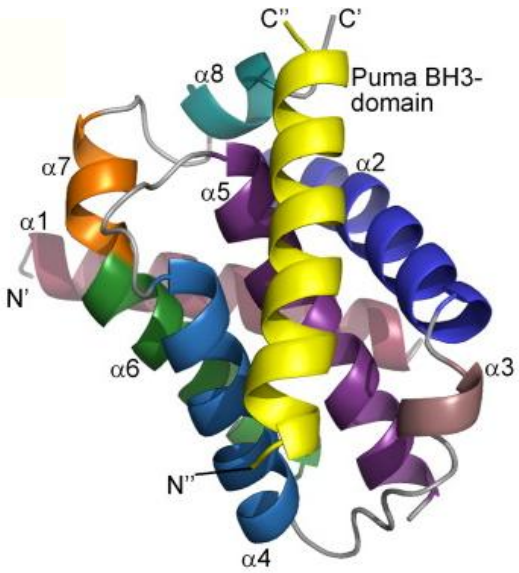

Figure 1.17: The structure of Bfl-1 in complex with Puma.
To elucidate this structure, the author's used a truncated form of Bfl-1, lacking the 20 amino acids of the C-terminal α9 helix, and mutated hydrophobic residues expected to be solvent exposed to hydrophilic residues (P104K, C113S). These mutations were far away from the BH3 binding site. The Puma BH3 domain (yellow) is shown bound to the BH3 binding domain of Bfl-1, which involves the helixes α2-5 [416].

Most pro-survival Bcl-2 proteins contain a transmembrane domain at their C-terminus which gives localisation to the OMM (Figure 1.14); however, Bfl-1 does not contain a well-defined transmembrane domain. Even so, the C-terminus of Bfl-1 has been shown by Brien et al. (2009) to be important in determining the function and localisation of the protein [417]. This research theorised that, similar to Bax, the C-terminal α9 helix of Bfl-1 can exist within the hydrophobic groove, or exposed from the globular core, where it acts as an anchor to the mitochondria and regulates the pro-survival function of the protein (Figure 1.18). Bfl-1 also lacks the N-terminal loop of charged amino acids, a region sensitive to proteases, present in most other pro-survival proteins [418]. The lack of this N-terminus appears to increase the anti-apoptotic activity and may lengthen the biological half life of the protein; when the N-terminus loops of Bcl-2 and Bcl-xL were deleted, the anti-apoptotic activity was much higher than that of the wild type proteins [419].

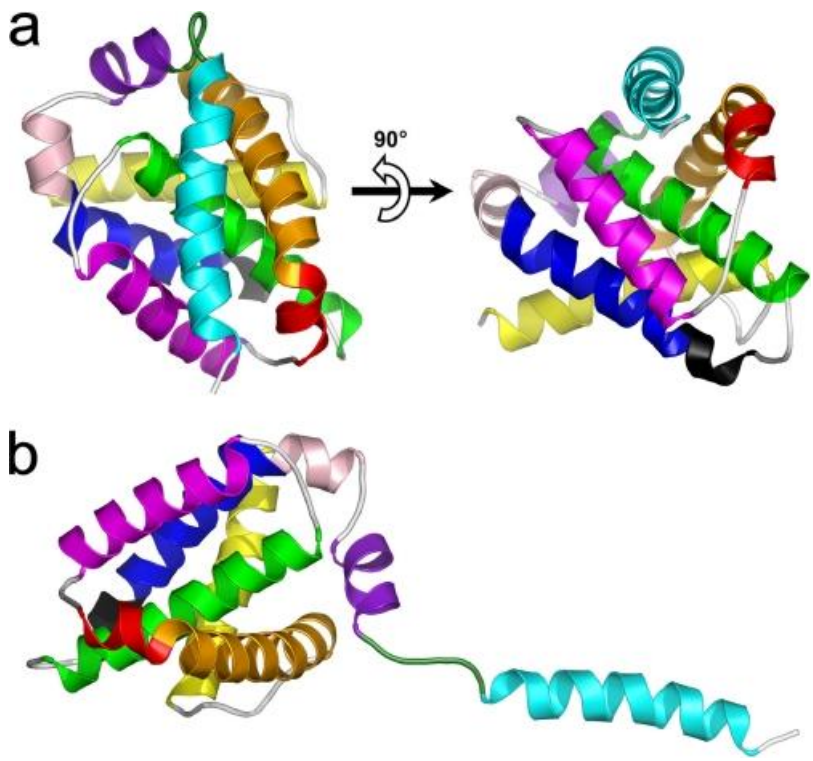

Figure 1.18: Results from the molecular modelling of full length Bfl-1 based on the crystal structure of Bfl-1 in complex with the Bim BH3 domain.
The authors suggest that Bfl-1 exists in two conformations, one with the C-terminus helix α9 (turquoise) inserted into the hydrophobic BH3 groove of Bfl-1 (a), the other with the C-terminus tail free for insertion into membranes (b). This model of full length Bfl-1 also demonstrated the amphipathic nature of the C-terminal helix which is often observed in transmembrane domains and membrane anchors. The authors therefore assessed the localisation of Bfl-1 and found that when the C-terminus helix α9 was removed, radioactive tagged Bfl-1 lost association with the mitochondria in PBLs. Figure taken from Brien et al. 2009 [417].

One copy of the Bfl-1 gene has been found in humans [413], with four A1 copies in mice [413,420], A1-a, A1-b, A1-c and A1-d. The mouse versions are coded from chromosome 9 and contain 2 exons. A1-a, A1-b and A1-d are nearly identical, but A1-c contains a point mutation which results in a truncated protein [420]. The multitude of A1 isoforms in the mouse provides a significant challenge in the creation of a knock-out mouse. An A1-a knockout mouse presented 50% less mast cells after allergic stimuli [379], and enhanced apoptosis in peripheral blood neutrophils [324]. Alternately, a conditional transgene-driven shRNA was used which knock-downed A1-a, A1-b and A1-d, although with different efficiencies in different cell types, being much more successful in thymocytes than mature lymphocytes and resulting in no obvious phenotype [421]. The mouse and human proteins contain 72% homology, and although the BH4 domain is present in Bfl-1 but completely lacking in the murine A1 protein, the proteins display very similar structures [414,416]. A splice variant of human Bfl-1 has also been distinguished called Bfl-1 Short (Bfl-1S).

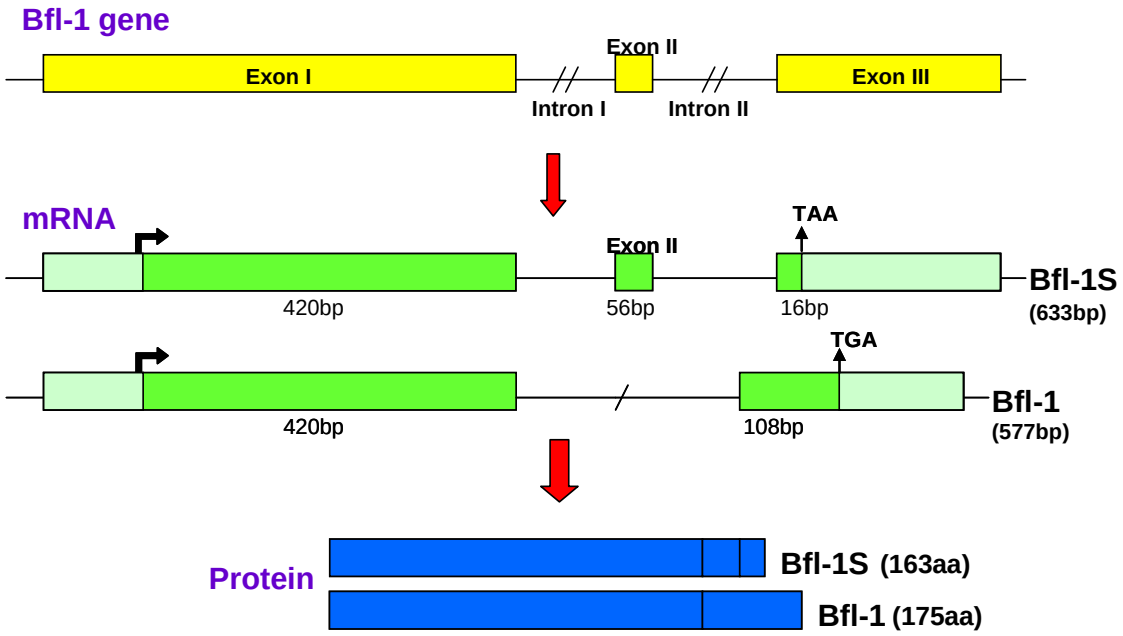

Figure 1.19: Alternate splice variants for the Bfl-1 gene.
Two isoforms exist for Bfl-1 which result from alternate splicing during transcription. The shorter isoform results from the inclusion of exon 2 near the 3' end in the mRNA. This 56 base pair insert creates a frame shift which brings the stop codon forward by 72 base pairs to produce a shorter protein with an open reading frame (ORF) of 163 amino acids. Exon 2 is excluded from the longer isoform to result in an ORF of 175 amino acids.

1.6.6 Bfl-1S

Bfl-1S, although recognised to exist in many papers, has only been explored in detail in one study, so there is limited information on its role in either healthy or cancerous cells. It contains the four BH domains but lacks 12 amino acids in the positively charged C-terminus which results in Bfl-1S being localised to the nucleus [422]. Bfl-1S was found predominantly in the lymph nodes and B-lymphoid leukaemia cells when tagged with GFP. This research also found that Bfl-1S could act in a dominant negative manner on pro-apoptotic Bax when they were coexpressed and that the expression of Bfl-1S gave protection to cells following treatment with the apoptosis inducer, staurosporine (STS), possibly by sequestering Bid at the nucleus region and inhibiting its cleavage.

The two isoforms arise from alternate splicing during transcription (Figure 1.19). The mRNA coding for the shorter isoform contains an additional 56 base pair (bp) exon (exon II) which is lacking from the mRNA of the full-length isoform. The inclusion of exon II creates a frame shift which brings the stop codon forward by 72bp resulting in early translational termination to code for a protein with an open reading frame (ORF) of 163 amino acids. When exon II is not included in the mRNA, the ORF codes for the full-length, 175 amino acid, protein. This splicing has been observed in other genes, such as

caspase 2, which has two isoforms which result from a frame shift following the inclusion or exclusion of an exon during transcription [423].

1.6.7 The Localisation of Bfl-1

Reports as to the intracellular localisation of Bfl-1 vary, with some finding it localised to the mitochondria despite the charged amino acids in it C-terminus [424], while others find it in the nucleus of apoptotic cells and the cytoplasm of resting cells [425]. One study by Yang et al. (2005) added green fluorescent protein (GFP) to Bfl-1 to discover the intracellular localisation and instead found that fusion with GFP at either the C- or N-terminus converted Bfl-1 into a potent pro-apoptotic protein and induced cell death [426]. However this discovery has not been confirmed by other research groups such as Fan et al. [427] and Simmons et al. [371], who have used GFP to tag Bfl-1, as commercial antibodies which recognise the protein have only become available in recent years.

1.6.8 Bfl-1 as a Target for Therapeutic Agents

The anti-apoptotic effects of the pro-survival proteins have been targeted using BH3-mimetics, such as ABT737 and Navitoclax. However, these target a range of pro-survival proteins whereas more specific inhibitors may cause less toxic side-effects. A few screens for possible Bfl-1 inhibitors have been carried out resulting in the unearthing of gambogic acid and *N*-aryl maleimides as potential inhibitors [428,429]. Unfortunately, gambogic acid also caused cell death in cells with deficiencies in the effector proteins, causing serious side-effects, and the *N*-aryl maleimides have yet to be explored in a biological setting. Also emerging as potential candidates for the role are apogossypol derivatives and peptide aptamers [430,431]. Another mechanism to downregulate Bfl-1 expression is to target the NFκB pathway, although this has the potential for plenty of off-target side effects. It has been reported that in human melanoma cells, using proteasome inhibitors can increase the effects of radiotherapy via suppression of the NFκB pathway [432], and steroids like guggulsterone that suppress NFκB activation can also suppress the upregulation of Bfl-1 [433]. However, drugs designed specifically for Bfl-1 will not emerge until the protein is better understood, and its importance in cancer has been more widely demonstrated. This thesis aims to determine the importance of Bfl-1 in metastatic melanoma, and its potential as a drug target in this infamously chemo-resistant form of cancer.

1.6.9 The Expression Profile of Bfl-1 in the NCI60 Microarray

A panel of 60 cell-lines derived from human cancers has been used by the National Cancer Institute (NCI) to screen over 100,000 possible anti-cancer drugs since 1990. These cell-lines have been examined by microarray analysis for gene expression patterns to give an NCI60 array [437], which has been used to examine mRNA and protein expression, chromosomal aberrations, DNA copy number and mutational status, with all this data made available as a public resource (http://biogps.gnf.org/). In fact a selection of ninety three cell-lines derived from twenty two different cancer types are now present in the array [438]. The expression of a gene can be linked to the phenotype of a cell when a large database such as this is created and hence, by looking at the expression patterns in the array, the cell-specificity of a novel gene can be inferred. The NCI60 array is used not only to determine expression levels of genes, but also to test chemical compounds for cytotoxicity across the cell-lines. Hence, relationships between expression levels and chemo resistance can be observed. An in depth exploration of the NCI60 determined that expression levels of Bcl-x showed a positive correlation with resistance to chemotherapy agents, independent of p53 status [439]. The same study observed that Bax and Bcl-2 conversely showed no correlation with drug sensitivity.

Although cell-lines derived from human cancers differ from normal and cancerous tissue, they are much more accessible than the primary materials. As such, they have been used extensively as experimental models of cancer. In general, the expression patterns of the different cell-lines seen in the National Cancer Institute's NCI60 microarray are relatively consistent with the primary tissue type when the clustering is based on mRNA expression patterns [437,438].

The NCI60 uses the Affymetrix Human Genome U133A Array (Affymetrix, USA), which contains 14,500 well characterised human genes. Fluorescent labelled cDNA is obtained from the test cell mRNA which is labelled with the fluorophore Cy5-dUTP. mRNA from a reference pool of mRNA from 12 cell-lines is then labelled with Cy3-dUTP. The labelled test cDNA is hybridised to the probe on the chip and arrays are scanned using a GeneChip Scanner 3000 measuring both channels of fluorescence. The comparison of the test mRNA to the reference allows a quantitative analysis of the gene expression across the cell-lines from the variation in the normalised Cy5/Cy3 ratio [437].

In an analysis of the NCI60 microarray, it could be observed that the pattern for Bcl-2 mRNA expression was extremely broad across all the cell-lines (Figure 1.20); however the other Bcl-2 family members showed more variation. There was no obvious correlation between Mcl-1, Bcl-w and Bcl-xl expression and cancer type and these genes were expressed in all the cell-lines tested. However, by interrogating the NCI60 array, it was observed that the mRNA expression profile for Bfl-1 with the 205681_at probe, unique for Bfl-1, showed that this pro-survival gene was highly and selectively expressed in melanoma cell-lines (Figure 1.21). As such, Bfl-1 was seen to be expressed over the threshold level in seven out of eight melanoma cell-lines tested (LOX IMVI, M14, MALME 3M, SkMel2 (low levels of Bfl-1), SkMel28, SkMel5, UACC257 and UACC62), and two lymphoma cell-lines (RS11846 and A361), but was not found to be present in most other cell-lines tested and when it was present, it was at a very low level (A549 (lung), HL60 and SR (B-cell leukemias), HT1080 (Colon), T24 (bladder)).

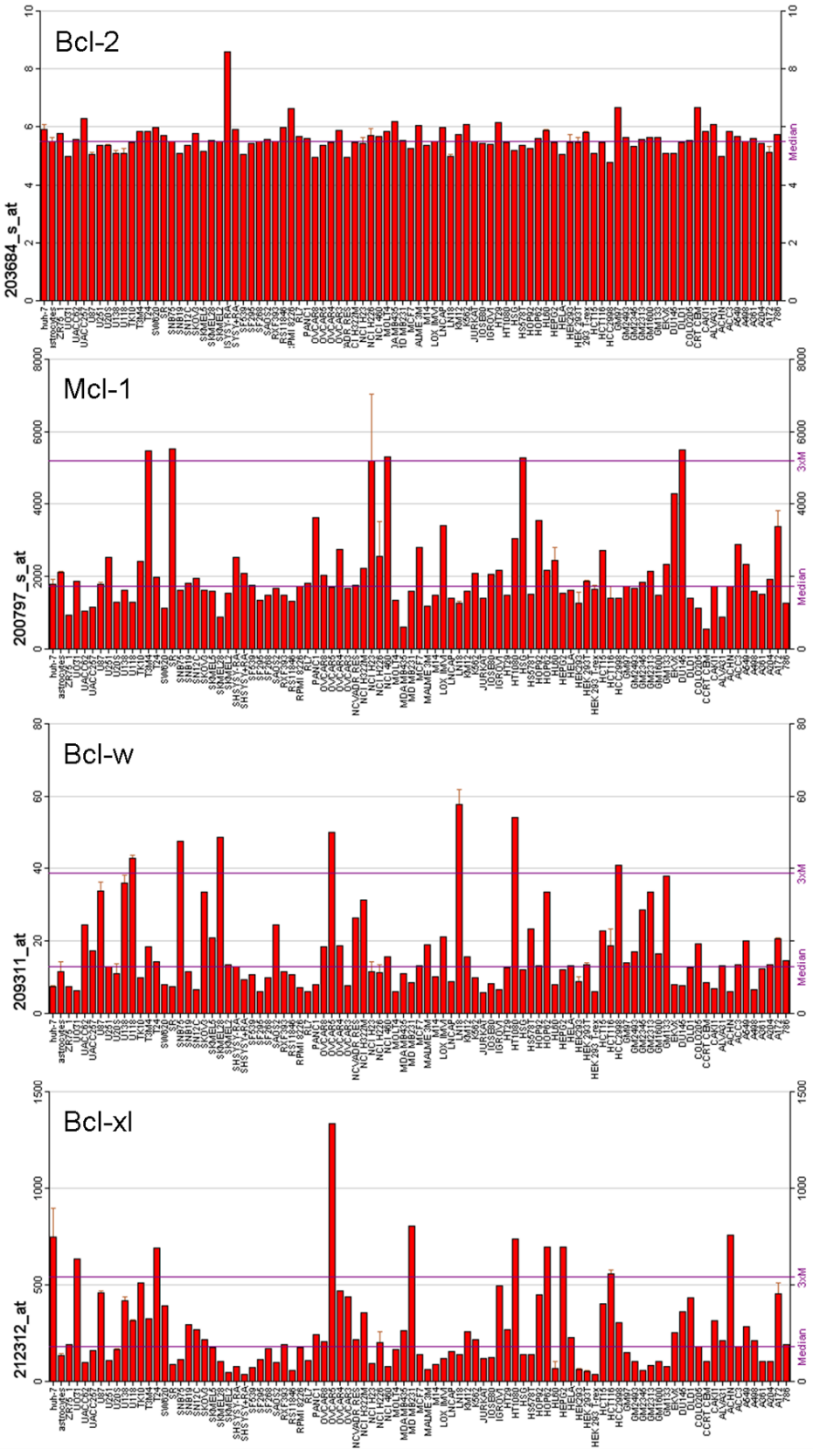

Figure 1.20: Microarray analysis of the expression of the pro-survival members of the Bcl-2 family in a selection of cell-lines based on the National Cancer Institute's panel of 60 cell-lines.

Total RNA was extracted from untreated cells and converted to cDNA. This cDNA was then labelled with a fluorophore during amplification by PCR. The fluorescent labelled cDNA hybridises to a probe on a GeneChip which recognises a specific gene. Arrays are scanned using a GeneChip Scanner 3000 and quantitatively analysed for expression of mRNA. (http://biogps.gnf.org/).

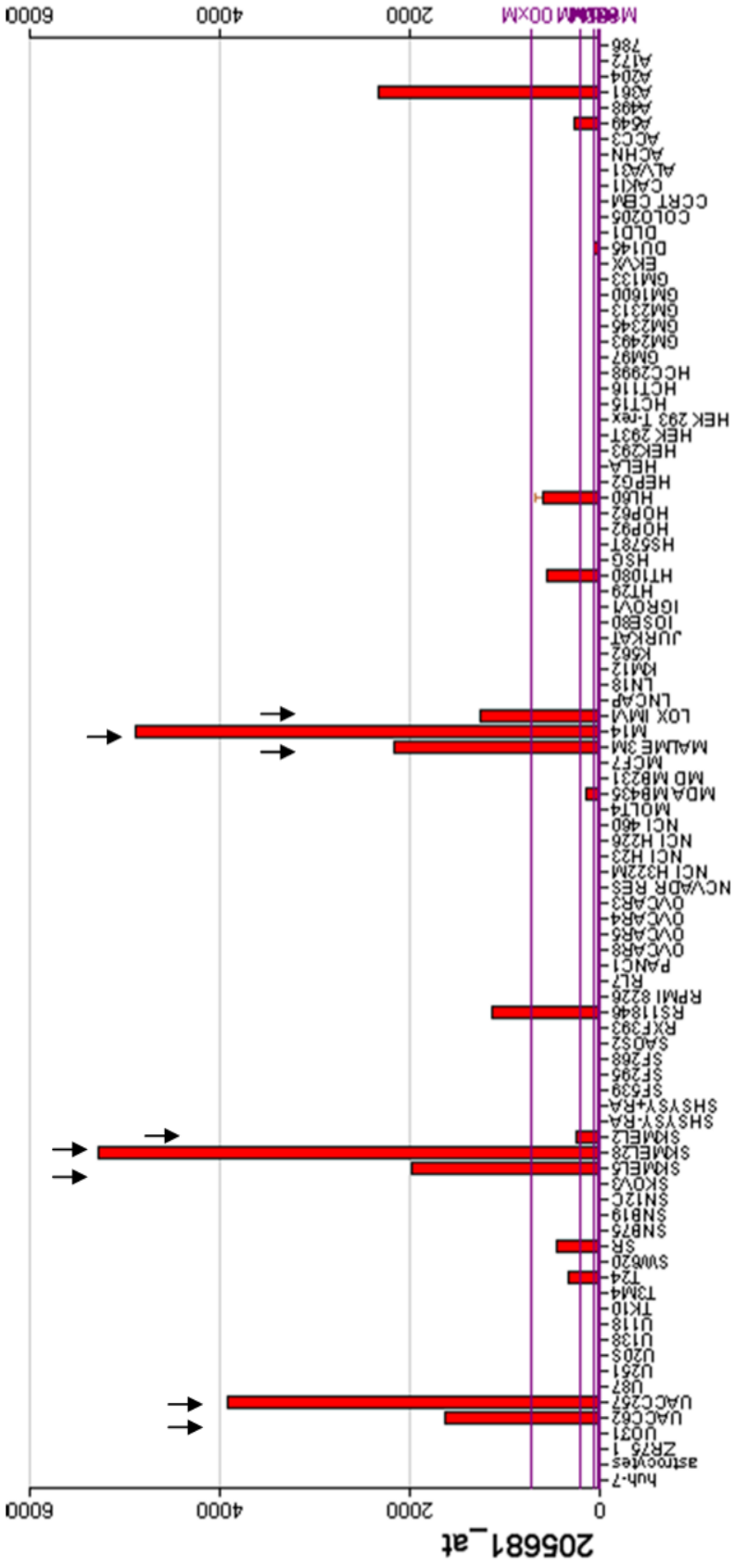

Figure 1.21: Microarray analysis of the pro-survival molecule Bfl-1 in a selection of cell-lines based on the National Cancer Institute's panel of 60 cell-lines.
RNA was extracted from untreated cells and converted to cDNA. This cDNA was then labelled with a fluorophore. The fluorescent labelled cDNA hybridises to a probe on a GeneChip which recognises a specific gene. Arrays are scanned using a GeneChip Scanner 3000 and quantitatively analysed for expression of mRNA. Melanoma cell-lines are indicated by the black arrows. (http://biogps.gnf.org/).

1.7 Hypothesis

The hypothesis to be explored in this thesis is that the pro-survival molecule Bfl-1, which the NCI60 microarray suggests is highly and specifically expressed in melanoma cells, is the cause of the high levels of intrinsic chemo resistance displayed in metastatic melanoma. Therefore, down-regulation of Bfl-1 should increase the effects of the existing chemotherapeutic agents and hence, Bfl-1 is a viable drug target in metastatic melanoma.

1.8 Aims and Objectives

This thesis aims to prove for the first time that Bfl-1 is over-expressed in melanoma and that melanoma cells rely on its expression to resist apoptosis caused by chemotherapeutic agents. It aims to characterise the protein in melanoma by exploring the pathways through which Bfl-1 is regulated, the half lives of the protein and mRNA, the degradation of the protein and the subcellular localisation of the protein. Furthermore, to discover the effects of down regulating Bfl-1 in melanoma cells in terms of their response to chemotherapeutic agents.

2: MATERIALS AND METHODS

2.1 Materials

All chemicals used were of molecular grade and obtained from Sigma-Aldrich (St. Louis, USA) unless otherwise stated.

2.2 Tissue Culture

MM200, SkMel28 (supplied by P. Hersey, University of Newcastle, Newcastle, New South Wales, Australia), SkMel31, Colo205 (ATCC, Manassas, USA), A375, UACC62, G361 (supplied by J. Blaydes, University of Southampton, Southampton, UK) cell-lines were cultured in Dulbecco's Modified Eagle Medium (DMEM) (Invitrogen, Paisley, UK) supplemented with 10% heat inactivated Foetal Calf Serum (FCS) (Lonza, Wokingham, UK), 100μg/ml penicillin and streptomycin (Invitrogen), 1mM pyruvate (Invitrogen) and 2mM L-Glutamine (Invitrogen). Ramos, Raji (ECACC, Sigma-Aldrich, St. Louis, USA), K562 (supplied by K. Shimada, Nagaya University, Nagaya, Japan) and PC3 (ATCC) cell-lines were cultured in RPMI medium (Invitrogen) with the same supplements as above. Transfected A375 cell-lines were cultured in DMEM with supplements as above plus geneticin at 1mg/ml (GIBCO, Invitrogen). Primary melanocytes (Lonza) were maintained in Melanocyte Growth Medium-4 (MGM-4) containing growth factors, cytokines and supplements (recombinant human (rh) fibroblast growth factor-B, calcium chloride, bovine pituitary extract, phorbol 12-myristate 13-acetate (PMA), rh-insulin, GA-1000 (gentamicin sulphate amphotericin-B), Hydrocortisone, Endothelin 3 and FCS) (Lonza). Adherent cells were passaged using trypsin/ethylenediaminetetraacetic acid (EDTA) solution (Invitrogen). To split primary melanocytes, trypsin/EDTA was diluted 1:1 in EDTA/versene (Lonza) solution before trypsin neutralising solution (Lonza) was added at a 1:1 dilution after detachment. All cell-lines were maintained in a 37ºC 5% CO_2 humidified incubator in tissue culture flasks (Fischer, Loughborough, UK).

2.3 Cell Quantification

Concentrations of cells were determined using a Coulter Particle Counter Z1 according to the manufacturers' instructions (Coulter Electronics, Luton, UK).

2.4 Molecular Biology

2.4.1 Plasmid Analysis by Restriction Digestion

Restriction digests were performed to identify if the correct insert was present in the plasmid vector. Approximately 30μg of plasmid DNA, 1μl of each restriction digest

enzyme (10u/µl) (Promega, Southampton, UK) and 2µl 10X buffer (Promega) (Buffer used depended on which enzymes were used) in a final volume of 20µl were incubated in a waterbath at 37ºC for 1 hour. Subsequently, DNA was separated by gel electrophoresis.

2.4.2 DNA gel electrophoresis

Gel electrophoresis was used to analyse DNA by separating it based on size. 6X Orange loading dye (10 mM Tris-HCl (pH 7.6), 0.15% orange G, 0.03% xylene cyanol FF, 60% glycerol, 60 mM EDTA) (Fermentas, York, UK) was added to the samples, which were routinely run on a 0.7% agarose gel (0.7g agarose, 100ml Tris-acetate-EDTA (TAE) buffer, 5µl GelRed (Biotium, Cambridge, UK)) run at 160mA (7V/cm) for 45 minutes using 10µl of O'GeneRulerTM 1kb or 100bp DNA Ladders (0.1µg/µl) (Fermentas, York, UK) as references for DNA size. The DNA was visualised under UV light and if required the band of interest was extracted using a QIAX II gel extraction kit (Qiagen).

2.4.3 DNA extraction

For use in downstream techniques, DNA was extracted from agarose gels and purified using a QIAX II gel extraction kit according to the manufacturers' instructions. Accordingly, the band excised from the gel was heated for 10 minutes at 50˚C in QX1 buffer and 10µl Qiax II resin to dissolve the gel. The resin contains silica-gel particles which bind nucleic acids in the presence of chaotropic salt, which is contained in the QX1 buffer. The beads were washed once with QX1 buffer to remove any remaining agarose, and twice with PE buffer (containing ethanol) to remove salt contaminates. DNA was eluted from the beads in TE buffer (10mM Tris, pH 7.5, and 1mM EDTA) at 50˚C for 5 minutes and stored at -20˚C.

2.4.4 DNA Ligation

Ligation was performed to anneal two pieces of DNA, for example of a PCR fragment into an empty vector.

2.4.4.1 TOPO Vector Ligation

The TOPO vector has been developed to easily ligate with DNA fragments and therefore was routinely used to clone and sequence DNA inserts. DNA of interest was ligated into zero blunt TOPO vector using the TOPO TA cloning kit (Invitrogen). No additional ligase is required for this ligation as TOPO is linearised with topoisomerase I covalently bound

and single thymidine overhangs. 1µl TOPO vector, 1µl salt solution (1.2M NaCl, 0.06M $MgCl_2$) and 8µg of the DNA of interest (e.g. PCR product extracted from a DNA gel) in a final volume of 6µl were incubated for 15 minutes at room temperature.

2.4.4.2 Expression Vector Ligation

DNA sequences were sub-cloned and ligated into an expression vector which was typically used to transfect cells for expression of the protein coded for by the insert DNA. To ligate the DNA of interest into an expression vector, 3µl 10X ligation buffer (300mM Tris-HCl (pH 7.8 at 25˚C), 100mM $MgCl_2$, 100mM DTT, 10mM ATP) (Promega), 3µl T4 ligase (Promega), approximately 30µg insert DNA and 1µg/µl (8µl) vector in a final volume of 20µl were incubated overnight at 4ºC.

2.4.5 Transformation of plasmid DNA into Bacteria

Plasmid DNA obtained from the ligation of insert DNA into a vector was transformed into bacteria in order to amplify it and remove un-ligated DNA. Plasmid DNA was transformed into TOP10 E.coli or JM109 E.coli (Invitrogen).

2.4.5.1 TOP10 Bacteria

DNA ligated into the TOPO vector (described in section 2.3.4.1) was transformed into TOP10 E.coli (Invitrogen). The ligation mixture was added to a stock vial of TOP10 (60µl from Invitrogen stock) and subjected to heat shock (42ºC for 45 seconds). The bacteria were then placed in ice for 2 minutes before 500µl of prewarmed SOC medium (Super Optimal Broth with added glucose) (2% tryptone, 0.5% yeast extract, 10mM NaCl, 2.5mM KCl, 10mM $MgCl_2$, 10mM $MgSO_4$, 20mM glucose) (Invitrogen) was added. The tube was then incubated at 37ºC for 1 hour with shaking before the tube was centrifuged (2,400G for 5 minutes (Eppendorf centrifuge 5415R)). Supernatant was then removed and bacterial pellet was resuspended in 200µl of SOC and spread on an agar plate containing ampicillin (100µg/ml). Plates were left at 37ºC overnight and incubated upside down to produce tighter colonies.

2.4.5.2 JM109 Bacteria

For DNA ligated into expression vectors, JM109 bacteria were used. 100µl JM109 E.coli bacteria were transformed with 200µl 0.1M $CaCl_2$ added to the 30µl of ligation mixture

and the mixture was incubated on ice for 30 minutes. The JM109 bacteria were then heat shocked at 42ºC for 45 seconds and covered with ice for 2 minutes. The ice was removed and 500µl prewarmed SOC medium was added. The tube was then incubated at 37ºC for 1 hour with shaking. Bacteria were centrifuged (2,400G for 5 minutes (Eppendorf centrifuge 5415R)), the supernatant was removed and the pellet was resuspended in 200µl of SOC and added to an agar plate containing the relevant antibiotic (100µg/ml), to incubate overnight at 37ºC. The agar plates were incubated upside down to produce tighter colonies.

2.4.6 Isolating Plasmid DNA from Bacterial Cultures

Following overnight incubation of transformed bacteria on agar plates, ten individual distinct colonies were routinely picked from each agar plate. The miniprep technique was used to extract the plasmid DNA from the bacteria to determine which of these bacterial colonies contained the relevant plasmid DNA. Once this was established, one clone was grown in a larger culture of transformed bacteria and the maxiprep technique was employed to yield high quantities of the plasmid DNA.

2.4.6.1 Miniprep

Each colony was grown up in 6mls of Lunia Bertani (LB) broth (1% Tryptone, 0.5% Yeast Extract, 1% NaCl, pH7, containing the relevant antibiotic) for 6 hours, or overnight in 10mls, at 37ºC. 1µl from each colony was pipetted onto an antibiotic-containing agar plate to make a master plate. The rest was centrifuged (3,000G for 10 minutes (Mistral 300i Sanyo)) and plasmid DNA was isolated using a QIAPrep spin miniprep kit 250 (Qiagen, Crawley, UK) according to the manufacturers' instructions. This miniprep kit lyses the cells by alkaline lysis, precipitates the genomic DNA and protein in a high salt buffer (cleared by centrifugation) and purifies the plasmid DNA using a spin column which contains a silica membrane that the DNA binds to. The DNA in the column was washed with buffer PB (to remove endonucleases) and buffer PE (containing ethanol to remove salts). Plasmid DNA was then eluted in 30µl low salt elution buffer. DNA obtained from the miniprep was subjected to restriction digest and examined by agarose gel electrophoresis to identify positive colonies containing the correct plasmid DNA. Once identified, one of the positive colonies was picked from the master plate, grown up for 6 hours at 37ºC in 6mls LB broth, spun down as before and resuspended in 0.7ml of broth and 0.3ml glycerol (autoclaved) as a master stock to be stored at -20ºC.

2.4.6.2 Maxiprep

To obtain higher quantities of plasmid DNA, a positive colony containing the relevant plasmid DNA was grown in 10mls LB broth overnight. The following day this was added to 100mls LB broth and grown up overnight so that maxiprep using HiSpeedPlasmid Maxikit could be performed to extract the plasmid DNA. The maxiprep kit is a scaled up version of the miniprep kit yielding much higher quantities of DNA.

2.4.7 Characterisation of DNA

The plasmid DNA was quantified using a Nanodrop ND1000 spectrophotometer according to the manufacturers' instructions (Thermo Scientific, Wilmington, USA). The nanodrop measures the quantity and purity of the DNA by measuring light absorbance. The quality of the DNA is measured through ratios of absorbance between two wavelengths: 260/280 and 260/230. Nucleotides, RNA and DNA absorb at 260nm. Contaminants which absorb around 280nm include protein and phenol whereas contaminants which absorb at 230nm include carbohydrates. The 260/280 ratio should be close to 1.8 for 'pure' DNA and 2.0 for 'pure' RNA, and between 2.0-2.2 for the 230/280 ratio.

2.5 Western Blot Analysis

Western blot analysis was used to analyse the presence of proteins in various cells before and after treatment. Lysates were prepared from cells and proteins were separated using SDS-PAGE and analysed by western blot to visualise them.

To prepare lysates, cells were harvested and washed with ice-cold PBS (Lonza) before lysis on ice for 30 minutes with Onyx Lysis Buffer (1M Tris, 5M NaCl, 1M $MgCl_2$, 1M EGTA, 0.01% Triton-X-100, 0.1% Glycerol, 1M NaF, 700mM Na_3VO_4), 1% Protease Inhibitor) after which cells were centrifuged at 15,700G at 4ºC for 15 minutes (Eppendorf centrifuge 5415R). Lysates were stored at -20ºC, quantified by Bradford Assay using protein assay reagent (BioRad, Hemel Hempstead, UK) and an ELISA plate reader (Dynatech MR4000) (Dynatech, Boston, USA). Once quantified, 15 to 30µg of protein lysates were diluted with dH_2O to give a final volume of 25µl. 7.5µl of 4X reduced loading buffer (2M Tris HCl pH6.8, 40% Glycerol, 20% Sodium Dodecyl Sulphate (SDS), Bromophenol Blue. Before use, add 900µl 4X loading buffer to 100µl 2-mercaptoethanol (2-ME)) was added and the lysates were boiled at 100ºC for 5 minutes and centrifuged (1 minute at 15,700G). Proteins were separated on a 10% or 4-12% Bis-Tris NuPAGE pre-cast gel (Invitrogen) run at 150V in MOPS buffer (0.01M 3-(N-

morpholino)propanesulfonic acid (MOPS), 0.01M Tris, 0.7mM SDS, 2.05mM EDTA) using the *Surelock* system from Invitrogen. The transfer of the proteins to the membrane was carried out at 30V for 60 minutes in NuPAGE Transfer Buffer (TB) (Invitrogen) with 10% methanol, diluted in dH_2O, in an XCell II TM Blot Module (Invitrogen). Either methanol-activated polyvinylidene fluoride transfer (PVDF) membrane (Millipore, Watford, UK) or nitrocellulose membrane (GE Healthcare, Amersham, UK) were used.

Table 2.1: Primary antibodies used in the western blotting protocol.

Specificity	Species	Source	Clone Number	Working dilution
A1/Bfl-1	Rat	WEHI	51B2	2μg/ml
A1/Bfl-1	Rabbit	Cell Signaling Technology	4647S	2μg/ml
A1/Bfl-1	Rabbit	Epitomics	EP517Y	1:500
Phospho-ERK1/2 (Thr202/Tyr204)	Rabbit	Cell Signaling Technology	9101S	1:500
ERK1/2	Rabbit	Cell Signaling Technology	9102	1:1000
Phospho-AKT (Ser473)	Rabbit	Cell Signaling Technology	4060B	1:1000
AKT	Rabbit	Cell Signaling Technology	9272	1:1000
β-Actin	Mouse	Sigma	A228	1:10,000
FLAG	Rabbit	Tenovus	-	1:500
Bcl-2	Mouse	BD BioSciences	3F11	1:500
Bcl-xL	Mouse	BD BioSciences	44	1:500
Bcl-w	Rat	Tenovus	13F9	1:500
Mcl-1	Rabbit	Abcam	Y37	1:1000
S100-β	Rabbit	Millipore	EP1576Y	1:1000
GAPDH	Mouse	Abcam	8245	1:1000
α-Tubulin	Mouse	Cell Signaling Technology	2144	1:1000
Phospho-IκBα (Ser 32)	Rabbit	New England BioLabs	14D4	1:1000
COX IV	Rabbit	Cell Signaling Technology	4844	1:1000

The membranes were blocked with 5% (w/v) milk solution (non-fat dried milk in TBS-0.05%-Tween (TBS: 0.05M Tris, 0.15M NaCl, pH 7.4 with dH_2O and HCl.)) for 1 hour

and washed in TBS-0.05%-Tween. Membranes were probed with primary antibodies (see Table 2.1) (antibodies diluted in 5% BSA, 0.05% Azide, 0.05% Tween in TBS) for 1 hour at room temperature, or overnight at 4ºC. Horse radish peroxidase (HRP) conjugated secondary antibodies (GE Healthcare UK Ltd.) (1:5000 dilution in TBS-Tween) were incubated for 1 hour. Protein bands were visualised using enhanced chemiluminescence (ECL) Immobilon Western HRP Substrate (Millipore), SuperSignal® West Pico Chemiluminescent Substrate (Pierce) or Lumigen TMA-6 (GE Healthcare) (diluted 1:5 before use) on the membranes for 5 minutes. Membranes were analysed using a UVP BioImager system (UVP, Cambridge, UK) and VisionWorksLS acquisition and analysis software or the Xograph developer (Xograph Healthcare Ltd., Tetbury). Western Blots were quantified using VisionWorks software with a rolling disk size of 200.

2.6 Death Assays

Cell death was measured through propidium iodide staining and analysed using flow cytometry. This assay was adapted from the method developed by Nicoletti et al. [434] for the rapid measurement of fragmented DNA. Cells were passaged into 12-well plates (Fischer) at $1x10^5$cells/ml and allowed to settle overnight. Before treatment, floating cells were removed from wells and fresh media was added. After treatment for 24-48 hours, both floating and adherent cells were harvested into FACS tubes and centrifuged (3,000G, Sorvall RT7 Plus, Thermo Scientific, MA, USA), the supernatant was removed and the cells were stained with 250µl of hypotonic fluorochrome solution (50µg/ml propidium iodide in 0.1% Sodium Citrate, 0.1% Triton-X-100) for at least 1 hour at 4˚C. Cells were analysed by flow cytometry using a FACScan (BD Biosciences, Oxford, UK) using CellQuest Pro software (BD Biosciences). Routinely, 10,000 events were collected, as identified by the forward scatter and side scatter threshold parameters.

2.7 Quantitative Analysis of Nucleic Acids

2.7.1 RNA Extraction

Total RNA was extracted in order to analyse mRNA levels present in cells under various treatment conditions. Total RNA was extracted from cultured cells using a PureLink™ Micro-to-Midi Total RNA Purification System (Invitrogen) according to the manufacturer's instructions. Briefly, $5x10^6$ cells were harvested, collected and resuspended in lysis buffer (containing 2-mercaptoethanol (2-ME)). Nucleic acids were precipitated by 70% ethanol and added to a spin column where the RNA bound to the silica-based membrane. The RNA was washed with several alcohol based buffers before being eluted in

RNAase-free water and quantified by spectrophotometry on a Nanodrop ND-1000 (Thermo Scientific). RNA was stored at -80ºC for a maximum of 18 hours prior to conversion to cDNA.

2.7.2 cDNA Synthesis

RNA was converted to cDNA so that PCR could be carried out to give a quantitative analysis of mRNA levels present in cells cultured under various treatment conditions. 5µg of RNA was converted to cDNA using Superscript II First-strand synthesis system for RT-PCR (Invitrogen) according to the manufacturer's instructions. In brief, the RNA was incubated with 1µl 10mM deoxynucleotide triphosphates (dNTPs) and 1µl 50µM oligo$(dT)_{20}$ primer for 5 minutes at 65˚C (to denature nucleic acids) before being left on ice for 1 minute. 2µl 10X reverse transcriptase (RT) buffer, 4µl 25 mM $MgCl_2$, 2µl 0.1 M Dithiothreitol (DTT), 1µl 40 U/µl RNaseOUT™, 1µl 200 U/µl SuperScript™ III RT were added and these were incubated for 50 minutes at 50˚C (for cDNA synthesis). cDNA synthesis was terminated at 85˚C for 5 minutes and the mixture was chilled to 4˚C. 1µl RNase H was added and the reaction was incubated at 37˚C for 20 minutes (to remove residual unconverted RNA). cDNA was stored at -20ºC prior to analysis by PCR.

2.7.3 Polymerase Chain Reaction (PCR)

PCR was used to analyse the presence of mRNA of various genes in cells which were cultured under various treatments. 1µl of 0.2µg/µl cDNA was added to 10µl 2X Green GoTaq® Reaction Buffer (pH 8.5) containing DNA polymerase (400µM dATP, 400µM dGTP, 400µM dCTP, 400µM dTTP and 3mM $MgCl_2$) (Promega) and 7µl dH_2O. 1µl 100ng/µl of forward primer and 1µl 100ng/µl of reverse primer (Invitrogen) (Table 2.2) was added to each 20µl reaction. Human GAPDH or actin primers were used as the internal control for cDNA quantity. PCR was performed on a PTC-100 Programmable thermal controller (MJ Research, Minnesota, USA) (PCR cycle; 94ºC for 5 minutes, 94ºC 30 seconds (denaturation of the double stranded DNA), 57ºC 1 minute (annealing of the primers to the DNA), 72ºC 2 minutes (extension of the primers), steps 2-4 for 25 cycles, 72ºC 10 minutes, 4ºC forever). Samples were separated by size on a 0.7% agarose gel with O'GeneRulerTM 1kb DNA ladder for size reference. Fluorescence was detected using UVP BioImager system (UVP, Cambridge, UK) and VisionWorks software (UVP).

2.7.4 Quantitative PCR (qPCR) with SyberGreen

qPCR was used to produce a quantitative analysis of the levels of mRNA present in cells. 1µl of 0.1µg/µl cDNA was added to 10µl 2X SYBR® Green master mix from DyNAmo™ SYBR® Green qPCR Kit (containing modified *Thermus brockianus* DNA Polymerase, SYBR Green I dye, optimized PCR buffer, 5 mM $MgCl_2$, dNTP mix including dUTP) (Finnzymes, Espoo, Finland) and 3µl dH_2O. 3µl 100ng/µl of forward primer and 3µl 100ng/µl of reverse primer (Invitrogen) (Table 2.2) was added into each 20µl reaction. Each sample was examined in triplicate and an internal control of β-actin was used as a reference for cDNA quantity. qPCR was performed according to the following PCR cycle; 95ºC 15 minutes, 94ºC 15 seconds (denaturation double stranded DNA), 50ºC 30 seconds (annealing of primers to DNA), 72ºC 30 seconds (extension of primers). The qPCR plate is then read, and steps 2-5 were repeated 45 times, with the melting curve from 60ºC to 95ºC, assessed every 1ºC to identify contamination or mis-priming, before incubation at 4ºC forever. Fluorescence signals were detected using chromo4 continuous fluorescence detector and DNA Engine Opticon Software (BioRad).

2.7.5 qPCR with Taqman

qPCR was also performed using Taqman probes, which required a different protocol to account for the difference in the technology of the systems. Taqman primers bind at higher temperatures than the SyberGreen dye and do not require an extension step to produce fluoresence. 1µl of 0.1µg/µl cDNA was added to 10µl Platinum® Quantitative PCR SuperMix-UDG (Platinum® *Taq* DNA polymerase, Mg^{2+}, uracil DNA glycosylase (UDG), proprietary stabilizers, and deoxyribonucleotide triphosphates, with dUTP instead of dTTP) (Invitrogen), 1µl of Taqman probe (Invitrogen) and 8µl H_2O. Samples were run in triplicate and β-actin or B2M (Invitrogen) was the internal control. qPCR was performed according to the following PCR cycle; 50ºC 2 minutes, 95ºC 2 minutes, 95ºC 15 seconds (denaturation of double stranded DNA), 60ºC 30 seconds (annealing of reporter probe). The qPCR plate is then read, and steps 3-5 repeated for 40 cycles, before incubation at 4ºC forever.) Fluorescence signals were detected using chromo4 continuous fluorescence detector and DNA Engine Opticon Software (BioRad). Housekeeping gene expression was quantified using a TaqMan® Express Human Endogenous Control Plate (Applied Biosystems). Here, cDNA was added for 3 cell-lines per plate to wells containing pre-mixed taqman reactions and the plate was run under the same PCR cycle, read by the same machine and analysed in the same way as the taqman probes.

Table 2.2: Primers used for PCR and SyberGreen qPCR.

Primer	Direction	Sequence
HuBfl-1 BamHI	Forward	5'AGGATCCGATGACAGACTGTGAATTTGGATATATT3'
HuBfl-1 HindIII	Reverse	5'CCAAGCTTGTCAACAGTATTGCTCAGGAGAGATAG 3'

2.7.6 DNA Sequencing

DNA sequencing was used to confirm the identity of DNA fragments and elucidate any mutations present. Dye-terminator sequencing labels each ddNTP with a different fluorescent dye in a single reaction. The bases can then be identified as each dye emits light at a different wavelength, resulting in four different colours. DNA inserted into the TOPO vector was sequenced using primers for the T7 and sp6 sequences present in the TOPO vector. The sequencing reaction contained 2µl Big Dye Terminator v1.1 (Applied Biosystems), 2µl 5x sequencing buffer (Applied Biosystems), 1µl 100ng/µl primer (T7 or sp6) (Invitrogen) and 100ng cDNA for a total volume of 10µl, made up with dH_2O. This mixture was amplified using the PCR programme for sequencing as described: step 1; 96˚C for 1 minute (primary denaturation), step 2; 96˚C for 10 seconds, step 3; 50˚C for 5 seconds (annealing of primers), step 4; 60˚C for 4 minutes (extension of DNA). Steps 2-4 were repeated for 25 cycles and the reaction was cooled to 4˚C). The DNA was then precipitated when the 10µl reaction was transferred to 1.5ml eppindorfs containing 1µl 3M sodium acetate and 25µl 100% ethanol. The samples were centrifuged at 15,700G for 30 minutes at 4˚C (Eppendorf centrifuge 5415R) and the supernatant was carefully removed. DNA was washed with 125µl 70% ethanol and centrifuged at 15,700G for 5 minutes. The supernatant was removed and the DNA was resuspended in 10µl Hi-Di™ formamide (Applied Biosystems) which denatures the DNA, preserves the sample and prevents evaporation. Sample electrophoresis was carried out on a 3130xl genetic analyser (Applied Biosystems) and analysed using SeqMan Lasergene software (DNASTAR, Madison, USA).

2.8 Transfection

Transfection techniques were used to insert plasmid DNA into cells in order for cells to express proteins not native to the cell for over-expression assays or for detection of tagged proteins. Different cell types required different transfection protocols, which are described below.

2.8.1 Electroporation

Electroporation is a technique which temporarily punches holes in the cell with an electric pulse. The plasmid DNA can then enter the cell through these holes. As such, electroporation is a good transfection technique to use for large DNA constructs. Cells were harvested when they were in exponential growth and $5x10^6$ cells were re-suspended in serum free media (DMEM or RPMI depending on the cell-line). 800µl of cells were added to 0.4cm electroporation cuvettes along with 30µg of 0.5µg/µl DNA. Cells were incubated with DNA for 10 minutes on ice then subjected to electroporation at 300V/cm, 960uFD capacitance. The volume from the cuvettes was mixed with 10mls complete medium at room temperature, incubated on ice for 10 minutes, then at room temperature for 10 minutes. A further 20mls complete medium was added and the cells were incubated for 10 minutes at room temperature. Cells were plated into three 96-well plates per electroporated sample, 100µl/well. After 48 hours, geneticin was added at 1mg/ml. Wells with individual colonies were grown up to form stably transfected cell-lines.

2.8.2 Nucleofection

Nucleofection is a form of electroporation developed by amaxa to transfect cells which proved resistance to transfection by standard electroporation. It involves the use of the specific currents and reagents, optimised for different cell types, and even different cell-lines. Nucleofection is an advance of electroporation as it opens the nuclear membrane as well as the cell membrane, allowing constructs to be transfected straight into the nucleus.

Cells were harvested and resuspended to obtain $1x10^6$ cells/200µl sample resuspended in nucleofector solution (Lonza). 200µl of cells were transferred to a 0.4cm Gene Pulser Cuvette (Bio-Rad) and 2µg of DNA was added to the cells. The cuvette was inserted into the cuvette holder on the Nucleofector machine (Amaxa Biosystems, Lonza) where the cells were subjected to pre-set electroporation programmes. Different cell-lines were subjected to different pre-set programmes according to the manufacturer's instructions (Table 2.3). The cuvette was removed from the Nucleofector and 500µl complete warm medium was added. The cells were then transferred, using the special plastic pipettes provided with the kit to prevent damage and loss of cells, to 2ml complete warm media in a 6-well plate. Cells were cultured at 37˚C, 5% CO_2. For production of stable transfected cell-lines, geneticin was added 24 hours after transfection at 1mg/ml.

Table 2.3: Nucleofection protocols

Cell-line	Nucleofection Solution	Nucleofector Programme
A375	V	X-001
B16	V	P-020
SkMel28	V	X-001

2.8.3 Lipofection

Lipofection is a different technique for transfection of plasmid DNA or siRNA into cells that involves small lipid vesicles rather than an electric current. It is a gentler transfection technique than electroporation and it often displays very high transfection efficiency. Liposomes containing the synthetic lipid N-[1-(2,3-dioleyloxy)propyl]-N,N,N-trimethylammonium chloride (DOTMA) spontaneously interact with DNA in solution to form lipid-DNA complexes. These liposomes containing the DNA are then added to cells where the vesicles fuse with the cell membrane, allowing uptake of the DNA. 2.5µg of 0.5µg/µl plasmid DNA added to 500µl Opti-MEM® and 6.25µl of Lipofectamine 2000 (Invitrogen) added to 500µl Opti-MEM®, were incubated at room temperature for 5 minutes then mixed together and incubated at room temperature for 20 minutes. The Lipofectamine and DNA were then added dropwise to cells plated in 6-well plates at 40-60% confluence. To produce stably transfected cell-lines, the selection agent geneticin was added at 1mg/ml, 48 hours after transfection. Once colonies had formed in the 6-well plates, they were picked and re-seeded into 96-well plates and grown up under continuing geneticin selection.

2.8.4 siRNA Transfection

Lipofection was also used to transfect siRNA into cells, through a slightly adapted technique. Routinely, siRNA at a final concentration of 40nM was added to 250µl Opti-MEM® and 5µl Lipofectamine 2000 to 250µl Opti-MEM®. These were firstly incubated separately at room temperature for 5 minutes before the siRNA mix was added to the Lipofectamine 2000. The mixtures were vortexed vigorously and centrifuged briefly before being incubated at room temperature for a further 30 minutes. During the incubation, the media on cells, which had been seeded at the appropriate density and allowed to settle overnight, was replaced with fresh complete warm medium. The lipofectamine/siRNA mixture was then added dropwise to cells. siRNA was routinely left on the cells for 48 hours before analysis. Bfl-1 siRNA was obtained using the Invitrogen online siRNA

designer. Negative control siRNA was selected which contained an equal GC percentage as Bfl-1 siRNA and does not target any gene product (Silencer negative control #1 siRNA, Applied Biosystems).

Table 2.4: siRNA primer sequences

Name	Sequence 5'-3'
BCL2A1HSS100957	ACAACCUGGAUCAGGUCCAAGCAAA
BCL2A1HSS100958	GGACAAUGUUAAUGUUGUGUCCGUA
BCL2A1HSS100959	UCAAGAAACUUCUACGACAGCAAAU

2.8.5 293T Transfection

293T cells are a cell-line developed as an easily transfectable over-expression system. 293T cells can be used to determine the transfectability of DNA constructs and to analyse the resulting protein. 293T cells are transfected using a calcium phosphatase transfection method with reagents from Qiagen. The calcium phosphatase precipitates DNA and the resulting complex can then enter the cells. Semi-adherent 293T cells were cultured in DMEM and passaged using EDTA/Versene. To transfect these cells, the nonliposomal lipid Effectene transfection reagent from Qiagen was used. 1µg of 0.5µg/µl plasmid DNA was added to the DNA-condensation buffer, Buffer EC, to a total volume of 150µl. 8µl Enhancer (Qiagen) was added and the solution was mixed by vortexing for 1 second. The mixture was incubated at room temperature for 5 minutes, then 25µl Effectene transfection reagent (Qiagen) was added and the mixture was vortexed for 10 seconds. The mixture was left at room temperature for 10 minutes to allow transfection-complex formation. 1ml growth medium was then added and the mixture was added dropwise to cells plated out at $0.5x10^6$cells/well in a 6-well plate overnight so they were 40-80% confluent. Cells were incubated at 37˚C for at least 24 hours before lysates were generated or selection was added.

2.8.6 293F Transfection

293F cells are the suspension version of 293T cells and have also been developed for easy transfection. 293F cells were used for similar reasons as 293T cells, but were transfected using a lipid based system similar to lipofection. Suspension 293F cells were cultured in Freestyle 293 medium (Invitrogen) and transfected using the 293fectin™ reagent (Invitrogen) which has been specifically designed for use with 293F cells. 1µg of 0.5µg/µl plasmid DNA was added to 300µl Opti-MEM® reduced serum medium (Invitrogen) whilst

15µl 293fectin™ (Invitrogen) was added to 300µl Opti-MEM® and incubated at room temperature for 5 minutes. The DNA and 293fectin were mixed and incubated at room temperature for 30 minutes. 293F cells were seeded at $1x10^5$cells/ml in 12-well plates. The DNA-fectin was added dropwise to the cells and the plates were placed in a rocking incubator at 37ºC. Cells were checked after 6 and 24 hours by flow cytometry (100µl cells with 100µl FACS flow) for transfection of the fluorescently tagged DNA constructs. After 24 hours lysates were generated and samples were run by western blot to check transfection of the non fluorescent DNA constructs.

2.8.7 Fluorescence Microscopy

Fluorescence microscopy was used to visualise cells expressing fluorescently labelled DNA constructs and was carried out using a CX41 Biological microscope (Olympus, Southend-on-Sea, UK) and Cell^B software (Olympus) according to the manufacturers' instructions.

2.8.8 Cell Sorting

Cell sorting is used to achieve pure populations of cells (for example to remove unsuccessfully transfected cells), or cells expressing a particular level of expression of a given protein. Cells for cell sorting were grown to sufficient quantities and then sorted according to forward scatter (FSC), side scatter (SSC) and fluorescence (FL-1/FL-2) parameters using a FACS Aria flow cytometer (BD BioSciences) with CellQuest Pro software (BD BioSciences). Sorted cells were collected into a FACS tube coated with FCS to minimise impact and breakage of the cells. These cells were then washed and returned to culture conditions (37˚C, 5% CO2) under selection with the relevant antibiotic.

2.9 Clonogenic Assay

The clonogenic assay was used to determine the clonogenic survival of cells after chemotherapeutic treatment. Cells were seeded at $2x10^5$cells/ml in 6-well plates, left to settle overnight and then treated with drug for 24 hours. Cells were trypsinized and washed in fresh medium to remove drugs. Cells were seeded in a 96-well plate at cell densities from 1-2,400 cells/well (12 wells of each density) in 70% fresh media and 30% media taken from growing cells (centrifuged and filtered) to provide optimal growing conditions. Clonogenicity was measured by counting the number of wells with colonies of >50 cells after 10 days of culture.

2.10 Subcellular Localisation

The localisation of proteins within cells was explored using various techniques including subcellular fractionation and microscopy.

2.10.1 Mitochondrial Isolation

Intact mitochondria were isolated from cells in order to elucidate the proteins located at the mitochondria. This was performed using a mitochondria isolation kit for cultured cells (Thermo Scientific) following the manufacturer's instructions. A reagent-based method was used in combination with differential centrifugation to separate the mitochondrial and cytosolic fractions. EDTA-free protease inhibitor was added to reagents A and C before use. Cells were cultured in tissue culture flasks to obtain $2x10^7$ cells per sample. These cells were harvested, centrifuged at 850G for 2 minutes and resuspended in 800µl reagent A by vortexing for 5 seconds at medium speed before incubation on ice for 2 minutes. 10µl reagent B was added and cells were subjected to 5 seconds vortexing at high speed every minute for 5 minutes. 800µl reagent C was then added and mixed in by inverting the tube before centrifugation at 700G for 10 minutes at 4˚C. The supernatant was then transferred to a new tube and centrifuged at 3,000G for 15 minutes at 4˚C. The supernatant from this step contained the cytosol fraction and the pellet contained the mitochondria. The cytosol fraction was removed to a new tube and 500µl reagent C was added to the pellet before centrifugation at 12,000G for 5 minutes. The pellet was maintained on ice before mitochondrial lysis by vortexing for 1 minute in 2% CHAPS buffer (CHAPS in TBS, TBS as described in section *2.5*). The mitochondria in CHAPS buffer were then centrifuged at high speed for 2 minutes, presenting the soluble protein in the supernatant for analysis by Bradford Assay (BioRad). Proteins in the cytosol and mitochondria fractions were then analysed by western blot (section *2.5*). Mitochondria isolation efficiency was assessed through western blotting for the presence of COX IV, as a marker of mitochondria, and actin, as a marker of the cytosol.

2.10.2 Indirect Immunofluorescence

Protein localisation was also visualised by microscopy techniques. Cells were plated out in tissue culture plates at $1x10^5$cells/ml and allowed to settle overnight onto coverslips coated with Poly-L-Lysine (PLL). Growth medium was removed and the coverslips were washed 3 times with PBS before cells were fixed using 4% formaldehyde in PBS for 15 minutes on ice. Coverslips were washed a further 3 times with PBS and permeabilised using 0.25%

saponin in PBS for 20 minutes at room temperature. From this point, coverslips were washed with PBS containing 0.05% saponin. Coverslips were washed 3 times and blocked using 0.25% Normal Goat Serum (NGS) for 20 minutes to 2 hours at room temperature. The NGS was washed off and the coverslips were removed from the tissue culture plate and placed cell-side down on a drop of primary antibody. The coverslips were incubated with the primary antibody (Table 2.5) overnight at 4˚C in a chamber containing wet tissue to prevent drying out of the coverslips. The next morning, coverslips were placed in individual petri dishes and washed 3 times, with the third wash left rocking for 20 minutes. Incubation with the secondary antibody (goat anti-(relevant species) conjugated to alexa 488 fluorophore) (Invitrogen) was in the same chamber as before, the coverslips were again placed cell-side down on a drop of secondary antibody for 1 hour at room temperature. Cells were then washed 3 times, in the dark, with a 5 minute wash on the third wash. Coverslips were then placed cell-side down on a microscope slide on a drop of Hard-set Vectashield with Dapi nuclear stain (Vector Laboratories, Inc. USA). These were left to dry in the dark before examination using fluorescent or confocal microscopy.

In some experiments, cells were treated with MitoTracker® Red CMXRos (Invitrogen) at 100nM for 30 minutes in warm serum-free media. Excess MitoTracker was washed off with PBS before the cells were fixed using 4% formaldehyde in PBS for 15 minutes on ice.

Table 2.5: Primary antibodies used in IHC

Specificity	Species	Source	Clone	Working Dilution
Bfl-1	Rat	WEHI	51B2	1:50-1:200
Bfl-1	Rabbit	Cell Signaling Technology	4647S	1:100-1:200
FLAG	Rabbit	Tenovus	-	1:100-1:250
Lamp1	Biotinylated	Abcam	H4A3	1:100-1:250

2.10.3 Confocal Microscopy

Confocal microscopy was used to obtain co-localisation pictures of cells for subcellular localisation. This type of microscopy is ideal for co-localisation studies as it can eliminate out-of-focus light through the combination of a spatial pinhole and point illumination, giving a picture of a slice through the cell. Confocal microscopy was performed on a Leica TCS SP5 (Leica Microsystems, Milton Keynes, UK) and analysed using LAS AF software (Leica Microsystems).

3: AN ANALYSIS OF BFL-1 EXPRESSION IN MELANOMA

3.1 Introduction

As has been detailed in the introduction the pro-survival members of the Bcl-2 family serve to block apoptosis and have been seen to be upregulated in many chemo resistant cancers [435,436]. As the lesser studied member of the family, we were particularly interested in Bfl-1. Bfl-1 has previously been seen to be upregulated in B-cell chronic lymphocytic leukemia, large B-cell lymphomas and acute myeloid leukemia [373-375], and in melanoma cell-lines (Figure 1.21). In these cells, over-expression is thought to tip the balance between the pro-survival and pro-apoptotic members of the Bcl-2 family in favour of cell survival. For this reason, Bfl-1 has been theorised to lend to the intrinsic resistance to chemotherapy seen in many of the cancers where it is over-expressed [395].

In this chapter, I confirmed the expression pattern of Bfl-1 mRNA and protein in a panel of melanoma cell-lines. I then went on to characterise Bfl-1 by determining its half life, the signalling pathways through which it is regulated and the factors which control its degradation.

3.2 Bfl-1 mRNA Expression in Melanoma Cells

I decided to follow on from the analysis of the NCI60 microarray by investigating Bfl-1 expression in our own panel of melanoma cell-lines, looking at the levels of both mRNA and protein. To do this, I selected melanoma cell-lines, including some seen in the NCI60 array (Figure 1.21), and examined the levels of Bfl-1 mRNA and protein present. I also included the colorectal cell-line Colo205 as a non-melanoma BRaf mutant cell-line and the lymphoma cell-line Raji as lymphoma cell-lines in the NCI60 were seen to express Bfl-1, albeit at a lower level than melanoma cell-lines. The known characteristics of these cell-lines are presented in Table 3.1, based on database and literature searches.

Table 3.1: Characteristics of the cell-lines, including the mutations they express and their origins.
Information obtained from papers and the American Type Culture Collection (ATCC) and Sanger Institute cell-line databases, alongside some published references.

Melanoma Cell-lines	Cancer type and Origin	BRaf status	N-Ras Status	P53 status	Additional information	References
A375	Malignant melanoma, metastatic phenotype	V600E, homozygous	WT	WT	CDKN2A mutant, WT PTEN	[66] ATCC
G361	Malignant melanoma, metastatic phenotype	V600E heterozygous	WT	Mutated	WT PTEN WT EGFR CDKN2A mutant WT myc, kit	ATCC, Sanger
MM200	Melanoma	V600E	WT	WT	No PTEN as a result of a missense mutation	[440,441] Sanger
SkMel28	Malignant Melanoma	V600E	WT	Mutated	EGFR mutant, PTEN missense mutation, but protein expressed at normal level	[36,66,441] Sanger
SkMel31	Malignant melanoma	V600E, heterozygous	WT	Mutated	Derived from same original sample as SkMel28	Sanger
UACC62	Malignant melanoma	V600E	WT	WT	PTEN mut CDKN2A mut	Sanger
Controls						
Colo205	Colorectal, large intestine carcinoma, adenocarcinoma.	V600E	WT	Mutated	APC mutant SMAD4 mutant	Sanger
Raji	Burkitt's lymphoma	WT	WT	WT	-	ATCC, Sanger

The melanoma cell-line SkMel28 was picked from the microarray as a positive for Bfl-1 expression and the colorectal cell-line Colo205 was used as a negative control. Another melanoma cell-line not screened by the NCI60, A375, was also examined for levels of Bfl-1. Initially RT-PCR using GoTaq green was used to examine the levels of Bfl-1 mRNA present in total RNA extracted from the two melanoma cell-lines grown in culture compared to the colorectal cell-line (Figure 3.1A). Actin was used as an internal control for the quantity and quality of cDNA in each sample. A water control was also included in every PCR to check the specificity of the primers, and no bands were ever seen in these lanes.

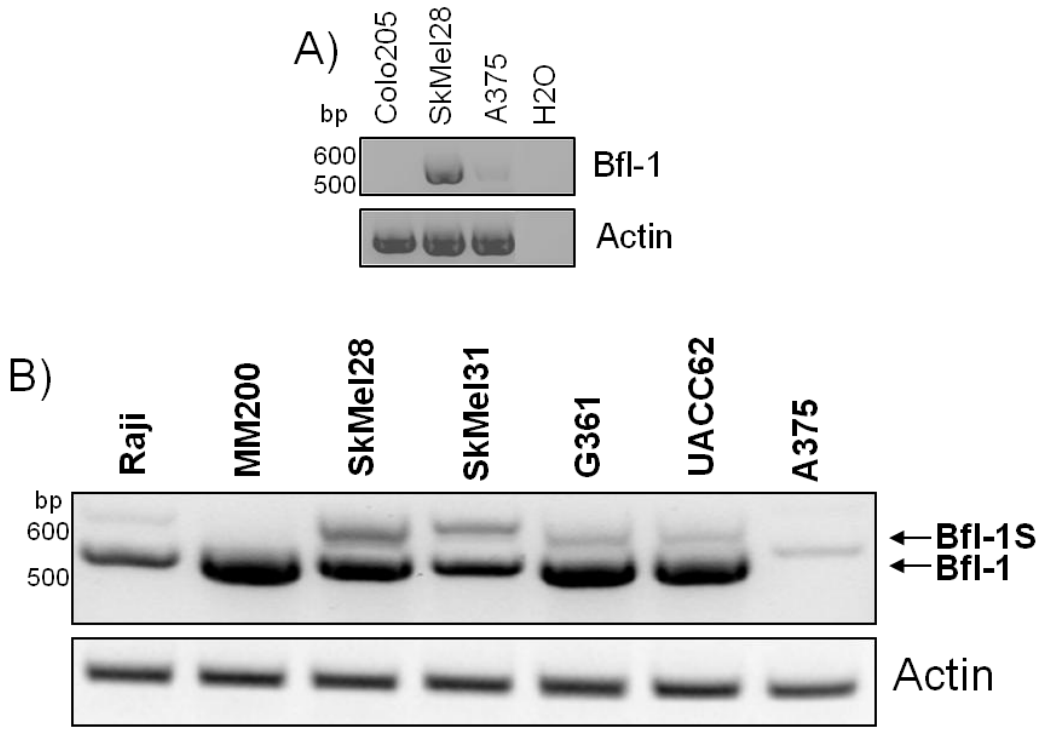

Figure 3.1: RT-PCR to analyse the level of Bfl-1 mRNA expression in a panel of cell-lines.
A) Total RNA was extracted from the untreated melanoma cell-lines in culture and converted to cDNA. cDNA was then amplified by PCR using Bfl-1 primers (Invitrogen) and separated by gel electrophoresis. Actin mRNA was amplified as an internal control. Bfl-1 negative (Colo205), Bfl-1 highly expressing (SkMel28) and Bfl-1 low expressing (A375) cell-lines were found. B) A more comprehensive panel of cell-lines, including a greater selection of melanoma cell-lines, was examined using the same method to determine the levels of Bfl-1 mRNA. Actin mRNA was amplified as an internal control and the gel was run for a longer time allowing further separation of cDNA bands. Two bands were detected in most cell-lines, representing Bfl-1 and the splice variant Bfl-1S. These data are representative of three independent experiments using independently acquired cDNA.

In agreement with the NCI60 microarray, the colorectal cell-line Colo205 had undetectable levels of Bfl-1, whereas Bfl-1 could be seen to be expressed in both the melanoma cell-lines examined, but at very different levels. SkMel28 expressed high levels of Bfl-1 mRNA compared to the very low levels seen in A375 (Figure 3.1A). Subsequently we assessed a larger panel of melanoma cell-lines to identify how the expression of Bfl-1 mRNA varied within melanoma cell-lines (Figure 3.1B). Actin was again used as the internal control. Again, Bfl-1 was seen at a low level in A375 cells, but in the five other melanoma cell-lines, MM200, SkMel28, SkMel31, G361 and UACC62, Bfl-1 mRNA was present at high levels. All these melanoma cell-lines appeared to express similar levels except SkMel31, which expressed a lower level of Bfl-1 mRNA. Additionally, a Burkitt's lymphoma cell-line, Raji, was tested for Bfl-1 as the mRNA was observed at significant levels in two lymphoma cell-lines in the NCI60 microarray. Raji cells contained levels lower than the majority of the melanoma cell-lines, but higher than A375 cells.

Furthermore, two bands were observed by PCR representing the Bfl-1 and Bfl-1S isoforms, as confirmed by sequencing (section 3.3). As detailed in section 1.6.6 in the introduction, the larger PCR band represents the transcript that encodes the shorter protein isoform, Bfl-1S, as the additional 56 base pair exon present in the larger band moves the stop codon forward in the sequence to result in a shorter protein.

The proportion of the isoforms appeared to be relatively different in SkMel28, SkMel31, G361, UACC62 and Raji cell-lines, when calculated using densitometry. The notable exception was MM200 cells, which appeared to express the full-length Bfl-1 isoform only. In A375 cells only the full-length isoform was visible, however the levels were so low that it cannot be concluded that A375 cells express the full-length isoform and not the shorter Bfl-1S isoform. The cell-lines which contained Bfl-1S had a ratio of Bfl-1: Bfl-1S of between roughly 3:1 (SkMel28) and 5:1 (UACC62 and Raji). To get a more quantitative result of the expression levels of Bfl-1 mRNA, qPCR was performed using a Taqman probe.

The Bfl-1 Taqman probe, which contains a fluorophore and a quencher, anneals to the template Bfl-1 cDNA. As PCR amplification occurs, the fluorophore is cleaved from the quencher by the exonuclease activity of the Taq polymerase as it extends the primer. This degradation of the Taqman probe removes the fluorophore from its close proximity to the quencher, allowing the fluorophore to fluoresce. During the qPCR reaction, the thermal cycler records a measurement of the fluorescence released by the Taqman probe, generating the graphs seen in 2. The point on the graph when the cDNA has been amplified enough to produce a level of fluorescence to cross the threshold line (i.e. above background noise) is taken as the cycle threshold (Ct) number. This was the number used to analyse the data in a quantitative manner, with each increasing Ct number representing a doubling in DNA quantity. The Bfl-1 Taqman probe spans exons 1 and 2, hence it can recognise both full length Bfl-1 and the shorter Bfl-1S isoforms.

Initially we validated the qPCR assay and the Taqman probe by examining the raw data from qPCR with the Bfl-1 Taqman probe (2). As can be seen, cDNA from the highest Bfl-1 expressing cell-line (MM200) had an average Ct value of 23.5 whereas the low expressing cell-line (A375) had a Ct value of 29.2. This confirmed the different levels of Bfl-1 initially observed in MM200 cells and A375 cells by RT-PCR (Figure 3.1), and

along with the tightness of the curves for the triplicate samples analysed for each cell-line, revealed the specificity and reliability of the Bfl-1 Taqman probe.

Subsequently the quantitation of the Taqman assay was examined by a titration of the amount of cDNA initially added to the qPCR reaction. cDNA isolated from the melanoma cell-line UACC62 was used as these cells appeared to express a high level of Bfl-1 mRNA, with both isoforms present (Figure 3.3). The titrations show that as the quantity of cDNA added to a qPCR reaction was increased, the quantity of Bfl-1 cDNA detected increased in a linear manner, demonstrating that the Taqman protocol for qPCR was quantitative. The level of actin cDNA detected also increased in a linear manner.

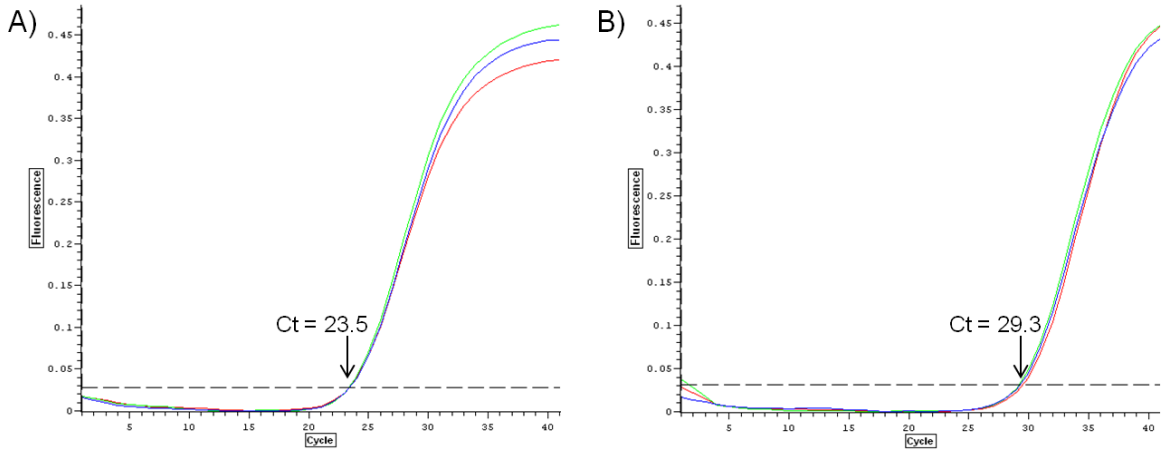

Figure 3.2: Validation of Bfl-1 expression using qPCR with Taqman probes for Bfl-1 in melanoma cell-lines.
Total RNA was isolated from untreated cells in culture. RNA was converted to cDNA and qPCR was performed. Graphs show the cycle threshold (Ct) value of A) MM200, a cell-line with high Bfl-1 expression and B) A375, a cell-line with low Bfl-1 expression. Graphs show a triplicate of the same cDNA sample taken from untreated cells in culture and amplified by qPCR using Taqman probes (Applied Biosystems).

The validation of the primers in Figure 3.2 allows us to utilise an addition analysis of the qPCR results; In addition to Ct numbers, the quantity of cDNA detected can also be represented by 'fold difference' to allow comparison between different samples. This difference was calculated using the following formula:

$$\text{Fold difference} = 2^{-((\delta Ct \text{ housekeeping gene}) - (\delta Ct \text{ Bfl-1}))}$$

$$\text{I.e. Fold difference} = 2^{-((\text{actin}^{\text{control}} - \text{actin}^{\text{target}}) - (\text{Bfl-1}^{\text{control}} - \text{Bfl-1}^{\text{target}}))}$$

This calculation converts the Ct numbers into a representative view of the quantity of Bfl-1 mRNA present in different cells or different conditions.

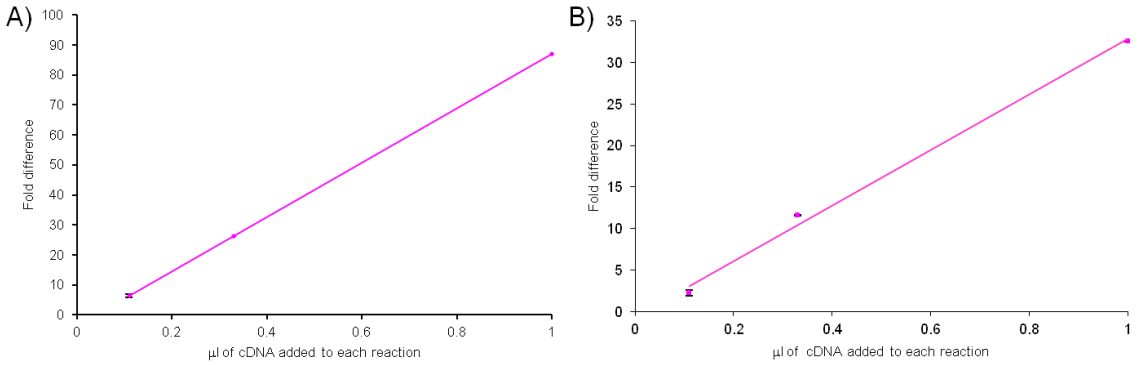

Figure 3.3: Sensitivity of Taqman qPCR probes in a melanoma cell-line.
Total RNA was extracted from untreated UACC62 cells in culture and 5µg was converted to cDNA. A) Bfl-1 cDNA was amplified by qPCR using Taqman primers (Invitrogen). B) Actin cDNA was amplified as the internal control for cDNA quantity. A titration of three-fold difference in concentration of cDNA was performed to analyse the quantitative accuracy of the Taqman probe for Bfl-1.

Having established the reliability and linearity of the assay, Taqman qPCR was used to determine the levels of Bfl-1 mRNA in the panel of melanoma cell-lines and the lymphoma cell-line, Raji (Figure 3.4). As before, Colo205 was used as a negative control for Bfl-1 and actin was the internal control for the quantity and quality of cDNA present in each qPCR reaction. Taqman qPCR showed that levels of Bfl-1 mRNA expression varied more in the melanoma cell-lines than could be observed by RT-PCR, but with a similar pattern of expression. Bfl-1 mRNA was expressed at the highest level in SkMel28 cells, followed by UACC62, then MM200 and G361, with SkMel31 expressing less Bfl-1, in accordance with the RT-PCR. The lymphoma cell-line Raji expressed less Bfl-1 than these melanoma cell-lines, but Bfl-1 was still present in these cells at a higher level than in the melanoma cell-line A375.

To confirm that actin was a reliable housekeeping gene for comparing the quality and quantity of cDNA in the different cell types, we assessed a wide panel of potential housekeeping genes using a plate of Taqman probes. The concentration of cDNA was measured using nanodrop technology (as detailed in section 2.4.7) before samples were loaded onto the plate, ensuring that the cDNA samples obtained from all three cell-lines were at the same concentration. From this, actin was determined to be expressed at a relatively consistent level over the different melanoma cell-lines (Figure 3.5). Interestingly, other commonly used housekeeping genes, such as GAPDH, showed much greater variation. Through early experiments, both at the cDNA and protein level, actin was consistently expressed at very similar levels across all the cell-lines tested. As such, we routinely used actin as an internal control for the quantity and quality of both cDNA and protein added to each experiment.

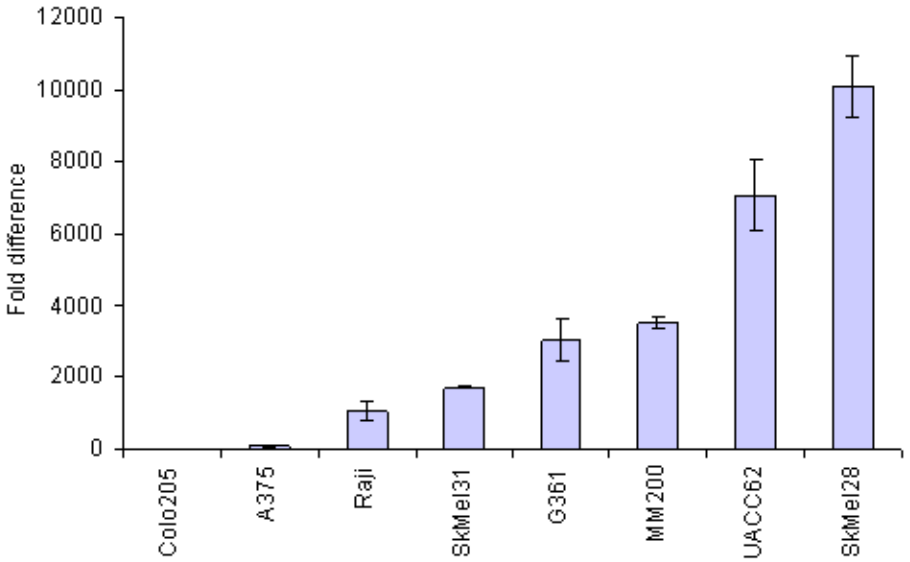

Figure 3.4: Relative levels of Bfl-1 mRNA in a panel of melanoma cell-lines.
Total RNA was extracted from untreated cells (Colo205, Raji, A375, SkMel31, G361, MM200, UACC62 and SkMel28) in culture and converted to cDNA which was then amplified by qPCR with Taqman primers. Levels of Bfl-1 cDNA were normalised with levels of actin cDNA and standardised to levels of Bfl-1 in Colo205. Error bars are standard deviations of triplicate reactions.

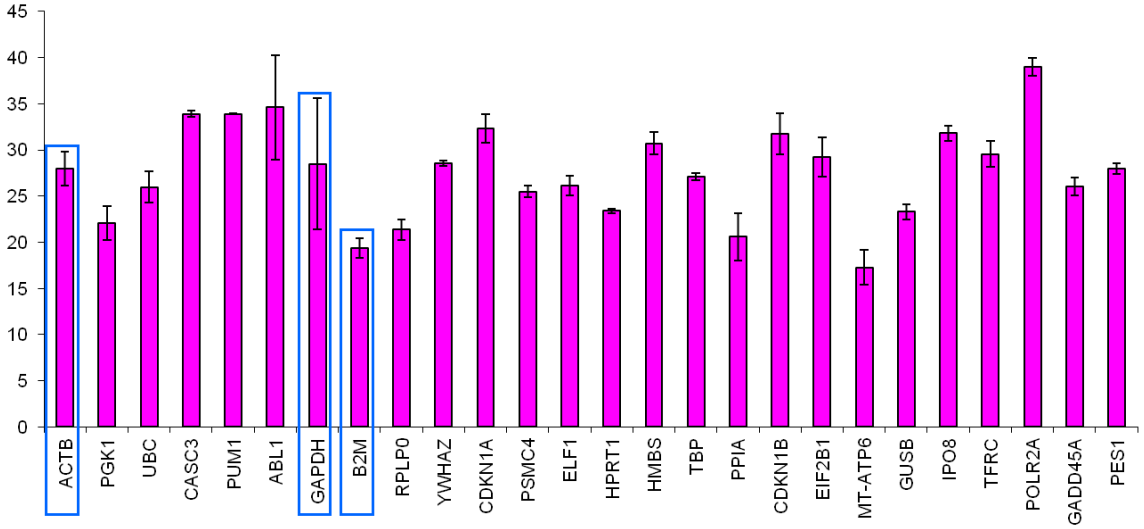

Figure 3.5: Housekeeping genes for Taqman qPCR.
An array of taqman probes for housekeeping genes was tested across three cell-lines to determine which genes could be used as reliable controls for the quantity of cDNA added to each qPCR reaction. The genes marked by blue boxes are the ones most commonly used in research (ACTB is β-actin). Error bars represent the standard deviations of all three cell-lines combined across two independent experiments, resulting in duplicate samples for each cell-line with each gene.

Having determined the expression patterns of Bfl-1 mRNA and the presence of both the full-length and short isoforms in melanoma cells, we confirmed that the bands seen on the RT-PCR gel were indeed Bfl-1 and Bfl-1S by sequencing the cDNA.

3.3 Sequencing Bfl-1 mRNA in Melanoma Cells

We sequenced Bfl-1 cDNA obtained from our panel of melanoma cell-lines and compared the sequence to the published sequence of Bfl-1. Total RNA was obtained from untreated cells in culture and converted to cDNA. The Bfl-1 cDNA was amplified by PCR using primers designed specifically for human Bfl-1, and the bands were separated by gel electrophoresis to facilitate extraction of the Bfl-1 product. This amplified product was then ligated into the blunt ended TOPO vector (Invitrogen), transformed into TOP10 bacteria and colonies were grown on agar plates overnight. TOPO is a linearised vector which has a 3' deoxythymidine (T) overhang which complements the 3' deoxyadenine (A) overhang generated by *Taq* during PCR. The 3' T overhang in the vector is activated by a covalent bond with topoisomerase I. As topoisomerase I is already present within the vector, the ligation of the DNA of interest can be performed very quickly and efficiently. The construct can then be transformed into the competent bacteria strain TOP10 E.coli (Invitrogen). The TOPO vector also includes resistance genes for ampicillin and kanamycin for selection of positive bacterial colonies containing the insert when grown on an agar plate containing one of these antibiotics.

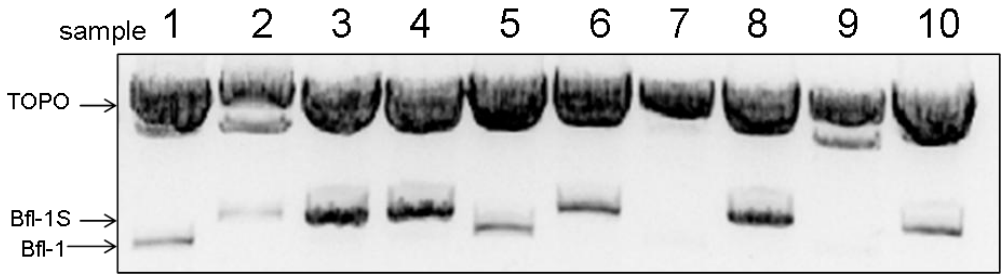

Figure 3.6: Restriction digest for Bfl-1 from the cell-line UACC62.
Total RNA was isolated from untreated cells, converted to cDNA and Bfl-1 cDNA was amplified by PCR. The amplified product was ligated into the blunt TOPO vector and subjected to restriction digest with EcoRI. Samples which contained bands of the correct size for Bfl-1 cDNA were then sequenced. Both Bfl-1S (samples 2, 3, 4, 6 and 8) and full-length Bfl-1 (samples 1, 5 and 10) were observed.

Twenty-four hours after the transformed TOP10 bacteria were spread on agar plates containing ampicillin, colonies were picked and grown up in LB broth until sufficient bacteria existed to perform minipreps to isolate the plasmid DNA. Ten colonies for each plasmid were then assessed by restriction digest using EcoRI, sites for which are present at both sides of the insert site in the TOPO vector, (Figure 3.6) to identify if they contained the inserted PCR product. DNA from colonies which had the correct sized product were then sequenced using T7 and sp6 primers, the sequences of which are present in the TOPO

vector on either side of the insert site. A typical result, shown for UACC62 cells is indicated in Figure 3.6.

As indicated previously (Figure 3.1) both full-length Bfl-1 and Bfl-1S size products were observed in most cell-lines (SkMel28, SkMel31, UACC62, G361 and Raji) and this was confirmed by sequencing. Sequencing determined that the smaller band was indeed full-length Bfl-1 and that the larger band included the 56 base pair insert which represents exon 2 and codes for the shorter Bfl-1S isoform. Sequencing also revealed that all the melanoma cell-lines tested, except for MM200 cells, contained three previously documented polymorphisms in some, if not all, of the ten samples tested [442]. I have labelled these polymorphisms relating to their position within the coding region of the Bfl-1 gene, G056A, T117G and G245A. These polymorphisms have been documented previously in the SNP database (http://www.ncbi.nlm.nih.gov/snp) and all of them result in an amino acid change (Table 3.2). Studies of the population frequencies of these three SNPs show that in general they are present at similar levels in Caucasians and Asians but at lower levels in Africans (http://hapmap.ncbi.nlm.nih.gov). In Caucasian populations, the SNPs exist either all together or not at all, with the major GTG allele being present in 71% of people, meaning only 29% of the Caucasian population expresses the minor AGA allele (see Appendix B). However, in the Asian and African populations, more combinations of the SNPs are seen. In Asian and African populations, the G allele for G056A is present in a higher percentage of people than either of the other two SNPs. In fact in African populations, the T allele for T117G is present in just 43% of the population compared to 92% with the G allele for G056A and 80% with the G allele for G245A.

Table 3.2: The polymorphisms observed in Bfl-1 mRNA all result in residue changes in the protein.
Reports for each SNP can be found on the SNP website under the reference numbers in this table.

Polymorphism site	Reference SNP Cluster Report	Allele change	Residue change
G056A	rs1138357	T**G**C → T**A**C	Cys → Tyr
T117G	rs1138358	AA**T** → AA**G**	Asn → Lys
G245A	rs3826007	G**G**C → G**A**C	Gly → Asp

In the melanoma cell-lines we sequenced, the polymorphisms were either all present i.e. the minor AGA allele, or none of them were present, i.e. the major GTG allele. There were

no samples that we sequenced which contained one or two of the polymorphisms. All three polymorphisms were present in exon 1, therefore upstream of where the 56 base pair exon 2 insert appears in mRNA coding for Bfl-1S. Indeed, the presence of the polymorphisms appeared to have no correlation with the presence of the 56 base pair insert, hence the polymorphisms were present, or not, regardless of whether the mRNA coded for the full-length or the short isoform. A typical result of a sequencing reaction for a sample which contained the three polymorphisms is shown in Figure 3.7.

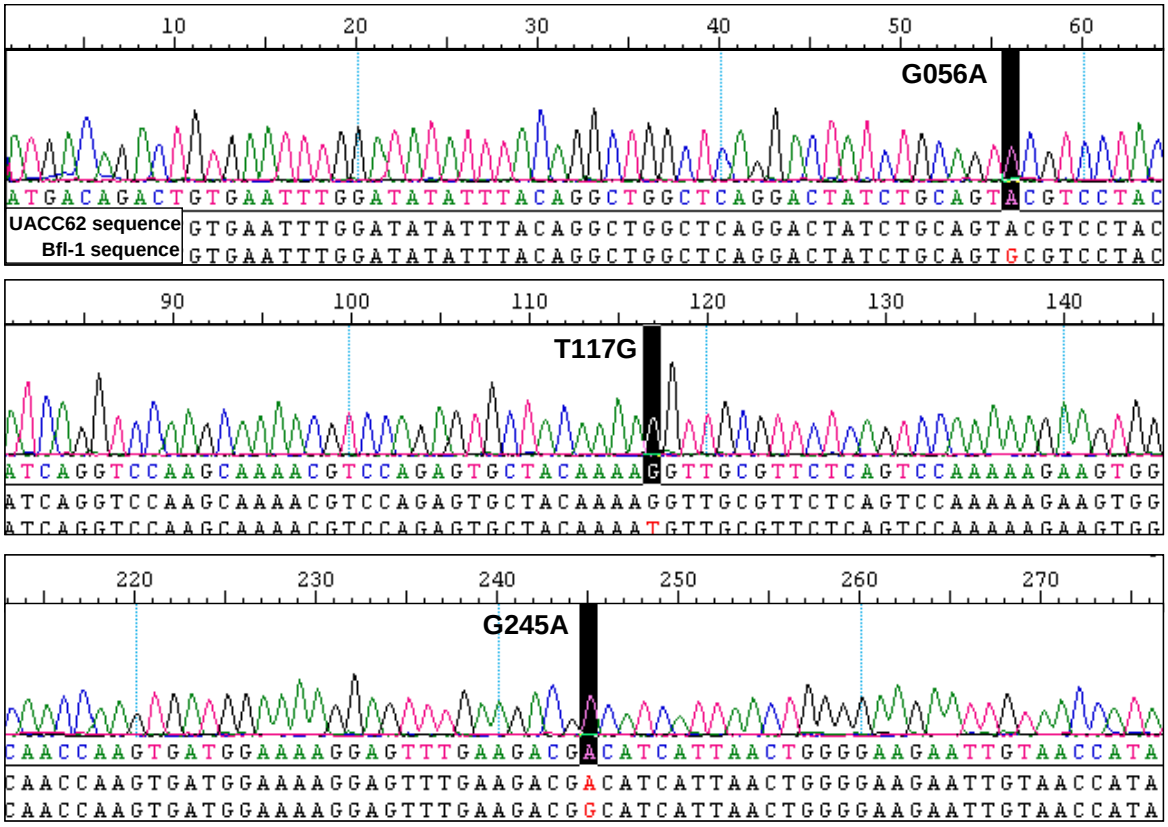

Figure 3.7: A fluorogram of a typical sequencing reaction highlights the three polymorphisms observed in melanoma cell-lines.
Presented here are the three fractions of DNA sequence containing the polymorphisms from the cell-line UACC62 compared with the known human Bfl-1 sequence. During the sequencing reaction, each nucleotide base is labelled with a different fluorophore that emits light at unique wavelengths, which is then detected by the genetic analyser and presented as a DNA sequence trace chromatograph as seen here. These data are representative of all the samples which contained the polymorphisms.

SkMel28 and SkMel31 cell-lines appeared to carry the minor AGA allele in a homozygous manner and were present in both the full-length and short isoforms from mRNA obtained from these cells. However G361 and UACC62 appeared to be heterozygous, with only some of the transcripts containing the minor AGA allele. This could mean that either the cells contain 2 different alleles, or, because mRNA was taken from multiple cells, some of the cells contained the SNPs while others did not. Although the shorter isoform was not observed in successfully sequenced samples from UACC62 or G361, our previous PCR

indicated that these cell-lines do express both isoforms, and bands representing both of the isoforms were observed after restriction digest in both cell-lines (Figure 3.6). Interestingly, the MM200 cells appeared to contain none of the polymorphisms in any of the samples, and, again agreeing with our previous PCR, only had mRNA coding for the full-length protein. Unfortunately, the PCR band seen for A375 cells could not be analysed as not enough Bfl-1 mRNA could be isolated from these cells to be converted into cDNA for sequencing. A summary of the presence of the polymorphisms, and the 56 base pair insert, in the melanoma cell-lines tested is presented in Table 3.3.

Table 3.3: A summary of the presence of polymorphisms found in Bfl-1 mRNA isolated from melanoma cell-lines.
Ten colonies from the cDNA from each melanoma cell-line were sequenced and the frequency of the polymorphisms was determined. In addition, the number of colonies expressing the Bfl-1S isoform was assessed.

Cell-line	Contained polymorphisms	Contained no polymorphisms	Bfl-1 sequence	Bfl-1S sequence
SkMel28	10	0	9	1
MM200	0	10	10	0
UACC62	6	4	10	0
G361	6	4	10	0
SkMel31	10	0	6	4

Having characterised the existence of the major and minor alleles, and the different full length and short isoforms, we examined whether they correlated with the mRNA expression pattern seen across the cell-lines. This analysis revealed that MM200 was the only cell-line which contained only the major allele and none of the shorter isoform, but the level of Bfl-1 mRNA was not significantly different from the other melanoma cell-lines. Additionally, although SkMel28 and SkMel31 appeared to always contain the polymorphisms, they have completely different expression levels, with SkMel28 having very high levels of Bfl-1 mRNA while SkMel31 has much lower levels. G361 and UACC62 both contained the minor allele in 60% of our samples, but the level of mRNA was different between them and therefore we concluded that the polymorphisms had no effect on the expression level of mRNA in melanoma cells.

However, each polymorphism results in an amino acid change in the resultant protein, with a bulkier side chain for G245A where a glycine is replaced with aspartic acid and G056A where cysteine is replaced by tyrosine. The T117G polymorphism results in an asparagine

replaced with lysine which is neither significantly more bulky, nor a change in charge. In fact, the only polymorphism that results in any charge change is G245A, which results in a more hydrophilic amino acid. As such, it is difficult to predict the effect these polymorphisms would have on the structure, function or regulation of the protein, especially given the fluid structure displayed by Bfl-1 [416]. However, the G245A polymorphism exists in the BH1 domain which forms part of the hydrophobic pocket in Bfl-1, which could be important in effecting the function of the protein. The other polymorphisms exist in the coding region between BH domains.

Having mapped these polymorphisms and the presence of both isoforms in most of our melanoma cell-lines, we were able to go on to examine whether they bore any relationship to the expression pattern of the protein, the half lives of the mRNA and protein and the regulation of the transcription and degradation of Bfl-1. To begin with, we examined the expression levels of Bfl-1 protein in the melanoma cell-lines to determine whether any relationship existed between the presence of the polymorphisms, or the ratio of full-length Bfl-1 and Bfl-1S, and the expression levels of the protein in melanoma.

3.4 The Expression of Bfl-1 Protein in Melanoma

It was interesting to observe how the levels of Bfl-1 mRNA varied across the melanoma cell-line panel and hence, I explored whether the protein levels correlated with mRNA expression pattern or the presence of the polymorphisms or different isoforms. Levels of Bfl-1 protein were determined by western blot using a rat monoclonal antibody specific for Bfl-1 (Gift from Professors Strasser and Huang, WEHI, Australia). Lysates were made from untreated cells in culture and 25μg of protein per sample was separated by SDS-PAGE and then subjected to analysis by western blot with actin as the internal control for the quantity of protein loaded (Figure 3.8). It was clear from the western blot that the levels of Bfl-1 protein also varied amongst the melanoma cell-lines. Bfl-1 protein was barely detectable in A375 cells, but it could be seen at high levels in SkMel28, UACC62, MM200 and G361 cells. Unfortunately, we cannot tell whether the Bfl-1 antibody can specifically detect both the full-length and short isoforms of the protein. The two isoforms are only 12 amino acids different in length, and we have not seen two distinct bands with this, or any of the commercially available Bfl-1 antibodies we tested.

To help make quantitative comparisons of protein expression levels we performed densitometry on the western blots using the UVP BioImager and the associated VisionWorks software with densitometry analysis. During this procedure, the density of

the Bfl-1 band was compared to the density of the control actin band and the relative amounts of Bfl-1 protein in each lane could be calculated. This analysis gives a more quantitative measure of the relative protein expression levels than the visualisation of the bands and also allows data from more than one western blot to be visualised as an average with standard deviations calculated, although it is not as reliably quantitative as Taqman qPCR. However, densitometry confirmed that SkMel28 cells had the highest level of Bfl-1 and so in each western blot the SkMel28 cell-line was taken as 100% and the other cell-lines were calculated as a percentage of Bfl-1 protein present compared to SkMel28. According to this analysis, MM200, UACC62 and G361 express around 30% less Bfl-1 than SkMel28 cells. This analysis also initially suggested that A375 cells expressed about 80% less Bfl-1 than SkMel28 cells, but this appeared to be an over-estimation of its expression due to background noise, as there was no clear band present. Hence, we stated that A375 cells had no Bfl-1 protein and took the densitometry of the A375 lane as being background noise. We recalculated the Bfl-1 levels to account for the background noise and found that MM200, UACC62 and G361 expressed about 40% less Bfl-1 than SkMel28 cells.

In summary, the level of Bfl-1 protein found in the cells was consistent with the level of Bfl-1 mRNA. As such, A375 cells contained the lowest levels of both Bfl-1 mRNA and protein, whereas SkMel28 cells contained the highest. However this association between mRNA and protein was not always direct as UACC62 cells expressed higher levels of mRNA than MM200, but they expressed very similar levels of the protein.

Typically, the expression level of each pro-survival protein is related to the expression levels of the rest of the Bcl-2 family. Hence, we explored the expression levels of the other four pro-survival members of the Bcl-2 family (Mcl-1, Bcl-2, Bcl-xl and Bcl-w) in our panel of melanoma cell-lines, and the colorectal cell-line Colo205 (Figure 3.9). The Bcl-x proteins were very uniformly expressed over the melanoma cell-lines. But interestingly, A375 cells, which express very low levels of Bfl-1, expressed a much higher level of Mcl-1 protein than any of the other cell-lines examined. It was also interesting to note that Colo205 cells, which have undetectable levels of Bfl-1 also expressed a much higher level of another pro-survival protein than the other cell-lines, Bcl-xl. Bcl-2 and Bcl-w were both expressed fairly consistently over all four cell-lines examined. Indeed, apart from the special cases in A375 and Colo205 respectively, Mcl-1 and Bcl-xl were also consistently expressed over the cell-lines. This high expression level of another pro-survival protein may explain why A375 had much lower levels of Bfl-1 than the other melanoma cell-lines.

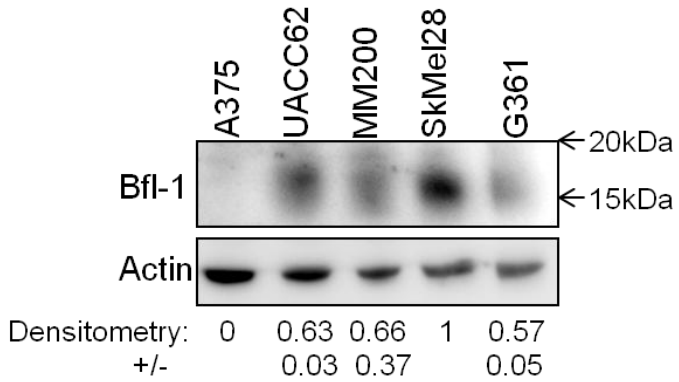

Figure 3.8: Bfl-1 protein expression in a range of melanoma cell-lines.
Cell lysates were generated from untreated cells in culture and 25μg of protein was separated by SDS-PAGE and assessed by western blot. The membrane was analysed and densitometry performed using the UVP BioImager and VisionWorks software. These data are representative of two experiments.

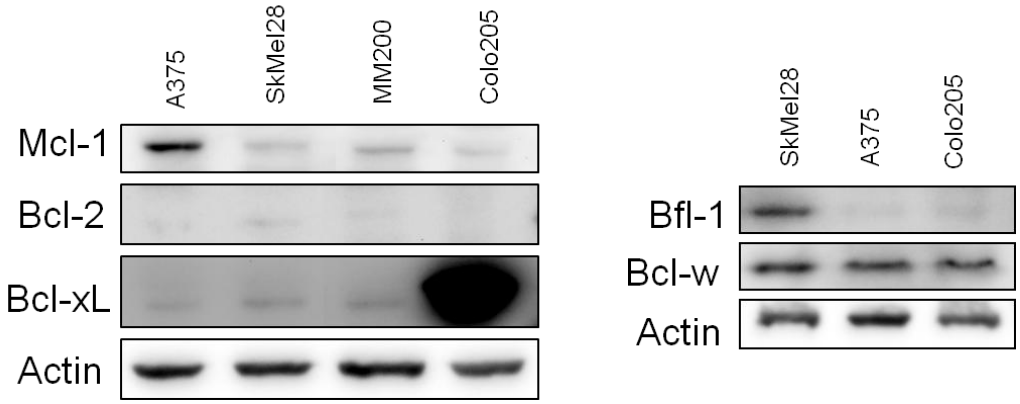

Figure 3.9: Pro-survival protein expression in a range of melanoma cell-lines.
Cell lysates were obtained from untreated cells, separated by SDS-PAGE and analysed by western blot. Two separate membranes were necessary to assess the expression of Bcl-w and Bcl-xL which are detected at the same size and by the same secondary antibody. These data represent three independent experiments.

3.5 The Half Lives of Bfl-1 mRNA and Protein in Melanoma Cells

To investigate the half life of Bfl-1 mRNA and protein in our panel of cell-lines, we used Actinomycin D and cycloheximide (CHX), respectively. Actinomycin D prevents the elongation of the mRNA chains by interfering with the RNA polymerase II enzyme. CHX prevents protein synthesis by inactivation of the enzyme transferase II which is responsible for peptide chain elongation.

The half life of Bfl-1 mRNA in two melanoma cell-lines, MM200 and SkMel28 was examined (Figure 3.10). To assess the half life of Bfl-1 mRNA, cells were treated with Actinomycin D at 10μg/ml for 1, 2, 4 or 6 hours or cells were left untreated. RNA was

extracted from the cells, converted into cDNA and Bfl-1 mRNA expression was assessed by qPCR with the Bfl-1 Taqman probe. Actin mRNA was amplified as the internal control for the quantity of cDNA loaded into each reaction and there was no evidence that actin mRNA was degraded through the experiment. These experiments revealed that the half life of Bfl-1 mRNA in SkMel28 cells was about 5 hours, whereas in MM200 cells, it was shorter, at around 2 hours.

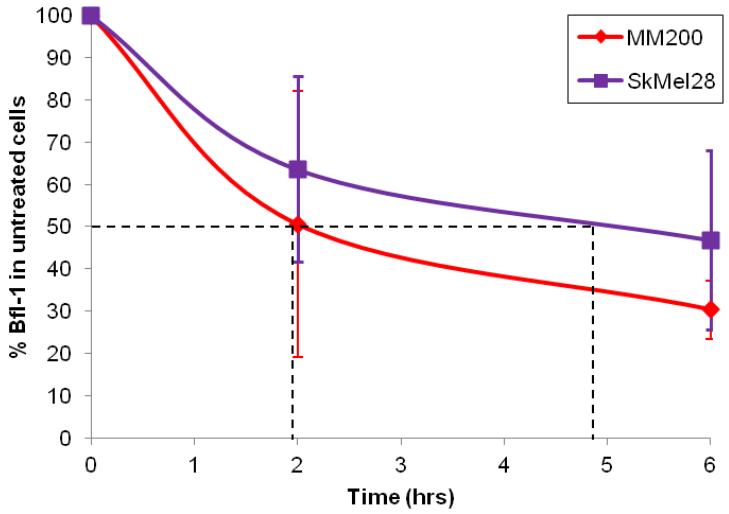

Figure 3.10: The half life of Bfl-1 mRNA determined by qPCR.
The melanoma cell-lines MM200 and SkMel28 were treated with Actinomycin D at 10µg/ml for 1, 2, 4 or 6 hours. Total RNA was extracted from the cells and converted to cDNA and qPCR was performed with the amount of Bfl-1 mRNA calculated as a percentage of that seen in untreated cells. The graph is representative of 3 experiments with each reaction performed in triplicate. The error bars represent the standard deviation from the mean across the independent experiments.

Subsequently, the half life of the Bfl-1 protein was determined in the two melanoma cell-lines (MM200 and SkMel28) (Figure 3.11). After treatment with CHX at 10µg/ml for 1, 2, 4, 6, 12 or 24 hours, cells were subjected to lysis, then the proteins were separated by SDS-PAGE and analysed by western blot. The Bfl-1 protein could not be detected after 12 hours in either melanoma cell-line and even after 1 hour there appeared to be less protein present in both cell-lines. This was in contrast to the loading control, actin, which appeared relatively stable throughout the experiment. Therefore, densitometry analysis of the western blots could be used to calculate the approximate half life of Bfl-1 in the melanoma cell-lines by normalising the level of Bfl-1 against the loading control, actin (Figure 3.12). The graphs in Figure 3.12 represent the amount of Bfl-1 protein as a percentage of that seen in untreated cells after subtracting the background signal from the membrane.

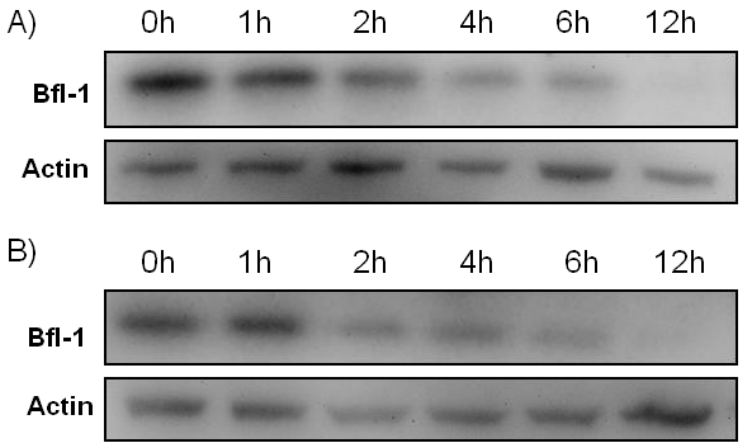

Figure 3.11: The half life of Bfl-1 protein in two melanoma cell-lines determined by western blot.
The melanoma cell-lines MM200 (A) and SkMel28 (B) were treated with cycloheximide at 10µg/ml for the indicated times. Cell lysates were generated and the proteins were separated by SDS-PAGE and Bfl-1 and actin were detected by western blot. These data are representative of three independent experiments.

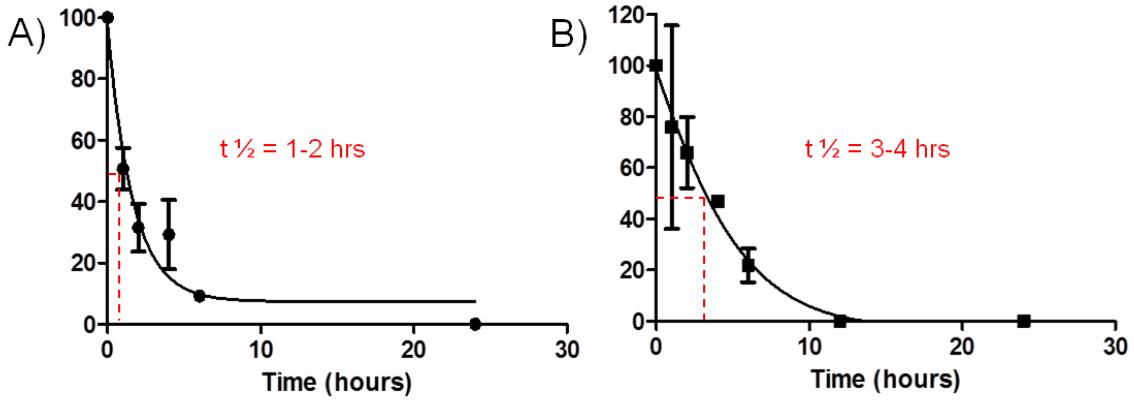

Figure 3.12: The half life of Bfl-1 protein in melanoma cell-lines as determined by densitometry.
MM200 (A) and SkMel28 (B) Cells were treated with cycloheximide at 10µg/ml for a series of time points. Cell lysates were generated and the protein was separated by SDS-PAGE and detected by western blot. The western blots were quantified using UVP BioImager and VisionWorks software to determine the half life of Bfl-1. Error bars represent the standard deviation from the mean from four independent experiments with MM200 (A) and from three independent experiments with SkMel28 (B).

These experiments looking at the half life of Bfl-1 mRNA and protein in melanoma cells revealed that in MM200 cells, both Bfl-1 mRNA and protein had shorter half lives than in SkMel28 cells. They also revealed that the half-lives of the mRNA and protein were not significantly different, with only a slightly shorter protein half life than mRNA half life.

We also looked at the half life of Bfl-1 mRNA and protein in the lymphoma cell-line Raji. Lymphoma cell-lines were also highlighted by the NCI60 microarray to express Bfl-1

mRNA, so we used Raji cells to obtain a comparison between the half lives in melanoma cells and a different cancer. The half life of Bfl-1 mRNA and protein in this lymphoma cell-line was longer than was seen in either melanoma cell-line tested. The mRNA half-life in Raji cells appeared to be over 6 hours and the protein was still present after 96 hours with a half life of over 48 hours (Figure 3.13). The half life of Bfl-1 protein and mRNA in melanoma cell-lines and the lymphoma cell-line are summarised in Table 3.4. MM200 cells consistently displayed the shortest half lives for both the mRNA and protein and Raji cells consistently displayed the longest. Only in the Raji cells did the half life of the protein appear to be longer than the half life of the mRNA, suggesting that the protein is more stable in the lymphoma cell-line than in the melanoma cells.

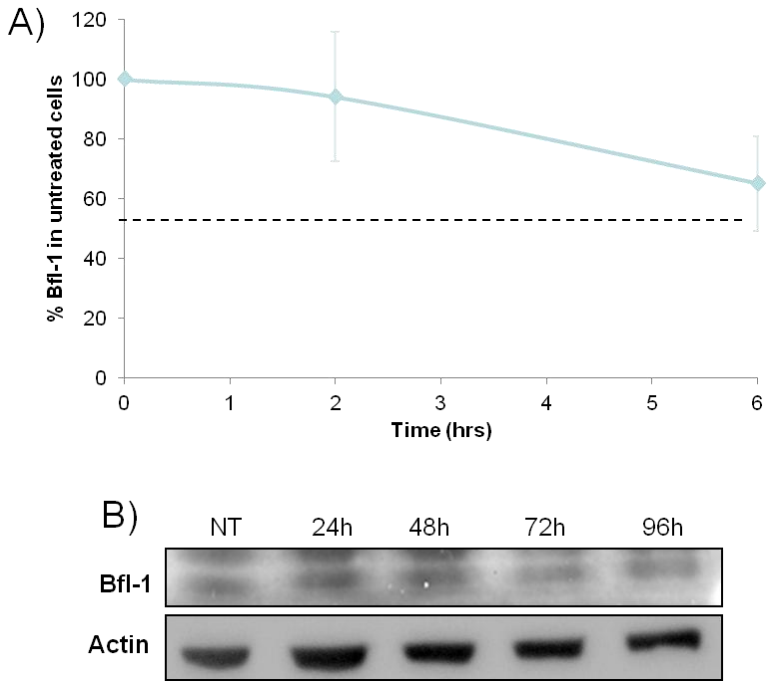

Figure 3.13: The half life of Bfl-1 mRNA and protein in the lymphoma cell-line Raji. A) Cells were treated with actinomycin d at 10mg/ml for 0, 2 or 6 hours. Total RNA was then extracted from the cells, converted to cDNA and subjected to qPCR with Taqman probes for Bfl-1 and actin. These data are representative of 3 independent experiments, each experiment performed in triplicate, with the error bars representing standard deviations between experiments. B) Cells were treated with cycloheximide at 10μg/ml for a series of time points. Cell lysates were generated and the proteins were separated by SDS-PAGE and detected by western blot. These data are from one experiment.

Table 3.4: The half lives of Bfl-1 mRNA and protein.
The half life of the mRNA was calculated from analysing qPCR data after cells were treated with Actinomycin D at 10μg/ml, total RNA was extracted and converted to cDNA. The half life of Bfl-1 protein was calculated from densitometry analysis of data from western blots where cells were treated with cycloheximide at 10μg/ml.

	Half life of Bfl-1 mRNA	Half life of Bfl-1 protein
MM200	2 hours	1-2 hours
SkMel28	5 hours	3-4 hours
Raji	>6 hours	>48 hours

To explore how the half life of Bfl-1 related to the other pro-survival Bcl-2 family members, the half lives of the other pro-survival proteins were investigated in SkMel28 cells by western blot (Figure 3.14). Lysates were taken from cells in culture treated with CHX at 10μg/ml for 2, 6, 24 or 48 hours and the western blots were probed for the pro-survival proteins. Both Bcl-2 and Bcl-xL displayed very long protein half lives compared to Bfl-1 within these cells. Indeed, the half life of Bcl-2 appeared to be somewhere between 6 hours and 24 hours, whereas the level of Bcl-xL did not seem to drop significantly even after 48 hours of treatment with the protein synthesis inhibitor. Mcl-1 was not detectable at significant levels in these cells for its half life to be analysed, and Bcl-w was not probed for as its band was present at the same size as Bcl-xL and both the primary antibodies for these proteins used the same secondary antibody.

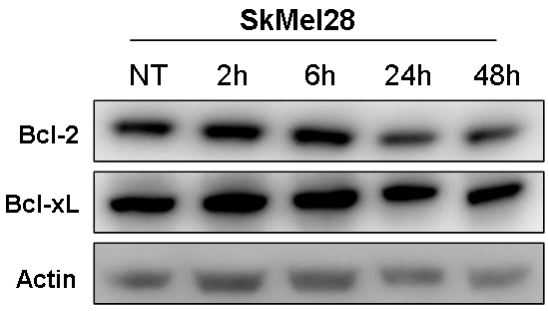

Figure 3.14: The half lives of the pro-survival proteins of the Bcl-2 family in melanoma cells.
The melanoma cell-lines SkMel28 and UACC62 were treated with cycloheximide at 10μg/ml for the indicated times. Cell lysates were generated; the proteins were separated by SDS-PAGE and detected by western blot. These data are representative of one experiment.

3.6 Degradation of the Bfl-1 Protein in Melanoma Cells

The half life of Bfl-1 tagged with GFP in FL5.12 pro-B-cells has been shown previously to be 2-3 hours, controlled by ubiquitin-proteasome turnover [406]. Hence, we investigated whether inhibition of the proteasome by the proteasome inhibitor MG132 would prevent the degradation of the untagged Bfl-1 protein in melanoma cells.

To explore this post-translational protein regulation, we added MG132 to cells at 50μg/ml, 10μg/ml and 2μg/ml for 12 hours (Figure 3.15). As a positive control for proteasomal inhibition by MG132 and to determine the optimal dose of the inhibitor, we assessed the expression of Mcl-1 and p-IκBα, two proteins known to be targeted for degradation by the proteasome [39,443]. We observed that the levels of Mcl-1 and p-IκBα accumulated with the doses of 10μg/ml and 2μg/ml, but not at 50μg/ml, possibly due to toxicity of the inhibitor at this high dose. However, even at the doses where Mcl-1 and p-IκBα were seen to accumulate, showing the proteasome was indeed inhibited, Bfl-1 was not seen to accumulate.

However, we further explored the theory that Bfl-1 is degraded by the proteasome by determining whether inhibition of the proteasome increased the half life of the protein. We did this by adding MG132 to two melanoma cell-lines in the presence of the protein synthesis inhibitor CHX for 2, 4 or 6 hours (Figure 3.16). At each of these timepoints, we also added MG132 alone or CHX alone to use as a direct comparison for the level of Bfl-1 protein after proteasome inhibition or protein synthesis inhibition alone. Indeed, when both proteasomal degradation and protein synthesis were inhibited, the half-life of the protein was seen to increase significantly when compared to the samples from cells with only protein synthesis inhibition. In fact, the half life increased from 1-2 hours in MM200 and 4-5 hours in SkMel28 to over 6 hours in both cell-lines (determined by densitometry from three independent experiments, data not shown). In MM200 cells when only MG132 was added, an accumulation of the protein was consistently observed at 4 hours but was seen to decrease again by 6 hours. However there was a steady accumulation of Bfl-1 observed in SkMel28 cells over time. This accumulation might not have been picked up in Figure 3.15 because by 12 hours (or in fact by 6 hours in MM200 cells) other factors, such as calpains, may become activated to degrade the protein [406].

In summary, these data indicates that the proteasome does indeed have a role to play in the degradation of the protein in melanoma cells, because the stability of the protein increases

when the proteasome is inhibited, giving it a longer half life, even if the levels do decrease eventually. Having explored the post-translational regulation of Bfl-1 in melanoma cells, we explored the signalling pathways involved in the regulation of Bfl-1 expression.

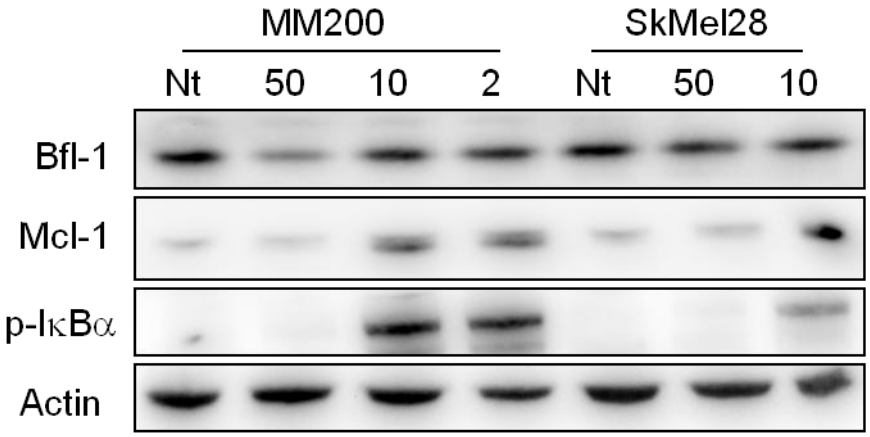

Figure 3.15 The pro-survival protein Mcl-1 and p-IκBα accumulate in the presence of the proteasome inhibitor MG132.
MG132 was added to the melanoma cell-lines MM200 and SkMel28 for 12 hours at 50μg/ml, 10μg/ml and 2μg/ml. Cell lysates were generated, the proteins were separated by SDS-PAGE and analysed by western blot. These data are representative of three experiments for Bfl-1 and one experiment for Mcl-1 and p-IκBα.

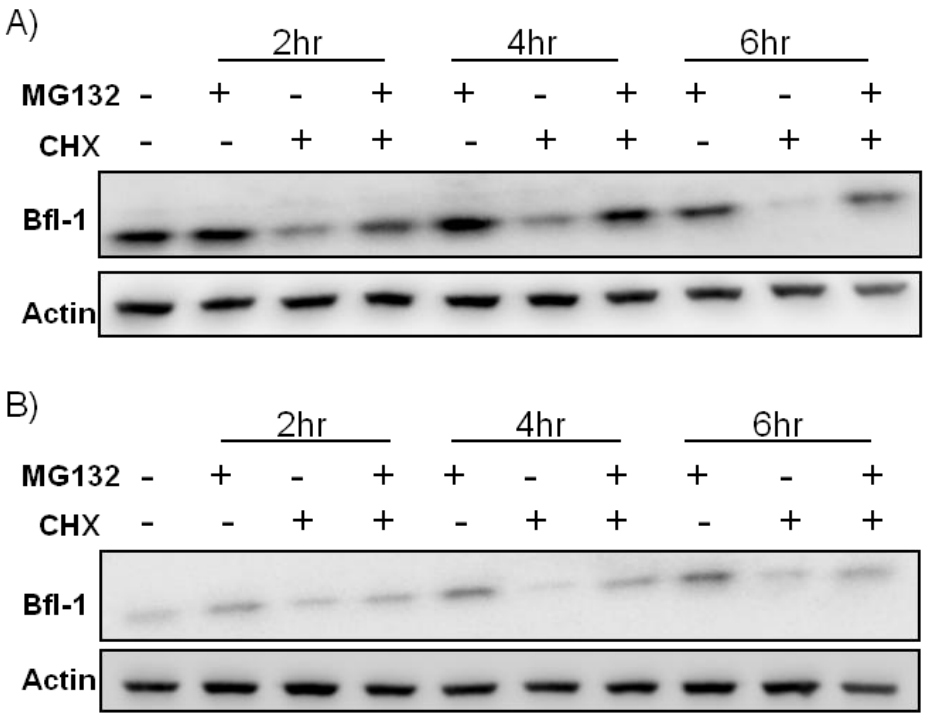

Figure 3.16: The proteasome inhibitor MG132 increases the half life of Bfl-1 protein in melanoma cells.
Two melanoma cell-lines (MM200 (A) and SkMel28 (B)) were treated with MG132 at 10μg/ml and/or CHX at 10μg/ml for the times indicated. Cell lysates were generated, the proteins were separated by SDS-PAGE and analysed by western blot. These data are representative of three experiments.

3.7 Determination of the Signalling Pathways Important in Bfl-1 Regulation

To assess which signalling pathways are important for Bfl-1 expression in melanoma cells we employed a series of well-established pathway selective inhibitors and explored the effect they had on Bfl-1 mRNA and protein expression.

Initially we explored inhibition of the NFκB pathway to confirm previous work by Zong et al.[235] who used northern blotting to demonstrate that the transcription of Bfl-1 was regulated through this pathway across a selection of cell types including T- and B-cells. Other groups have confirmed this work in a variety of cell types, including cancer cells [59,398,399]. However at the protein level they have had to use tagged protein due to the lack of high quality commercial antibodies for Bfl-1, and to our knowledge, this regulation has never been confirmed in melanoma cells.

The NFκB pathway inhibitor BAY 11-7082 was added to two melanoma cell-lines, MM200 and SkMel28, at 10μM, 2μM and 0.08μM for 24 hours (Figure 3.17A). Cell lysates were generated and the level of Bfl-1 protein was examined by separation of proteins by SDS-PAGE and detection by western blot. BAY 11-7082 works by inhibiting the phosphorylation of IκBα which is responsible for the activation of NFκB, as demonstrated in Figure 3.17C. Treatment of cells with BAY 11-7082 was seen to decrease the levels of Bfl-1 expression at the highest dose of 10μM and the middle dose of 2μM. In SkMel28 cells Bfl-1 expression was equal to that seen in the untreated cells at the lowest dose of the inhibitor, but in MM200 cells, Bfl-1 was still expressed at a lower level than in untreated cells. We also inhibited this pathway using an IKK inhibitor (Calbiochem, IKK2 inhibitor IV), which inhibits the pathway upstream of IκBα (Figure 3.17C). When this inhibitor was added to the melanoma cell-lines for 48 hours at various doses, it also resulted in decreased levels of Bfl-1 protein, further confirming the importance of the NFκB pathway in the regulation of Bfl-1 in melanoma cells (Figure 3.17B).

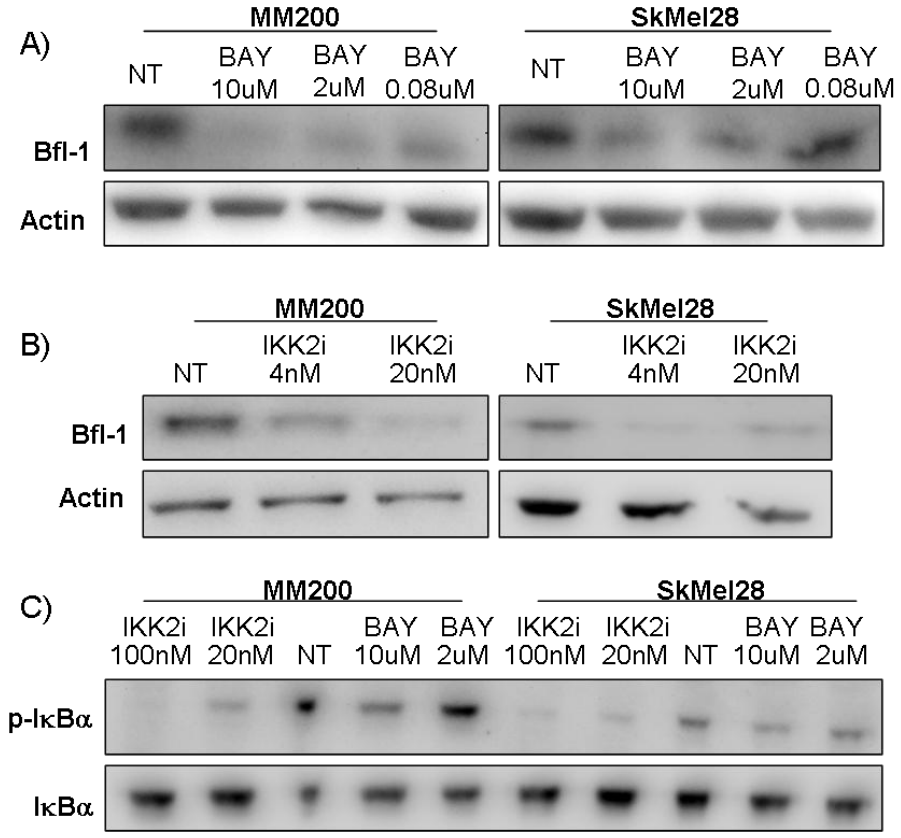

Figure 3.17: Inhibition of the NFκB pathway causes a decrease in the level of Bfl-1 expression in melanoma cell-lines.
(A) The melanoma cell-lines SkMel28 and MM200 were treated with BAY 11-7082 for 24 hours at 10μM, 2μM and 0.08μM. (B) The same cell-lines were treated with IKK2 inhibitor IV for 48 hours at 4nM and 20nM. (C) The specificity of the inhibitors was demonstrated by probing the western blot for p-IκBα after 24 hours treatment with the inhibitors. For all experiments, cell lysates were generated and the proteins were separated by SDS-PAGE and detected by western blot. Each of these data is representative of three independent experiments.

To determine whether other pathways were involved in the regulation of Bfl-1 expression, the MEK/ERK and Akt cell survival pathways were also explored using pathway-specific inhibitors. The MEK/ERK pathway was examined because 70% of melanomas carry the BRaf mutation [53]. This mutation results in a continuous growth signal through the MEK/ERK pathway, so we looked to determine if this continuous signal had any significance in the high expression of Bfl-1 in melanoma.

The melanoma cell-lines, MM200 and SkMel28, were treated with PD0325901 (PD901), a highly potent and specific inhibitor of MEK 1&2. This potent inhibition of MEK1/2 blocks the effects of the activating mutation in BRaf. PD901 was added to cells in culture at 50nM, determined as the optimal dose by previous work in the lab [343], for 24 hours or 48 hours before cell lysates were generated from the cells (Figure 3.18A). A downstream

target of BRaf and MEK1/2, phospho-ERK (p-ERK), was assessed by western blot to ensure the inhibitor was active in these cells over the time-frame measured (Figure 3.18B). The phosphorylation of ERK1/2 by MEK1/2 was shown to be inhibited by PD901 proving that the signalling pathway had indeed been inhibited. Interestingly, the inhibition of the Ras/Raf/MEK/ERK pathway appeared to have opposite effects in the two cell-lines tested, despite the fact that they both carry the BRaf mutation. In MM200 cells, the inhibition of MEK resulted in a decrease in the level of Bfl-1 protein, whereas in SkMel28, an increase of protein was routinely observed after MEK inhibition (Figure 3.18).

The Akt pathway is a parallel cell survival pathway to the MEK/ERK pathway that is also frequently upregulated in cancer cells, sometimes through the NRas mutation and sometimes through the deletion or mutation of PTEN, as in MM200 cells. Therefore, we explored the importance of this pathway on Bfl-1 expression using the Akt1/2 kinase inhibitor, Akt Inhibitor VIII (Calbiochem). The Akt1/2 inhibitor blocks the activation of Akt1 and Akt2 through their pleckstrin homology domains, leading to a decrease in the level of phosphorylated, and therefore activated, Akt, as demonstrated in Figure 3.18C. Initially, a dose range with the inhibitor was performed to determine its activity and optimal dose (Figure 3.18C) over 48 hours, and from this a dose of 1μM was determined as the optimal dose and added to cells for 24 or 48 hours before cell lysates were generated (Figure 3.18A). The effects of the Akt inhibitor were directly opposite to the effects seen with the MEK inhibitor. In MM200 cells, levels of Bfl-1 protein increased after Akt inhibition, whereas in SkMel28 cells, the levels were seen to display no difference after Akt inhibition (Figure 3.18A and Figure 3.19C). This suggests that overall Akt inhibition does not have a significant effect on Bfl-1 protein levels in either MM200 or SkMel28 cells.

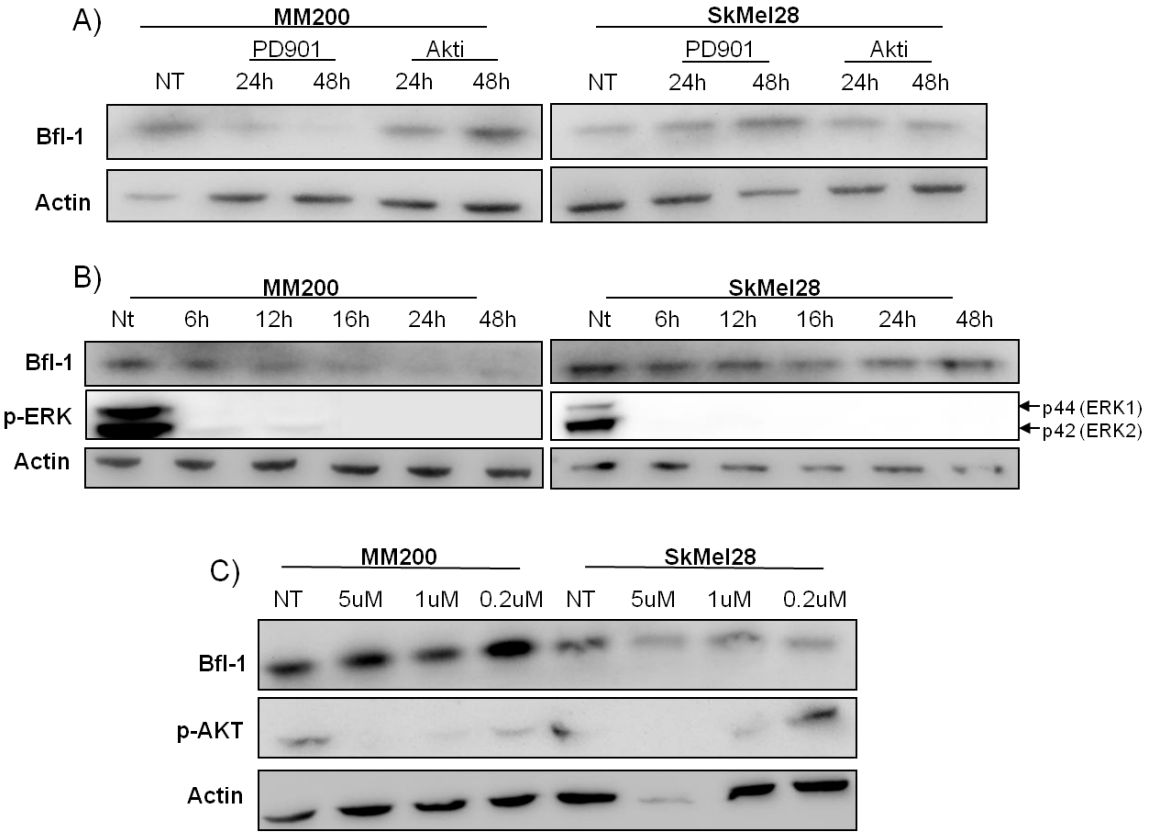

Figure 3.18: Inhibiting the MEK/ERK pathway or the Akt pathway in melanoma cells-lines.
(A) The MEK inhibitor PD901 (50nM) or the Akt inhibitor Akt1/2 (1μM) were added to two melanoma cell-lines, SkMel28 and MM200, for 24 or 48 hours. Cell lysates were generated and the proteins were separated by SDS-PAGE and detected by western blot. (B) PD901 was added to cells at 50nM for the times indicated before cell lysates were generated. (C) Akt1/2 inhibitor was added to cells at the doses indicated for 48 hours before cell lysates were generated. Each of these data is representative of at least three independent experiments.

We also explored the effects the signalling inhibitors have on the levels of Bfl-1 mRNA using Taqman qPCR. Inhibitors were added to the two melanoma cell-lines MM200 and SkMel28 at the optimal doses already described (PD901 50nM, Akt1/2 inhibitor 1μM and BAY 11-7082 2μM), for 6 or 24 hours before RNA was extracted from the cells, converted to cDNA and subjected to qPCR (Figure 3.19A and B). The results show that the level of Bfl-1 mRNA significantly drops after 24 hours in both cell-lines in the presence of the NFkB inhibitor, agreeing with the effects on the protein levels (Figure 3.17A). However the MEK inhibitor, PD901, which caused an increase in the level of protein seen in SkMel28 cells, resulted in significantly lower levels of Bfl-1 mRNA in this cell-line. In MM200 cells, where the level of Bfl-1 protein drops after MEK inhibition, no difference was seen in the levels of mRNA after addition of the inhibitor to the cells. The Akt inhibitor, which causes an increase in the level of Bfl-1 protein in MM200 cells, caused no

significant difference in mRNA levels in MM200. However there was a lower, but not statistically significant, level of mRNA in SkMel28 cells, where an associated drop in Bfl-1 protein levels was also observed.

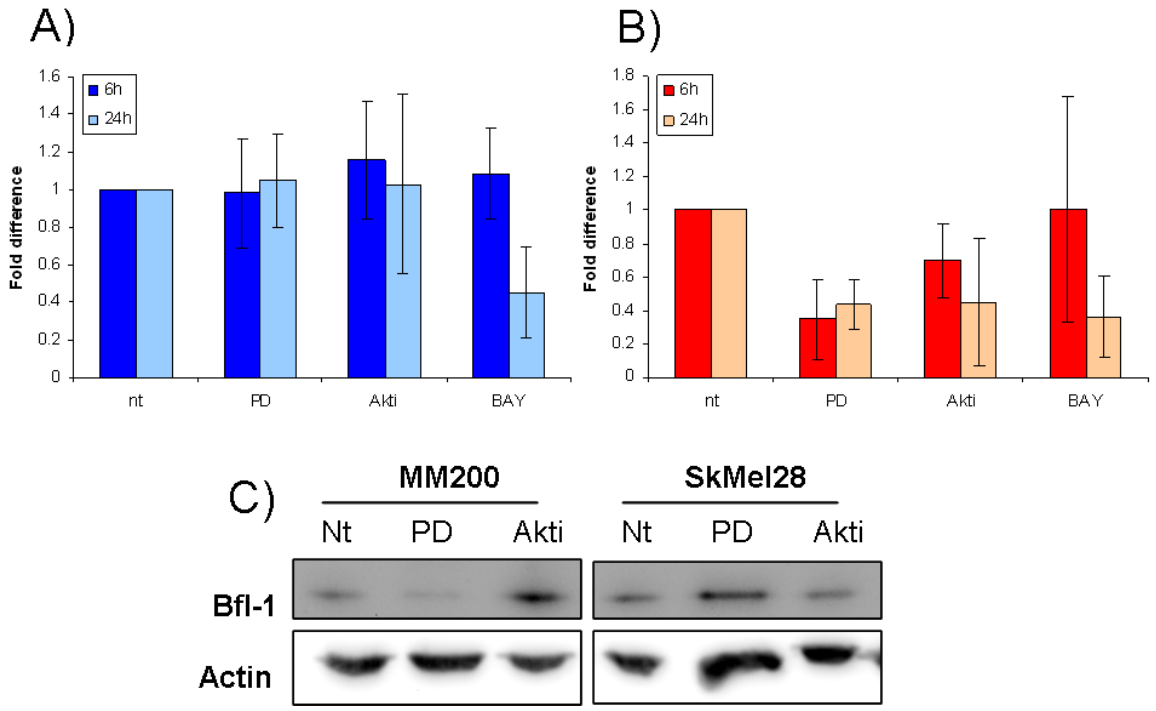

Figure 3.19: The effects of the pathway specific inhibitors on the level of Bfl-1 mRNA and protein in melanoma cells.
The MEK inhibitor, PD901, was added to cells at 50nM, the Akt1/2 inhibitor was added at 1μM and the NFκB inhibitor, BAY 11-7082, was added at 2μM. The inhibitors were left on MM200 cells (A) and SkMel28 cells (B) for 6 or 24 hours before RNA was extracted from the cells, converted to cDNA and subjected to qPCR using Taqman primers for Bfl-1. The 6 hour timepoints are representative of 2 independent experiments and the 24 hour timepoints are representative of 3 independent experiments. Each experiment was performed in triplicate and the error bars represent the standard deviation from the mean over all experiments. (B) The signalling inhibitors were added at the same doses as for the qPCR for 48 hours before cell lysates were generated, proteins separated by SDS-PAGE and analysed by western blot. These data are representative of at least 3 independent experiments.

We also explored the effects of the signalling inhibitors BAY11-7082 and PD901 on the ratio of Bfl-1 and Bfl-1S mRNA in melanoma cells (Figure 3.20A and B). Cells were treated with the drugs for a range of time-points up to 24 hours. Total RNA was extracted from the cells, converted to cDNA and subjected to RT-PCR. Although a dip in the total levels of both isoforms was seen in UACC62 cells treated with PD901, the ratio of the two isoforms remained the same. In fact, after treatment with the DNA damaging agent Etoposide and the microtubule disrupter Paclitaxel, the ratio also remained the same and the total levels also were unchanged by the presence of the drugs (Figure 3.20C and D).

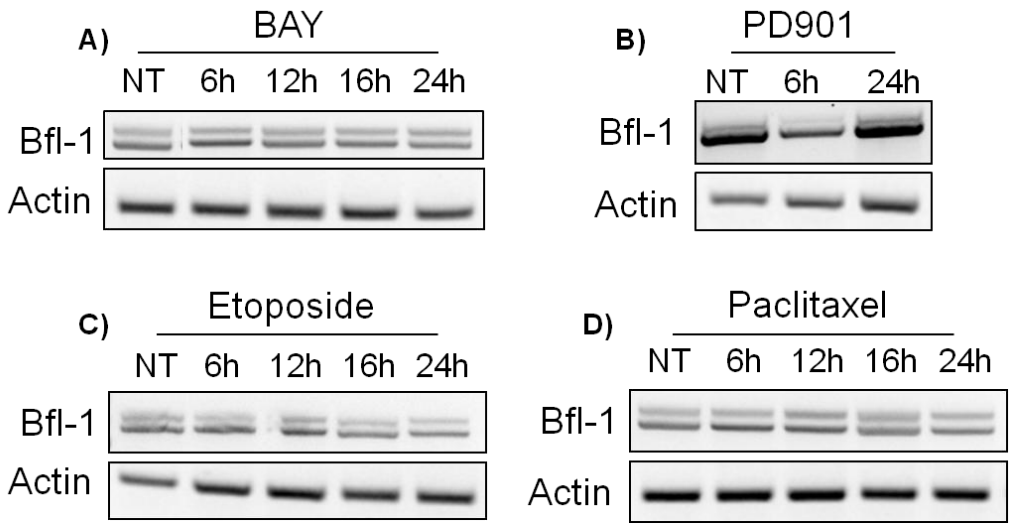

Figure 3.20: The effects of signalling inhibitors and chemotherapeutic drugs on levels of Bfl-1S in melanoma cells.
SkMel28 cells (A, C and D) and UACC62 (B) cells were treated for the times indicated with BAY11-7082 (BAY 10μg/ml), PD901 (50nM), Etoposide (10μg/ml) or Paclitaxel (10μg/ml). After treatment, total RNA was isolated from the cells and converted to cDNA. cDNA was amplified by PCR using primers specific for Bfl-1 and DNA bands were separated by gel electrophoresis. These data are representative of one experiment each.

3.8 Chapter 3 Conclusions

In this chapter, the characterisation and regulation of Bfl-1 in melanoma cells was explored by assessing the expression pattern across a range of melanoma cell-lines, the degradation of the protein by the proteasome and its regulation through the cell survival signalling pathways. The mRNA transcribed was also sequenced and the proportion of the full-length and short isoforms expressed was assessed alongside the mRNA and protein half lives.

We found that across our panel of melanoma cell-lines (with the exception of A375 cells) the Bfl-1 protein and mRNA were highly expressed (Figure 3.8 and Figure 3.4), correlating with the high and specific expression of Bfl-1 in melanoma seen in the NCI60 microarray (1). We also checked Bfl-1 expression in a Burkitt's lymphoma cell-line (Raji) as the NCI60 microarray also highlighted Bfl-1 to be expressed in lymphomas. We found, again, that our data correlated with the NCI60 microarray, as Raji cells expressed Bfl-1 protein and mRNA, but at a lower level than observed in almost all our melanoma cell-lines. Additionally, we probed a colorectal carcinoma cell-line (Colo205) for levels of Bfl-1 and found that the protein was undetectable, and the mRNA was expressed at a very low level. Hence, the expression pattern of Bfl-1 in our panel of cell-lines was consistent with that observed in the NCI60 microarray.

We also probed the panel of cell-lines for the other pro-survival proteins and found that they were generally similar over the range of melanoma cells, with Bcl-xL being expressed to a much higher level in Colo205 cells (Figure 3.9). Mcl-1 expression proved interesting, as in the melanoma cell-lines with high Bfl-1 expression, Mcl-1 was almost undetectable, yet was highly expressed in A375 cells, which have undetectable levels of Bfl-1. A possible hypothesis at this stage may be that as a cancer progresses, it becomes reliant upon a particular pro-survival protein which is then over-expressed to the extent that other pro-survival proteins become superfluous. This theory could be explored by looking at the levels of the pro-survival proteins in non-cancerous cells and by using siRNA to knock-down the over-expressed protein to determine whether this increases the sensitivity of the cancerous cells to apoptosis. However, why it is Bfl-1 which becomes over-expressed in melanoma cells is difficult to explain; Melanomas originate from melanocytes, which have been shown to rely on Bcl-2 expression for their survival [164], but have not been specifically linked to high levels of Bfl-1. However, studies have suggested that the NFκB pathway becomes activated upon transformation of the melanocyte, likely through the activation of the G-protein coupled receptor CXCR2 [444]. When mouse melanocytes were stimulated with chemokines for CXCR2, they were seen to display the ability to grow colonies on soft-agar plates, representing their tumourigenic potential [445]. Indeed, the NFκB pathway has been shown to be constitutively activated in melanoma cells [446], which would result in an increase in the expression of its transcriptional targets.

When we explored the expression levels of Bfl-1 mRNA, we observed both the long and short isoforms of the protein, which were confirmed by sequencing, in every cell-line which expressed detectable levels of Bfl-1 mRNA, except for MM200 cells which appeared to only express the longer, more common isoform (Figure 3.1). Indeed, in every other cell-line, about 30-40% of the mRNA detected belonged to the shorter isoform. The antibody for Bfl-1 protein could not distinguish between the full-length and shorter isoforms, possibly because the two isoforms are only 12 amino acids different in length, so we were unable to compare the relative expression of the two isoforms at the protein level. In fact, it is difficult to suggest a reason for the lack of Bfl-1S in MM200 cells, or to predict the effects this would have in the cells, as very little is known about the regulation of Bfl-1S expression. The only study to mention the shorter isoform apart from the characterisation study by Ko et al. [422], postulated that Bfl-1S was important in mast cell protection, as it was only present in activated mast cells, not resting ones, suggesting there could be a separate regulation system for Bfl-1S and full length Bfl-1 transcription. [378]. We

can determine whether Bfl-1S becomes activated upon tumourigenesis of melanocytes by probing primary melanocytes for the shorter isoform. Bfl-1S has been shown to compliment Bfl-1 activity by also protecting cells from apoptosis [422], so we could also determine whether in melanoma cells, the presence of Bfl-1S gives any additional protection from apoptosis by comparing the viability of MM200 cells against the other melanoma cell-lines. Additionally, as high quality antibodies for Bfl-1 are developed, perhaps the two protein isoforms will eventually be separately detectable, or an antibody will be designed specifically for exon 2, present in only the shorter isoform, and the different expression levels can be explored at the protein level.

When we sequenced the Bfl-1 mRNA transcripts from our panel of melanoma cell-lines, we found that several contained three common polymorphisms in the exon 1 region of the gene. The presence of these three single nucleotide polymorphisms (SNPs) has previously been linked with a genetic predisposition to atopic dermatitis in children by Gray et al. [442]. However, there are as yet no other studies which have explored how these SNPs might alter the function of Bfl-1. The only cell-line not found to contain the SNPs in any of the ten individual clones sequenced was MM200 (Table 3.3). The cell-lines SkMel28 and SkMel31 appeared to contain only Bfl-1 transcripts containing the three SNPs whereas G361 and UACC62 contained both the major (GTG) and minor alleles (AGA) for Bfl-1. Gray et al. also determined the presence of another polymorphism in Bfl-1 [442], within the promoter region of the gene, which is outside the region of Bfl-1 which we sequenced, as is the other known SNP which is present in the 3' untranslated region of the gene. The SNP present in the promoter region may have an effect on the transcription of the gene, and it may be that, given most of our melanoma cell-lines contain polymorphic Bfl-1, individuals expressing these SNPs, i.e. the minor allele, may have a genetic predisposition to developing melanoma, as seen with the increased likelihood of developing atopic dermatitis[442]. A large scale study of the presence of the SNPs in melanoma patients may be useful to determine this.

Population frequencies show that it is the population which is least prone to melanoma, i.e. African origin, which has on average the lowest frequencies of the SNPs. African populations have the lowest frequency of the G056A and G245A A alleles, although the highest frequency of T117G G allele. These frequencies are very different from the Caucasian population, which is the most prone to developing melanoma, where 71% of the population carry the major allele (GTG), while 29% carry the minor allele (AGA). Therefore, the presence of G056A and G245A A alleles appear to possibly be related to the

development of melanoma, but perhaps the absence of the T117G G allele, which is present in 57% of Africans but only 29% of Caucasians, is also a contributing factor. However, there are other factors, such as skin colour and the production of pigment, which are known to determine the varying sensitivities of the different populations to the development of melanoma. Therefore, the determination of whether the presence of polymorphic Bfl-1 does lend a predisposition to melanoma would have to be explored within one population, i.e the Caucasian population. One way to address this would be to use a melanoma mouse model such as the BRaf constitutively active mouse. The major or minor Bfl-1 alleles could then be knocked-in and the mice could be treated with UV to generate melanomas and determine whether mice with the minor allele for Bfl-1 were more or less sensitive to melanoma development than the mice containing the major allele for Bfl-1.

Any change in Bfl-1 function may be a consequence of the substitution of the amino acid residues resulting from each of the three SNPs we found. However, Bfl-1 protein has a fluid nature to its structure, and only one of the SNPs is present in a BH domain. This SNP is the G245A A allele, which results in a bulkier and more hydrophilic side chain being present in the hydrophobic BH3-binding pocket as a glycine is replaced by an aspartic acid. This may result in a decreased ability to bind to the BH3 domains of the other Bcl-2 family members, but this remains to be proven.

When the protein half life was elucidated, it was seen to correlate broadly with the mRNA half life (Table 3.4), at least in melanoma cells. However, in Raji cells we saw a much longer half life for the protein, suggesting that there may be cell specific post translational differences. Bfl-1 protein has a significantly shorter half life than the other pro-survival proteins of the Bcl-2 family explored, agreeing with previous studies which showed the longer half lives of the Bcl-x proteins [447]. As such, Bcl-2 has been shown to have a half life of around 10 hours [448], which appears to be similar in SkMel28 cells (Figure 3.14). The exception to this was Mcl-1 which was not detectable in cells with high Bfl-1 expression, but is known to also have a relatively short half life, similar to Bfl-1 [333]. In MM200 melanoma cells, the half life of both the Bfl-1 mRNA and protein were significantly shorter than in the SkMel28 melanoma cells. This may be significant to the level of Bfl-1 expression in these cells, as MM200 cells have been shown to express less Bfl-1 protein compared to SkMel28 cells.

We also speculated as to whether the level of degradation of the protein varied in the different melanoma cell-lines and whether it contributed to the different levels of protein seen in the cell-lines. Hence, the importance of the proteasome in the degradation of Bfl-1 protein was explored using the proteasome inhibitor MG132. MG132 was observed to significantly increase the half life of the Bfl-1 protein in both melanoma cell lines examined (Figure 3.16). But despite this, an accumulation of Bfl-1 was not observed in cells treated with MG132 for more than 4 hours in MM200 cells or 12 hours in SkMel28 cells. It should be noted that the proteasome inhibitor MG132 blocks all proteasome activity, including the degradation of IκBα [449] (Figure 3.15). Hence, a potential explanation is that although the proteasome is potentially blocked from degrading Bfl-1, Bfl-1 does not accumulate as the NFκB pathway which regulates the transcription of the protein is also significantly blocked by the inhibitor, resulting in no net increase or decrease in Bfl-1 levels during the term of the assay (Figure 3.21). However, there is still evidence that Bfl-1 is degraded through the proteasome, as the half life was seen to increase in the presence of MG132. These data agree with the literature which has suggested that Bfl-1 is degraded through the proteasome [407]. However there is also evidence in the literature that Bfl-1 is degraded by calpains [406], which is something we did not explore, but could be determined using commercially available calpain inhibitors.

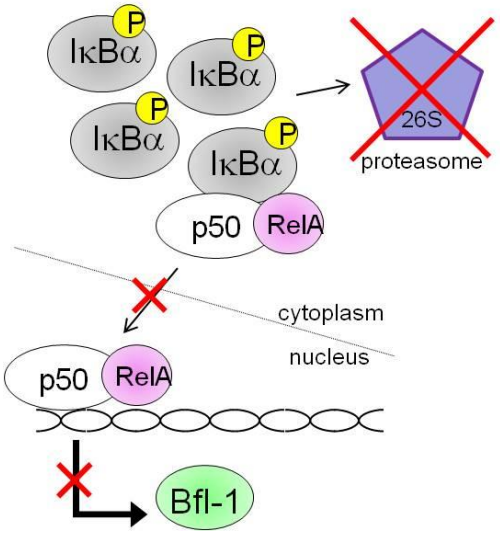

Figure 3.21: The proteasome inhibitor blocks the degradation of Bfl-1, but also blocks the transcription of Bfl-1 through the accumulation of IκBα.
When the proteasome is inhibited, IκBα accumulates in the cell, resulting in the lack of free p50/RelA for translocation to the nucleus where they act as transcription factors to Bfl-1.

In terms of the regulation of Bfl-1 protein and mRNA levels, it is clear from our results and evidence in the literature that the NFκB pathway is very important in melanoma cells [235]. Inhibition of this pathway with several pathway-specific inhibitors resulted in lower levels of both the Bfl-1 protein and mRNA (Figure 3.17 and Figure 3.19). However, our data also indicated some surprising effects on Bfl-1 levels after blocking the MAPK and Akt pathways in the melanoma cell-lines. After inhibition of the MAPK pathway, the level of Bfl-1 protein in SkMel28 cells was seen to increase while the level of mRNA decreased, whereas in MM200 cells, the mRNA level did not alter, but the protein level decreased. Although the Akt inhibition results were not as consistent as the MEK inhibition results, typically after Akt inhibition, the level of mRNA in both cell-lines did not change significantly, but the protein level increased in MM200.

The increase in protein level despite the associated decrease in mRNA after MEK inhibition in SkMel28 cells suggests an increase in translation efficiency or increased stability of the protein. The increased stability may be through an off-target inhibition of the proteasome or calpains, or perhaps stabilisation of a chaperone or scaffold protein for Bfl-1. The proteasome is understood to be controlled by phosphorylation events, although the kinases responsible for its activation are yet to be determined [450]. It may be that kinases in the MAPK pathway have some role to play in the activation of the proteasome, so blocking this pathway blocks the degradation of Bfl-1 protein by the proteasome.

The same theories could also be applied for the increase in protein level after Akt inhibition in MM200 cells despite the lack of a change in mRNA levels. However, apparently in these two melanoma cell-lines, the protein stability or translational efficiency are under different regulatory pathways. This could be as a result of the presence of polymorphic Bfl-1 and the shorter Bfl-1S isoform in SkMel28 cells whilst MM200 cells express only the long isoform and the major allele which lacks any polymorphisms. The presence of the SNPs in the minor allele and their related amino acid residue changes may affect the post-translational regulation of the protein. It may also be that Bfl-1S is under a different regulation from the full-length protein, so inhibiting different pathways would affect the total level of Bfl-1 in SkMel28 cells differently than in MM200 cells. This could be checked by RT-PCR, which separates out the two isoforms. Indeed, we examined the levels of Bfl-1 and Bfl-1S mRNA after treatment with a range of drugs, including some of the pathway inhibitors. The ratio of the two isoforms remained the same regardless of treatment with the MEK inhibitor, the NFκB pathway inhibitor or a DNA damaging agent

or microtubule disrupter. A wider range of drugs need to be used, for example the Akt inhibitor.

The differences in the regulatory pathways in the two cell-lines could also be as a result of the differing PTEN status between the cell-lines. The presence of a hyper-activated Akt pathway, due to the lack of PTEN, generally leads to the upregulation of the NFκB pathway [228]. SkMel28 cells express active PTEN, so the Akt pathway must be blocked endogenously, hence why blocking it further with an Akt inhibitor did not lead to a significant decrease in Bfl-1 expression levels. However MM200 cells have no PTEN protein, so the Akt pathway is presumably active in these cells. This would suggest that blocking Akt in MM200 cells would result in a decrease in NFκB activity and an associated decrease in the levels of Bfl-1. However, the opposite is observed in these cells suggesting that the MAPK pathway may have a more important role in the regulation of the NFκB pathway, possibly because of the presence of the BRaf mutation. Indeed, when the MAPK pathway was blocked in MM200 cells, the level of Bfl-1 protein did decrease. SkMel28 cells also express the BRaf mutation, and an associated decrease in Bfl-1 mRNA levels was observed after MEK inhibition in these cells. However, the dissociation between protein and mRNA levels after MEK or Akt inhibition in these cells suggests that it is more likely due to the reasons defined in the previous paragraph rather than the PTEN or BRaf statuses.

Having characterised the transcription, translation and regulation of Bfl-1 in melanoma cells, in the next chapter, its role and function in regulating apoptosis will be explored.

4 : THE EFFECTS OF OVER-EXPRESSION OR KNOCK DOWN OF BFL-1 ON THE TREATMENT OF MELANOMA WITH CHEMOTHERAPEUTICS

4.1 Introduction

In the previous chapter we confirmed that Bfl-1 was expressed highly and specifically in melanoma cells and characterised it further by determining its regulation and the half lives of both its mRNA and protein. Subsequently we aimed to elucidate the role and function of Bfl-1 in melanoma cells. It has already been shown that tumours, such as lymphomas, with high levels of the pro-survival molecule Bfl-1 are highly resistant to chemotherapy treatments. As such, over-expression of Bfl-1 in NFκB null cells was associated with increased resistance to apoptotic stimuli [59] and when Bfl-1 was knocked down in malignant B-cells, cells displayed an increased sensitivity to apoptosis [385]. It is therefore evident that there is a correlation between the expression levels of Bfl-1 and the sensitivity of these cells to apoptosis. However, to date, it has not been proven that Bfl-1 expression in malignant melanoma has any relation to the high level of chemo resistance observed in this cancer.

In this chapter, we explored the relationship between the sensitivity of our panel of melanoma cell-lines to apoptosis and the level of Bfl-1 they expressed. We then determined the effects of artificially over-expressing Bfl-1 in A375 cells, the melanoma cell-line we found to express undetectable levels of Bfl-1. We also looked at the effects of knocking down Bfl-1 expression in our cell-lines using siRNA technology. We explored these relationships in order to determine whether Bfl-1 was a viable drug target in melanoma.

The chemotherapeutic drugs used in this chapter have all been clinically trialled for the treatment of metastatic melanoma, showing more promise for future therapy than the current standard of care, decarbazine. The mode of action for these drugs is summarised in Table 4.1. Cisplatin is a DNA damaging agent widely used in the treatment of metastatic melanoma often as part of a combined therapy including Vinblastine and Decarbazine [451]. Cisplatin targets fast dividing cells, such as cancer cells, but is only modestly active in melanoma so it is often used in combination with other agents. Paclitaxel has also been seen to have some success in clinical trials for metastatic melanoma. In a 2006 trial 45% of patients saw a small but significant improvement when it was used in combination with Carboplatin [452] and it has had success in combination with Tamoxifen [453]. Etoposide has been trialled with Cisplatin [454] with varying degrees of success in metastatic melanoma cases. Vincristine is used in melanoma treatment, including as part of the CVD (Cisplatin, Vincristine and Decarbazine) regimen. More recently, MEK inhibitors have been trialled in metastatic melanoma as 70% of melanomas carry the BRaf mutation and the majority of

the others carry a mutation in Ras, both of which lead to the up-regulation of the MAPK pathway (AstraZeneca and Array BioPharma Inc., 2006). Although the initial trial results were not hugely impressive, MEK inhibitors are still being explored in clinical trials as the biological rationale is strong for their potential success in treating melanoma.

Table 4.1: **Mode of action of chemo therapeutic agents.**

Drug name	Mode of Action
PD0325901 (PD901)	Acts as a MEK (MAP kinase or ERK kinase) inhibitor. When MEK is inhibited, Bim is not phosphorylated and targeted for degradation, therefore Bim remains active and the cells are more prone to undergo apoptosis.
Etoposide	DNA damaging agent that reversibly affects topoisomerase II [455], a nuclear enzyme which can relax super-coiled DNA by performing a transient double-stranded break. This is associated with the formation of a protein-DNA complex, which can be trapped on the DNA by Etoposide, resulting in DNA breaks which are not repaired, so the cell cannot replicate.
Cisplatin	Causes platinum complexes to form in cells which bind to and cause 1,2 intrastrand cross-linking between purine bases in DNA. This stops division by mitosis and eventually leads to apoptosis.
Paclitaxel	Stabilises microtubules by polymerisation of β-tubulin so they are not broken down during cell division. It also binds directly to Bcl-2, a pro-survival protein, changing its function and initiating apoptosis [456].
Vincristine	Binds tubulin dimers and stops the assembly of microtubules and also causes the phosphorylation and inactivation of Bcl-2, leading to apoptosis [457].

Previous studies exploring Bfl-1 often used over-expressed Bfl-1 tagged with a fluorescent protein, which either fluoresce green or yellow (GFP or YFP, respectively) for easy detection by flow cytometry or microscopy [371]. This was a convenient way of measuring Bfl-1 activity in a cell or examining sub-cellular location before antibodies for Bfl-1 recently became available. Another way groups visualised Bfl-1 was by tagging Bfl-1 with the polypeptide protein tag, FLAG, which can then be detected using a range of high quality and reliable FLAG antibodies [417]. For examining Bfl-1 as a therapeutic target, short hairpin RNAs [385] or small inhibitory RNAs [458] have been used to knock down the expression of Bfl-1.

4.2 Exploring the Sensitivity of Melanoma Cell-lines to a Range of Chemotherapeutic Agents

As previously stated melanomas are highly resistant to many therapeutic agents, so we treated a range of melanoma cell-lines with commercially available chemotherapeutic drugs and measured the levels of apoptosis by flow cytometry. Each drug was given at a range of doses for 48 hours before the cells were collected and examined using hypotonic propidium iodide (PI) staining. Following hypotonic treatment, the outer plasma membrane loses its structural integrity and PI enters the nucleus, intercalates with DNA and fluoresces. This fluorescence can be captured by flow cytometry and is proportional to DNA content. Therefore PI can be used to measure cell DNA content and can be used for cell cycle analysis. As the cells undergo apoptosis, oligo nucleosomal fragmentation occurs resulting in DNA content less than that of a healthy cell and a sub-G1 peak is seen allowing calculations of the degree of apoptosis (Figure 4.1).

The histograms displayed in Figure 4.1 clearly show that different chemotherapeutic agents had varying effects on the state of the cell cycle within all three melanoma cell-lines examined compared to the untreated profiles. For example, cisplatin caused a much higher percentage of DNA in the Sub G1 area of the graph whereas the MEK inhibitor PD901 caused a significant arrest in the G1 phase of the cell cycle. These effects are examined in more detail later.

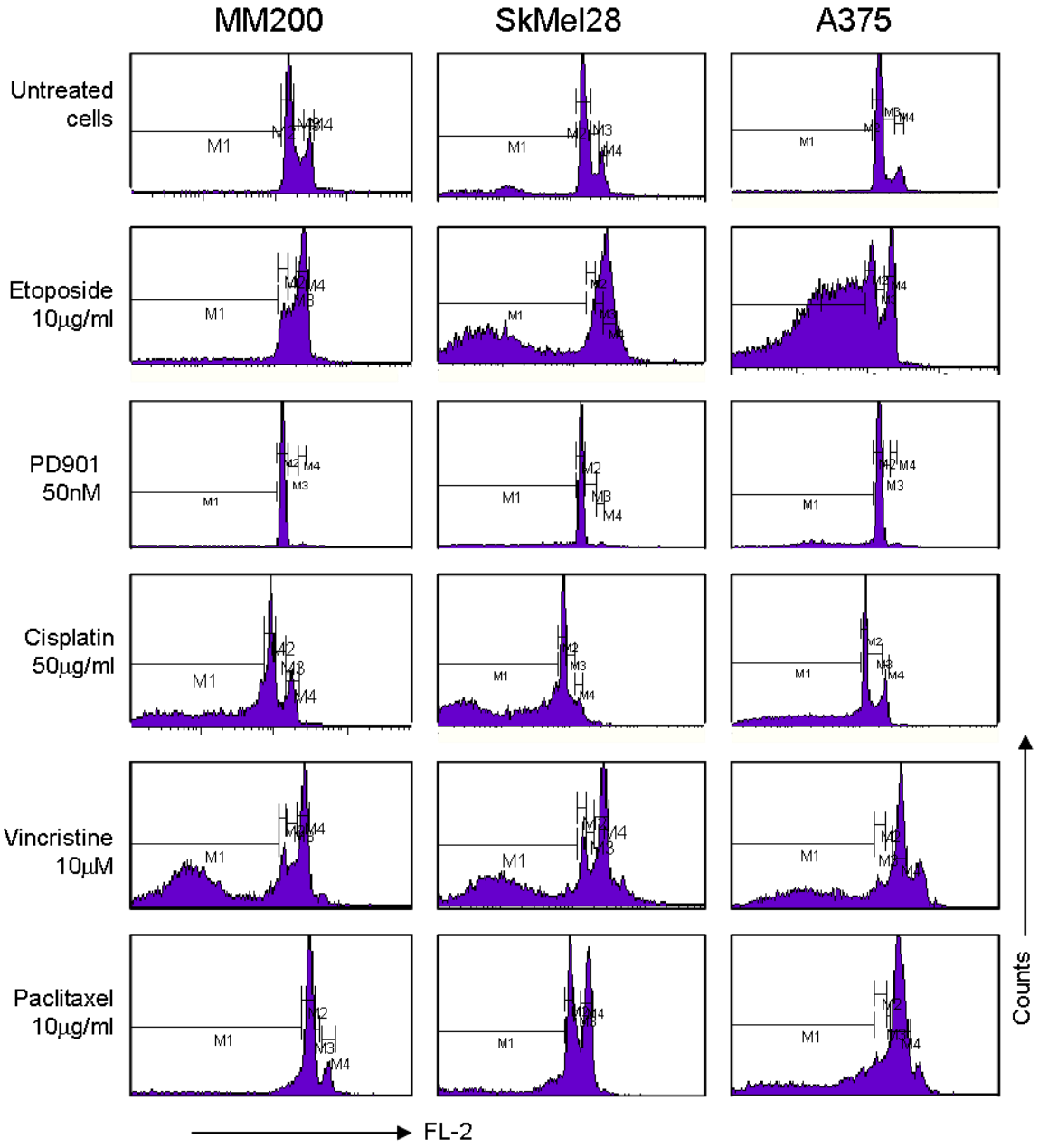

Figure 4.1: Example flow cytometry histograms showing cell cycle status after treatment of melanoma cells with chemotherapy agents.
Cells were treated with drugs at the doses shown for 48 hours. Cells were harvested and stained with propidium iodide and analysed by flow cytometry. Cells are gated to show the sub-G1 (M1), G1 (M2), S (M3) and G2/M (M4) phases of the cell cycle. These data are representative of at least three independent experiments.

To confirm that hypotonic PI staining was indeed a measure of apoptosis, we treated the melanoma cells with both the chemotherapeutic drug and a pan-caspase inhibitor, QVD (Q-VD-OPh, Sigma-Aldrich) (Figure 4.2). Inhibition of caspases blocks the completion of apoptosis, so we could determine whether the chemotherapeutic drugs killed cells through apoptosis by measuring whether the death was blocked in the presence of caspase inhibitors. Cells were treated with QVD at 10µM or 25µM for 30 minutes before the addition of the range of chemotherapeutic agents for 48 hours. Cells were treated for 48

hours in order to obtain sufficient levels of cell death for our analysis, as after 24 hours only low levels of cell death were observed. After 48 hours of treatment, both floating and adherent cells were harvested, stained with hypotonic PI and analysed by flow cytometry. The results display evidence that Etoposide, PD901, Paclitaxel and Cisplatin all cause cell death through a pathway which is blocked by caspase inhibition, i.e. apoptosis. However, caspase inhibition only partly blocked cell death caused by the microtubule disrupter Vincristine and completely failed to block cell death caused by the NFκB inhibitor BAY11-7082, even at the higher dose of 25μM. This suggests that for Vincristine, the death caused was only partially through apoptosis and for BAY11-7082 it was through a death pathway which was independent of caspases. Bfl-1 has been proposed to be involved in the blocking of the intrinsic apoptosis pathway which is completed through the caspase cascade. As such, we explored the relationship between Bfl-1 expression and cell death through apoptosis caused by Etoposide, PD901, Cisplatin, Paclitaxel and Vincristine, but not at BAY11-7082. First we examined the relationship following MEK inhibition.

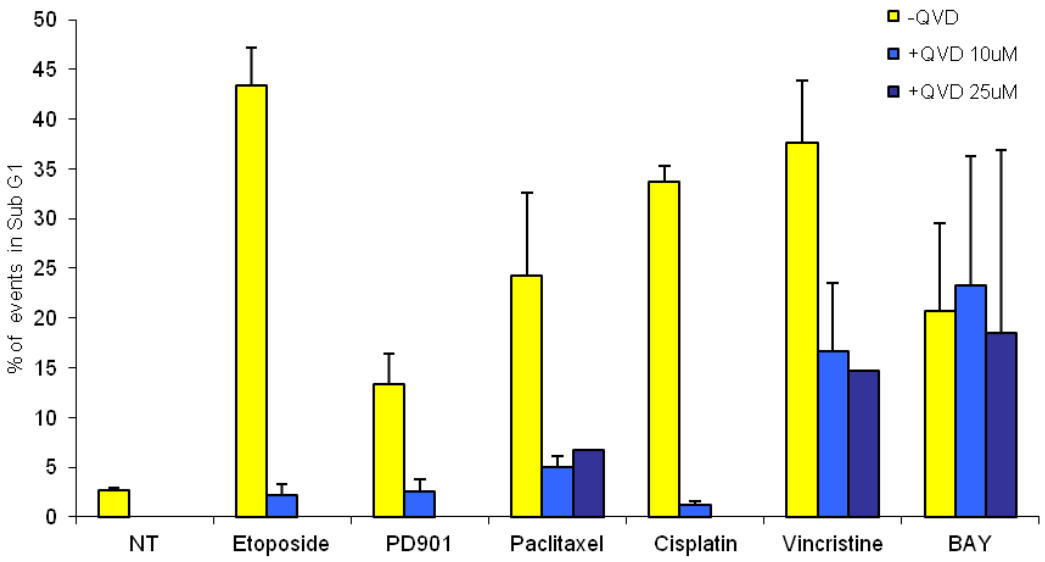

Figure 4.2: Effect of the pan-caspase inhibitor QVD on cell death in melanoma cells after the addition of chemotherapeutic drugs.
The melanoma cell-line A375 was treated with a range of chemotherapeutic agents (Etoposide 10μg/ml, PD901 50nM, Paclitaxel 10μg/ml, Cisplatin 50μg/ml, Vincristine 10μM and BAY11-7082 10μM) for 48 hours. QVD was added (10μM or 25μM) to some samples for 30 minutes before the drugs were added and the QVD remained present on the cells when the drugs were added. Both floating and adherent cells were harvested, stained with hypotonic PI and analysed by flow cytometry. Error bars represent the standard deviation from the mean and these data represent three independent experiments.

Despite the disappointing results of MEK inhibitors in clinical trials, this class of drugs are still being developed for the treatment of melanoma as they block survival signals through the MAPK survival pathway which is over-activated in the 70% of melanomas which express the activating BRaf mutation. Hence, we examined the effect of the MEK inhibitor PD901 on our panel of melanoma cell-lines. Cells were treated with PD901 at a range of doses from 0.5nM to 50nM, based on previous work in our lab [343], for 48 hours before both floating and adherent cells were harvested and stained with hypotonic PI and analysed by flow cytometry. In all experiments, solvent controls (DMSO) were run alongside treated and untreated cells. The profiles for the solvents are not shown as they match the untreated profiles very closely, probably because only 1µl of solvent was added to each 1ml of medium for all the drugs used as the stock concentration was 1000X the standard treatment dose. In fact, there was very little difference in the cell cycle profile of the untreated cells between independent experiments.

As expected, PD901 inhibited the phosphorylation of ERK, hence inhibiting cell survival signalling through the MEK/ERK pathway in melanoma cells (Figure 4.3A). A range of drug concentrations were examined and showed that melanoma cells died in a dose responsive manner to MEK inhibition (Figure 4.3B). However, even at the highest drug concentration of 50nM, levels of apoptosis higher than 30% were not observed in the majority of our melanoma cell-lines (Figure 4.3C). Instead, PD901 resulted in a large G1 arrest in every cell-line compared to their untreated profiles (Figure 4.1, and data not shown). MM200 cells, which expressed high levels of Bfl-1, were especially protected against cell death after MEK inhibition and displayed a large G1 arrest of over 90% compared to 60% of cells being in the G1 phase in healthy untreated samples. G361 cells, which expressed a moderate level of Bfl-1, were the only cells to display more than 30% apoptosis, dying at a level of 60%. This was about three times the level of apoptosis measured in A375 cells which expressed very low levels of Bfl-1. In fact, SkMel28 and UACC62 cells, which expressed very high levels of Bfl-1, presented similar levels of apoptosis to SkMel31 and A375 cells, which were at the lower end of the Bfl-1 expression scale. As such, higher expression levels of Bfl-1 in our panel of melanoma cells did not appear to provide protection from the apoptosis caused by MEK inhibition.

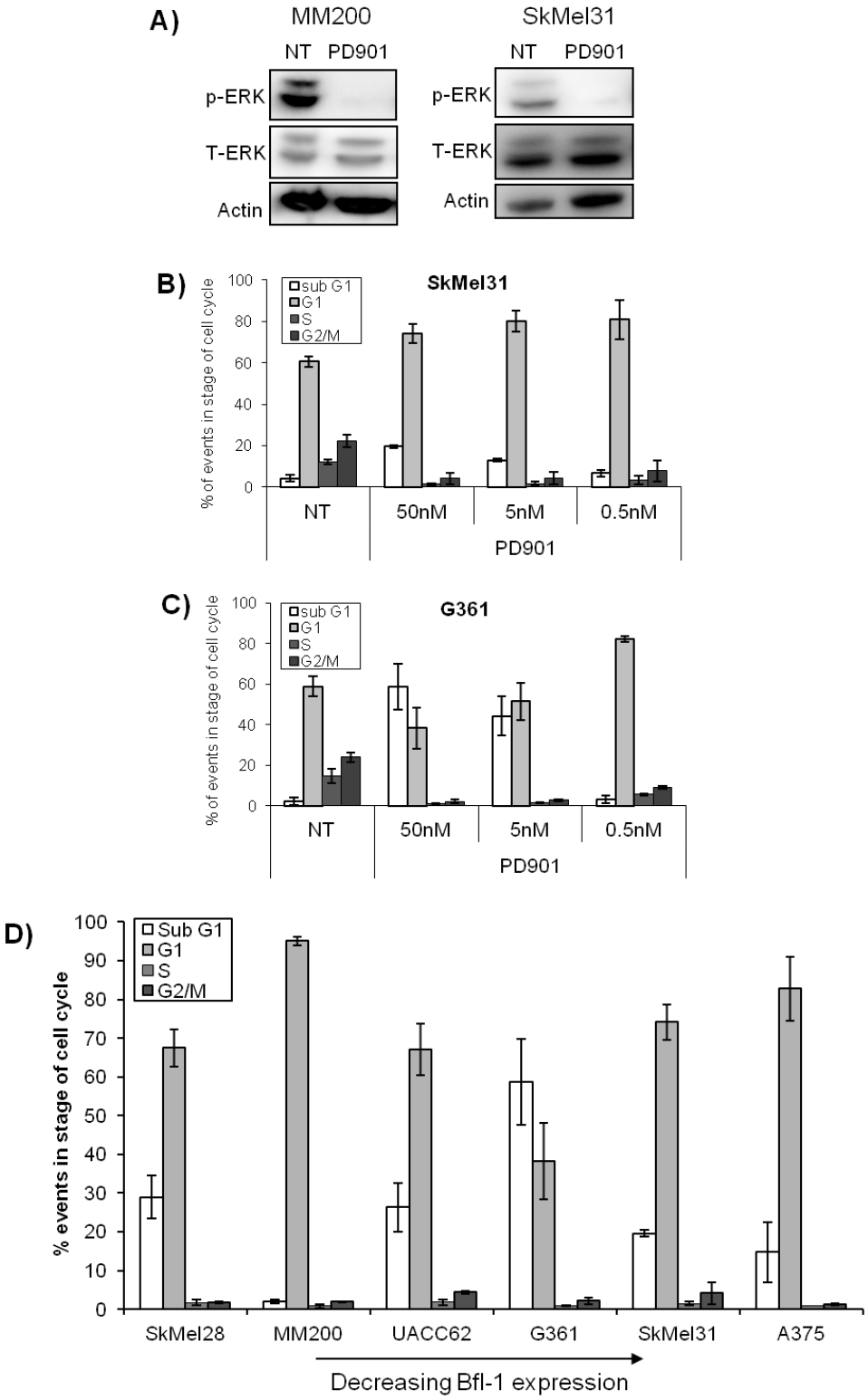

Figure 4.3: The effects of the MEK inhibitor PD0325901 (PD901) on cell cycle progression and cell death in melanoma cell-lines.
A) Cells were treated with PD901 at 50nM for 24 hours before lysates were generated and proteins were separated by SDS-PAGE and analysed by western blot for p-ERK, T-ERK and actin as a loading control. These data represent three independent experiments. B) and C) Cells were treated with PD901 at a range of doses for 48 hours before both floating and adherent cells were harvested, stained with hypotonic propidium iodide for half an hour and analysed by flow cytometry. D) Cells were treated with PD901 at 50nM for 48 hours and analysed as before. Bars represent the mean plus and minus the standard deviation from at least 3 independent experiments.

Despite the lack of correlation between Bfl-1 expression levels and apoptosis caused by MEK inhibition, we also explored the relationship of Bfl-1 expression and resistance to cell death after treatment with other chemotherapeutic agents used in the treatment of melanoma. These drugs were split into two classes; DNA damaging agents and drugs which block the normal processing of microtubules during mitosis. As before, melanoma cells were treated with the drugs for 48 hours at a range of doses, and analysed by flow cytometry with hypotonic PI staining.

Melanoma cells were treated with the DNA damaging agent Etoposide at a range of doses, from 0.4μg/ml to 10μg/ml. These concentrations were previously determined as an optimal range for causing apoptosis in other cell-lines in our lab [459]. In the majority of our melanoma cell-lines, this range of doses resulted in a clear dose response, with higher levels of cell death consistently being observed after treatment with Etoposide at 10μg/ml compared to the levels of cell death at 0.4μg/ml (Figure 4.4B). The exception to this dose response was in MM200 cells, which showed high levels of resistance to Etoposide treatment at all the doses tested (Figure 4.4A). In fact, although the levels of cell death did not change significantly at any dose of Etoposide, these cells displayed the highest G2/M arrest at the middle dose of 2μg/ml. A time course assay for Etoposide treatment demonstrated that after 24 hours, levels of cell death were still relatively low even after treatment with Etoposide at 10μg/ml (Figure 4.4D). However, after 48 hours, levels of apoptosis in most of the cell-lines increased to markedly higher levels which we could use to analyse the relationship of Bfl-1 expression to protection from cell death. Interestingly, A375 cells displayed no greater level of cell death for the longer time points of 72 or 96 hours than at 48 hours, while MM200 and SkMel28 cells continued to display higher levels of cell death with time.

The majority of our melanoma cell-lines displayed a high level of apoptosis in response to Etoposide at the top dose of 10μg/ml after 48 hours of treatment (Figure 4.4C). A375 cells exhibited the highest sensitivity to cell death at 10μg/ml out of the cell-lines tested. G361 and MM200 cells exhibited the largest resistance to Etoposide-induced cell death. SkMel31 and SkMel28 underwent cell death at roughly double the amount seen in MM200 and G361 cells. UACC62 cells had the highest level of cell death in the group of cell-lines with high levels of Bfl-1 expression, but this was still about 15% lower than the death seen in A375 cells. Across the range of cell-lines, when levels of cell death were lower, a G2/M arrest was seen in the cells (Figure 4.1 and Figure 4.4C), which was also observed at the

lower doses in cells which underwent high levels of apoptosis after 10μg/ml Etoposide treatment (Figure 4.4B).

The higher level of apoptosis in A375 cells, which express very low levels of Bfl-1, compared to the cell-lines which express high levels of Bfl-1 lent a positive correlation between higher Bfl-1 expression and resistance of cells to Etoposide-induced apoptosis. However, this was not a clear association, as UACC62 cells and MM200 cells, which express similar levels of Bfl-1, varied greatly in their sensitivity to Etoposide and SkMel28 cells, which express the highest level of Bfl-1, were more sensitive to Etoposide treatment than G361 cells. These results suggest that the lack of Bfl-1 in melanoma does not directly correlate with sensitivity to Etoposide treatment, but that other factors are also involved in resistance to Etoposide in melanoma cells.

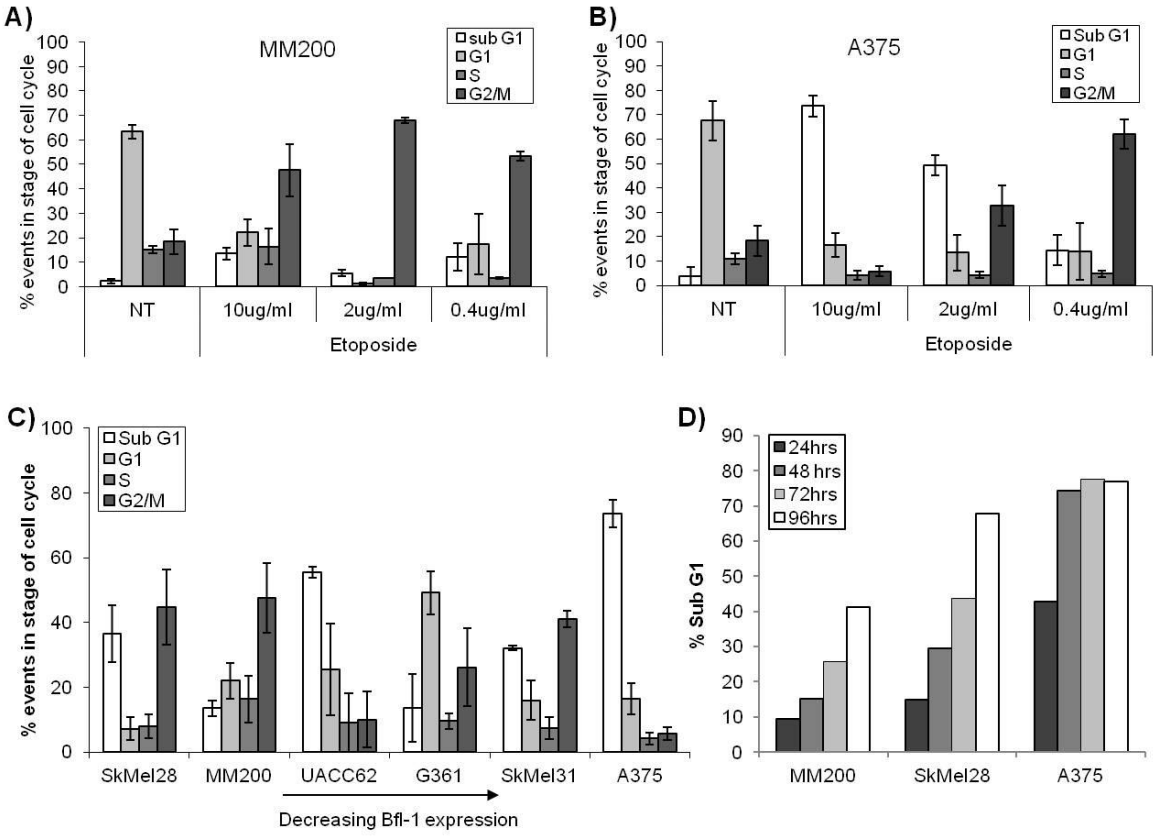

Figure 4.4: The effects of Etoposide on cell cycle progression and cell death in melanoma cell-lines.
Cells were treated with Etoposide at a range of doses (A and B) or at 10μg/ml (C and D) for 48 hours (A, B and C), or a range of time points (D) before both floating and adherent cells were harvested, stained with hypotonic propidium iodide for 30 minutes and analysed by flow cytometry. Bars represent the mean plus and minus the standard deviation from of at least 3 independent experiments.

The other DNA damaging agent we tested on our panel of melanoma cell-lines was Cisplatin. Cells were treated with Cisplatin at a range of doses including 2μg/ml, 10μg/ml

(data not shown) and 50μg/ml, based upon concentrations typically used in the literature. Cisplatin caused consistently high levels of 38-55% cell death at the top dose of 50μg/ml across the panel of melanoma cell-lines (Figure 4.5A). The only cell-line which displayed a lower level of apoptosis in response to Cisplatin treatment was UACC62, which only underwent 17.4% apoptosis. In fact all the cell-lines displayed a dose dependent level of apoptosis, except UACC62 cells. In general however, at the lowest dose of Cisplatin, less cell death was observed and cells were seen to arrest in the G2/M stage of the cell cycle (Figure 4.5B). Levels of cell death after Cisplatin treatment at 50μg/ml were very similar in A375, SkMel31 and MM200 cells, with slightly more cell death seen in SkMel28 and G361 cells and less seen in UACC62 cells. The largest G2/M arrest after Cisplatin treatment at 2μg/ml was observed in A375, MM200 and G361 cells, with SkMel28 cells exhibiting a lower percentage of cells in G2/M arrest at this dose, similar to the levels seen in SkMel31 and UACC62 cells. The highest and lowest doses of Cisplatin treatment were presented here to highlight the effects across the panel of cell-lines of the different doses on their cell-cycle profiles.

UACC62 cells, with their high levels of Bfl-1 expression, displayed the highest resistance to Cisplatin-induced apoptosis, however all the other cell-lines responded to Cisplatin treatment in a manner apparently independent of their Bfl-1 expression levels. Therefore, a correlation between Bfl-1 expression and protection from Cisplatin induced cell death cannot be deduced.

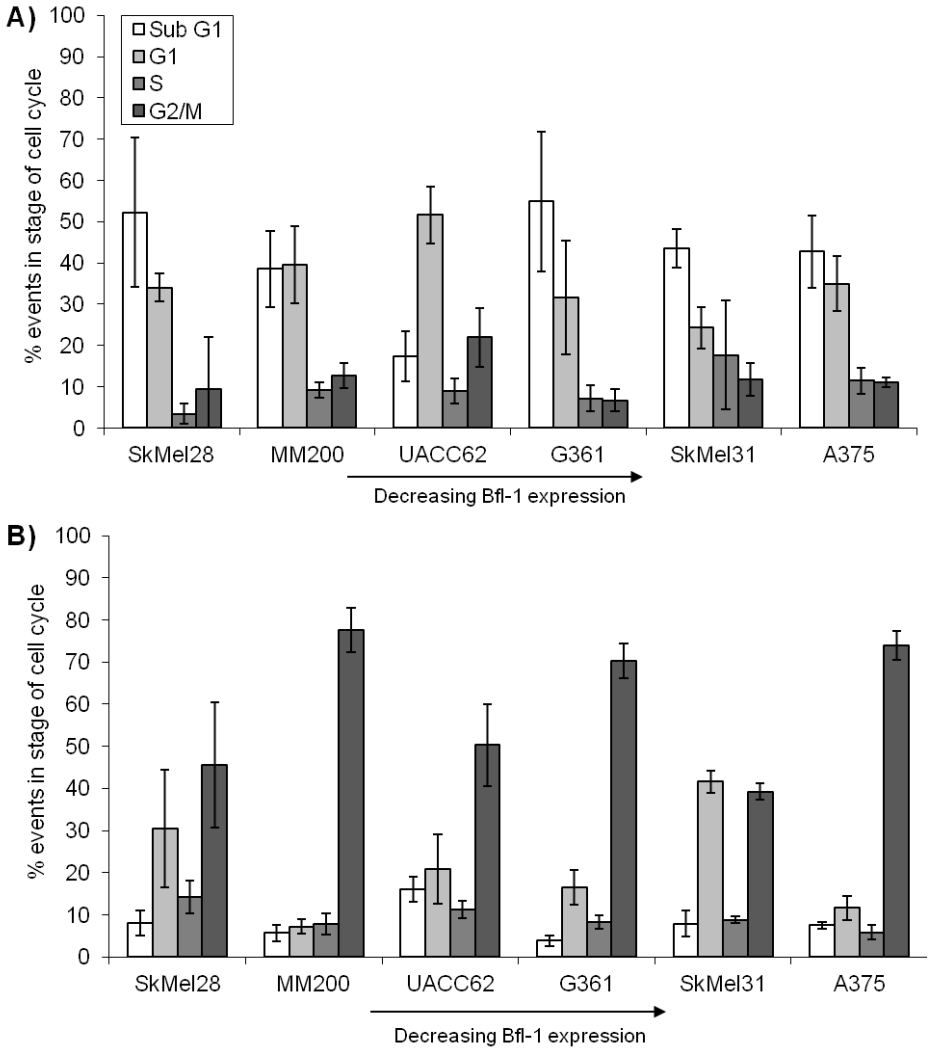

Figure 4.5: The effects of Cisplatin on cell cycle progression and cell death in melanoma cell-lines.

Cells were treated with cisplatin for 48 hours (at 50μg/ml in A and 2μg/ml in B) before both floating and adherent cells were harvested, stained with hypotonic propidium iodide for 30 minutes and analysed by flow cytometry. Bars represent the mean plus and minus the standard deviation from at least 3 independent experiments.

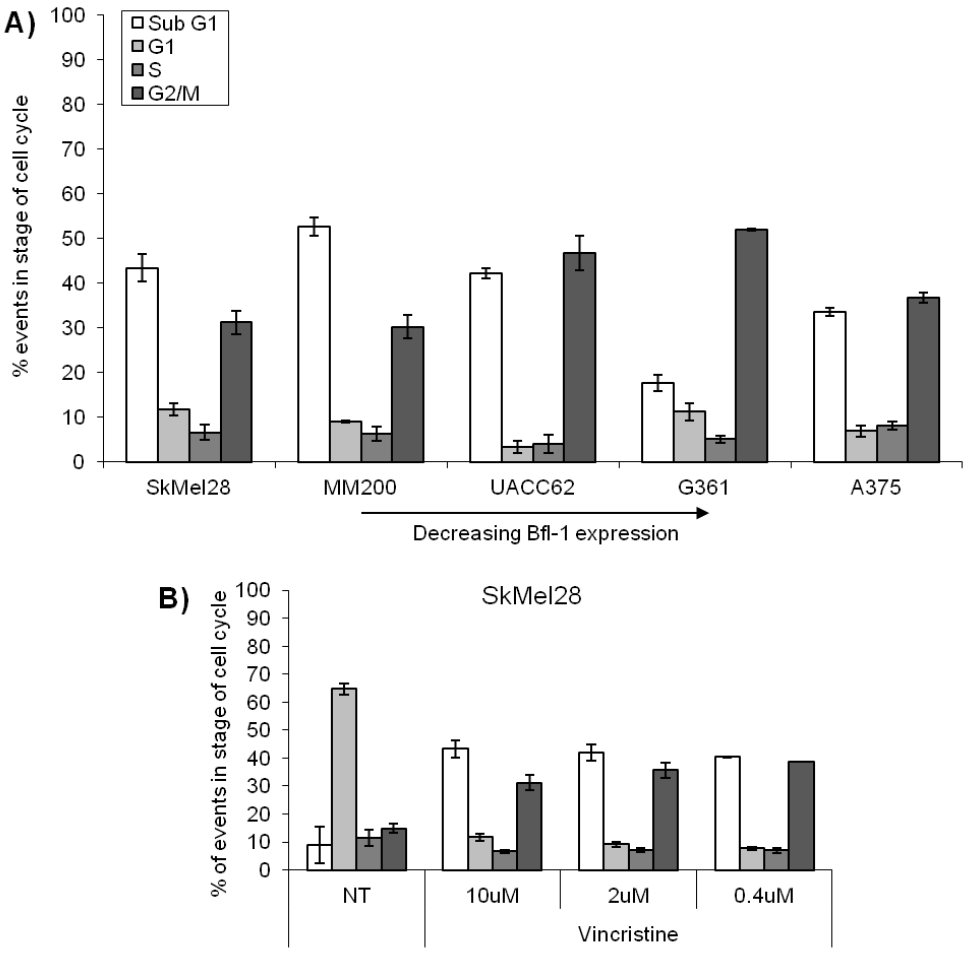

Figure 4.6: Effects of Vincristine on cell cycle progression and cell death in melanoma cell-lines.
Cells were treated with Vincristine at 10μM (A) or a range of doses (B) for 48 hours before both floating and adherent cells were harvested, stained with hypotonic propidium iodide for 30 minutes and analysed by flow cytometry. Bars represent the mean plus and minus the standard deviation from at least 3 independent experiments.

The other types of drug that we tested because of their routine use in the treatment of metastatic melanoma were drugs which affect the microtubules in the cell. We explored the effects of the microtubule disrupter Vincristine and the microtubule stabiliser Paclitaxel on our panel of melanoma cell-lines.

Vincristine irreversibly binds to microtubules during the S phase of the cell cycle, preventing the assembly of the mitotic spindle and causing cell cycle arrest. Cells were treated with Vincristine (also called Vincristine sulphate) at a range of doses from 0.4μM to 10μM based on previous research that determined cell cycle arrest occurred in G2/M at 100nM in breast cancer cells [460]. When cells were treated with Vincristine at 10μM, at least 30% of cells were in G2/M arrest and at least 30% were dead in all the cell-lines tested (Figure 4.6A). There was no dose response from 0.4μM to 10μM seen in any of the cell-lines in terms of the level of cell death diminishing at lower doses (Figure 4.6B). Cell death

was observed at the highest level in MM200 cells, but this was only about 5% higher cell death than the level seen in SkMel28 and UACC62 cells which again exhibited only about 5% more death than A375 cells. Cell death was seen to be the lowest in G361 cells. Therefore, high Bfl-1 expression did not relate to protection of the cells from Vincristine-induced apoptosis.

Paclitaxel also acts on microtubules, but instead of preventing their assembly, it stabilises them so that during cell division they cannot be dissociated. We treated our panel of melanoma cells with Paclitaxel at a range of doses from 0.4μg/ml to 10μg/ml to observe whether the expression of Bfl-1 protects melanoma cells from Paclitaxel-induced apoptosis. MM200 and SkMel28 cells, which expressed the highest level of Bfl-1 exhibited lower levels of cell death than cell-lines with lower levels of Bfl-1 (Figure 4.7). However G361 and UACC62 cells underwent higher levels of apoptosis than A375 cells. A G2/M arrest was observed in A375 cells, which expressed the lowest levels of Bfl-1 expression. However, as with Vincristine, a dose response was not observed and no correlation with higher Bfl-1 expression and lower levels of cell death were seen after Paclitaxel treatment in our panel of melanoma cells.

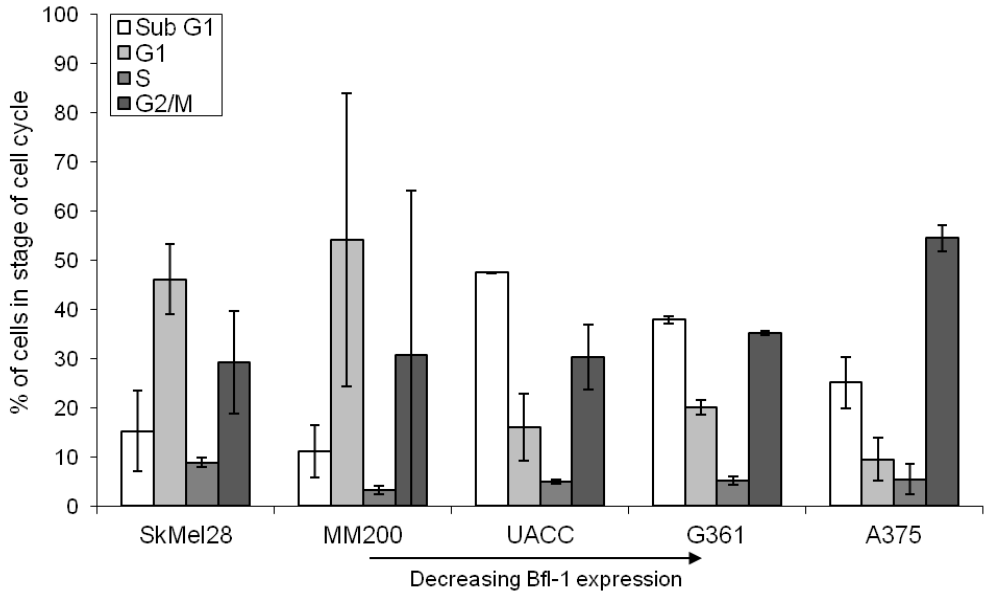

Figure 4.7: Effects of Paclitaxel on cell cycle progression and cell death in melanoma cell-lines.
Cells were treated with Paclitaxel at 10μg/ml for 48 hours before both floating and adherent cells were harvested, stained with hypotonic propidium iodide for half an hour and analysed by flow cytometry. Bars represent the mean plus and minus the standard deviation from at least 3 independent experiments.

As only a weak correlation, if any, was detected between the amount of cell death after treatment with chemotherapeutic agents and the level of Bfl-1 expressed in each melanoma cell-line we concluded that there must be other factors which affected the sensitivity of the cells to apoptosis.

4.3 The Effect of the Over-Expression of Bfl-1 on Chemo Resistance in Melanoma Cells

To directly assess the role of Bfl-1 in the chemo resistance of melanoma cells we employed the twin strategies of the over-expression and knock-down of Bfl-1. Initially we chose to over-express Bfl-1 in A375 cells that were sensitive to Etoposide and expressed very low levels of Bfl-1. To do this we generated expression vectors containing full length Bfl-1 after first cloning it into the TOPO vector (see Appendix). In order to minimise the risk of any mutation in the Bfl-1 coding sequence, we initially amplified Bfl-1 from cDNA taken from peripheral blood leukocytes (PBLs), as opposed to a melanoma cell-line. Sequencing revealed that the Bfl-1 isolated contained none of the polymorphisms we observed in our melanoma cell-lines and was the more common full-length isoform. The vector maps of the constructs are presented in the Appendix.

4.3.1 Transfection of the Bfl-1 Constructs into 293F Cells

To validate the expression plasmids and to show that the fusion proteins would result in stable production of Bfl-1 and its over-expression, Bfl-1-pcDNA3, Bfl-1FLAG and Bfl-1YFP plasmids were transfected into 293F cells. 293F cells are part of the FreeStyle™ 293 Expression System (Invitrogen) which has been optimised for the transient production of proteins in a suspension cell-line. The DNA constructs were transfected into the 293F cells using 293 fectin, a cationic lipid transfection agent optimised for use with 293F cells. Cell lysates were prepared 24 hours after transfection; the proteins were separated by SDS-PAGE and detected by western blot using the WEHI Bfl-1 antibody. Bfl-1 (16kDa), Bfl-1FLAG (17kDa) and Bfl-1YFP (43kDa) could be detected easily in just 2.5μg of protein lysates showing that they were highly over-expressed in the 293F cells (Figure 4.8). As the DNA constructs were of good quality and resulted in high levels of protein production, they were transfected into the melanoma cell-line A375 which we have shown expresses very low basal levels of Bfl-1 protein and mRNA.

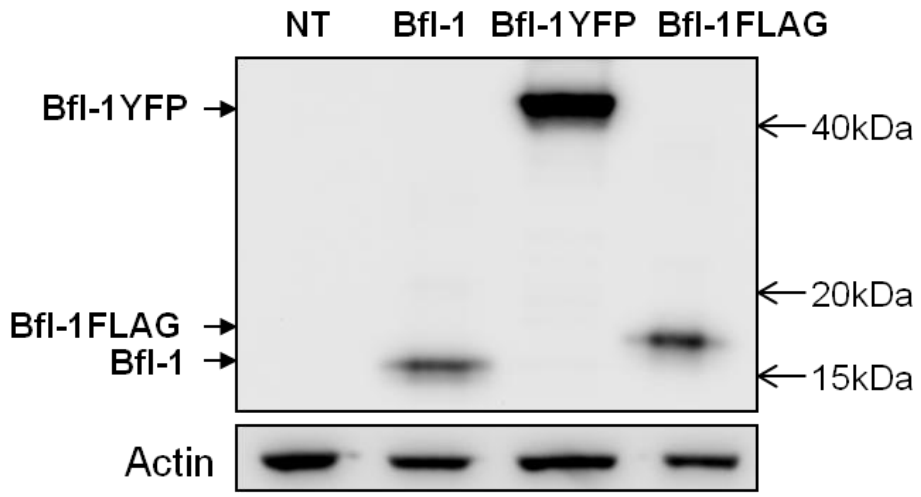

Figure 4.8: Transfection of expression constructs encoding Bfl-1 proteins in 293F cells.
Expression constructs encoding for Bfl-1 proteins were transfected into 293F cells using 293 fectin. After 24 hours, cell lysates were generated and 2.5μg of protein was separated by SDS-PAGE and detected by western blot using the WEHI Bfl-1 specific antibody. These data are representative of over three independent experiments.

4.3.2 Transfection of the Bfl-1 constructs into a Melanoma Cell-line

Bfl-1 constructs were transfected into the melanoma cell-line A375, which allowed us to directly compare cells with high Bfl-1 expression to cells with very low Bfl-1 expression levels. A range of transfection methods were attempted, as described in chapter 2, with varying success rates. The success of the transfection and selection was analysed by western blotting of the clonal population (obtained from the expansion, under selection, of a single overexpressing clone) with the Bfl-1 antibody (Figure 4.9). After exploring various transfection methods, Bfl-1FLAG and Bfl-1YFP were routinely transfected into A375 cells by lipofection, but Bfl-1pcDNA3 proved very difficult to transfect into these cells. Routinely, A375 cells were transfected with the constructs for 48 hours, then the antibiotic geneticin was added to select for successfully transfected cells. Once geneticin treatment had resulted in death of untransfected cells and colonies had started forming, cells from colonies were seeded into 96 well plates and wells with colonies derived from single cells were grown up under selection and tested for the expression of the construct by western blot.

Cells successfully transfected with Bfl-1YFP then underwent further selection through fluorescence-activated cell sorting using a FACS Aria II. This separated the cells on the basis of their YFP positivity based on the assumption that cells expressing more Bfl-1YFP would have higher fluorescence in the FL-1 channel due to expression of YFP. Sortinf

produced a Bfl-1YFP expressing cell-line with 94% positively transfected cells after cell sorting (Figure 4.10).

The empty vector pcDNA3 was routinely transfected into A375 cells alongside the protein constructs in order to provide a control for the selection process, as the process itself may have favoured resistance to apoptosis regardless of the successful transfection of the Bfl-1 constructs.

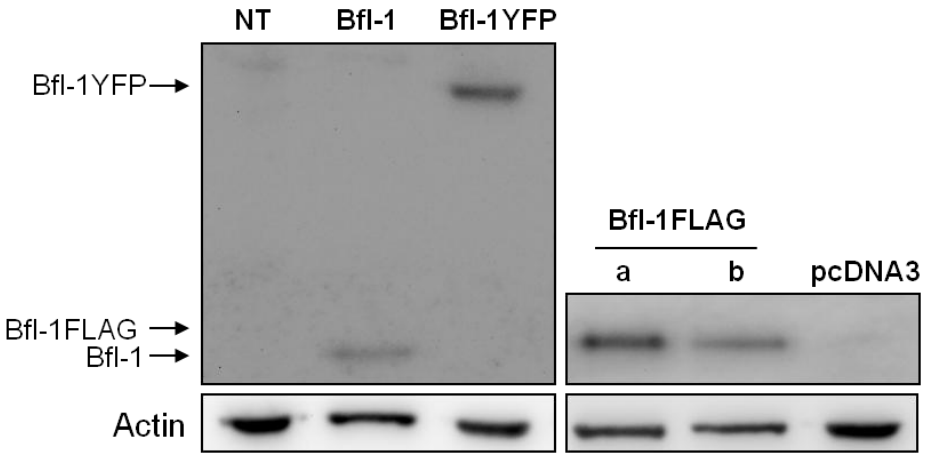

Figure 4.9: Transfection of expression constructs encoding for Bfl-1 proteins in A375 melanoma cells.
The expression constructs encoding Bfl-1 fusion proteins were transfected into A375 cells by lipofection. After 24 hours, cell lysates were generated and 25µg of protein was separated by SDS-PAGE and detected by western blot using the WEHI Bfl-1 specific antibody. Bfl-1pcDNA3 and Bfl-1YFP constructs are shown alongside untransfected A375 cells on the left, whilst on the right are two separately transfected samples for Bfl-1FLAG and A375 cells transfected with the empty construct pcDNA3. These data are representative of over three independent experiments.

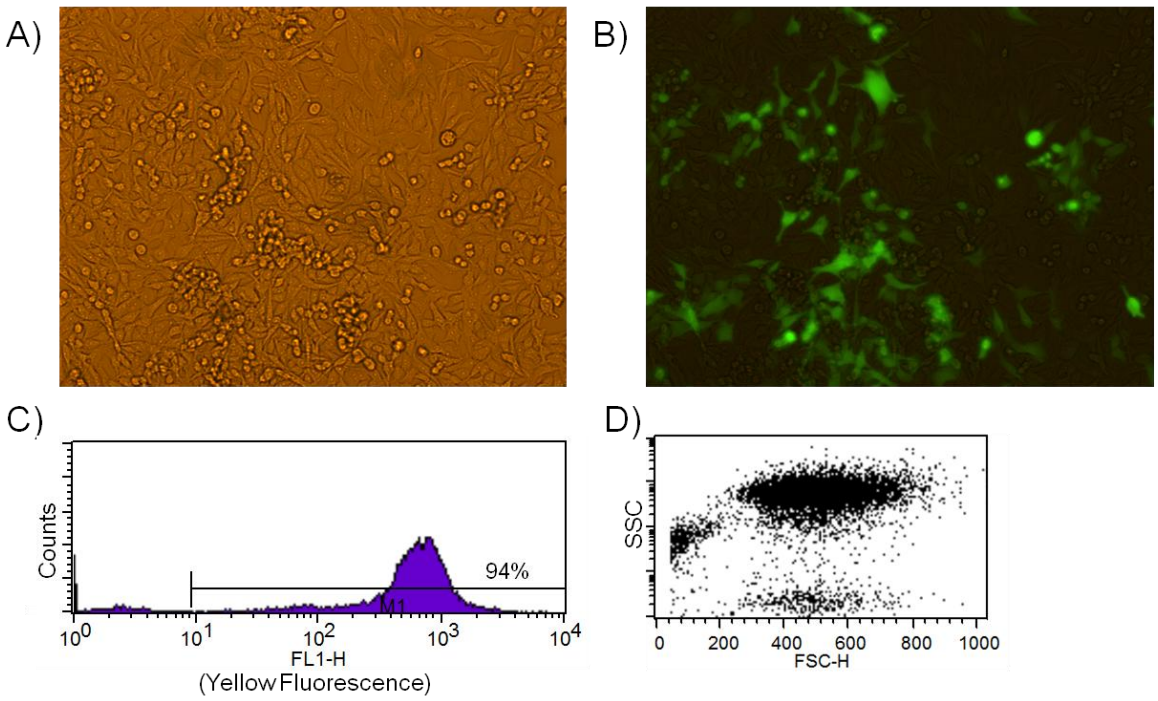

Figure 4.10: Microscopy and flow cytometry analysis of Bfl-1YFP in A375 cells.
Bfl-1YFP was transfected into the melanoma cell-line A375 via lipofection. Cells were qualitatively checked for yellow fluorescence after selection with geneticin for 48 hours by microscopy; under white light to visualise all the cells (A) and UV light for the transfected cells (B). After cell sorting by flow cytometry, cells were quantitatively analysed by flow cytometry (C, D) to obtain the percentage of positively transfected cells. The histogram shows the percentage of transfected cells based on their fluorescence.

4.3.3 The Effect of the Over-Expression of Bfl-1 on Cell Death after Treatment with Chemotherapeutic Agents

The transfection of Bfl-1YFP and Bfl-1FLAG into A375 melanoma cells gave us the opportunity to examine the relationship between Bfl-1 expression and sensitivity to chemotherapeutics by direct comparison between the wild type cells and the cells over-expressing Bfl-1. A375 cells transfected with Bfl-1YFP or pcDNA3, as the control, were treated with a selection of chemotherapeutic agents chosen from the original panel used on the melanoma cell-lines earlier in this chapter. The drugs were chosen to represent the different mechanisms by which they work; Paclitaxel acts as a microtubule inhibitor, Etoposide as a DNA damaging agent and PD901 as a MEK inhibitor. Cells were treated with the drugs at the doses indicated (Figure 4.11) for 48 hours before cells were harvested and stained with hypotonic PI. Cell cycle analysis was performed by flow cytometry. A dose dependent response was seen in the mock-transfected cells in response to Etoposide and PD901, but not Paclitaxel. Basal levels of cell death in untreated cells were equal in the mock and Bfl-1 transfected cells. The transfected cells consistently exhibited lower levels of cell death than the mock cells after treatments with all the drugs tested. The only

exception to this was at the lowest dose of Etoposide where wild-type and transfected cells showed death at a similar level.

Statistical analysis of the results by two-tailed t-test showed that when cells were treated with Paclitaxel, PD901 and the top two doses of Etoposide, the difference in the cell death between mock-transfected and Bfl-1 transfected cells was statistically significant with a p value under 0.05. This supports the hypothesis that over-expression of Bfl-1 protects cells from apoptosis caused by various chemotherapeutic reagents.

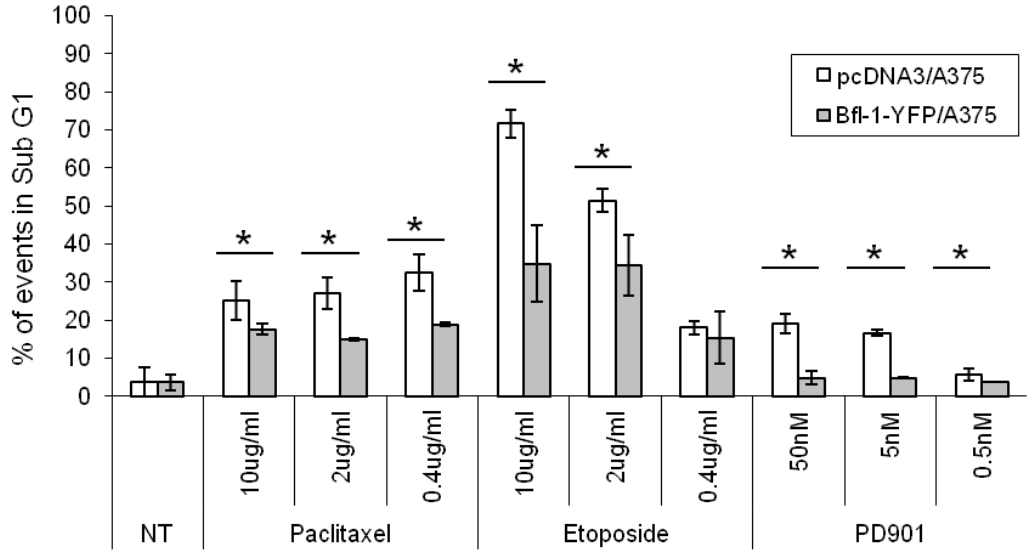

Figure 4.11: Apoptosis resistance against chemotherapeutic agents in A375 melanoma cells transfected with Bfl-1YFP.
Levels of apoptosis in pcDNA3 transfected A375 cells were higher than in A375 cells transfected with Bfl-1YFP when treated with dose ranges of Paclitaxel, Etoposide and PD901. Cells were treated with the drugs at the doses indicated for 48 hours and samples were stained with hypotonic propidium iodide and analysed by flow cytometry. Bars represent the mean plus and minus the standard deviation from of 3 independent experiments. * represents a $p<0.05$, as analysed by two-tailed t-test.

We also examined the effect of the over-expression of Bfl-1 on the clonogenic potential of A375 cells (Figure 4.12). To do this we transfected A375 cells with Bfl-1FLAG, or the empty pcDNA3 vector as a control. Transfected cells were treated with Etoposide at a range of doses for 24 hours before the drug was washed off. Cells were counted and resuspended in conditioned media and seeded into 96 well plates at a range of 1-2400 cells per well. Cells were then left to grow under culture conditions and after 10 days, the number of wells containing colonies (positive wells) was counted. In general, the cells transfected with Bfl-1FLAG had a higher clonogenic potential after treatment with Etoposide than the control A375 cells which were mock transfected with the empty vector

(Figure 4.12). The results of a single experiment are presented here which are representative of four experiments. Although the absolute numbers of positive wells differed between experiments, increased clonogenicity seen in A375 cells transfected with Bfl-1FLAG was always observed when cells were treated with Etoposide at 0.4μg/ml.

After treatment with Etoposide at 10μg/ml, no cell clones grew through in either the Bfl-1FLAG or control populations, but after treatment at 0.4μg/ml and 0.08μg/ml, although there was quite a high variation between experiments, cells containing Bfl-1FLAG generally produced more colonies than the control cells. For example, in the presented experiment, the transfected cells produced three times as many positive wells after Etoposide treatment at 0.4μg/ml at 89 cells/well and four times as many after Etoposide treatment at 0.08μg/ml at 9 cells/well. This suggests that the expression of Bfl-1 gives cells a long-term clonogenic survival benefit after treatment with this chemotherapeutic drug.

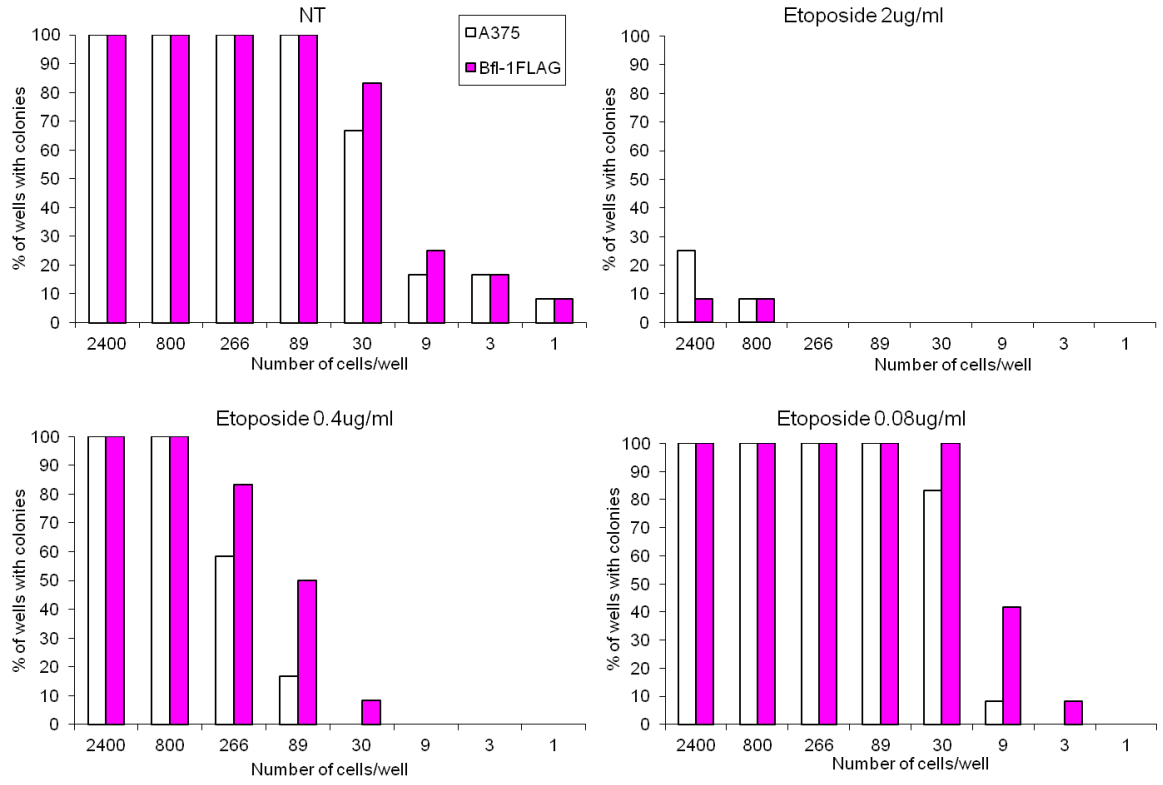

Figure 4.12: Clonogenicity of A375 cells following transfection of Bfl-1FLAG.
A375 cells were transfected either with Bfl-1FLAG (pink bars) or the empty pcDNA3 vector (white bars) and treated with Etoposide at a range of doses for 24 hours. The drug was then washed off and cells were seeded in 96 well plates at a range of 1-2400 cells per well. After 10 days, the numbers of wells containing colonies at each concentration of cell/well were counted. These data are from one experiment but are representative of four independent experiments.

4.4 The Effect of Knocking-Down Bfl-1 Expression in Melanoma Cells

Having found that the over-expression of Bfl-1 in a melanoma cell-line could increase the resistance of the cells to apoptosis after treatment with some therapeutic agents, the next step was to examine whether knock down of Bfl-1 would re-sensitise melanoma cells to apoptosis.

4.4.1 siRNAs Knock-Down the Expression of Bfl-1

To determine whether lower levels of Bfl-1 could make the melanoma cell-lines more sensitive to chemotherapeutic agents, we explored whether siRNAs could be used to specifically and efficiently knock-down Bfl-1 expression in the melanoma cell-lines MM200 and SkMel28. siRNAs were designed using the Invitrogen online siRNA designer and the three theoretically most effective siRNAs were chosen, named BCL2A1HSS100957 (957), BCL2A1HSS100958 (958) and BCL2A1HSS100959 (959) (Invitrogen) (sequences in Table 4.2). siRNAs were transfected into melanoma cell-lines by lipofection and cell lysates were generated 48 hours later for separation of the proteins by SDS-PAGE and analysis by western blot. The siRNA 957 was found to knock down the expression of Bfl-1 in both the melanoma cell-lines tested (Figure 4.13). Importantly this knock-down was observed to be specific for Bfl-1 and not other Bcl-2 family members such as Bcl-2 (Figure 4.13). The siRNAs 958 and 959 did not decrease the levels of Bfl-1 expression in the melanoma cell-lines. In fact, 958 and 959 appeared to stabilise the Bfl-1 protein.

To assess whether the knock-down effect was dose-dependent, siRNA 957 was transfected into cells at a range of doses, from 40nM to 0.32nM (Figure 4.14). A dose dependent knock-down of Bfl-1 was observed with 957 siRNA, and at 40nM, knock-down was determined to be over 80% in both MM200 and SkMel28 cells by densitometry analysis. Therefore, 957 siRNA was used as the Bfl-1 specific siRNA in further experiments at a dose of 40nM. A control siRNA was obtained from Applied Biosystems which contained the same GC percentage as the Bfl-1 siRNA, had a sequence which did not target any known gene product and had no effect on cell proliferation, viability or morphology. This control siRNA was also used at a dose of 40nM and was important to control for the effects of siRNA delivery in the cells. The untreated cells (NT) were cells which had lipofectamine and OptiMem medium added, but with no siRNA present.

Table 4.2: siRNA sequences for knock down of A1 expression in melanoma cell-lines.

Name	Sequence 5'-3'
BCL2A1HSS100957	ACAACCUGGAUCAGGUCCAAGCAAA
BCL2A1HSS100958	GGACAAUGUUAAUGUUGUGUCCGUA
BCL2A1HSS100959	UCAAGAAACUUCUACGACAGCAAAU

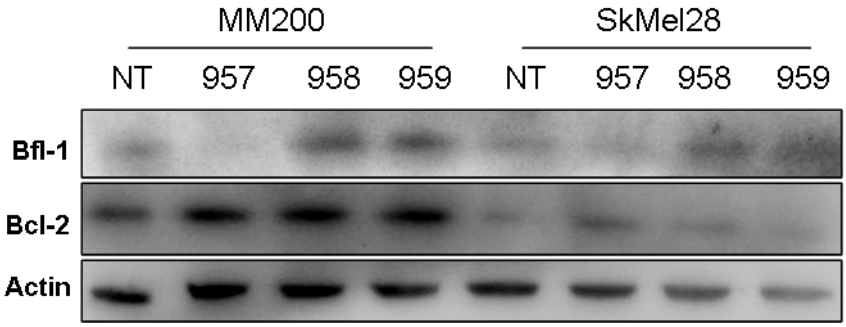

Figure 4.13: Knock down of Bfl-1 expression in melanoma cell-lines with siRNA.
The melanoma cell-lines MM200 and SkMel28 were transfected with 40nM of 3 different siRNAs BCL2A1HSS100957 (957), BCL2A1HSS100958 (958) and BCL2A1HSS100959 (959). After 48 hours cell lysates were generated and the proteins were separated by SDS-PAGE and analysed by western blot for Bfl-1, Bcl-2 and actin. These data are representative of 3 independent experiments and show clear knock down of Bfl-1 with 957 but no knock down of Bcl-2.

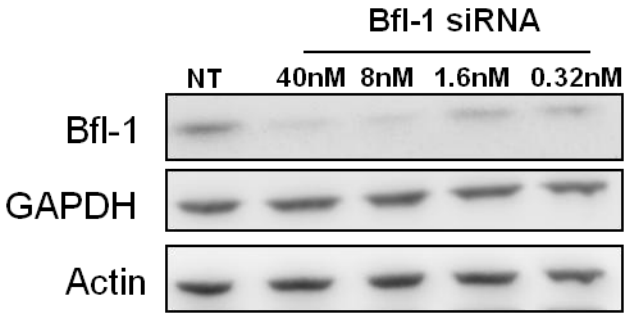

Figure 4.14: Dose response of Bfl-1 knock-down in MM200 cells after 957 siRNA treatment.
MM200 cells were treated with 957 siRNA at a range of doses as shown, or left untreated. After 48 hours cell lysates were generated and proteins were separated by SDS-PAGE and analysed by western blot for Bfl-1, GAPDH and actin. GAPDH was used as an additional control to actin. These data are representative of 2 independent experiments.

Having optimised the doses for the efficient knock down of Bfl-1 with siRNA, we went on to examine the effects of this knock down on the levels of apoptosis in cells after treatment with a range of chemotherapeutic agents. In these experiments, siRNA and lipofectamine was removed from the cells in order to treat them with the chemotherapeutics, so we

determined how long after the removal of siRNA Bfl-1 remained knocked-down for in order to find out how long we could leave the drugs on the cells for. Therefore, we treated melanoma cells with the Bfl-1 siRNA and the control siRNA for 48 hours, then washed the siRNA off the cells and generated lysates at 0, 24 and 48 hours after siRNA removal (Figure 4.15). Western blot analysis showed that the level of Bfl-1 was significantly lower up to 48 hours after the removal of the Bfl-1 specific siRNA, but that it was most efficiently knocked down for 24 hours after siRNA removal, as protein levels began to recover by 48 hours. This western blot also showed that the control siRNA did not significantly lower Bfl-1 expression levels at any time point. Therefore, in the subsequent death assays, we transfected the cells with the siRNA for 48 hours, then removed it and treated the cells with the chemotherapeutic agents for a further 24 hours before both floating and adherent cells were collected, stained with hypotonic PI and analysed by flow cytometry for apoptosis and cell cycle arrest.

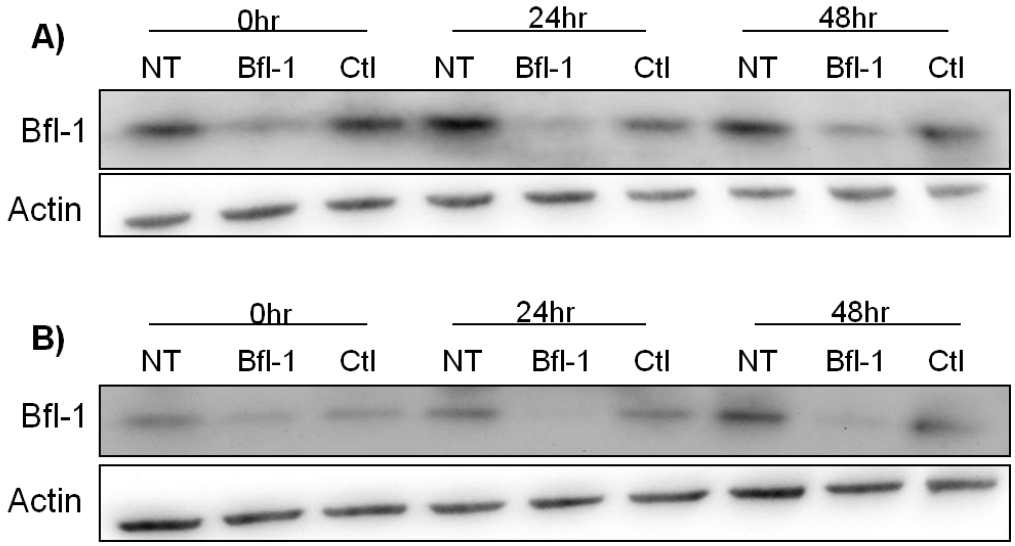

Figure 4.15: Kinetics of Bfl-1 re-expression following knock-down in melanoma cell-lines by siRNA treatment.
MM200 (A) and SkMel28 (B) cells were transfected with 957 Bfl-1 siRNA, or the control siRNA (Ctl), at 40nM for 48 hours. After this, siRNA was washed off the cells and lysates were generated at 0, 24 and 48 hours after siRNA removal. Proteins were separated by SDS-PAGE and analysed by western blot. These data are representative of two independent experiments.

4.4.2 The Effects of the Knock-Down of Bfl-1 on the Sensitivity of Melanoma Cells to Chemotherapeutic Agents

Having determined that siRNAs could be used to efficiently knock down the expression levels of Bfl-1 in our melanoma cells, we went on to explore the effects that decreasing the

level of Bfl-1 expression had on the ability of the melanoma cells to resist apoptosis induced by a range of chemotherapeutics. Firstly, we treated melanoma cells with Bfl-1-specific and control siRNA at 40nM for 48 hours, then treated them with the panel of chemotherapeutic agents we previously used to determine whether knock down of Bfl-1 sensitised the cells to apoptosis (Figure 4.16). The presence of the control siRNA induced a slightly higher level of background cell death than untreated cells, and the level was further enhanced, although not to a statistically significant level, when cells were treated with Bfl-1 specific siRNA. Hence the procedure of transfection by lipofection killed a small proportion of the cells. However, SkMel28 cells displayed significantly greater levels of cell death than were seen with the control siRNA when Bfl-1 knock-down was combined with PD901, Cisplatin or Paclitaxel treatment. Statistical significance was determined by two-tailed t-tests with a p value of <0.05. The sensitivity of cells to Etoposide and Vincristine treatment was not significantly affected by Bfl-1 knock-down in these melanoma cells.

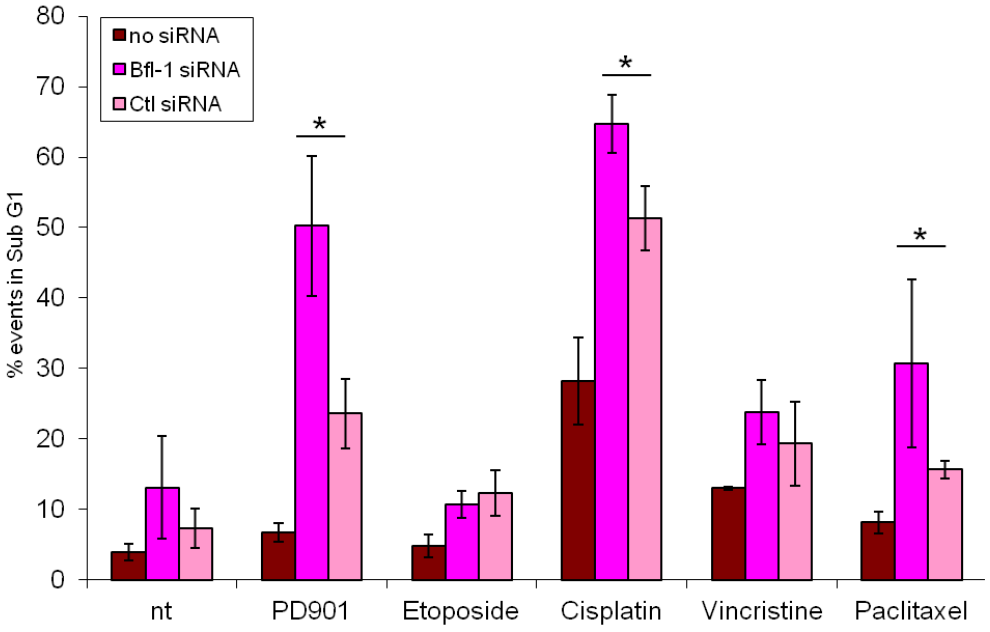

Figure 4.16: Sensitivity of melanoma cells to a range of chemotherapeutic agents after Bfl-1 knock-down.
SkMel28 cells were transfected with Bfl-1 or control siRNA (Ctl) at 40nM for 48 hours. Then cells were treated with chemotherapeutic agents (PD901 50nM, Etoposide 10µg/ml, Cisplatin 50µg/ml, Vincristine 10µM and Paclitaxel 10µg/ml) for a further 24 hours before both floating and adherent cells were harvested, stained with propidium iodide for 30 minutes and analysed by flow cytometry. Error bars are representative of the mean plus and minus the standard deviation from three independent experiments. * represents a $p<0.05$, as analysed by two-tailed t-test.

Having determined that the sensitivity of our melanoma cell-lines to Paclitaxel, Cisplatin and PD901-induced apoptosis was increased when Bfl-1 expression was knocked-down, I examined whether the degree of Bfl-1 knock-down correlated directly with the level of the increase in sensitivity. Hence, I treated cells with a range of Bfl-1 siRNA doses from 0.32nM to 40nM and then left cells untreated for 24 hours or subjected them to PD901 or Paclitaxel treatment (Figure 4.17). In SkMel28 and MM200 cells, a dose response was seen depending on the concentration of Bfl-1 siRNA used, with the response being clearer in SkMel28 cells, particularly after PD901 treatment. I previously showed by western blot that lower concentrations of siRNA were less effective at knocking down Bfl-1 (Figure 4.14), and here we see levels of cell death reflect the same pattern. In SkMel28 cells, treatment with PD901 resulted in significantly higher levels of cell death than the control siRNA at Bfl-1 siRNA concentrations of 40nM and 8nM. With siRNA at 1.6nM, cell death levels were equal to the control siRNA and by 0.32nM, cell death levels were heading towards the levels found in untreated cells. A similar pattern was seen after Paclitaxel treatment, although only the top dose of 40nM of Bfl-1 siRNA treatment resulted in significantly higher cell death than the control siRNA. In MM200 cells, Paclitaxel treatment resulted in significantly higher levels of cell death than the control when Bfl-1 siRNA was added at 40nM, 8nM and 1.6nM, with a more gradual decrease in cell death levels than was seen in SkMel28 cells. PD901 treatment in MM200 cells yielded no significant increase in cell death levels over the control siRNA, but levels still fell in response to lower Bfl-1 siRNA concentrations. In conclusion, drugs that were more effective when Bfl-1 was knocked down were reliant on the level of knock-down for the level of their effectiveness in our melanoma cell-lines.

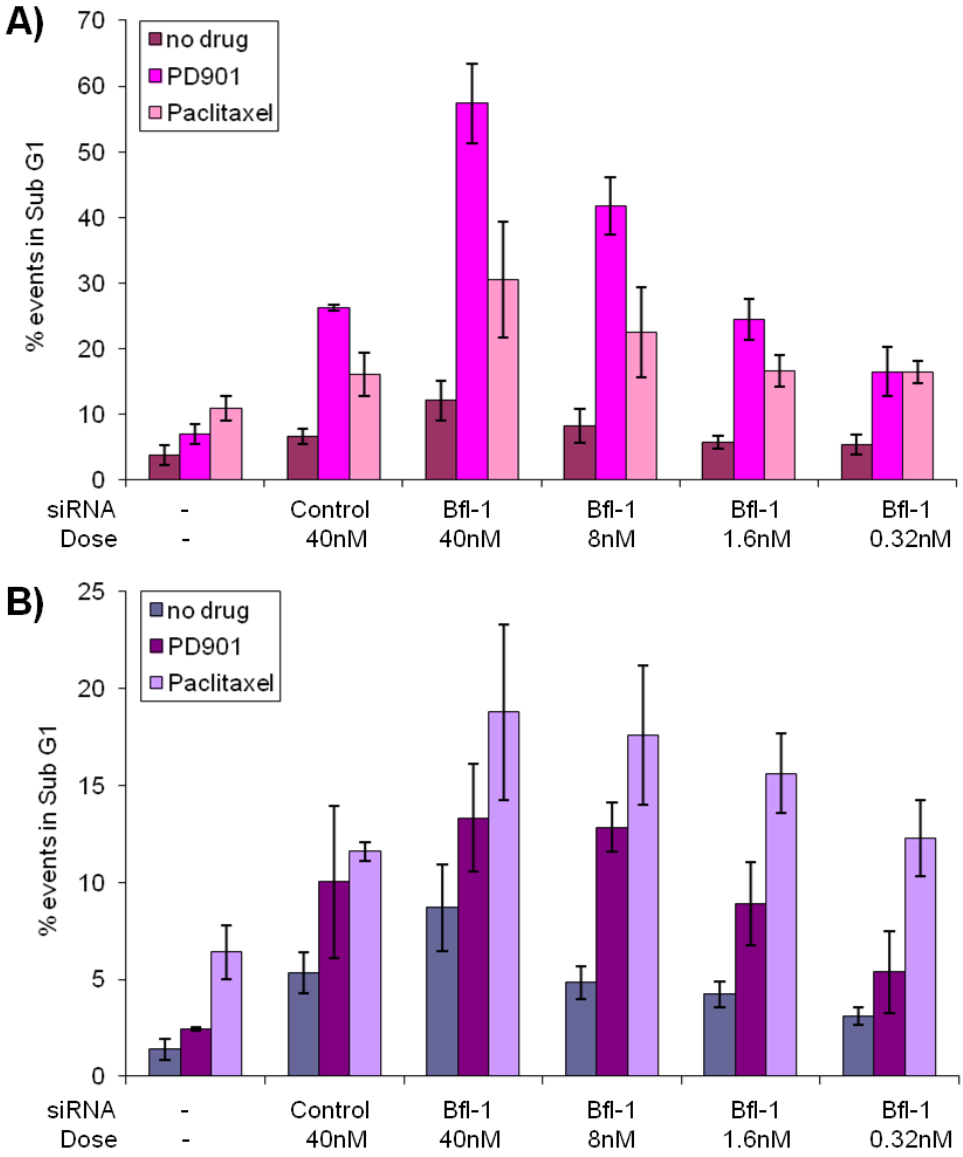

Figure 4.17: Sensitivity of melanoma cells to chemotherapeutics following differing levels of Bfl-1 knock-down.
SkMel28 (A) and MM200 (B) cells were treated with Bfl-1 specific siRNA at a range of doses and compared with untreated cells and cells treated with the control siRNA dosed at 40nM. Cells were incubated with siRNA for 48 hours, then siRNA was removed and cells were treated with either PD901 at 50nM or Paclitaxel at 10µg/ml for a further 24 hours. Both floating and adherent cells were harvested and stained with propidium iodide for 30 minutes. Cell death was analysed by flow cytometry. Error bars represent the mean plus and minus the standard deviation from three independent experiments.

In addition to examining the effect of knocking down native Bfl-1 in melanoma cells, I also tested the sensitivity of our A375 cells over-expressing Bfl-1FLAG to Bfl-1 knock-down. Firstly, I examined whether our Bfl-1-specific siRNA successfully knocked down Bfl-1FLAG. To do this we treated transfected cells with Bfl-1 siRNA, or the control siRNA, for 48 hours, washed the siRNA off and left them untreated for a further 24 hours to mimic the timings used in the death assay experiments. Cell lysates were then generated and protein expression was examined by western blot (Figure 4.18). Bfl-1FLAG was

efficiently knocked down by Bfl-1 siRNA in the over-expressing cells, while the presence of the control siRNA had no significant impact on Bfl-1 expression. Hence, I performed the death assay in the manner previously described on mock-transfected A375 cells and A375 cells over-expressing Bfl-1FLAG (Figure 4.19). Bfl-1 knock-down in wild-type A375 cells had no effect on the background level of cell death, or that seen after treatment with PD901 or Etoposide compared to the levels seen with the control siRNA. Surprisingly however, cells treated with Bfl-1 siRNA were more sensitive to Paclitaxel treatment than cells treated with the control siRNA, despite the very low levels of Bfl-1 present in A375 cells.

A375 cells over-expressing Bfl-1FLAG were sensitive to Bfl-1 knock-down in response to treatment with all three chemotherapeutic agents tested, but background levels of cell death were no higher after Bfl-1 knock-down compared to the control siRNA. Interestingly, after Bfl-1 knock down in these cells, levels of cell death were greater than those observed in the wild-type cells, jumping from less than 30% cell death to around 40% cell death in transfected cells, while cell death levels after treatment with the control siRNA remained similar between the mock and Bfl-1 transfected cells. This may suggest that some of these cells, which previously expressed very low levels of Bfl-1, quickly became reliant on its expression for their survival.

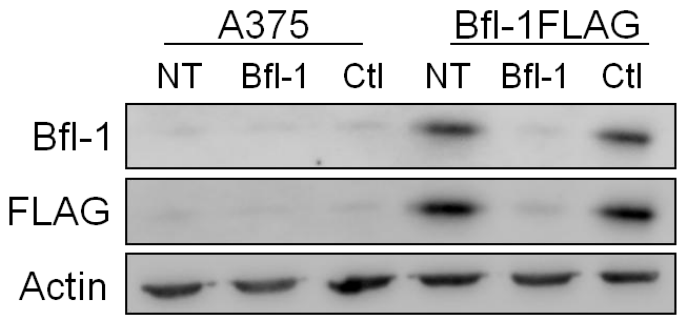

Figure 4.18: Knock-down of over-expressed Bfl-1FLAG in A375 cells.
A375 cells transfected with the empty vector pcDNA3 and A375 cells transfected with Bfl-1FLAG were treated with Bfl-1 specific and control (Ctl) siRNA or left untreated for 48 hours. Cell lysates were then generated, proteins were separated by SDS-PAGE and analysed by western blotting.

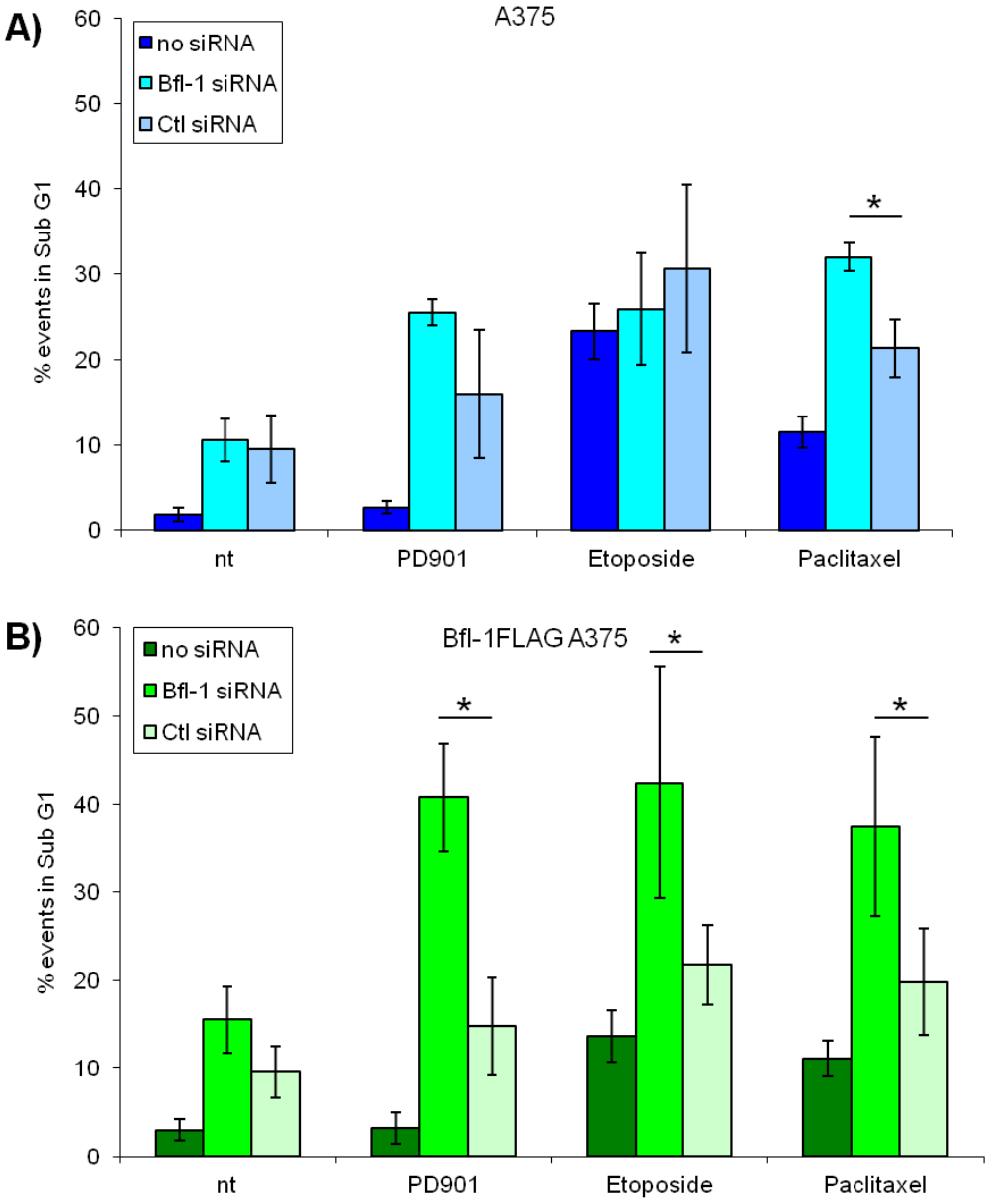

Figure 4.19: Sensitivity to chemotherapeutic agents after Bfl-1 knock-down in A375 cells transfected with Bfl-1FLAG.
A375 cells (A) and A375 cells transfected with Bfl-1FLAG (B) (transfected cells were expanded from a single clone, under selection) were subjected to siRNA treatment with Bfl-1 specific and control (Ctl) siRNA at 40nM for 48 hours. Then they were treated with chemotherapeutic agents (PD901 50nM, Etoposide 10μg/ml and Paclitaxel 10μg/ml) for a further 24 hours. Floating and adherent cells were harvested, stained with propidium iodide for 30 minutes and analysed by flow cytometry. Error bars represent the mean plus and minus the standard deviation from three independent experiments.

4.5 Chapter 4 Conclusions

In this chapter I have explored the role of Bfl-1 in melanoma cells and its importance in protecting these cells from apoptosis triggered by chemotherapeutic agents. Firstly, I treated the panel of melanoma cell-lines with a range of chemotherapeutic agents to

determine if the level of Bfl-1 expression related to the sensitivity of each cell-line to apoptosis.

Initially, I confirmed that the chemotherapeutic agents we used did indeed induce cell death through the apoptotic pathway. This was important to determine as Bfl-1 is involved in protecting cells from cell death through the intrinsic apoptosis pathway. By blocking caspases, the executioners of the intrinsic pathway, using a pan caspase inhibitor I showed that the majority of the drugs did indeed induce apoptosis. The clear exception was the NFκB inhibitor BAY11-7082, where cell death was not blocked by the addition of the caspase inhibitor (Figure 4.2). In fact, previous work has shown the BAY11-7082 kills cells through necroptosis, a specialised programmed necrotic pathway [461]. Cell death caused by Vincristine was also only partially blocked by the caspase inhibitor, suggesting that Vincristine also triggers cell death through a pathway other than apoptosis. Vincristine has previously been shown to cause death associated with lysosomal changes [462], as well as through apoptosis [463]. Etoposide, Cisplatin, Paclitaxel and MEK inhibitors have all been shown to induce cell death through apoptosis, agreeing with our data [464-467].

Having determined which of the chemotherapeutic drugs caused cell death through the apoptotic pathway, I further examined their effects on melanoma cells and explored whether their effectiveness bore any relationship to the expression level of Bfl-1.

Theoretically, cells containing the activating BRaf mutation should be sensitive to MEK inhibition as they rely on the constitutively activated MAPK pathway for survival. However, I did not observe high levels of cell death in our melanoma cell-lines (Figure 4.3), all of which expressed one, if not both, mutated alleles for BRaf (see Table 3.1). Conversely, previous work in our lab demonstrated that melanoma cells which did contain the mutated form of BRaf were more sensitive to MEK inhibition-induced apoptosis than melanoma cells expressing wild-type BRaf, however it should be noted that melanoma cells in general were more resistant to PD901 treatment than other cancer types, such as colorectal cells, containing the BRaf mutation due to their low levels of Bim expression and high levels of pro-survival protein expression [343]. In all our cell-lines I observed a marked arrest in the G1 phase of the cell cycle, sometimes leading to cell death. This agrees with previous findings that the blockade of the MAPK pathway results in G1 arrest and apoptosis in tumours which had an activating mutation in the pathway [468].

The DNA damaging agents Etoposide and Cisplatin were both seen to result in arrest in the G2/M phase of the cell cycle and to translate to high levels of apoptotic cell death (Figure 4.4 and Figure 4.5). Indeed, after Etoposide treatment, previous work has consistently shown cell cycle arrest in the G2/M phase, and the resulting translation to cell death, across a range of tumour types [466,469,470]. Etoposide forms a complex with topoisomerase II on DNA, so that cleaved DNA breaks cannot be repaired. Cells are arrested in G2, as this is the stage in the cell cycle when topoisomerase II reaches its peak in activity [471]. At the high dose of 10μg/ml of Etoposide, the cell cycle arrest was translated into cell death which presumably occured when the cells entered mitosis (Figure 4.4). There appeared to be some correlation between the level of Bfl-1 expression and the susceptibility of these cells to apoptosis with A375 cells displaying the highest level of cell death.

Cisplatin causes platinum complexes to form in the DNA and was also seen to cause arrest in the G2/M phase of the cell cycle in our melanoma cells (Figure 4.5). Cisplatin has been shown to arrest cell cycle in the G2 phase across a range of tumour types and it is the lack of progression across the G2/M transition which leads to apoptotic cell death [467,472,473]. The G2 arrest could be seen as the result of the formation of platinum adducts during the S phase of the cell cycle where DNA is replicated. However when the damage was too great (at 50μg/ml), at least 40% of the cells underwent apoptosis regardless of the levels of Bfl-1 expression in the cell-line. High expression of Bfl-1 induced through strong NFκB pathway signalling has been shown to give human bladder cancer cells resistance to Cisplatin treatment [398], however here we have no conclusive evidence that Bfl-1 protected melanoma cells from Cisplatin treatment. Previous work has shown that Cisplatin activated the ERK pathway to result in higher levels of cell death than when ERK signalling was blocked, independent of p53 status [474]. In our cells, the ERK pathway was already activated by the BRaf mutation, which may be why high levels of cell death were seen across the whole panel of melanoma cell-lines tested, irrespective of Bfl-1 expression. It would be interesting to measure the levels of ERK activation after Cisplatin treatment and to explore whether addition of PD901 blocked Cisplatin-induced apoptosis in our melanoma cells. It would also be interesting to assemble a much larger panel of cell-lines including other cancer types with high Bfl-1 expression, such as lymphomas, to determine whether our melanoma cells were more resistant to treatment with these DNA damaging agents than other cancer types despite the fairly high levels of apoptosis displayed in some of the lines.

Vincristine irreversibly binds to microtubules and spindle proteins in the S phase of the cell cycle and thereby disrupts the formation of the mitotic spindle, causing arrest of the cell cycle in metaphase [475]. Some studies have also observed transient cell cycle arrest in both the G1 and G2 phases of the cell cycle after treatment with Vincristine [460,476]. I observed cell cycle arrest in the G2/M phase of the cell cycle, agreeing with the understanding that Vincristine triggers metaphase arrest (Figure 4.6). Bfl-1 expression did not appear to protect cells from the cell death caused by Vincristine, but interestingly, inhibition of IKK2, the upstream regulator of NFκB, which is responsible for the transcription of Bfl-1, was previously shown to enhance Vincristine cytotoxicity in lymphoma cells [477].

Paclitaxel, instead of preventing the formation of the mitotic spindle, binds to the microtubule polymer, preventing it from disassembly thereby causing a transient arrest at the metaphase checkpoint after which cells either revert back to the G2 phase or undergo cell death [478]. Indeed, I routinely saw 30% arrest in the G2/M phase in the melanoma cell-lines compared with about 10% in untreated cells (Figure 4.7). In fact A375 cells displayed about 50% G2/M arrest. Levels of cell death varied over the cell-lines, with 50% cell death seen in UACC62 cells but only around 10% seen in MM200 and SkMel28 cells. Despite the low cell death, SkMel28 and MM200 cells did show increased G2/M arrest compared to untreated cells, with fewer cells in the G1 phase. This G2/M arrest showed that Paclitaxel was at high enough concentrations to be active in the cells, but that these two cell-lines were particularly resistant to Paclitaxel-induced cell death at 10μg/ml. The level of Paclitaxel-induced cell death did not directly correlate with Bfl-1 expression levels, although the two highest expressing cell-lines were the most resistant to this treatment and A375 cells, although they underwent less cell death than UACC62 and G361 cells, displayed a large G2/M arrest instead.

In summary, I did not see a clear correlation in our cell-lines between resistance to chemotherapy-induced apoptosis and the level of Bfl-1 protein they expressed. This was perhaps not surprising given the multi-faceted nature of apoptosis induction.

After the lack of clear evidence that high Bfl-1 expression lent melanoma cells resistance from the range of chemotherapeutics, we investigated its effect on apoptosis more directly by directly regulating its expression, firstly by over-expressing Bfl-1 in A375 cells. These transfected cells plainly had higher resistance to the chemotherapeutics than the mock transfected cells and fewer cells underwent apoptosis as a result, confirming that high Bfl-1 expression made cells more resistant to chemotherapeutics (Figure 4.11). The other

important role of cancer drugs other than the initial killing of tumour cells is to prevent the proliferation of cells which survive the initial treatment. Cells that avoid cell death at the first stage can go on to proliferate, selecting for clones with increased resistance to the drug. I explored whether over-expression of Bfl-1 resulted in higher clonogenic potential for the A375 melanoma cells. Although the actual clone numbers obtained were rather variable between experiments, in general the trend was clear; that transfected cells with higher levels of Bfl-1 expression had higher clonogenic potential than the mock-transfected cells (Figure 4.12). Several factors may have caused this variation within the clonogenic experiments, such as different transfection efficiencies between samples, different levels of growth factors in the conditioned media and errors in the counting of cells before they were seeded into 96 well plates. On the whole, results from this assay suggest that high Bfl-1 expression provides cells with higher long-term survival and clonogenic potential. An important follow-up experiment for this would to be to knock-down native Bfl-1 expression in a melanoma cell-line and determine whether the cells lost clonogenicity.

Having shown that high levels of Bfl-1 expression did indeed make cells more resistant to chemotherapeutics, I explored whether knock-down of Bfl-1 would increase the sensitivity of cells to these drugs. We achieved efficient knock-down of up to 80% of Bfl-1 using siRNA technology (Figure 4.14). Through this process I was able to measure the levels of cell death resulting from chemotherapeutic agents in melanoma cells with native levels of Bfl-1 against the same melanoma cells with much lower levels (Figure 4.16). SkMel28 cells showed increased sensitivity to PD901 with more than double the cell death level seen after treatment with Bfl-1 siRNA compared to the control siRNA. A lower level of increased sensitivity to Cisplatin and Paclitaxel treatment after Bfl-1 knock-down was also observed in SkMel28 cells with between 10-15% extra cell death compared to the control siRNA. MM200 cells were less sensitive to Bfl-1 knock-down, only displaying higher levels of cell death as a result of Paclitaxel treatment.

The reasons behind this differential cell and drug sensitivity are currently unclear. However, Bfl-1 protein expression in SkMel28 cells was routinely seen to rise after PD901 treatment (Chapter 3), while in MM200 cells it was seen to fall. Bfl-1 knock-down in SkMel28 cells sensitised them to PD901 treatment, possibly because Bfl-1 expression was an important defence against this trigger in these cells, while in MM200 cells it was not. A study of the affects of MEK inhibition across a panel of melanoma cell-lines determined that the BH3-only proteins Bmf and Bim were essential for MEK inhibitor-induced

apoptosis [445]. Bfl-1, with its structural plasticity, has been shown to bind both the promiscuous protein Bim and the more selective Bmf [416]. Therefore, in the absence of Bfl-1 expression to block these BH3-only proteins, MEK inhibition became more effective in these cells. Presumably, the MM200 cells were not more sensitive to PD901 treatment after Bfl-1 knock-down because they had other defences upon which they relied more heavily than the induction of high levels of Bfl-1 protein. The effects of MEK inhibition on the levels of the other pro-survival proteins, and indeed the other BH3-only proteins such as Bim and Bmf, in MM200 cells should be explored and may elucidate why MM200 cells were relatively resistant to Bfl-1 knock-down. For example, another study on the effects of MEK inhibition indicated it was the inactivation of Bad which helped cells evade MEK inhibition-induced death, which is a protein Bfl-1 does not associate with [306].

Paclitaxel treatment was the one drug which MM200 cells became more sensitive to after Bfl-1 knock-down, and SkMel28 cells also displayed higher cell death with Paclitaxel after Bfl-1 knock-down. Induction of Bfl-1 expression has been seen to give leukemia cells resistance to Paclitaxel treatment [375], and I also observed this in our transfected A375 cells (Figure 4.11). In fact, Paclitaxel was one of the drugs where a weak correlation was seen between native Bfl-1 expression and resistance to its treatment (Figure 4.7). Previous research on the mechanism by which Paclitaxel-induced apoptosis occurs has confirmed the involvement of the Bcl-2 family. Deletion of Bim incurred partial resistance to Paclitaxel-induced apoptosis [304] while lower levels of Mcl-1 expression have been shown to re-sensitise Paclitaxel-resistant cells to Paclitaxel treatment [479]. Paclitaxel can cause phosphorylation of Bcl-2 which appeared to protect the protein from proteasomal degradation and therefore enhance its pro-survival effects [480] and over-expression of Bcl-xL prevented Paclitaxel-induced apoptosis in leukemia cells [481]. This research confirms the importance of pro-survival proteins in the protection of cells from Paclitaxel-induced apoptosis and highlights Bfl-1 as a major regulator in melanoma cells.

No increase in sensitivity to cell death was seen after Bfl-1 knock-down to Etoposide, Vincristine or the background levels of cell death in either MM200 or SkMel28 cells. Lack of an increase in background cell death suggests that Bfl-1 only takes on its pro-survival role after apoptosis has been triggered in these cells. In resting cells, Bfl-1 may be in an inactive form, possibly in the cytoplasm, and after apoptosis has been initiated Bfl-1 binds the activator BH3-only proteins at the mitochondria. Etoposide treatment has been shown to initiate apoptosis involving the Bcl-2 family, so it was surprising to see no increase in the sensitivity of the cells after Bfl-1 knock-down. Bfl-1 over-expression has been shown

to protect cells from Etoposide-induced apoptosis [411] and I also saw this in our transfected A375 cells (Figure 4.11), although the level of protection appears to vary between cell types [406]. In fact, Etoposide has been shown to activate the NFκB pathway, resulting in an increase in the transcription of Bfl-1 which can then protect cells from apoptosis [59]. Perhaps the activation of the NFκB pathway by Etoposide was sufficient to replace the Bfl-1 which had initially been knocked down by siRNA treatment and this could be confirmed by western blotting for Bfl-1 after drug treatment. Cisplatin treatment in SkMel28 cells was marginally more effective when Bfl-1 was knocked down in comparison to the control siRNA, whereas in MM200 cells Bfl-1 knock-down had no effect. Previous work has shown that knock-down of Bfl-1 with shRNA in malignant B-cells sensitised cells to Cisplatin, among other chemotherapeutic agents [385], suggesting that B-cells are more sensitive to Cisplatin treatment than melanoma cells after Bfl-1 knock down.

Interestingly, cells transfected with an over-expressed Bfl-1 construct appeared to become more reliant on Bfl-1 for survival from chemotherapeutic agents than the original wild-type cells were (Figure 4.19). Drugs, such as Etoposide, which were not made more effective by the knock-down of native Bfl-1 in melanoma cells, were more effective after knock-down of the over-expressed Bfl-1 construct in transfected cells. Knock-down of Bfl-1 in wild-type A375 cells did not increase the levels of cell death after treatment with PD901 or Etoposide, or the background cell death, as expected in a cell-line with very little Bfl-1 expressed. However, surprisingly, Paclitaxel treatment did result in higher levels of cell death after Bfl-1 knock-down, in native A375 cells expressed very little Bfl-1, the reason for this is unclear.

Meanwhile, A375 cells transfected with Bfl-1FLAG underwent significantly higher levels of cell death after treatments with PD901, Etoposide and Paclitaxel when Bfl-1 was knocked down, compared to the control siRNA. This suggests that while the transfected cells were proliferating with high Bfl-1 expression levels, they became more dependent, or 'addicted', to Bfl-1. This mirrors the 'oncogene addiction' observed in cancers, where the cells become reliant on one mutated oncogene for survival of the tumour. It would be interesting to explore the levels of the other pro-survival proteins in A375 cells after transfection with Bfl-1FLAG, particularly Mcl-1 levels. Wild-type A375 cells which expressed very low levels of Bfl-1 expressed high Mcl-1, which is the most similar pro-survival protein in the Bcl-2 family to Bfl-1. It is possible that Bfl-1 expressed at such high levels in the transfected cells made Mcl-1 redundant so that when Bfl-1 was taken away

again, there was not enough Mcl-1, or other pro-survival proteins, in the cell to protect them from cell death.

In conclusion, in this chapter I explored the role of Bfl-1 in melanoma and its importance in the chemo resistance of this cancer type. Although no clear correlation between the endogenous protein and sensitivity to chemotherapeutics was found in the panel of melanoma cell-lines, Bfl-1 was proven to act as a pro-survival molecule in melanoma cells and its knock-down increased the effectiveness of some already existing chemotherapeutic agents. There is enough evidence here to suggest the further exploration of Bfl-1 as a potential drug target in melanoma.

5 : THE SUBCELLULAR LOCALISATION OF BFL-1

5.1 Introduction

In chapters 3 and 4, I characterised Bfl-1 in melanoma cell-lines by examining its regulation, degradation and genetic profile, and elucidated its importance in protecting melanoma cells from the apoptosis usually triggered by chemotherapeutic agents. However, another important factor in characterising the protein was to determine its subcellular localisation.

Subcellular localisation is an important factor in understanding the function and site of action of a protein. It can also be used to determine the viability of a protein for drug targeting, for example, proteins on the plasma membrane provide more easily accessible targets than those contained within micro organelles. Interestingly, aberrant subcellular localisation of proteins has been observed in some cancers, which may result in, or be the result of, proteins having differing functions in cancerous cells compared to healthy cells, such as the phosphoprotein BRCA1 in breast cancer [482].

Subcellular localisation can be determined through laboratory techniques including subcellular fractionation and staining with fluorescently tagged antibodies, or tagging the protein directly with a fluorescent tag, such as GFP or YFP, for detection by microscopy techniques. In addition, computational techniques, which profit from the increased knowledge of known protein localisations, to predict the localisation of a new protein, are becoming increasingly faster and more accurate [483].

The subcellular localisations of some of the other members of the pro-survival Bcl-2 family have already been determined. Using subcellular fractionation and western blotting techniques in melanoma cell-lines, VanBrocklin et al.[445] found Bcl-2 in the mitochondrial fraction whilst Bcl-xL was present in the cytosolic fraction and Mcl-1 present in both, although at a higher level in the cytosolic fraction. In healthy lymphocyte cells subcellular fractionation and confocal microscopy showed Bcl-2 to be associated with the mitochondria, endoplasmic reticulum and nuclear envelope [484]. Bcl-w was also found to associate with intracellular membranes by subcellular fractionation and confocal scanning laser microscopy in transformed cell-lines [450]. In HeLa cells Mcl-1 was observed near the internal face of the plasma membrane, but after cleavage by caspases moved to the mitochondria where it bound Bim [485]. Hsu et al.[486] also observed that after initiation of apoptosis in leukemia cells, Bcl-xL relocated from the cytosol to the membrane fraction, although they did not identify the specific membrane it moved to. This work suggests that

in general, the pro-survival members of the Bcl-2 family exist in soluble forms in the cytosol and in membrane bound forms present across a selection of internal membranes.

Bfl-1S itself has been observed to be localised to the nucleus via residues in its C-terminus [422], but in general Bfl-1 has been observed in the cytosol or mitochondrial membrane [235,424,425]. Due to the lack of any Bfl-1 antibodies which could recognise non-denatured Bfl-1, these studies used tagged proteins transfected into cells to determine the subcellular localisation of Bfl-1. In this chapter we aimed to identify the localisation of the native protein in melanoma cells.

5.2 Detection of Native Bfl-1 in Melanoma Cell-lines

I began by determining whether any of the Bfl-1 antibodies I had access to would specifically bind Bfl-1 for subsequent detection by confocal microscopy. These antibodies included commercially available Bfl-1 specific antibodies from Epitomics and Cell Signaling Technology, as well as the antibody from WEHI which was used to detect Bfl-1 by western blotting in previous chapters. Three cell-lines were stained with each antibody to determine the specificity of the antibodies for Bfl-1. The three cell-lines were SkMel28, which expressed high levels of Bfl-1, A375 which expressed very low levels of Bfl-1 and Colo205 where Bfl-1 was undetectable, as demonstrated by western blotting (Figure 5.1). Cells under culture conditions were grown on coverslips coated with Poly-L-Lysine, an attachment factor which improves cell adherence, to an appropriate confluence. Slides were then fixed with 4% formaldehyde (PFA) and permeabilised with saponin to allow the antibody to enter the cells. Non-specific binding of the primary antibody was blocked using normal goat serum (NGS) before cells were stained with the primary antibody overnight at 4ºC. Subsequently, the excess primary antibody was washed off and cells were incubated with the fluorescently tagged secondary antibody for 1 hour at room temperature. The nuclear dye Dapi, contained in the mounting media Vectashield, was also added to identify the nuclei of the cells (data not shown). Fluorescence was detected using a Leica TPS SP5 confocal microscope.

In this experiment, each cell-line was visualised for the same exposure time and at the same magnification for the individual antibodies. The antibodies we tested all detected staining in the Bfl-1 negative Colo205 cells. In fact the Epitomics antibody fluoresced at higher levels in the Colo205 cells than in SkMel28 cells which have high levels of Bfl-1 (Figure 5.1). The Epitomics and WEHI antibodies also demonstrated fluorescence in the Bfl-1 low expressing A375 cell-line. This data suggested that none of the antibodies we

had access to could specifically detect native Bfl-1 in our cells and as yet, no commercially available antibodies claim to be able to detect Bfl-1 by immunohistochemistry.

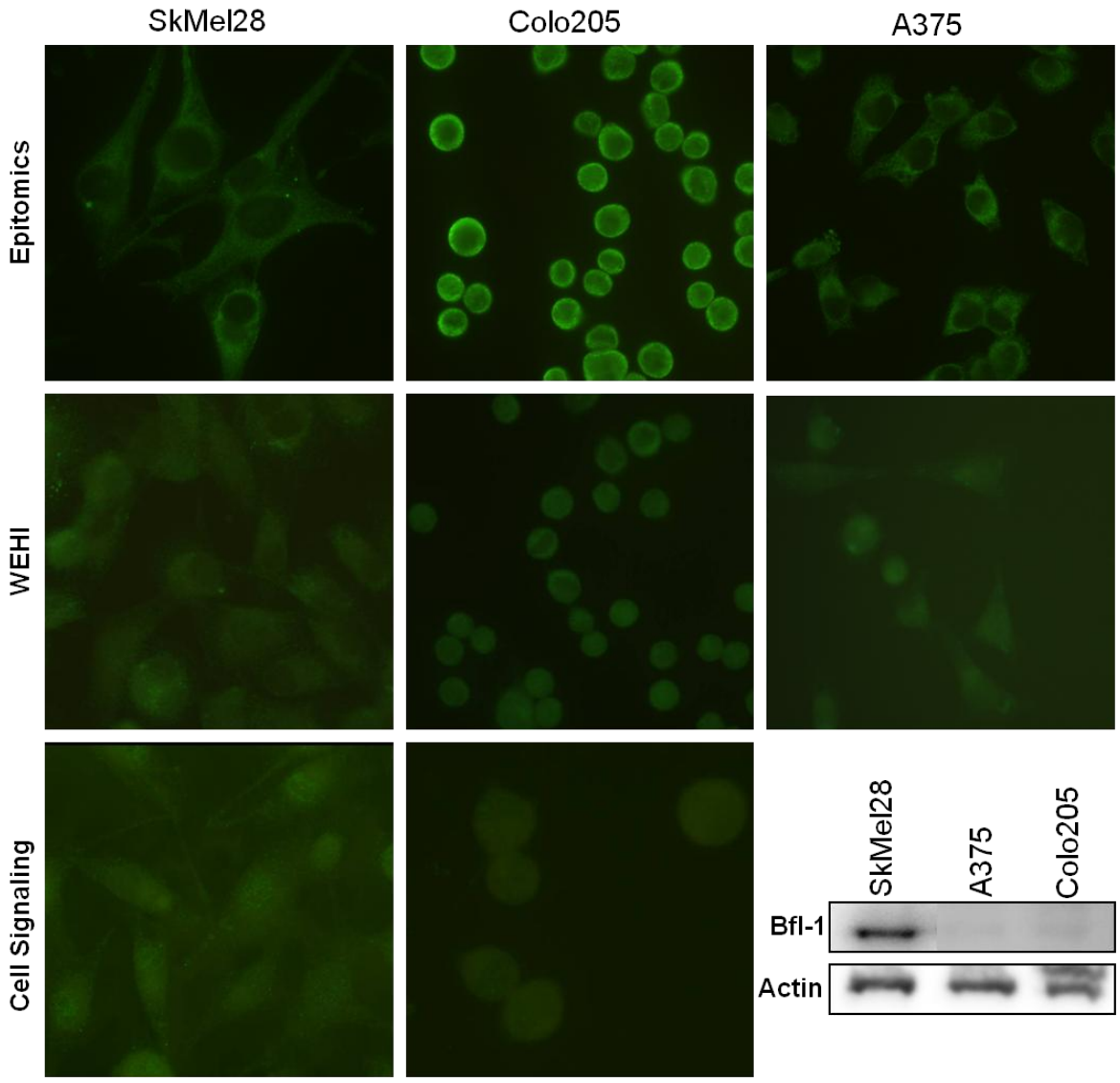

Figure 5.1: Antibodies for Bfl-1 cannot detect native Bfl-1 by indirect immunofluorescence.
For the western blot, lysates were generated from untreated cells, separated by SDS-PAGE and analysed by western blot. For microscopy, cells were grown on coverslips, fixed with formaldehyde and permeabilised with saponin. After blocking with normal goat serum, cells were incubated with the primary antibodies overnight then the secondary antibody for 1 hour. Secondary antibodies were tagged with the fluorophore alexa 488 which was then detected by confocal microscopy with 100X magnification. These data are representative of one experiment for Cell Signaling Technology and Epitomics antibodies and over three independent experiments for the WEHI antibody.

As I was unable to detect native Bfl-1 in our melanoma cell-lines using this technique, we employed a subcellular fractionation technique using a mitochondria isolation kit from Thermo Scientific. This kit was a reagent based technique which used differential centrifugation to produce mitochondria and cytosol fractions. Nuclei and cell debris are isolated first before the mitochondria and cytosol fractions are separated. These fractions

contained all the membrane bound proteins associated with the mitochondria and all the soluble proteins present in the cytosol of these cells and could be analysed by western blotting. Each fraction was subjected to protein quantitation so that the same concentration of protein was loaded to the western blot from both the mitochondria and cytosol fractions. Cytochrome-c oxidase IV (COX IV) is a protein bound to the internal membrane of the mitochondria [487] and was used as a marker for mitochondrial isolation, whilst actin was used as a cytosol marker to determine the purity of each fraction.

Having established effective separation of mitochondrial and cytosolic fractions, as observed with these protein markers, I probed the melanoma cell-lines MM200 and SkMel28 for the presence of native Bfl-1 in the mitochondria and cytosol fractions by separating the proteins by SDS-PAGE and analysing them by western blot using the WEHI Bfl-1 antibody (Figure 5.2). I observed that in both melanoma cell-lines, Bfl-1 was present in both fractions, but at a higher concentration in the mitochondria rather than the cytosol fraction.

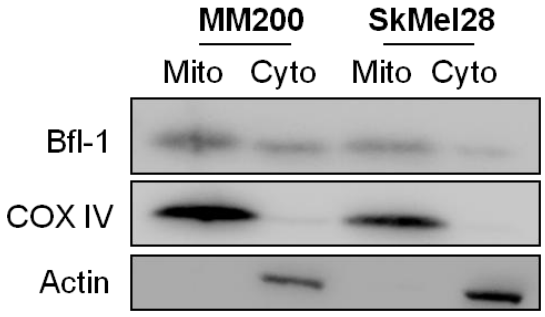

Figure 5.2: Subcellular localisation of Bfl-1 in melanoma cells.
MM200 and SkMel28 cells in culture were harvested and subjected to subcellular fractionation using the mitochondria isolation kit from Thermo Scientific, which is a reagent based method for the separation of these fractions from whole cells. Lysates were generated and subjected to SDS-PAGE and analysed by western blot. COX IV was used as a marker for mitochondria and actin was used as a marker for cytosol. These data are representative of four independent experiments.

We then went on to confirm these subcellular fractionation results by performing indirect immunofluorescence using the tagged protein constructs produced in chapter 4.

5.3 Detection of Bfl-1 in Over-Expressed Systems

The constructs Bfl-1YFP, Bfl-1FLAG and Bfl-1 alone were produced as described in Appendix I. We used these constructs to determine the subcellular localisation of Bfl-1 by indirect immunofluorescence. Firstly, we transfected the constructs into 293F cells, which over-express protein constructs at very high levels. We did this to test whether the

antibodies could detect the protein at these high levels before we attempted to detect them at lower, more physiological levels. 293F cells were transfected with the constructs using the 293fectin system as before and left to grow for 24 hours before fixation.

The Bfl-1YFP construct was detected through the fluorescence emitted by the YFP protein present on the N-terminus, therefore requiring no further staining with an antibody. Bfl-1FLAG was detected using an antibody specific for the FLAG tag, present on the C-terminus, and the Bfl-1 construct was detected using the WEHI Bfl-1 antibody. The secondary antibodies for detecting the FLAG and Bfl-1 monoclonal antibodies were tagged with the green fluorophore alexa 488. The method for the staining of these cells was as described in section 5.2, with the addition of the mitochondrial stain MitoTracker Red CMXRos. This is a reduced dye that enters actively respiring cells where it is oxidised and fluoresces when sequestered around the mitochondria. It was added to cells on coverslips for 30 minutes at 100nM before they were fixed. Throughout this chapter the Bfl-1 protein staining is represented as green and the mitochondria are shown in red. The overlays between the green and red appear yellow where the two signals are co-localised.

Transfection of the Bfl-1 constructs into 293F cells showed that Bfl-1 co-localised with the mitochondria in this system (Figure 5.3). Untreated 293F cells (Figure 5.3) and 293F cells treated with the secondary antibody alone (data not shown) yielded very low levels of background signal in the green channel. This confirmed that the subsequent staining we saw was as a result of the binding of the antibodies to the protein constructs in the cells. The Bfl-1FLAG and Bfl-1 constructs appeared to localise to the mitochondria in these cells, as shown by the overlay pictures. However the Bfl-1YFP construct appeared to be more generally dispersed throughout the cell, present mostly in the cytoplasm but with no clear co-localisation to the mitochondria. Subsequent analysis revealed that cells transfected with Bfl-1YFP appeared to display apoptotic morphology, with collapsed nuclei and loss of the healthy rounded shape usually seen with these cells, perhaps explaining the altered distribution of Bfl-1 in these cells. Staining was clearer with the FLAG antibody than with the Bfl-1 antibody, producing a stronger signal which more clearly demonstrated the localisation of the protein, probably because the FLAG antibody was more sensitive than the Bfl-1 antibody.

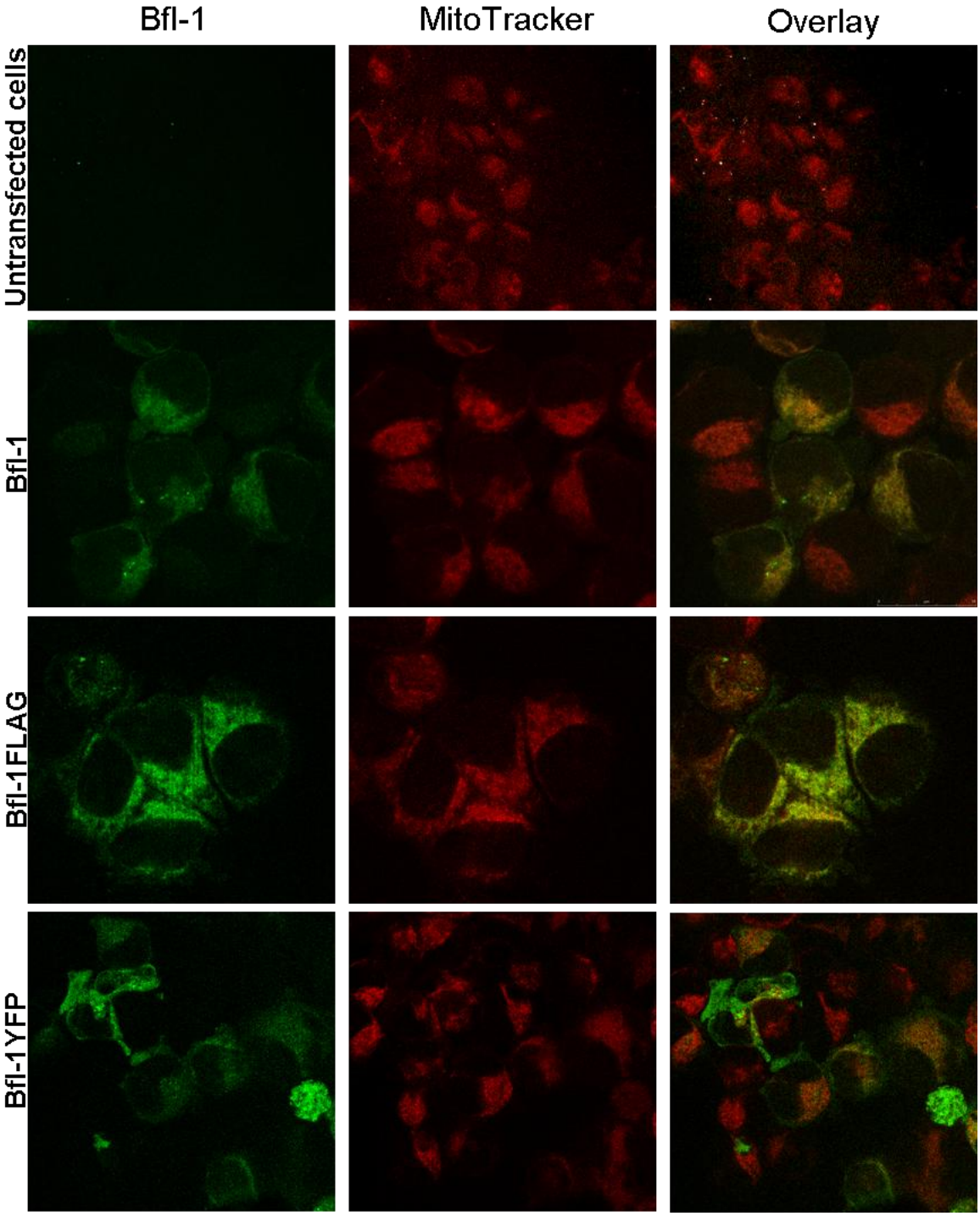

Figure 5.3: Localisation of Bfl-1 protein expressed in transfected 293F cells.
293F cells were transiently transfected with Bfl-1 constructs by 293fectin. 24 hours after transfection mitochondria were visualised by incubation of 293F cells with 100nM MitoTracker Red CMXRos dye (Invitrogen) for 30 minutes prior to fixation for indirect immunofluorescence. The Bfl-1 constructs were detected using different antibodies; Bfl-1 was detected using the WEHI Bfl-1 antibody, Bfl-1FLAG was detected using FLAG antibody and Bfl-1YFP was detected through the YFP fluorescence. These pictures were taken at 100X magnification. Bfl-1 and Bfl-1FLAG also had an additional 2X optical zoom to further magnify these pictures to examine the co-localisation of the protein and the mitochondria. These data are representative of two independent experiments.

Having successfully detected the protein products of our tagged constructs in 293F cells, we went on to examine the localisation of the constructs in a melanoma cell-line. The cell-line A375 was used as it naturally contained very low levels of native Bfl-1 protein. These cells proved difficult to transfect with our constructs. We applied techniques such as electroporation, lipofection and nucleofection with the most successful technique being lipofection. However even this method yielded a very low transfection efficiency so that on a coverslip covered in cells, only a minor proportion of cells were successfully transfected. We also found that the cells did not retain the constructs for long, even under selection, so growing a population from a single transfected cell did not result in a higher percentage of cells expressing the tagged proteins.

The Bfl-1-FLAG and Bfl-1YFP constructs were transfected successfully into these cells, but the untagged Bfl-1 construct was not. Therefore, no pictures were obtained for untagged Bfl-1 in A375 cells. However, we were able to detect Bfl-1-FLAG using the FLAG antibody and Bfl-1YFP through its native fluorescence (Figure 5.4). Both the Bfl-1YFP and Bfl-1FLAG constructs appeared to co-localise with the mitochondria in these melanoma cells, agreeing with the results of the subcellular fractionation of native Bfl-1 in melanoma cell-lines (Figure 5.2). Staining of untransfected A375 cells with the WEHI Bfl-1 antibody resulted in some weak fluorescence, but this did not relate to Bfl-1 expression, as shown in Figure 5.1 and confirmed by the non-specific staining seen in the sample stained with the secondary antibody only. Similarly, low levels of background green fluorescence were detected in A375 cells transfected with Bfl-1FLAG stained with only the secondary antibody (data not shown).

The expression constructs for Bfl-1 resulted in an over-expressed level of Bfl-1 in both A375 and 293F cells. In both these cell types, Bfl-1 was therefore expressed at higher levels than the native protein in any of the melanoma cell-lines. In fact, the protein was expressed at a higher level in 293F cells than A375 cells making the protein in the 293F cells the easiest to detect by indirect immunofluorescence.

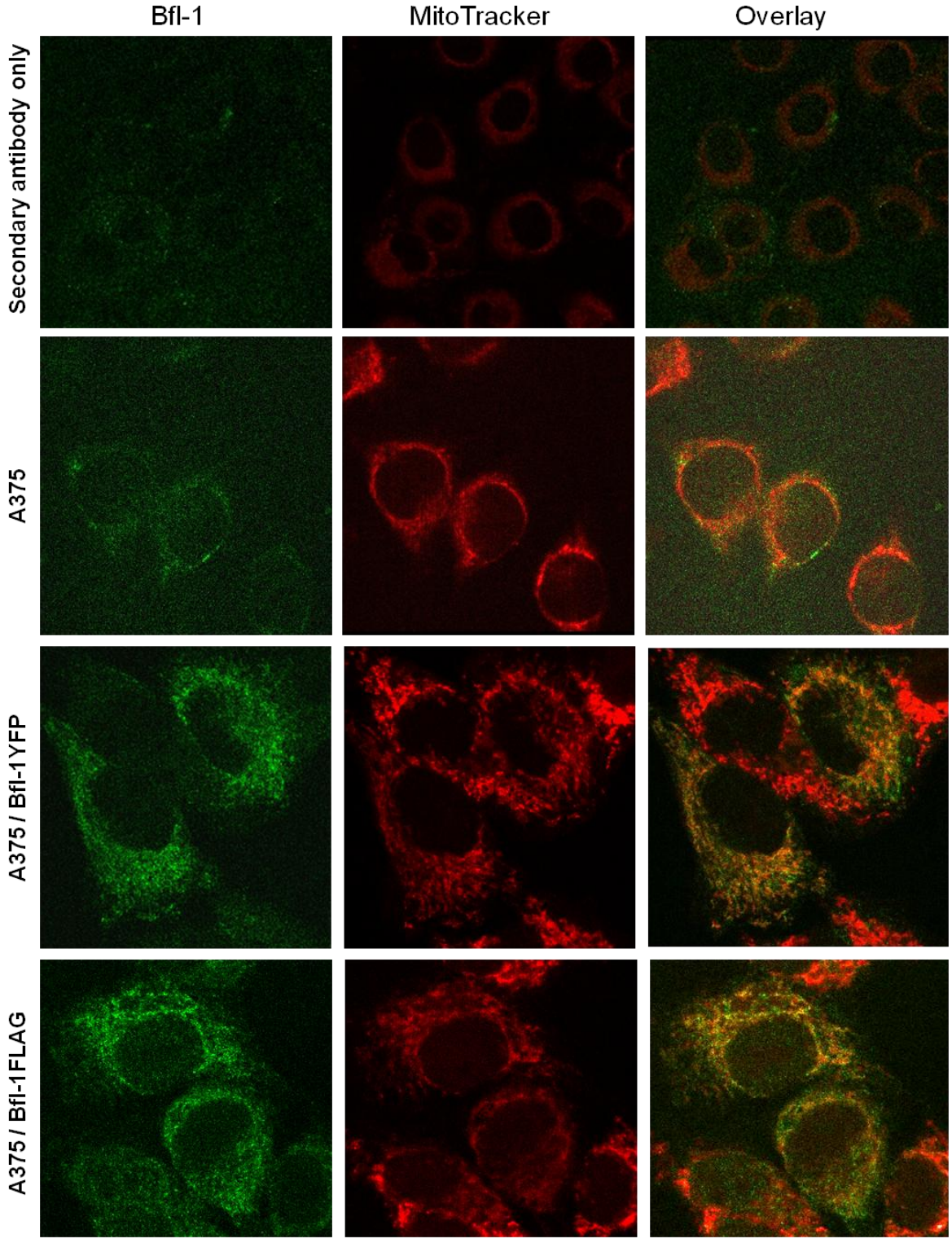

Figure 5.4: Localisation of Bfl-1 proteins expressed in transfected A375 melanoma cells.

The Bfl-1 constructs were transiently transfected into A375 cells by lipofection. 24 hours after transfection, cells were stained with Mitotracker Red CMXRos at 100nM for 30 minutes before being fixed for indirect immunofluorescence. Bfl-1FLAG was detected using the antibody for FLAG while Bfl-1YFP was detected through the fluorescence emitted by the YFP tag and A375 cells were stained with the WEHI Bfl-1 antibody. The cells were visualised by confocal microscopy with these pictures taken at 100X magnification. Bfl-1YFP and Bfl-1FLAG were also viewed with an additional 2X optical zoom to further view the co-localisation. These data are representative of one experiment for Bfl-1YFP and more than three independent experiments for Bfl-1FLAG and untransfected cells stained with the secondary antibody only, or the Bfl-1 WEHI antibody.

5.4 The Effect of Chemotherapeutics on the Subcellular Localisation of Bfl-1 in A375 Cells

In healthy resting cells, Bfl-1 appeared to be localised to the mitochondria, with some additional expression in the cytoplasm. In other cells and with other Bcl-2 family members such as Bcl-2, apoptosis stimulation can change the localisation of the proteins. Therefore, to assess if Bfl-1 redistributed after apoptotic stimuli, I challenged transfected cells with chemotherapeutic agents and probed them for the localisation of Bfl-1. I used the Bfl-1FLAG construct in A375 cells in these experiments, as detection of Bfl-1FLAG with the FLAG antibody resulted in the best staining. PD901 (50nM) and Etoposide (10μg/ml) were added to A375 cells 24 hours after transfection with Bfl-1FLAG for a further 24 hours. Drugs were then washed off the cells which were incubated with MitoTracker red for 30 minutes before being fixed and stained for FLAG as before (Section 5.2).

The overlays show that Bfl-1FLAG was localised to the mitochondria in resting cells and also in cells challenged with chemotherapeutic agents (Figure 5.5). I utilised a tool on the LAS microscope software to demonstrate in graphical form the co-localisation of Bfl-1 and mitochondria staining (Figure 5.6). To produce these graphs, a line in drawn across the cell and the intensity of each colour channel along that line is represented as a histogram on the graph. These graphs confirm this analysis of the microscopy pictures as peaks in the red line, representing the mitochondria, were aligned with peaks in the green line, representing Bfl-1. In addition to a large degree of co-localisation between Bfl-1 and mitochondria, this analysis demonstrated that a substantial amount of Bfl-1 was also present outside of the mitochondria. For example, the untreated cells in Figure 5.6 had several green peaks which were present when the red channel was dipped.

Interestingly, Bfl-1 appeared to associate more closely with the mitochondria after cells were treated with the apoptosis inducer Etoposide (Figure 5.5 and Figure 5.6), whereas treatment with PD901 provided less convincing evidence of a closer association of Bfl-1 with the mitochondria. Etoposide induces death at a much higher level in A375 cells than PD901, suggesting that Bfl-1 responds to apoptotic triggers by localising to the mitochondria and that the stronger the trigger, the more Bfl-1 is sequestered to the mitochondria. Another way of analysing co-localisation would be to employ co-localisation coefficients such as Pearson's co-localisation coefficient, used by Chaturvedi et al. to demonstrate co-localisation between the BCR and phosphorylated kinases [488]. However, more cells than we were able to visualise are needed to successfully apply this technique.

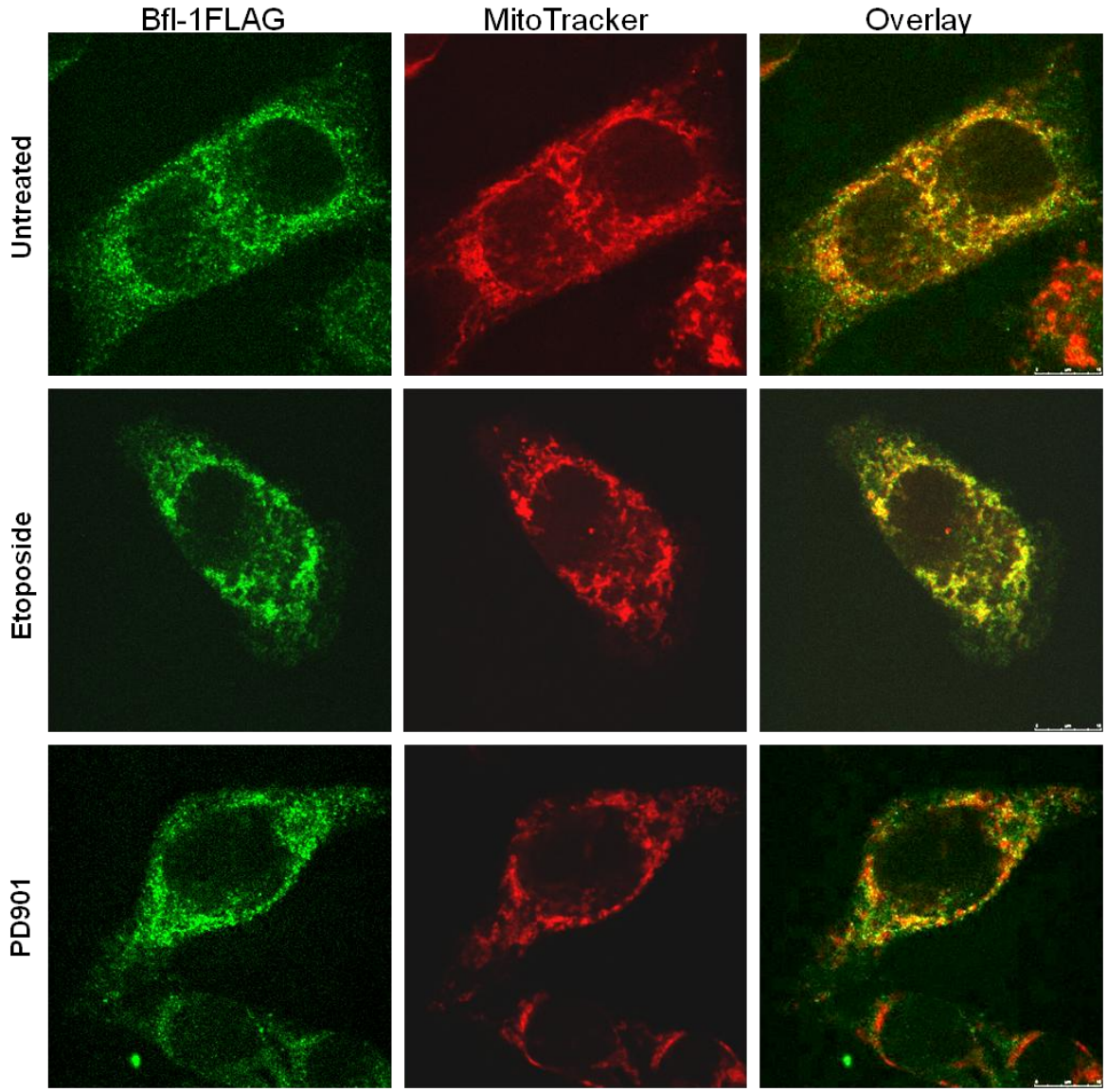

Figure 5.5: The subcellular localisation of Bfl-1FLAG in A375 melanoma cells after treatment with chemotherapeutic drugs.
A375 cells were transfected with Bfl-1FLAG by lipofection. 24 hours after transfection, cells were treated with Etoposide (10μg/ml) or PD901 (50nM) for a further 24 hours. Drugs were then washed off and cells were stained with MitoTracker Red (100nM) for 30 minutes before fixation for indirect immunofluorescence. The primary antibody used for detection of Bfl-1FLAG was the FLAG antibody. The cells were visualised by confocal microscopy and these pictures were at 100X magnification with an additional 2X optical zoom for closer examination of co-localisation. These data are representative of three independent experiments.

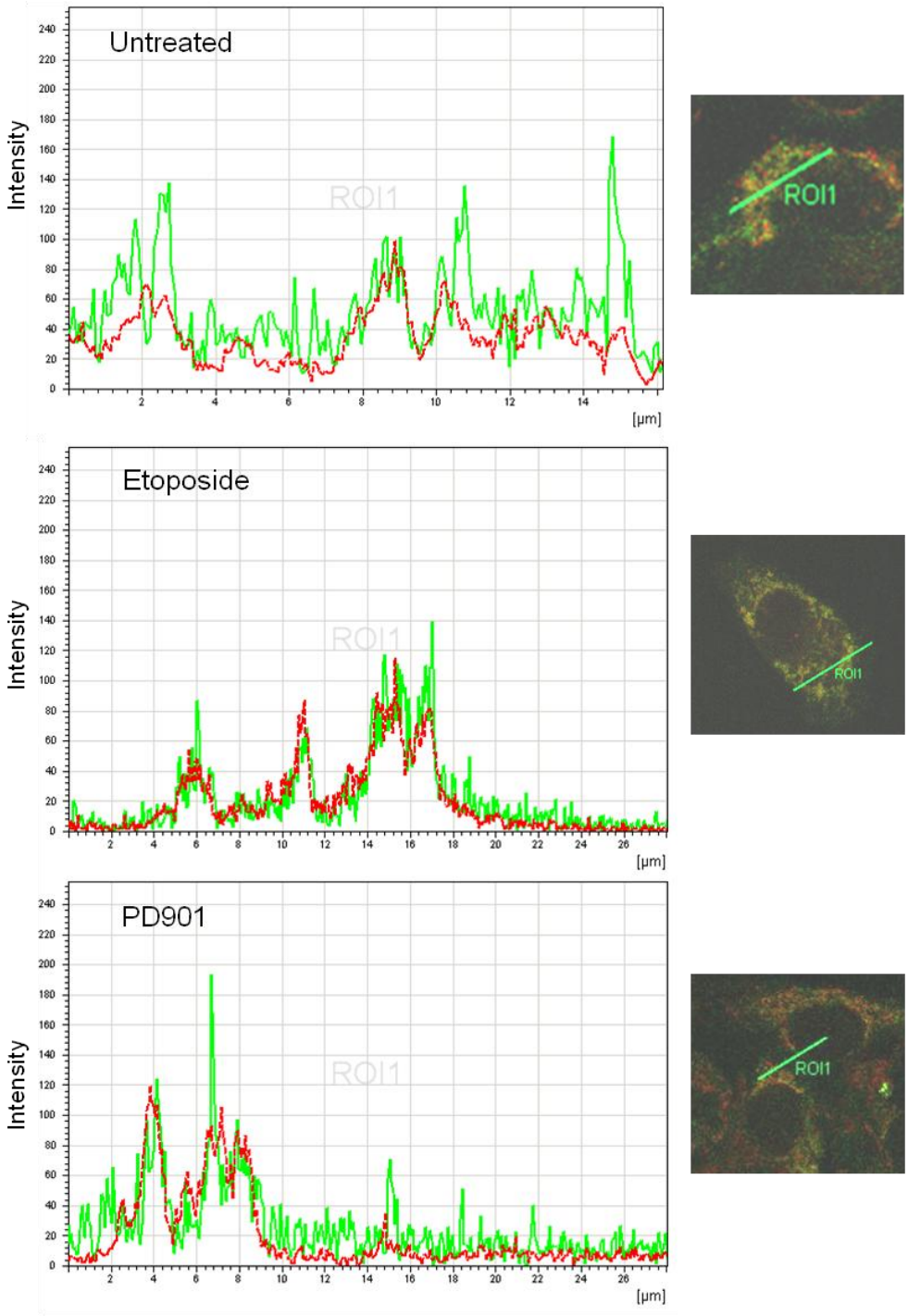

Figure 5.6: Graphical representations of the distribution of Bfl-1FLAG in apoptotic A375 melanoma cells.

A375 cells transfected with Bfl-1FLAG were treated with Etoposide (10mg/ml) or PD901 (50nM) for 24 hours. Drugs were washed off and the cells were stained with MitoTracker Red (100nM, 30 minutes) before fixation for indirect immunofluorescence. Bfl-1FLAG was detected using the FLAG antibody. The cells were visualised by confocal microscopy at 100X magnification with an additional 2X optical zoom. LAS software on the microscope was then utilised to convert the intensity of each colour channel into graphical format. A line was drawn through the picture of the cells with the red line representing the intensity of the mitochondria stain and the green representing Bfl-1FLAG. When the peaks align, the two signals are co-localised. Horizontal axis is length of line drawn through cells, vertical axis is intensity of fluorescence. These graphs are representative of numerous lines drawn across all angles of the cells seen here and also represent graphs from other cells from other experiments.

We also looked at the change in subcellular localisation of the native Bfl-1 protein in melanoma cells after treatment with Etoposide and PD901 by subcellular fractionation (Figure 5.7). SkMel28 cells (Figure 5.7) and MM200 cells (data not shown) were treated with Etoposide or PD901 for 24 hours before cells were harvested and mitochondria were isolated. Unfortunately, the mitochondria isolation kit requires a large number of cells in order to result in protein concentrations high enough to be detected by our Bfl-1 antibody. Hence, when cells were treated with Etoposide, not enough protein could be recovered to determine the localisation of native Bfl-1 (data not shown). However, after treatment with PD901, enough protein was recovered to detect Bfl-1 in the mitochondrial fraction (Figure 5.7). As before, the fractionation worked efficiently as evidenced by the detection of COX IV and actin. No protein was detected in the cytosolic fraction which might indicate that Bfl-1 was redistributed to the mitochondria. However, the level of protein generally in the PD901 treated cells was lower than that seen in the untreated cells, so the proportions could still be similar but at a level where we could not detect the protein in the cytosol. Therefore conclusive results cannot be drawn from these data. This decrease in Bfl-1 levels after PD901 treatment agreed with our previous results seen in SkMel28 cells where levels of Bfl-1 decreased or remained the same after 24 hours of treatment with PD901 but then rose after 48 hours of MEK inhibition. As such, subcellular fractionation could have been performed after 48 hours of PD901 treatment in SkMel28 to make use of this increase in Bfl-1 levels to determine the subcellular localisation of Bfl-1 after PD901 treatment in SkMel28 cells. However, the problem with treating cells for 48 hours was that a higher level of cell death was seen which would have limited the quantity of living cells available for the subcellular fractionation technique.

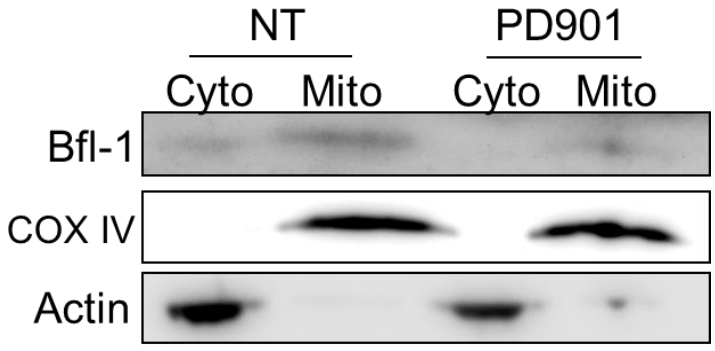

Figure 5.7: Localisation ofBfl-1 in melanoma cells treated with PD901.
SkMel28 cells were grown under culture conditions and treated with PD901 (50nM) for 24 hours before being harvested and separated into cytosolic (Cyto) and mitochondrial (Mito) fractions using the Thermo Scientific mitochondria isolation kit. Proteins were then separated by SDS-PAGE and analysed by western blot. These data are representative of two independent experiments.

5.6 Does Bfl-1 Co-localise with Other Micro-Organelles?

Having demonstrated the localisation of Bfl-1 to mitochondria in several systems using two independent techniques, we also examined the localisation of Bfl-1 to lysosomes. We chose lysosomes as they are present in the cytoplasm, where some Bfl-1 was observed.

To assess lysosomal co-localisation, A375 cells were transfected with Bfl-1FLAG and fixed for indirect immunofluorescence. As before, cells were stained for Bfl-1 using the FLAG antibody and for lysosomes using an antibody for lysosomal-associated membrane protein 1 (LAMP1), also known as CD107a. LAMP1 is a member of the glycoprotein family which make up the majority of the lysosome membrane.

Staining of the lysosomes revealed that Bfl-1FLAG was not associated with this organelle in A375 cells (Figure 5.8). Microscopy pictures clearly showed that lysosomes and Bfl-1 were not co-localised in these cells, as no yellow overlap was seen, and this was confirmed using the graphical representation which showed that the green (Bfl-1) and red (lysosomes) peaks did not align. The lack of any co-localisation, even random overlaps between the two colour channels, between lysosomes and Bfl-1 highlighted the reliability of our data that found Bfl-1 localised to the mitochondria.

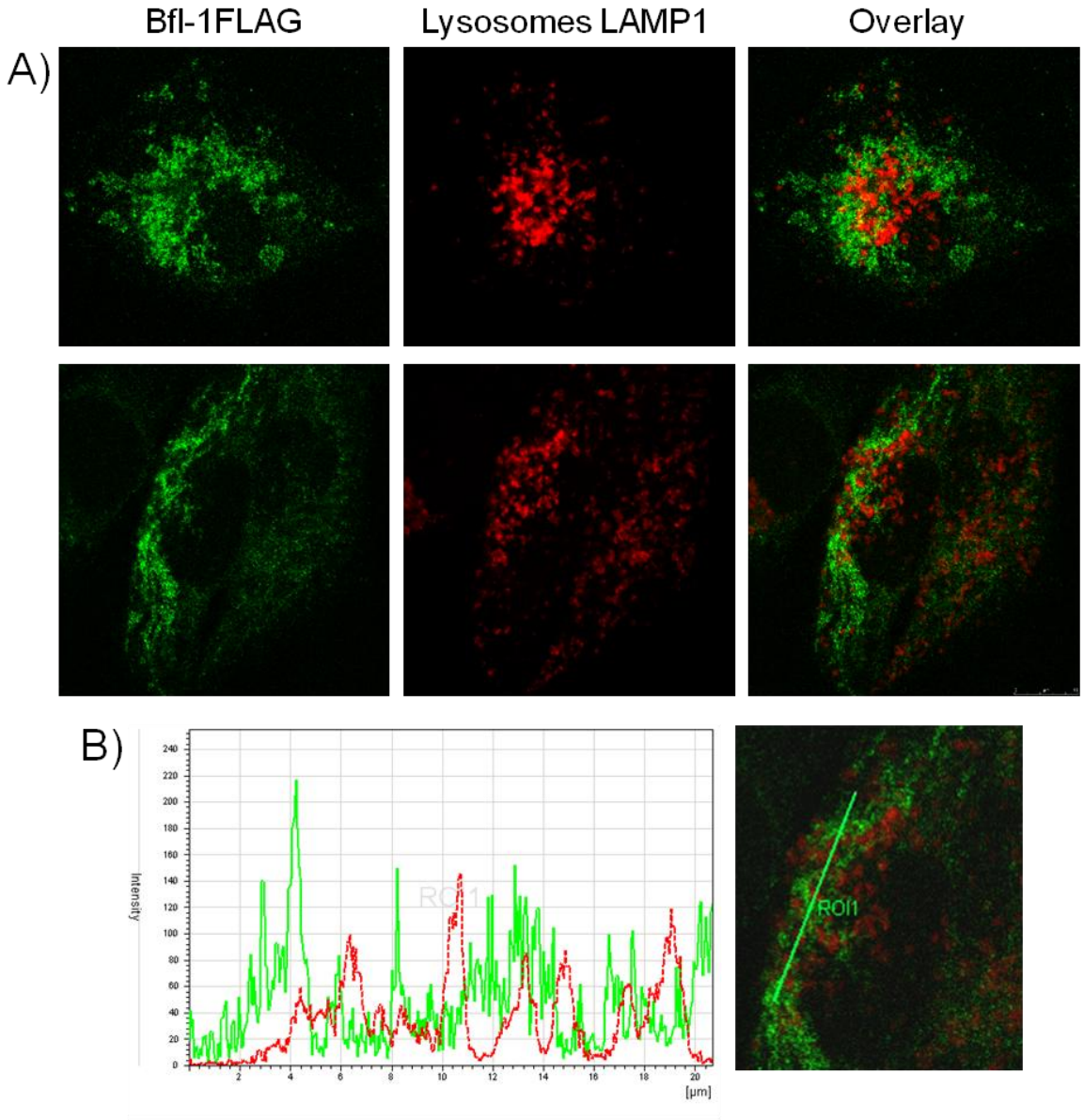

Figure 5.8: Lack of Bfl-1 co-localisation to lysosomes in A375 melanoma cells.
A375 cells were transfected by lipofection with Bfl-1FLAG. 24 hours after transfection, cells were fixed for indirect immunofluorescence. Bfl-1FLAG was detected using the FLAG antibody (green) and lysosomes were visualised using an antibody for LAMP1 (red). Cells were visualised by confocal microscopy, at 100X magnification with an additional 2X optical zoom, (A) and co-localisation was analysed using LAS software to produce a graphical representation, as previously described in Figure 5.6 (B).

5.7 Chapter 5 Conclusions

In this chapter I attempted to determine the subcellular localisation of the native Bfl-1 protein in melanoma cells and also used tagged proteins transfected into several cell systems, including a melanoma cell-line. I also explored the effects of apoptotic challenge by chemotherapeutic agents on the localisation of Bfl-1.

In all the systems we utilised for the detection of Bfl-1, Bfl-1 was seen to localise to the mitochondria of resting cells, with some protein also present in the cytosol. These results agree with previous work done on the subcellular localisation of Bfl-1. For example, Duriez et al. [424] determined Flag tagged Bfl-1 was present at the mitochondria in endothelial cells with a small amount also present in the cytosol. Werner et al. [411] also found HA-tagged-Bfl-1 in HeLa cells to be located mainly at the mitochondria in the perinuclear area of the cells, while outside the perinuclear area it was located at incidental mitochondria and was also diffuse, at a low level, throughout the cytoplasm. Indeed, although Orlofsky et al. [425] found Bfl-1 in the nucleus of some apoptotic cells and the cytoplasm of resting cells, the localisation to organelles within the cytoplasm was not explored, so it may have in fact agreed with our results and been mitochondrial.

The anomalous point in the data presented in this chapter was that Bfl-1YFP in 293F cells did not localise to the mitochondria in the way the other protein constructs did (Figure 5.3). In fact, in these cells, Bfl-1YFP appeared to induce apoptotic morphology while in A375 cells this expression construct localised to the mitochondria and the cells were protected from apoptosis by the presence of the construct (see Chapter 4). Interestingly, Yang et al. [426] tagged Bfl-1 with GFP and found that in 293T cells, the adherent version of 293F cells, the construct became pro-apoptotic, although it was still localised to the mitochondria. They found this was the case when they fused GFP to the N-terminus of Bfl-1, but that Bfl-1 tagged with other constructs such as glutatione S-transferase (GST) retained its pro-survival function. This difference in the action of different tags may be due to the size differences. YFP and GFP are much larger tags than FLAG or GST and therefore are more likely to interrupt the structure of Bfl-1 and thereby, the function. However, why Bfl-1YFP distressed 293F cells but gave A375 cells protection from apoptosis is unclear. Perhaps it comes from something specific to 293F and 293T cells to do with the over-expression of the protein or mis-folding problems.

All our constructs were made with the full-length cDNA isolated from healthy PBLs, containing no polymorphisms and did not include the shorter isoform Bfl-1S. The YFP tag was added to the N-terminus of Bfl-1 while the FLAG tag was added to the C-terminus. Apart from the difference seen in 293F cells, the addition of the tags to either end of the protein appeared to make little difference to the subcellular localisation of the protein. The importance of the C-terminus in the association of Bfl-1 with mitochondria has been demonstrated previously and the C-terminal α helix has been presented as a putative transmembrane domain [417]. The FLAG tag proved to be a useful tag for analysing the

subcellular localisation of Bfl-1 as its addition to the C-terminus failed to prevent the association of Bfl-1 with the mitochondria. In A375 cells, even the presence of the bulky YFP tag did not disrupt the ability of the protein to associate with the mitochondria. There have been suggestions that internal sequences in the protein may also have some responsibility for the mitochondrial localisation of Bfl-1 [406,489].

Previous research done for the determination of Bfl-1 subcellular localisation in overexpressed systems all presumably used the more common full-length isoform rather than Bfl-1S as none of them specified which isoform they used. We also used the full-length isoform for our overexpression systems. This may explain why the majority of projects, including ours, did not observe Bfl-1 to be present in the nucleus of resting cells, despite the finding by Ko et al. that Bfl-1S specifically localised to the nucleus [422]. Our subcellular fractionation technique removed nuclear and cellular debris so that any native Bfl-1 protein associated with the nucleus in the melanoma cells could not be picked up, even if our antibody was able to recognise both isoforms. It would be interesting to create a tagged construct for Bfl-1S and examine its localisation in overexpressed systems to determine whether it did indeed localise to the nucleus. In addition, nuclear isolation kits, similar to the mitochondrial isolation kit we used, provide nuclear and cytosolic fractions for the examination of proteins at these locations by western blotting. We could have explored this using our WEHI antibody, but realistically, this would only become a viable route for determining the presence of Bfl-1S in the nucleus once antibodies exist which can detect either both isoforms, or are specific for Bfl-1S.

In this chapter I also examined the effect of apoptotic stimuli on the localisation of Bfl-1. After challenge with chemotherapeutic agents we found that the localisation of Bfl-1 to mitochondria did not change significantly. Again this agrees with the literature, because despite the fact that other pro-survival proteins, such as Bcl-xL, have been seen to redistribute from the cytosol to the mitochondria after apoptotic challenge [486], HA-tagged-Bfl-1 was found not to alter location significantly after TNF receptor stimulation in HeLa cells despite the induction of cytochrome c release and apoptosis [411]. This lack of evidence for a closer association of Bfl-1 to the mitochondria may be because the majority of Bfl-1 is already found in the vicinity of the mitochondria before apoptotic challenge. Other Bcl-2 family proteins, such as Bcl-xL and Bax, are seen to translocate because in resting cells they are present as soluble forms in the cytosol and it is only after the initiation of apoptosis that they become membrane bound at the mitochondria [351,486].

We also hoped to examine the localisation of native Bfl-1 in melanoma cell-lines by paraffin embedding and sectioning the cell-lines, to reflect the paraffin embedding of tissue samples, in order to examine the localisation of Bfl-1 in primary samples of melanoma tumours obtained from the Cancer Sciences Unit tissue bank. However, the inability of any of the available Bfl-1 antibodies to detect the native protein by indirect immunofluorescence of paraffin embedded material prevented us from examining these, again highlighting the importance of developing higher affinity Bfl-1 antibodies which can detect the native protein.

In conclusion, the work in this chapter supports the majority of the data already presented in the literature for other cell types that Bfl-1 is localised mainly to the mitochondria in melanoma cells, and significant translocation of the protein after apoptotic challenge does not occur. However, the theories surrounding the structure and function of Bfl-1 in its role as a pro-survival protein suggest that it is present in both membrane bound and soluble forms in the cell where it binds the effector proteins or the BH3-only proteins either in the cytoplasm or at the mitochondria. If the subcellular localisation of Bfl-1 could be definitively determined, it might answer a few of these questions. If Bfl-1 is in fact already sequestered to the mitochondria in healthy cells and it does not translocate after the initiation of apoptosis, it suggests that Bfl-1 binds membrane-bound pro-apoptotic proteins at the mitochondria rather than binding their soluble forms and preventing them from becoming activated and translocating to the mitochondria. This theory would support the 'embedded together model', a combination model of the direct and indirect models of interactions between the Bcl-2 family proteins. The 'embedded together model' suggests that the pro-survival proteins bind BH3-only and effector proteins at the OMM in a dominant-negative manner [275,276], and that it is their binding to the mitochondrial membrane which mediates their function through the conformational changes required for their activation.

Currently, our available data, combined with previous research, suggests that Bfl-1 is located at the mitochondria where it acts as a pro-survival protein in the prevention of apoptosis. Importantly, higher affinity antibodies for Bfl-1 need to be produced for the further clarification of the localisation of native Bfl-1 in cells.

6 : EXPRESSION OF BFL-1 IN PRIMARY MELANOCYTES

6.1 Introduction

In most cases, malignant melanomas develop from nevi, which are clusters of melanocyte cells in the skin. Melanocytes are skin cells derived from the neural crest and are responsible for the production of the tanning pigment melanin. Melanin exists in two forms, the yellow/red pheomelanin and the brown/black eumelanin. It is packaged into vesicles called melanosomes in the melanocytes and transported out of the cells along microtubules in their dentritic arms (see Chapter 1, Figure 1.2) [39]. Melanosomes collect over the nucleus of keratinocytes in the skin where melanin then provides protection against harmful UV radiation by converting the radiation into harmless heat energy [41]. Indeed, pigmented melanocytes are less prone to UV related membrane damage than unpigmented melanocytes, suggesting it is the melanin within the cells which provides them with protection [449].

UV radiation increases the level of p53 in the keratinocytes surrounding the melanocyte cell [490]. Within keratinocytes, p53 then increases the transcription of melanocyte-stimulating hormone (MSH) which is secreted from the keratinocytes and interacts with the melanocortin-1 receptor (MC1R) on the cell surface of melanocytes [36]. It is this interaction which results in the production of more of the brown/black eumelanin rather than pheomelanin. However, UV radiation also results in a decrease in TGFβ expression in the keratinocytes [491]. TGFβ has been observed to inhibit melanocyte, but not melanoma, growth by blocking the progression of the cell cycle, and also to decrease melanin production [492,493]. A downstream target inhibited by TGFβ in melanocytes is PAX3, a member of the paired-box transcription factor family, which has also been implicated in the survival of melanocytes and in the production of melanin [494]. Indeed, it appears that many melanoma cell-lines derived from melanomas arising in sun-exposed skin have high expression levels of PAX3 which allow cell cycle progression and therefore survival [494]. Hence, UV radiation leads to less TGFβ in keratinocytes which means PAX3 is not blocked in melanocytes and can increase the production of melanin as well as allowing melanocytes to proceed through the cell cycle. As such, melanocytes in hairless SKH-2 mice were seen to proliferate in response to a single over-exposure of UVB radiation [440]. However, whether it is the same melanocyte cells which increase production of melanin as the ones which go on to proliferate after PAX3 stimulation is under debate, as evidence exists that the proliferating melanocytes come from a subset of immature melanocyte precursor cells [495]. This is important as it is the proliferating melanocytes which form nevi

which although initially benign can become malignant when they gain the ability to metastasise.

Cancers derived from keratinocytes include squamous and basal carcinomas which typically respond well to conventional treatments, with high survival rates. However cancers derived from melanocytes are much more aggressively metastatic and display strong resistance to current treatments resulting in much lower survival rates [51]. Melanocytes may not be more susceptible to gaining mutations than other cells in the skin, but once a DNA mutation has occurred, melanocytes appear to have a reduced ability, compared with other human fibroblasts, to repair the DNA damage [307]. In addition, melanocytes constitutively express high levels of the pro-survival protein Bcl-2 [164], which allows them to escape cell suicide. The combination of the inability to correct DNA mutations, the induction of proliferation caused by PAX3 expression after UV radiation and the ability to avoid apoptosis may be the unique set of pre-requisites, which under the right conditions, lead melanocytes to become cancerous.

Having characterised Bfl-1 in melanoma cell-lines, determined its importance in the intrinsic chemoresistance displayed by this cancer and its subcellular localisation, I wanted to characterise and explore the function of Bfl-1 in primary melanocytes. In order to do this, I obtained primary melanocyte cells from a range of sources and subjected them to similar experiments as the melanoma cells in chapters 3 and 4.

6.2 Melanocyte Characteristics

In total, five primary melanocyte samples were examined for Bfl-1 expression; the sources of these samples are defined in Table 6.1. The samples with high enough Bfl-1 content to be detected by our methods, were used to examine the regulation and subcellular localisation of Bfl-1.

The primary melanocytes which we received directly from Promocell and Lonza Clonetics™ were tested for purity by the companies before they were cryopreserved. The samples we received were guaranteed as being over 70% pure, as judged by morphology, Mel-5 expression and L-dopa conversion to dopa-melanin. Melanocyte samples from our collaborator Dr. Andre Ivanov were guaranteed by Invitrogen to contain <1% non-melanocyte cells on first culture after thawing, but had been passaged 26 times by his lab before being frozen down.

Given the varying passage status of the cells from different sources, we routinely checked the purity of the melanocytes by examining the morphology of the cells by microscopy throughout the culture passages and comparing them to the melanoma cell-lines (Figure 6.1). Primary melanocytes have a highly dendritic, or stellar, morphology and produce the dark pigment melanin (Figure 6.1, bottom left hand corner). Over time in culture, the cells become more rounded and lose their dendritic nature and produce less of the pigment. This change over time may be due to the outgrowth of the up to 30% of cells in the original sample judged not to be melanocytes, but it may also be due to the melanocytes themselves changing in culture. For example, melanocytes are extremely sensitive to trypsin, but require trypsin treatment to detach from the culture flask. Hence, we passaged the cells for a maximum of ten passages, but stopped earlier if they lost morphology and we judged them to no longer be a representative sample of primary melanocytes. This, combined with the slow proliferation rate of the melanocytes, limited the number of experiments which could be performed on each primary sample of melanocytes.

Table 6.1: Sources of the primary melanocyte samples used.

Sample reference number	Source	Reference/catalogue number
I	Normal human melanocytes from juvenile foreskin	Promocell, C-12400
II and III	Light pigmented donor, neonatal foreskin (Guaranteed for 16 population doublings. Passaged 26 times.)	Kind gift from Andre Ivanov, University of Glasgow, original source from Invitrogen, C-002-5C (both samples from same donor)
IV and V	Adult normal human epidermal melanocytes	Lonza Clonetics™ CC-2586 (different donors)

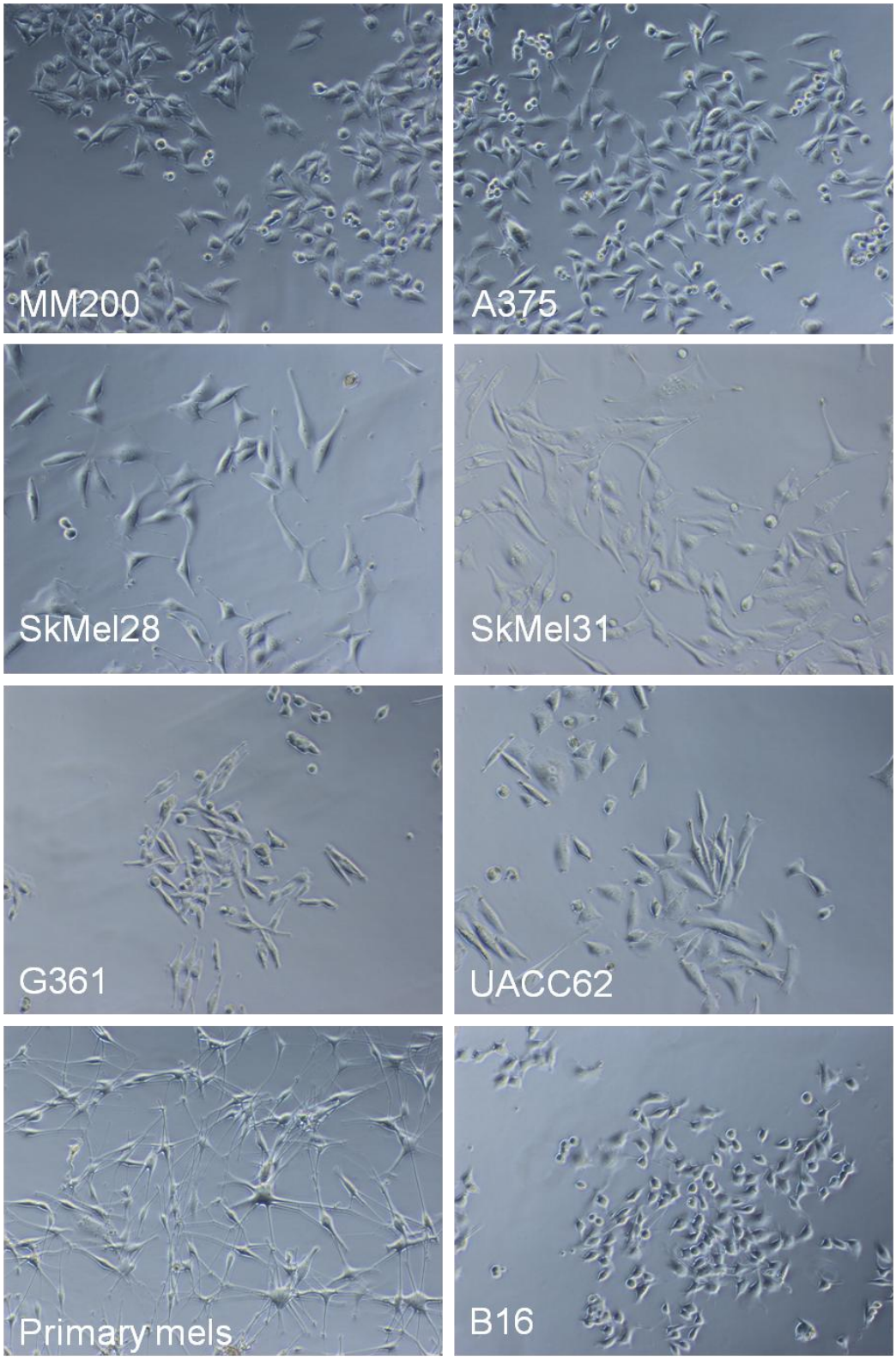

Figure 6.1: Morphology of primary melanocytes and melanoma cell-lines.
The human melanoma cell-lines MM200, A375, SkMel28, SkMel31, G361 and UACC62, the mouse melanoma cell-line B16 and primary melanocytes (Primary mels, sample V) were grown under culture conditions and photographed under light microscopy at 40X magnification.

We also checked the purity of some of the cultured samples for the routinely used melanocyte markers, S100β and tyrosinase. S100β is a calcium binding protein which the

NCI60 microarray shows is present in the same cell-lines that express high levels of Bfl-1, therefore mainly melanoma cell-lines (melanoma cell-lines are indicated by arrows in Figure 6.2A) but also in the cell-line A361 (Burkitt's lymphoma) and to a lesser extent, in SNB75 cells (CNS lymphoma). Melanoma cell-lines express S100β which is normally present in the cytoplasm or mitochondria of cells derived from the neural crest, such as melanocytes. Tyrosinase is a transmembrane protein found in melanosomes, with the catalytically active part of the protein within the melanosome and a small non-enzymatically essential part in the cytoplasm of the melanocyte. Tyrosinase is essential for the production of melanin in melanocytes and its activity has been related to the quantity of brown/black eumelanin produced by the cells [23]. We probed the primary melanocytes for both S100β and tyrosinase. S100β was visualised both by indirect immunofluorescence and western blotting, while tyrosinase expression was examined by western blot (Figure 6.2 B and C). S100β was present in the cytoplasm of both primary melanocyte samples and melanoma cell-lines, but not colorectal cancer cells. We also observed both S100β and tyrosinase in primary melanocytes by western blotting, although tyrosinase was not detected in the melanoma cell-line SkMel28. This loss of tyrosinase in the melanoma cell-line could be part of the cause for the loss of melanin production by cultured cells.

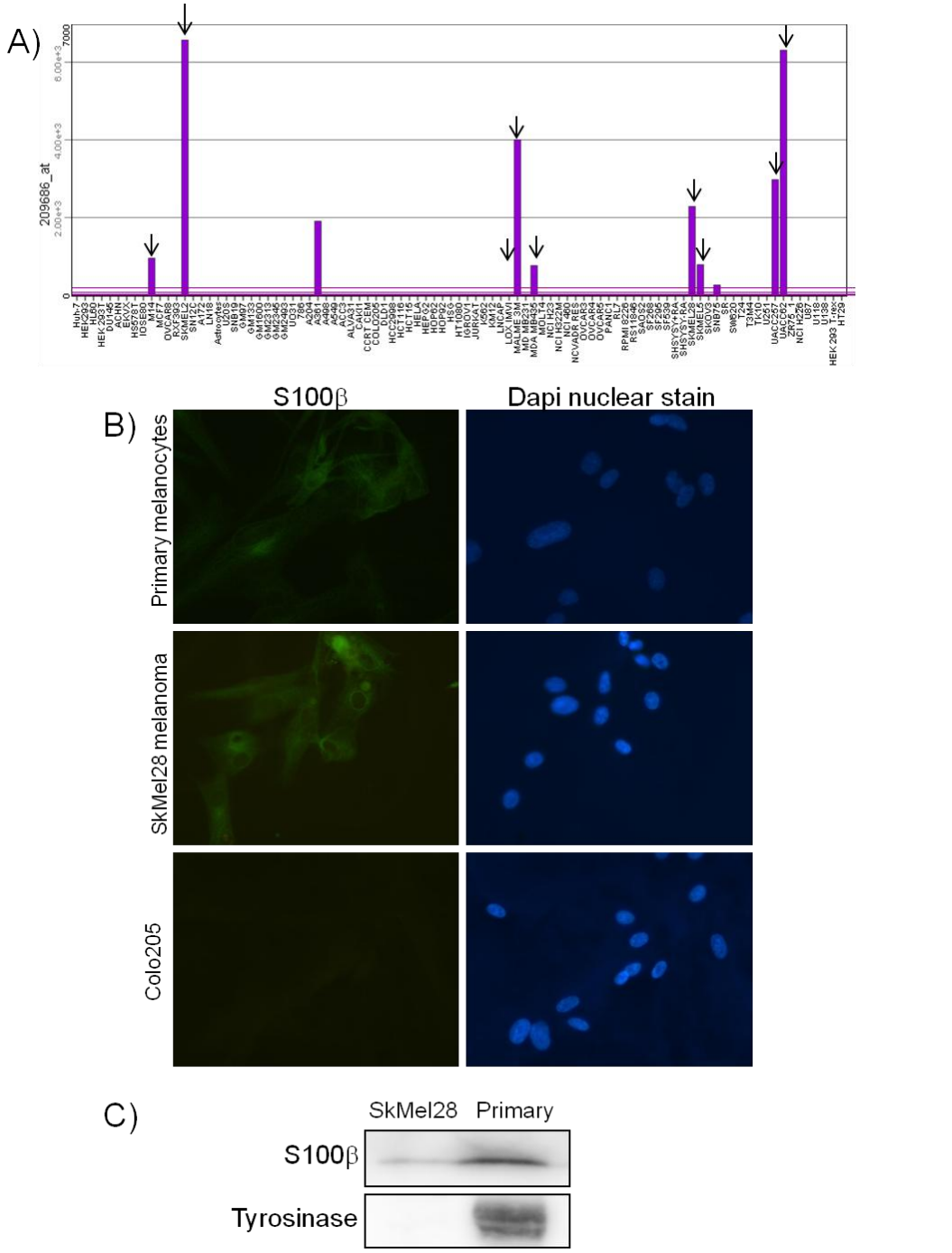

Figure 6.2: Expression of melanocyte markers in primary melanocytes and melanoma cells.

(A)The NCI60 microarray, which measured the level of expression of mRNAs across a range of cell-lines derived from cancers, demonstrated that S100β was expressed in all the melanoma cells that expressed Bfl-1 (Figure 3.1), as indicated by black arrows. (B) S100β was visualised in primary melanocytes and SkMel28 cells by staining with the S100β antibody and detected by fluorescence microscopy (green stain). Cells were also stained with Dapi to visualise the nucleus (blue stain). S100β was detected in primary melanocytes and the melanoma cell-line SkMel28, but not the colorectal cell-line Colo205. C) Lysates were generated from untreated cells, separated by SDS-PAGE and analysed by western blot for S100β and tyrosinase, both of which were observed in primary melanocytes, while melanoma cells expressed only S100β. B) and C) are both representative of 2 independent experiments on 2 separate melanocyte samples, III and IV.

6.3 The Expression of Bfl-1 in Primary Melanocytes

Having confirmed that the cells in the primary samples we obtained were indeed representative of primary melanocytes, we probed the melanocytes for their expression of Bfl-1 mRNA. We isolated total RNA from three separate melanocyte samples, converted it to cDNA and amplified Bfl-1 by RT-PCR. We then separated the DNA bands by gel electrophoresis and observed both the longer Bfl-1 and shorter Bfl-1S isoforms in all three samples, although the percentage of Bfl-1S seemed lower than in melanoma cells, such as G361 (Figure 6.3).

Subsequently, we sequenced Bfl-1 cDNA obtained from samples III and V. As in Chapter 3, Bfl-1 cDNA amplified by RT-PCR was extracted from the DNA gel and ligated into the blunt ended TOPO vector. This construct was transformed into TOP10 E.coli bacteria which were grown on an agar plate containing the selection agent kanamycin. Clones were subjected to restriction digest. As before, both the long and short Bfl-1 isoforms were observed (Figure 6.4). Five clones from each sample which contained DNA of the correct size for Bfl-1 or Bfl-1S were then sequenced using the T7 and sp6 primers present on either side of the insert site in the TOPO vector. This sequencing of primary melanocyte samples revealed that Bfl-1 mRNA from sample III contained only the major allele (GTG) for Bfl-1, whereas all the clones obtained from sample V contained the minor allele (AGA). This shows there is genetic variation between different primary melanocyte samples. Subsequently, we explored the expression levels of Bfl-1 protein in all five of our melanocyte samples.

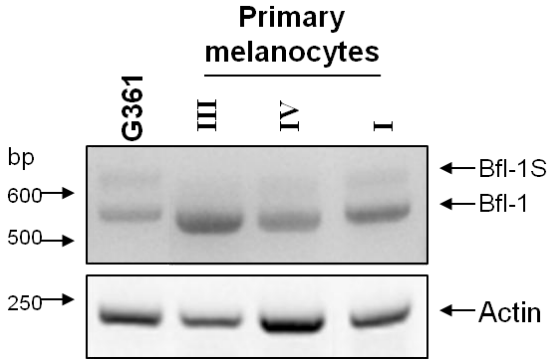

Figure 6.3: Bfl-1 mRNA expression in primary melanocytes.
Total RNA was extracted from low passage (p1) untreated cells in culture, converted to cDNA and amplified by PCR before being separated by gel electrophoresis. Actin was used as an internal control for cDNA quality and quantity.

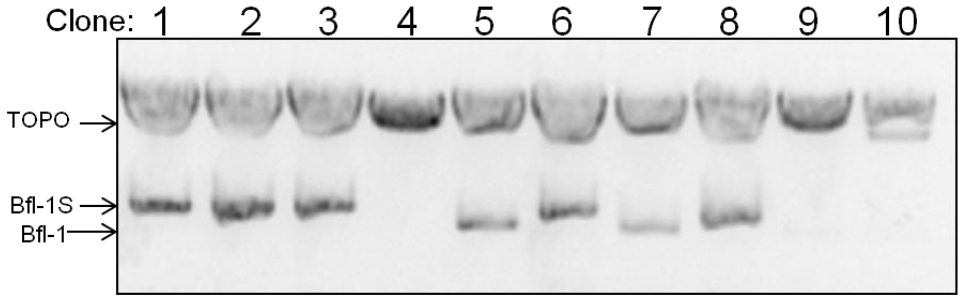

Figure 6.4: Restriction digest for Bfl-1 isolated from primary melanocytes and inserted into the TOPO vector.
Total RNA was isolated from low passage (p1) untreated cells, converted to cDNA and Bfl-1 cDNA was amplified by PCR. The amplified product was ligated into the blunt TOPO vector, expanded in TOP10 bacteria and the plasmid DNA was isolated by miniprep. Restriction digest with EcoRI revealed which clones contained Bfl-1 DNA. Samples which contained bands of the correct size for both the short or long Bfl-1 cDNA isoforms were then sequenced. Both Bfl-1S (clones 1, 2, 3 and 6) and full-length Bfl-1 (clones 5, 7 and 8) were observed (data shown from melanocyte sample III).

In order to explore the expression level of Bfl-1 protein in each melanocyte sample, lysates from untreated cells were generated, separated by SDS-PAGE and analysed by western blotting in comparison to the melanoma cell-lines SkMel28 and/or MM200 (Figure 6.5). The lysates from the different samples were obtained at different times, so it was not possible to run them all on one blot as protein in cell lysates can degrade over time. Hence primary melanocyte lysates were assessed in comparison to lysates from untreated MM200 and SkMel28 cells which display consistent levels of Bfl-1 expression over time. As such, a useful measure of the differing levels of Bfl-1 protein expression across the melanocyte samples could be established. Indeed, we did observe significant variations in the level of Bfl-1 between different primary melanocyte samples. Samples I and III contained higher levels of Bfl-1 protein than the other samples, with sample II in the middle and IV with the lowest expression level. Sample V also showed very low levels of Bfl-1 protein in this blot, but in other blots under untreated conditions and using the same Bfl-1 antibody (Figure 6.6 and Figure 6.7) this sample expressed much higher levels. This aberrant result may have been because the lysate for sample V used in the blot in Figure 6.5 was from cells which had been cultured for around 10 passages, whereas the other blots and other samples (I, II, III and IV) were analysed at earlier passages and primary cells can change significantly under culture conditions.

The expression of the other pro-survival proteins was also examined in the primary melanocytes, and although not every pro-survival protein was examined in every sample, there was a pattern to their expression profiles. The only other pro-survival protein to vary significantly in its expression between the primary melanocytes and the melanoma cell-lines was Bcl-xL. In both sample III and IV, where Bcl-xL levels were measured, Bcl-xL

was expressed at a higher level in the primary melanocytes than in the melanoma cells. This was independent of Bfl-1 expression, as in sample III Bfl-1 was highly expressed while in sample IV, Bfl-1 was expressed at low levels. Bcl-2, Mcl-1 and Bcl-w were expressed at relatively consistent levels in both melanocytes and melanoma cells, regardless of the variation in the level of Bfl-1 expression.

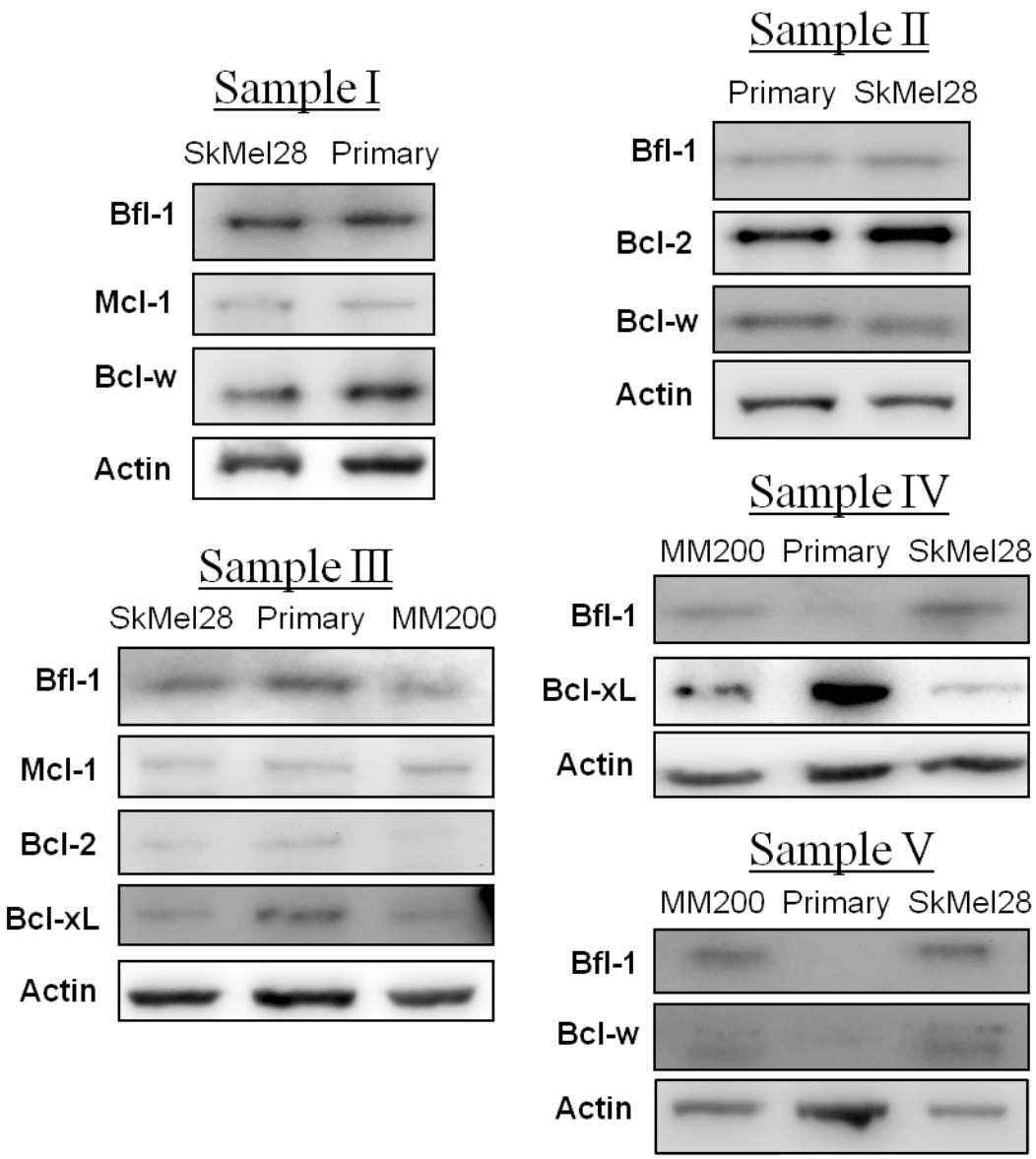

Figure 6.5: The levels of pro-survival proteins in primary melanocyte samples. Lysates were generated from untreated cells in culture. The proteins were then separated by SDS-PAGE and analysed by western blot. Bcl-2, Bcl-xL and Bcl-w are all detected at the same size by western blot which combined with the weakness of some of the antibodies, limited the number of pro-survival proteins which could be detected on each blot. Each blot is representative of one experiment, with 25μg of protein loaded on each gel. Sample I, II, III and IV were analysed at early passage numbers (p2-3) while sample V was analysed at p6.

6.4 Regulation of Bfl-1in Primary Melanocytes

Having established that the expression level and genetic profile of Bfl-1 can vary between primary melanocyte samples, we explored how the regulation of Bfl-1 expression in primary melanocytes compared to its regulation in melanoma cell-lines. To do this we explored the signalling pathways responsible for the regulation of Bfl-1 transcription and the role of the proteasome in the degradation of the protein.

Primary melanocytes and SkMel28 melanoma cells were treated with the range of signalling inhibitors previously defined in Chapter 3. IKK inhibitor IV was used to inhibit the NFκB pathway, the MEK inhibitor PD901 to inhibit the MAPK pathway and the Akt inhibitor Akt1/2 inhibitor was used to inhibit the Akt pathway. The cells were treated with the specific pathway inhibitors for 48 hours before lysates were generated, proteins were separated by SDS-PAGE and analysed by western blot (Figure 6.6).

After inhibition of the NFκB pathway with the IKK inhibitor IV, the level of Bfl-1 protein dropped significantly, indicating that in primary melanocytes, as in melanoma cells, Bfl-1 was regulated through the NFκB pathway. At the dose of 20nM, a decrease in the level of phospho-ERK was also observed in both the melanoma cells and the primary melanocytes. This was also accompanied by a decrease in phospho-Akt in both cell types. These drops were not observed at the higher dose of 100nM of the IKK inhibitor. This suggests that the blocking of the NFκB pathway with the IKK inhibitor at 20nM somehow resulted in the inhibition of the ERK and Akt pathways in these cells, or that the inhibitor had off-target effects, although the latter seems unlikely as it was not observed at higher doses.

After treatment with the Akt inhibitor, in both primary melanocytes and melanoma cells, the level of Bfl-1 protein did not drop significantly. However while the level of phospho-Akt was seen to drop in melanoma cells, showing the inhibitor targeted the Akt pathway, in the primary melanocytes the level of phospho-Akt barely changed, showing the inhibitor did not really work in these cells.

Interestingly, after treatment with the MEK inhibitor PD901, in SkMel28 cells the level of Bfl-1 protein routinely increased whereas in primary melanocytes (as in MM200 cells, Figure 3.20) the level dropped. In fact in primary melanocytes, after PD901 treatment the level of phospho-Akt significantly increased, indicating that when the MAPK pathway in these cells was blocked, the Akt pathway became more active. Conversely in SkMel28

cells the level of phospho-Akt dropped slightly after PD901 treatment. Therefore, the profile of Bfl-1 regulation in primary melanocytes matched the profile in SkMel28 cells closely with the one exception being after treatment with the MEK inhibitor PD901.

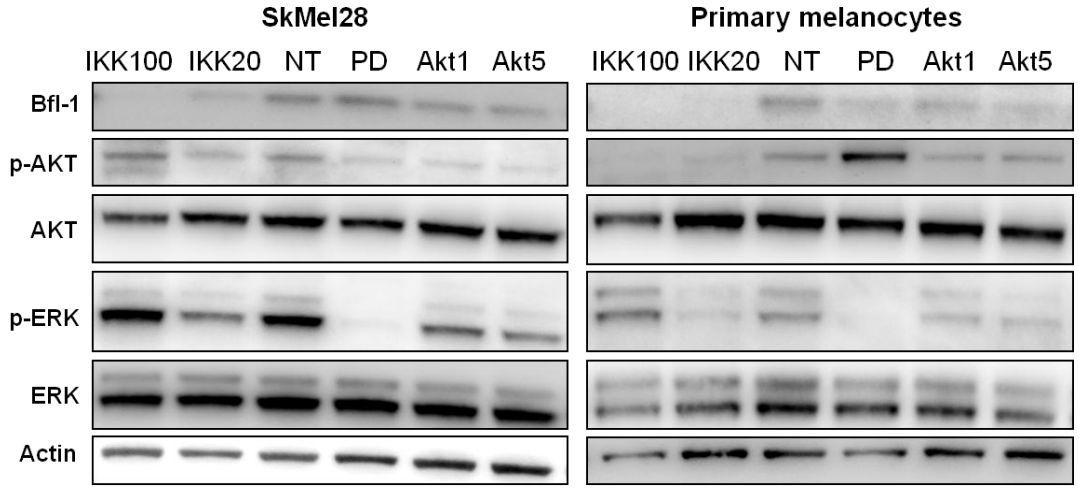

Figure 6.6: The regulation of Bfl-1 through signalling pathways in primary melanocytes.
Lysates were generated from cells treated with signalling inhibitors for 48 hours (IKK; IKK2 inhibitor IV at 100nM and 20nM, NT; non treated, PD; PD901 at 50nM, Akt; Akt inhibitor at 1μM and 5μM), 12μg of protein was loaded into each lane and proteins were separated by SDS-PAGE and analysed by western blot. These data are from melanocyte sample V taken at passage number 3.

We also explored the degradation of Bfl-1 protein in primary melanocytes by the proteasome. In order to do this we employed the same pulse-chase experiment using the protein synthesis inhibitor cycloheximide and the proteasome inhibitor MG132 as we did in Chapter 3 (Figure 3.18). Again, the results of this experiment in primary melanocytes matched those observed in melanoma cells (Figure 6.7). In primary melanocytes, Bfl-1 appeared to almost completely disappear after 2 hours of treatment with cycloheximide, suggesting the half life of Bfl-1 in primary melanocytes is equally as short as it was in melanoma cells, especially MM200 cells which had a protein half life of 1-2 hours. Indeed, after treatment with MG132, Bfl-1 appeared to accumulate in primary cells up until 4 hours, after which the level dropped again, matching the pattern observed in MM200 cells.

After treatment with MG132 and cycloheximide, the level of Bfl-1 protein was recovered in the absence of protein synthesis, although by 6 hours, the level of Bfl-1 fell again. This data suggests that the proteasome plays the same role in Bfl-1 degradation in primary melanocytes as it does in melanoma cells.

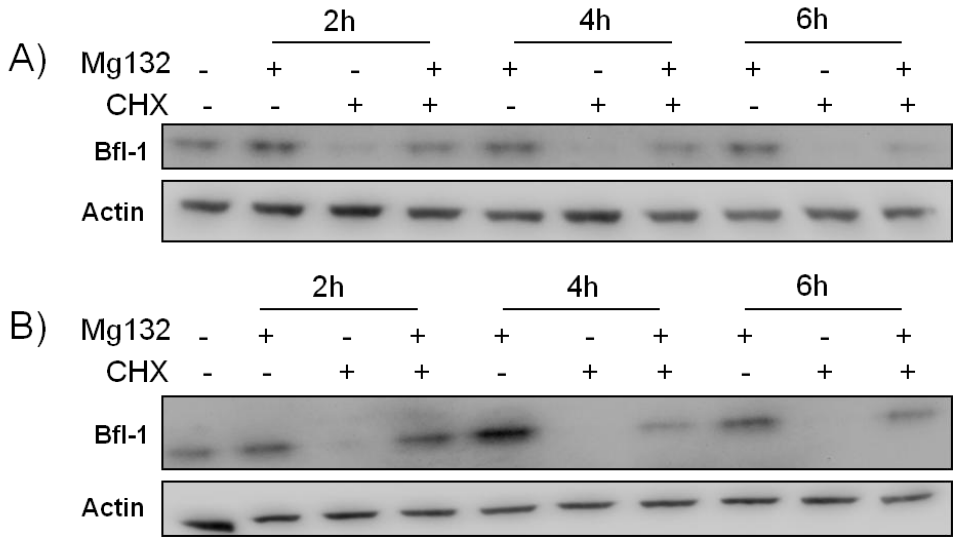

Figure 6.7: Degradation of Bfl-1 by the proteasome in primary melanocytes.
The proteasome inhibitor MG132 (10μg/ml) and the protein synthesis inhibitor cycloheximide (CHX) (10μg/ml) were added to the cells for the times indicated on UACC62 cells (A) or primary melanocytes (sample V) (B). Lysates were then generated, 15μg of protein was loaded into each lane and proteins were separated by SDS-PAGE and analysed by western blot. These data are representative of three independent experiments from two separate primary melanocyte samples (sample V twice at passage numbers 2 and 4 and II once at passage number 3).

6.5 Subcellular Localisation of Bfl-1 in Primary Melanocytes

Having determined that in melanoma cells, Bfl-1 was localised mainly to the mitochondria, but was also present in the cytoplasm, we aimed to determine if the localisation was similar in primary melanocytes. Unfortunately no antibodies were found that could specifically recognise the native Bfl-1 in cells for indirect immunofluorescence techniques (Chapter 5). However, we were able to carry out the Thermo Scientific mitochondria isolation kit on a sample of primary melanocytes (Figure 6.8). As can be seen, we managed to detect Bfl-1 in the mitochondrial fraction of the cells, although the signal was weak due to the low protein concentration recovered from the cells by the process. Although no Bfl-1 was detected in the cytoplasmic fraction, this may have been because the protein concentration was so low. As such it cannot be concluded from this experiment that Bfl-1 is localised entirely to the mitochondria in primary melanocytes, but it can be deduced that the majority of the Bfl-1 protein resides in the mitochondria in primary melanocytes, as it does in melanoma cells.

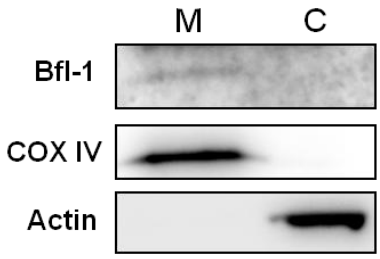

Figure 6.8: Subcellular localisation of Bfl-1 in primary melanocytes.
Primary melanocytes were subjected to subcellular fractionation using the mitochondria isolation kit from Thermo Scientific which provided mitochondrial (M) and cytosolic (C) fractions which were subjected to SDS-PAGE and analysed by western blotting. Due to low protein yields, only 10μg of protein was loaded into each lane for SDS-PAGE analysis. This experiment was from sample V at passage number 7.

6.6 The Effect of Knocking Down Bfl-1 Expression in Primary Melanocytes

Having characterised Bfl-1 in primary melanocyte cells we next explored the function and importance of the protein in these pre-cancerous cells for the ability to regulate apoptosis. Having concluded that knocking down Bfl-1 expression re-sensitised melanoma cells to chemotherapeutic agents, we attempted to knock down Bfl-1 using siRNA technology in primary melanocytes and repeated similar experiments to those performed in the melanoma cell-lines. siRNA specific for Bfl-1, or a control siRNA which contained the same GC percentage as Bfl-1 siRNA and did not target any known gene products, was added to cells for 48 hours before lysates were generated from the cells. Lysates were separated by SDS-PAGE and analysed by western blot to assess Bfl-1 knock down in primary melanocytes (Figure 6.9). Bfl-1 specific siRNA successfully knocked down Bfl-1 expression in primary melanocytes as it did in melanoma cells. The control siRNA did not knock down Bfl-1 expression in either the primary or cancerous cells, confirming the specificity of this effect. Subsequently, we treated cells with a range of chemotherapeutic agents to examine the sensitivity of primary melanocytes to the drugs compared to melanoma cells (Figure 6.10). We then examined the impact of knocking down Bfl-1 expression on this sensitivity (Figure 6.11) before examining the further impact of inhibiting the Bcl-x members of the pro-survival proteins of the Bcl-2 family using the BH3-mimetic ABT-737 (Figure 6.12). These experiments were performed in a similar manner to those in Chapter 4, with both floating and adherent cells being harvested, stained with hypotonic propidium iodide and analysed by flow cytometry to examine the percentage of apoptotic cells after each treatment.

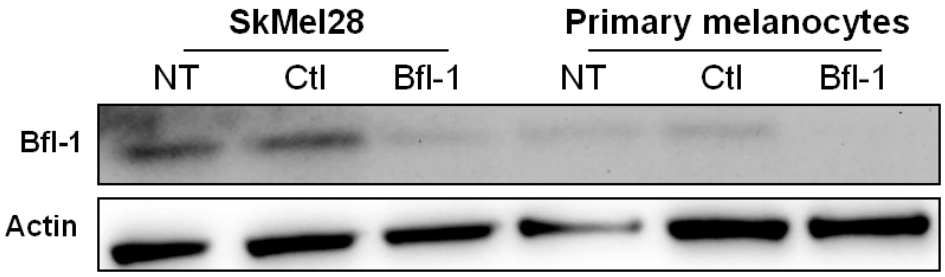

Figure 6.9: siRNA specific for Bfl-1 was used to knock down Bfl-1 expression in primary melanocytes and melanoma cells.
Cells were treated with 40nM Bfl-1 specific or control (Ctl) siRNA for 48 hours before lysates were generated. 15μg of proteins were separated by SDS-PAGE and analysed by western blot. This data is representative of two experiments from sample V at passage numbers 4 and 5.

We tested two different melanocyte populations in these experiments, expressing either high (sample III) or low (sample V) levels of Bfl-1. Initially, we compared the sensitivity of these two samples to a range of chemotherapeutic agents (Figure 6.10). Sample III appeared to show more cell death after treatment with Etoposide, PD901, Cisplatin and Paclitaxel compared to untreated cells, while sample V showed much less response to the compounds, with no drugs resulting in significantly higher levels of cell death than the background level. Levels of background death in both melanocyte samples were higher than melanoma cells, but very similar between samples. Hence, the melanocyte sample with low Bfl-1 expression was more resistant to these chemotherapeutic agents than the sample with high Bfl-1 expression and the melanoma cell-lines.

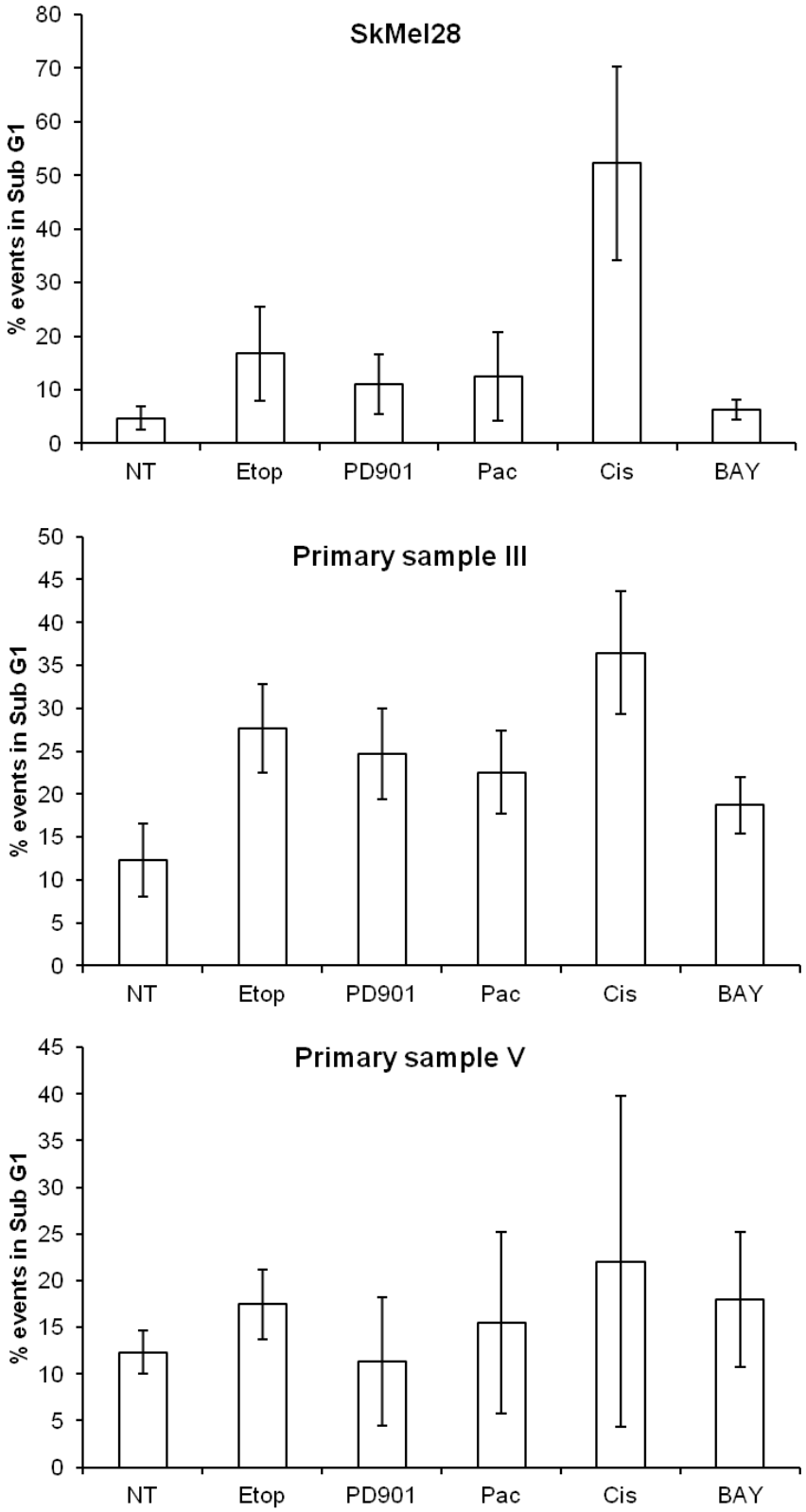

Figure 6.10: The sensitivity of primary melanocytes to chemotherapeutic agents.
Cells were grown under culture conditions and treated with a range of chemotherapeutic agents for 24 hours (Etoposide (Etop) at 10μg/ml, PD901 at 50nM, Paclitaxel (Pac) 10μg/ml, Cisplatin (Cis) 50μg/ml and BAY11-7082 (BAY) 10μM). Both floating and adherent cells were harvested, stained with propidium iodide for 30 minutes and analysed by flow cytometry. These data are representative of three independent experiments and error bars represent the standard deviation from the mean.

When Bfl-1 siRNA was added to the cells before treatment with the chemotherapeutic agents, it became evident that there were clear differences in the effects of Bfl-1 knock down on apoptosis levels between the two melanocyte samples tested in this experiment (Figure 6.11). Melanocyte sample III reacted to Bfl-1 siRNA in a similar manner to SkMel28 cells, with increased levels of apoptosis observed in cells with Bfl-1 knocked down. However sample V reacted very differently from either the other melanocyte sample or the melanoma cell-line, with no higher levels of cell death in cells with Bfl-1 knocked down compared to cells treated with control or no siRNA.

As was seen before, Bfl-1 knock down sensitised SkMel28 cells to both PD901 and Paclitaxel, but not the other chemotherapeutic agents tested. Melanocyte sample III on the other hand displayed a more consistent trend for higher levels of cell death when cells were treated with Bfl-1 siRNA in the presence or absence of any drugs. In fact, melanocyte sample III cells treated with Bfl-1 siRNA alone, in the absence of chemotherapeutic agents, underwent a significantly higher level of background cell death than cells which were left completely untreated or cells which were treated with control siRNA. The increase in cell death after Bfl-1 knock down in these untreated cells was similar to the level of increased cell death when Bfl-1 was knocked down after chemotherapy treatment. This suggests that rather than making the drugs more effective, the melanocytes were dying at a higher level because of the Bfl-1 knock down. This was different to the melanoma cells which displayed only a small increase in background death after Bfl-1 knock down which was amplified after treatment with selected drugs.

Primary melanocyte sample V showed no increase in cell death after Bfl-1 knock down either in the untreated cells or after treatments with chemotherapeutics. This correlated with the low levels of Bfl-1 expression in this sample. Hence we went on to explore the effect of inhibiting other pro-survival members of the Bcl-2 family. We did this by combining Bfl-1 knock down with treatment with ABT-737, the BH3 mimetic which inhibits the action of Bcl-2, Bcl-w and Bcl-xL (Figure 6.12).

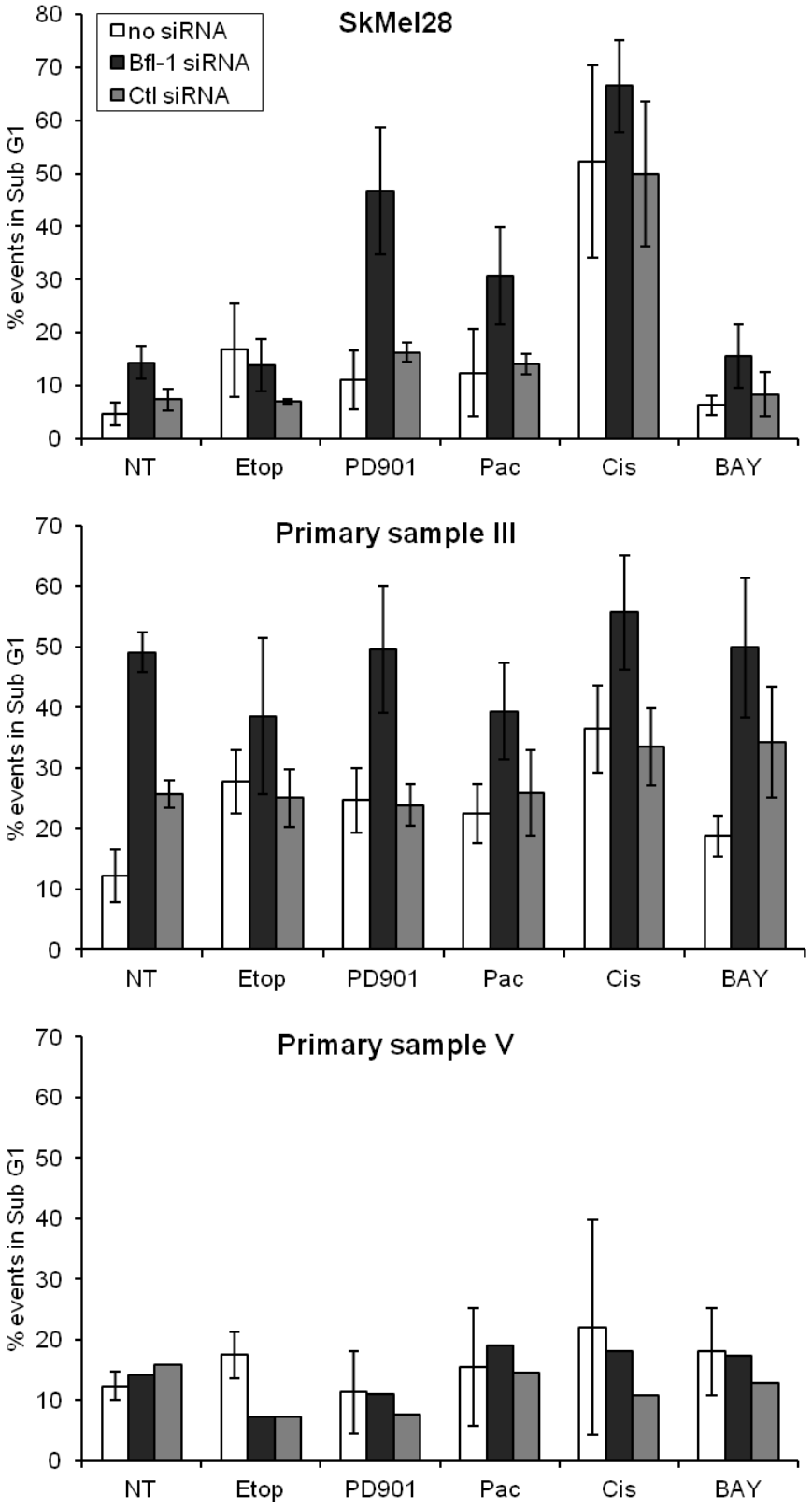

Figure 6.11: Sensitivity of primary melanocytes to a range of chemotherapeutic agents after Bfl-1 knock down.

Cells were treated with control (Ctl) or Bfl-1 specific siRNA at 40nM for 48 hours. siRNA was then washed off and cells were treated with chemotherapeutic agents for a further 24 hours (Etoposide (Etop) at 10μg/ml, PD901 at 50nM, Paclitaxel (Pac) 10μg/ml, Cisplatin (Cis) 50μg/ml and BAY11-7082 (BAY) 10μM). Both floating and adherent cells were then harvested, stained with propidium iodide and analysed by flow cytometry. These data are representative of three independent experiments (except for primary sample V) and error bars are representative of the standard deviation from the mean.

Interestingly, in melanocyte sample V the addition of ABT-737 did significantly increase the levels of cell death compared to untreated cells and this increase was regardless of which siRNA was present (Figure 6.12). This increase in cell death levels was also observed when ABT-737 was combined with most of the chemotherapeutic agents tested compared to the levels seen in cells treated with just the chemotherapeutic agents. Cell death was particularly increased when ABT-737 was combined with PD901 or Paclitaxel when compared to PD901 or Paclitaxel alone. In melanocyte sample V it was the addition of ABT-737 which had the significant impact on cell death levels, not the knock down of Bfl-1.

However, in melanocyte sample III and the melanoma cell-line, whilst the addition of ABT-737 raised the levels of cell death, these levels were consistently further raised by the knock down of Bfl-1. The addition of ABT-737 to sample III had much less impact on the levels of cell death than it did in sample V, only raising the cell death level by about 10% in untreated cells with Bfl-1 knocked down compared to an increase of around 30% in sample V and 25% in the melanoma cells. In sample III, this was only increased further when ABT-737 was combined with Paclitaxel and Bfl-1 siRNA, while in the melanoma cells the combination of ABT-737, PD901 and Bfl-1 siRNA also resulted in higher levels of cell death than Bfl-1 siRNA and ABT-737 without chemotherapeutics.

From this set of experiments, it became clear that melanoma cells had a more diverse reaction, in terms of the levels of apoptosis seen, to different chemotherapeutic agents than melanocytes did. In fact in the absence of ABT-737, and even in the presence of Bfl-1 siRNA, the primary melanocytes displayed nothing greater than background apoptosis after treatment with the array of chemotherapeutics alone. There were also clear differences between the melanocyte samples, with sample III which had high levels of Bfl-1 expression being sensitive to Bfl-1 knock down, while sample V which had low levels of Bfl-1 expression was more sensitive to treatment with ABT-737.

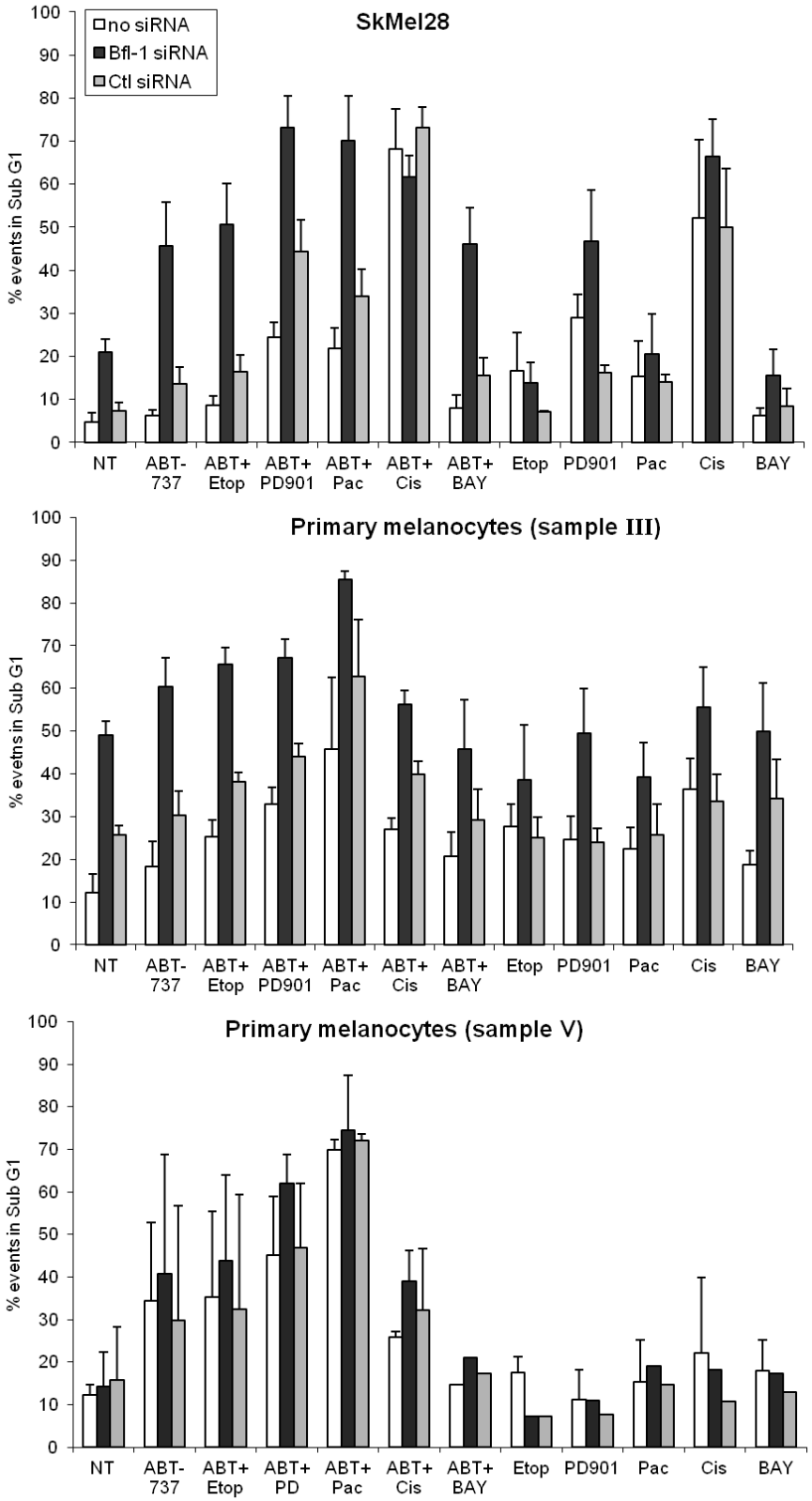

Figure 6.12: Sensitivity of primary melanocytes to chemotherapeutic agents when Bfl-1, Bcl-2, Bcl-xL and Bcl-w are inhibited.

Cells were treated with siRNA at 40nM for 48 hours before treatment with chemotherapeutic drugs (ABT-737 1μM, Etoposide (Etop) 10μg/ml, PD901 50nM, Paclitaxel (Pac) 10μg/ml, Cisplatin (Cis) 50μg/ml, BAY11-7082 (BAY) 10μM) for a further 24 hours. Both floating and adherent cells were then harvested and stained with propidium iodide and analysed by flow cytometry. These data are representative of three independent experiments each and the error bars represent the standard deviation from the mean.

6.7 Chapter 6 Conclusions

In this chapter, I began to characterise Bfl-1 in primary melanocytes. I looked at its expression levels, regulation, degradation, sub-cellular localisation and importance in protecting the cells from apoptosis triggered by chemotherapeutic agents. It became clear that the expression level of Bfl-1 protein amongst different samples of melanocytes varied significantly. This suggests that the levels of Bfl-1 in healthy melanocytes may vary between different patients, or that different clusters of melanocytes within an individual could express varying levels of Bfl-1. Alternatively, it may reflect differences in the source or passage number of the cells, which are both issues which could be addressed. Qualitative analysis of Bfl-1 mRNA from the melanocyte samples showed that mRNA coding for both the long and short isoforms was present in all the samples analysed, as in the majority of our melanoma cell-lines. However quantitative analysis of the levels of mRNA was not sufficient to determine whether the levels of mRNA correlated with the levels of protein in each sample as they did in the melanoma cell-lines.

I also sequenced Bfl-1 mRNA obtained from two of the melanocyte samples and found that one sample appeared to contain only the minor allele (AGA) for Bfl-1 which I had observed in the melanoma cell-lines, whereas the other sample contained only the major allele (GTG). This was an interesting observation which showed that Bfl-1 varies at the genetic level across different melanocyte samples. The presence of the SNPs (AGA) in all our melanoma cell-lines bar MM200 cells and their presence in some healthy primary melanocyte samples may suggest that melanocytes with the SNPs present are more likely to undergo transformation into malignant melanoma than melanocytes with wild-type Bfl-1 mRNA. This observation could be followed up with a wider scale investigation into the genetic profile of Bfl-1 in primary patients which could highlight whether the presence of the SNPs pre-disposes patients to developing malignant melanoma, as they do with atopic dermatitis [442].

The regulation of Bfl-1 in primary melanocytes appeared to be very similar to its regulation in melanoma cells in terms of the signalling pathways responsible for its expression level and its degradation by the proteasome. In fact the regulation of Bfl-1 in the melanocytes most closely reflected its regulation in MM200 cells rather than SkMel28 cells in terms of the expression levels of Bfl-1 after treatments with specific pathway inhibitors and the degradation pattern seen after the inhibition of the proteasome. This cannot be explained by the presence or absence of the SNPs in Bfl-1 as the melanocyte

sample examined did display all the 3 SNPs of the minor allele, akin to SkMel28 cells, differing from MM200 cells which displayed only the major allele which contained none of these 3 SNPs. The ratio of the two isoforms of Bfl-1 also cannot explain the similarity in the regulation of Bfl-1 between the melanocytes and MM200 cells as melanocytes contained both Bfl-1 and Bfl-1S isoforms, at a similar ratio to that observed in SkMel28 cells, whilst MM200 cells contained only the longer isoform. Another explanation could potentially be elucidated by looking at a wider range of melanoma cell-lines which would show whether the majority of melanoma cell-lines reflect the patterns of Bfl-1 regulation seen in MM200 cells or SkMel28 cells.

The subcellular localisation of Bfl-1 in primary melanocytes was also examined using a subcellular fractionation kit which allowed detection of the protein by western blot. This technique elucidated Bfl-1 to be present in the mitochondrial fraction, in a similar manner to the results seen in the melanoma cell-lines. The higher yield of protein from the melanoma cell-lines through this technique also showed Bfl-1 present, at a much lower level, in the cytoplasmic fraction and it remains possible that this would also be seen in melanocyte samples if enough protein could be isolated from these cells. Another way of determining the subcellular localisation of Bfl-1 in primary melanocytes would be through immunohistochemistry, but antibodies which are specific and sensitive enough to detect the native Bfl-1 protein have yet to be developed.

A key set of experiments in this chapter was to determine the importance of Bfl-1 in protecting primary melanocytes from apoptosis caused by chemotherapeutic agents. If melanoma cells were more sensitive to Bfl-1 knock down than primary melanocytes, Bfl-1 could be a viable drug target in the treatment of malignant melanoma. Again, more samples of primary melanocytes are needed to draw conclusions from this work, but we have already observed variation between our samples in their reliance on Bfl-1 for survival against chemotherapeutics. Two melanocyte samples were subjected to these experiments, one with high Bfl-1 expression (sample III) and one with low levels of Bfl-1 protein, (sample V).

The treatment of the two samples with a range of chemotherapeutic agents immediately showed the difference between the two samples. Sample III displayed a certain sensitivity to the drugs which was not seen at all in sample V (Figure 6.). Both samples underwent a background level of cell death of around 10%, but while sample III cells died at higher levels after drug treatment, the level of cell death in sample V was not significantly higher

than the background level. This data from sample V correlated with the observations that previous groups have made on the sensitivity of melanocytes to chemotherapeutic agents. In melanocytes, a single high dose of Cisplatin was shown to reduce the production of melanin but caused no apoptosis [443]. Melanocytes were also seen to be less susceptible to cell death caused by Etoposide, Cisplatin, Paclitaxel, or the MEK inhibitor PD184352, than melanoma cells [306,444,446].

When Bfl-1 was knocked down using siRNA technology, sample III was seen to be much more sensitive to Bfl-1 knock down than sample V. Higher levels of cell death after Bfl-1 knock down were observed in sample III while in sample V the levels remained consistent regardless of Bfl-1 knock down (Figure 6.11). In fact, sample V appeared to rely on the other Bcl-x pro-survival proteins for survival, as shown after treatment with ABT-737, which caused higher levels of cell death than Bfl-1 knock down after treatment with every chemotherapeutic agent tested (Figure 6.12). Sample III also showed a smaller level of reliance on the Bcl-x proteins for survival after treatment with Paclitaxel, but not the other chemotherapeutic agents, suggesting this sample of melanocytes were much more reliant on Bfl-1 for protection from apoptosis than the other pro-survival protein examined. The only pro-survival protein not knocked down or inhibited in these experiments was Mcl-1, and it would be interesting to also examine the importance of this protein in the survival of melanocytes.

In summary, the data presented in this chapter provided an insight into the role of Bfl-1 within melanocytes. I have shown that the expression level and reliance on Bfl-1 for survival varies between healthy primary melanocyte samples. The protein appears to display similar characteristics as it does within melanoma cells in terms of its regulation, degradation and sub-cellular localisation, yet in some melanocytes knock down of the protein did not change their sensitivity to apoptosis, suggesting that in some samples, it is other pro-survival proteins that these melanocytes rely on for survival.

7: CONCLUDING REMARKS

This project aimed to characterise the pro-survival molecule Bfl-1 and determine its importance in melanoma as a contributor to the intrinsic chemo resistance observed in metastatic melanoma. As detailed in the introduction, metastatic melanoma is becoming an increasingly problematic cancer in the developed world [47]. This is due to an ageing population, the increased use of sun beds and because metastatic melanoma displays an intimidating level of resistance to current therapies [496]. As such, survival rates are low as metastases of this cancer do not respond well to current therapies [51]. A key factor in this chemo resistance is the ability of melanoma cells to evade apoptosis. An examination of the NCI60 microarray initially provided evidence that Bfl-1 was highly and specifically expressed in melanoma cells (Figure 1.21). This expression pattern was very different from those of the other pro-survival proteins of the Bcl-2 family (Figure 1.20) and provided the original hypothesis that Bfl-1 was important in the chemo resistance of metastatic melanoma.

In order to characterise Bfl-1 in melanoma I examined its expression levels and half-lives, both at the mRNA and protein level, the regulation of the protein through signalling pathways and degradation pathways and its subcellular localisation. I also examined the sequence of the gene for the presence of the major and minor alleles for Bfl-1 and the prevalence of the different isoforms of the protein and the effect of chemotherapeutic treatment on the levels of Bfl-1 expression. Over-expression and knock down assays were used to determine the role and the importance of this pro-survival protein in the intrinsic chemo resistance seen in metastatic melanoma. This characterisation and elucidation of the role of Bfl-1 was explored using a panel of melanoma cell-lines, and was additionally assessed in pre-cancerous primary melanocytes.

The panel of melanoma cell-lines assessed were assembled to represent the spectrum of the disease, taking into account the diversity of the mutations observed in metastatic melanoma such as BRaf, NRas and PTEN status. Using cell-lines perhaps limits the applicability of this data to primary cancer cells in the body as the process of establishing immortal cell-lines invariably leads to differences from the cells they were derived from. However, cell-lines are much more easily accessible than the primary tissues and were a good place to start with the novel examination of Bfl-1 in melanoma. Furthermore, the National Cancer Institute's database of cell-lines derived from a selection of cancers (the NCI60) suggests that the expression patterns of mRNA remains largely similar between the cell-lines and the original tissues from which they are derived [437,438].

The NCI60 microarray measured the level of Bfl-1 mRNA, but within the panel of melanoma cell-lines I was able to explore the expression levels of both the protein and mRNA, which were both highly expressed in five out of our six melanoma cell-lines. A lymphoma cell-line was also shown to express Bfl-1, but the levels were at the lower end of the melanoma expression spectrum. Five samples of primary melanocytes were also probed for Bfl-1 protein expression and were found to express it at very different levels between samples, with some samples expressing Bfl-1 at a similar level to the melanoma cells, while others expressed much lower levels of the protein. The consistently high expression of Bfl-1 in melanoma cells compared to the variable levels in healthy melanocytes may suggest that Bfl-1 becomes over-expressed during the transformation process or that melanomas may be more likely to derive from melanocytes which already express high levels of Bfl-1. Whether this represents a sub-set or different differentiation stage of melanocytes is currently unknown. If we could successfully stain tumours for the expression of Bfl-1, we could check these theories.

Sequencing of Bfl-1 mRNA revealed that five of the six melanoma cell-lines (MM200 cells being the exception) expressed the minor allele for Bfl-1 which contained three defined SNPs while the samples of melanocytes examined varied with some expressing the major allele and some expressing the minor allele. This pattern reflects data presented in the HapMap database on the population frequencies of these polymorphisms. These data from the HapMap suggest that in the Caucasian population these three SNPs are either all present in the minor allele (AGA) or are all absent in the major allele (GTG) and the major allele is present in 71% of the Caucasian population.

The genetic element of Bfl-1 which was consistent between melanoma cells and primary melanocytes was the presence of the less common Bfl-1S isoform of Bfl-1 in both cell types. This isoform was present in all the primary melanocyte samples and five out of the six melanoma cell-lines, and was present at roughly 30-40% of the overall quantity of Bfl-1 mRNA. Unfortunately the two isoforms could not be differentiated at the protein level due to the similarity of size, with a difference of just 12 amino acids between Bfl-1S and Bfl-1 meaning two separate bands could not be distinguished by western blot. Currently there is an absence of antibodies which are known to detect the region of Bfl-1 that is altered during splicing, i.e. exon 2. It would be interesting to explore whether there is any difference in the function of the two isoforms of Bfl-1. This could be explored using expression constructs for both isoforms. After amplification by PCR and sequencing, both isoforms could be ligated into expression vectors for transfection for example into the

A375 melanoma cells, which express very low levels of native Bfl-1. Another way of creating two expression vectors would be through the use of Invitrogen's Gateway recombination cloning technology, which limits the number of steps to achieve an expression vector and helps to generate transfectants expressing equivalent levels of different proteins. The transfected A375 cells could then be used to compare the function of the two isoforms as well as characterising the proteins, assuming that the current Bfl-1 antibodies will detect Bfl-1S. Similarly, these methods could be utilised to examine any differences between the major and minor alleles for Bfl-1.

In both melanoma cells and primary melanocytes, Bfl-1 was consistently shown, using several different pathway specific inhibitors, to be regulated through the NFκB pathway, agreeing with previous research which defined this pathway as responsible for controlling the transcription of Bfl-1 in a range of other tissues and cancers [235,398,399]. We also examined the roles of the other survival pathways, the MEK/ERK pathway and the Akt pathway, in the regulation of Bfl-1 expression in melanocytes and melanoma cells. Inhibition of the MEK/ERK pathway consistently resulted in higher expression levels of Bfl-1 in SkMel28 cells, but not MM200 cells or primary melanocytes. Meanwhile, blocking the Akt pathway resulted in an increase of Bfl-1 protein in MM200 cells, but no increase in SkMel28 cells or primary melanocytes. The reasons for these inconsistencies in the regulation of Bfl-1 between melanoma cell-lines was discussed in detail in the conclusions section of chapter 3, where we postulated that they could be due to the differing PTEN status (MM200 cells have deleted PTEN, while SkMel28 cells contain active PTEN) or the differing ratios of the two isoforms of Bfl-1 in the two cell-lines (see section 3.8 for details). Melanocytes are known to express active PTEN, which is deleted during the transformation process [497]. This would support the theory that PTEN status is important in determining the response to Akt inhibition as melanocytes respond similarly to SkMel28 cells, which both contain active PTEN, while MM200 cells have deleted PTEN. However, PTEN status cannot explain the differing response to MEK inhibition between the cells as SkMel28 cells and melanocytes have different responses.

Additionally, post-translational control was seen to be very similar between melanoma cells and primary melanocytes. The proteasome was found to degrade the Bfl-1 protein in a similar manner in both systems. During a time course assay where the proteasome was blocked by MG132 and protein synthesis was blocked by cycloheximide, the protein half-life was seen to lengthen in both melanoma and melanocyte cells. However, after 4 hours, the level of protein did start to fall, despite the inhibition of the proteasome, suggesting

other factors may also have some influence in the degradation of the protein. In fact, previous work has suggested a role for calpains in the degradation of Bfl-1 [406].

All of this data on the regulation of Bfl-1 in melanoma cell-lines and primary melanocytes suggests that Bfl-1 does not become upregulated upon transformation of the cells, as the regulation of its expression does not change after transformation, leading me to theorise that if a melanoma sample had high Bfl-1 expression levels, the melanocyte it originated from already had high Bfl-1 levels. This would be difficult to determine without a very large study including samples from healthy individuals and follow up samples from all stages of melanoma development which could determine if there was a correlation between patients with high Bfl-1 expression in benign nevi and those that went on to develop metastatic melanoma. If this study was to be performed, the presence of the minor allele for Bfl-1 containing the polymorphisms would also be interesting to measure to determine if the polymorphisms lent a genetic predisposition to the development of metastatic melanoma, as they have been shown to do in the development of atopic dermatitis [442].

There is evidence in the literature which could support either theory. The theory that Bfl-1 would become upregulated during the transformation of melanocytes is supported by the fact that the NFκB pathway, which is responsible in the regulation of Bfl-1 expression, has been shown to become upregulated after the transformation of melanocytes [239] and NFκB regulated chemokines were observed at a higher level in melanoma than healthy cells [237,238]. Indeed, Bfl-1 overexpression, much like Bcl-2, was not seen to be tumourigenic itself in mice [391]. However, there is also evidence to support the theory that melanocytes with already high levels of Bfl-1 may be more susceptible to tumourigenesis than those with lower levels as there are studies which do support a tumour promoting role for Bfl-1. For example, Bfl-1, with CEBP, was shown to be essential for the transformation to anaplastic large cell lymphoma [387], and the overexpression of Bfl-1 in mice sensitized the animals to transformations caused by oncogenes such as E1A and myc [392,393], so it is feasible that Bfl-1 could have a tumourigenic role in melanoma development, possibly in combination with the BRaf mutation, or PTEN deletion.

The subcellular localisation of Bfl-1 was explored in detail in melanoma cells using tagged proteins for detection by microscopy and subcellular fractionation techniques to localise the native protein. All of this data together suggested that Bfl-1 was found localised to the mitochondria, even in resting non-apoptotic cells, but that it may become even more closely associated with the mitochondria after apoptotic stimulation. Subcellular

fractionation of primary melanocytes also suggested that Bfl-1 was localised to the mitochondria, although this was not explored in as much depth as in the melanoma cells. As discussed in detail in chapter 5, this correlated with some previous research in other cell types which found Bfl-1 localised around the mitochondria and at low levels in the cytoplasm [411,424], but completely disagreed with one study which found it in the nucleus of apoptotic cells and the cytoplasm of resting cells [425]. Theoretically, Bfl-1 should be located at the mitochondria, especially in apoptotic cells, where it interacts with other members of the Bcl-2 family to inhibit apoptosis [408,411]. This is true in both the direct and indirect theories of apoptosis inhibition within the Bcl-2 family, as both involve Bfl-1 binding to mitochondria-bound forms of Bax and Bak (Figure 1.13).

Having characterised Bfl-1 in melanoma and melanocyte cells, the next step was to explore the relative importance of the protein in both systems in the protection from apoptosis. In our panel of melanoma cell-lines, we did this by assessing the relative effects of Bfl-1 over-expression and knock down using siRNA. In primary melanocytes we assessed the role of Bfl-1 by employing siRNA. Firstly, we established which of our melanoma cell-lines expressed high (SkMel28, MM200 and UACC62), average (G361 and SkMel31) and very low levels of Bfl-1 (A375). These cells were treated with a range of chemotherapeutic agents but cells with less Bfl-1 were not found to be significantly more sensitive to apoptosis caused by chemotherapeutic agents than cells with higher levels of Bfl-1. The exception was a slight correlation between lower levels of Bfl-1 expression and higher sensitivity to Etoposide treatment. Of course, there are many other cellular factors which may influence the sensitivity of these cells to different chemotherapeutic agents regardless of Bfl-1 expression, such as BRaf mutation status which are discussed in detail in chapter 4. To more formally address the anti-apoptotic ability of Bfl-1 I employed the over-expression assays, where tagged Bfl-1 protein was transfected into A375 melanoma cells, which originally expressed very low levels of Bfl-1. These experiments confirmed that higher levels of Bfl-1 expression gave significant protection to cells from apoptosis caused by a range of chemotherapeutic agents, confirming its role as a pro-survival protein in melanoma cells.

Bfl-1 was then successfully knocked down in both melanoma cells and primary melanocytes using siRNA technology. As such, apoptosis caused by chemotherapeutic agents could be measured in cells expressing their native levels of Bfl-1 and compared directly with the apoptosis of the same cells in which Bfl-1 expression was lowered by

around 80%. This data could potentially provide the strongest argument for the importance of Bfl-1 as a potential drug target in the treatment of metastatic melanoma.

These knock down experiments provided some interesting results. Bfl-1 knock down was not always seen to lead to an increase in sensitivity to chemotherapeutic-induced apoptosis, but in some cases the effect was impressive. For example, the MEK inhibitor PD901 was much more effective in SkMel28 cells after Bfl-1 knock down, with levels of cell death rising from around 20% with the control siRNA to around 50% with Bfl-1 siRNA. Paclitaxel and Cisplatin were also more effective when used in conjunction with Bfl-1 knock down in these melanoma cells. These data imply that Bfl-1 serves to elicit resistance from these drugs in these cells. However, these results were not consistent across melanoma samples, with MM200 cells showing less increased sensitivity to Bfl-1 knock down when combined with PD901 or Cisplatin treatment. Therefore, it would have been interesting to look at the effects of Bfl-1 knock down in more members of our panel than just SkMel28 and MM200 cells as even across just two cell-lines, the effect of Bfl-1 knock down on MEK inhibitor-induced apoptosis was very different. MEK inhibitors are being widely trialled in the treatment of melanoma and other BRaf containing cancers, but are providing largely unimpressive clinical results (AstraZeneca and Array BioPharma Inc., 2010). Our data suggests that Bfl-1 expression may be an important factor in the resistance to MEK inhibition and indeed previous work has found that the effectiveness of MEK inhibitors in the treatment of melanoma depended on the expression levels of the pro-survival protein Mcl-1 during treatment [498]. Wang et al. showed that MEK inhibitors were more effective when Mcl-1 levels dropped after treatment while Konopleva et al. found that MEK inhibition enhanced the action of the BH3 mimetic ABT-737 by blocking the ERK-dependent induction of Mcl-1 [499]. In SkMel28 cells levels of Bfl-1 were seen to rise after treatment with PD901 while they dropped in MM200 cells. Indeed it may be the blocking of this unexplained rise in Bfl-1 expression after MEK inhibition that made SkMel28 cells so sensitive to MEK inhibition when Bfl-1 siRNA was present.

An additional interesting observation from these experiments was the response of the melanoma cells to the DNA damaging agent Etoposide. Etoposide was the only drug which was initially shown to display any correlation between the level of cell death it caused and the expression level of Bfl-1 across the melanoma cell-line panel. As such, A375 cells displayed much higher levels of cell death than the other melanoma cells which had higher levels of Bfl-1 expression. This pattern was confirmed in the over-expression system, where the over-expression of Bfl-1 in A375 cells gave these cells protection from

Etoposide-induced cell death. However in the knock down experiments, the loss of Bfl-1 did not sensitise any of the cells we tested to Etoposide-induced cell death. This suggests that while Bfl-1 can protect cells from Etoposide, other factors are also important in the protection of melanoma cells from Etoposide and may be able to substitute for its absence.

Interestingly, in primary melanocyte cells a substantial variation in sensitivity to Bfl-1 knock down was seen between samples of melanocytes. Only two melanocyte samples were subjected to the siRNA knock down assay, but the results between the two were very different. One sample, which had low levels of Bfl-1 expression, was completely unaffected by Bfl-1 knock down, while the other sample, which expressed a high level of Bfl-1 displayed a very consistent increase in cell death after Bfl-1 knock down regardless of which chemotherapeutic agent they were treated with. In fact, this increase in cell death was present in the melanocyte cells treated with Bfl-1 siRNA but no chemotherapeutic agents, showing that background death was significantly higher after removal of Bfl-1 from these cells. This suggests that these melanocyte cells rely on Bfl-1 for survival in general, not merely when they are challenged with apoptotic stimuli. Therefore as expected, the extent of Bfl-1 knock down and the effects of this knock down on survival appeared dependent on the level of expression of Bfl-1 in the cells. Presumably in the case where Bfl-1 expression was low, the cells relied on other pro-survival proteins for survival against apoptotic stimuli. As such, both samples were also treated with ABT-737, which inhibits Bcl-2, Bcl-w and Bcl-xL.

While both melanocyte samples and the melanoma cells underwent higher levels of cell death in response to ABT-737, it was the melanocyte sample with low levels of Bfl-1 which was the most sensitive to the inhibition of the Bcl-x proteins by ABT-737. In all cell samples, the combination of Bfl-1 knock down, ABT-737 treatment and Paclitaxel resulted in the highest levels of cell death, whilst in the melanoma cells, the combination of Bfl-1 knock down, ABT-737 and PD901 was also as effective. In both primary melanocyte samples, the combination of PD901 with either Bfl-1 knock down, ABT-737 treatment or a combination of both resulted in no higher level of cell death than these same treatments and combinations without PD901. Therefore, it was the inhibition of MEK in a BRaf mutant cell-line combined with the inhibition of pro-survival proteins which would appear to have the potential for the lowest level of side effects on healthy melanocyte cells.

The data from this series of experiments suggests that melanocytes and melanoma cells with high levels of Bfl-1 expression rely on this protein for survival against apoptotic

stimuli whilst melanocytes with low Bfl-1 expression rely on other members of the pro-survival proteins. These combination experiments, including Bfl-1 siRNA and ABT-737, left Mcl-1 as the only pro-survival protein of the Bcl-2 family not inhibited or knocked down in these cells. Unfortunately the level of Mcl-1 in these samples was not measured by western blot due to the lack of cells available for analysis and the low sensitivity of the Mcl-1 antibody on a membrane which had already been probed for Bfl-1 and other Bcl-2 pro-survival proteins. However it would be interesting to block Mcl-1 in primary melanocytes to determine the role it plays in the survival of these cells. As previously discussed, a new BH3 mimetic, TW-37 has been developed which targets Mcl-1 as well as Bcl-2 and Bcl-xL [346].

Another interesting observation found during the siRNA experiments was the exaggerated effect of knocking down the over-expressed Bfl-1 protein in A375 cells, discussed in detail in chapter 4. Surprisingly, A375 cells transfected with Bfl-1FLAG were much more sensitive to chemotherapy-induced apoptosis after Bfl-1 knock down than the native A375 cells which expressed very low levels of Bfl-1 protein. Presumably the Bfl-1 transfected cell-lines, over a matter of a few weeks, become reliant on Bfl-1 expression as a protection from apoptosis and down-regulate the other pro-survival proteins. When Bfl-1 was lost, the other pro-survival proteins or systems that native A375 cells relied upon for protection were then not sufficient to facilitate their resistance to the chemotherapeutic agents tested. It would have been interesting to assess the level of Mcl-1 and the other pro-survival proteins in the transfected cells compared with the native A375 cells, which expressed high levels of Mcl-1 in the absence of Bfl-1, to establish whether the large increase in Bfl-1 levels led to a related drop in the levels of the other pro-survival proteins. All of these siRNA and over-expression experiments showed how melanoma cells can rely upon Bfl-1 for protection from chemotherapy induced apoptosis and these experiments could be taken further into in vivo work.

Our approach to in vivo work would be to transfect melanoma cells with plasmids expressing a Bfl-1 specific short hairpin RNA (shRNA) based upon the siRNA sequence used here and then to inoculate immunodeficient mice (SCID or RAG-/-) with these cells or cells transfected with a scrambled control plasmid. Alternatively, systemic or intratumoral siRNA could be investigated to achieve Bfl-1 knock down. As such, xenografts in nude mice would allow tumours grown from human melanoma cells with knocked down Bfl-1 to be directly compared with those grown from melanoma cells with native Bfl-1 expression levels. These xenografts would allow the comparison of mice with

untreated tumours, tumours treated with Bfl-1 shRNA, tumours treated with chemotherapeutic agents alone and tumours treated with the combination of Bfl-1 shRNA and chemotherapies. The combination of Bfl-1 knock down and MEK inhibition would be especially interesting. The growth of the tumour after treatment and the mortality of the animals would demonstrate whether Bfl-1 inhibition enhanced the therapeutic ability of other chemotherapeutic agents, or was indeed effective alone.

However, xenografts are performed in immunodeficient mice and melanoma is an immunogenic cancer. Melanoma expresses a range of melanoma-associated antigens (MAGEs) [500], and Bfl-1 is a pro-survival protein which can be upregulated by inflammatory cytokines [370,379] and has been shown to be of importance in the immune response [378]. Therefore, ideally we would strive to test the effects of Bfl-1 knock down in melanoma in mice with a fully active immune system. One such model exists which combines the BRaf mutation with the deletion of PTEN, a combination seen in about 20% of melanomas. This combination results in the development of metastatic melanoma in these mice when the mutated BRaf is activated under the control of tamoxifen induced Cre recombinase. If Bfl-1 knock down could be achieved in these cells, the active immune system would make it a useful model for testing it as a target in melanoma. However, one complications is that this model utilises mice melanoma cells, rather than human cells, which contain 4 copies of the murine Bfl-1 protein, A1, which has proven difficult to knock down efficiently [420]. Although mouse models are still not ideal for representing real patients, they are a step onwards from the use of cell-lines and allow mechanistic studies which are not possible in patients.

The melanocyte samples we investigated were obtained from one site on a healthy patient, so we cannot tell from these samples whether the variations we saw (i.e. Bfl-1 expression levels) were differences between individuals or whether a single patient would have some melanocytes which expressed high Bfl-1 at the same time as having other melanocytes with low Bfl-1 expression. If all the melanocytes in an individual expressed high Bfl-1 and this was a factor that predisposed them to melanoma, knock down of Bfl-1 using a specific inhibitor might kill off all their healthy melanocytes as well as the cancerous ones. However if only some melanocytes expressed Bfl-1 and these were the ones in an individual that were predisposed to cancer, then a Bfl-1 inhibitor could potentially pre-treat these cells to prevent melanoma even developing alongside treating existing melanomas. If Bfl-1 expression did in fact increase during the transformation process then a Bfl-1 inhibitor could be used to kill cancerous cells, but might also possibly kill healthy

melanocytes that were expressing high levels of Bfl-1. In this case, a regimen combining a Bfl-1 inhibitor with chemotherapeutics which specifically target very fast proliferating cells could be successful, as cancer cells proliferate much faster than healthy melanocyte cells.

A Bfl-1 inhibitor could be very successful in conjunction with already existing chemotherapeutics such as the MEK inhibitor PD901 and the BH3 mimetic ABT-737 for overcoming the intrinsic chemo resistance observed in this cancer. There is bountiful evidence that cancers that become resistant to ABT-737 do so through the upregulation of Mcl-1 and Bfl-1 [332,345]. In this case a Bfl-1 specific inhibitor may be particularly useful. In fact, a new BH3 mimetic has been designed which can also target Mcl-1 as well as Bcl-2 and Bcl-xL [346], but a Bfl-1 specific inhibitor has yet to be elucidated.

This lack of a drug designed specifically to inhibit Bfl-1 may be due to the difficulty in designing a drug which targets a protein which displays structural plasticity and has a very similar hydrophobic groove to the other members of the Bcl-2 family [313]. Indeed, the crystal structure for Bfl-1 has only been elucidated when it is bound to a BH3-only protein due to its fluidity [416]. However, there are some molecules which have already been identified as potential Bfl-1 inhibitors, including gambogic acid and N-arly malemides [428,429], which could act as compounds from which a specific Bfl-1 inhibitor could be derived. In addition, peptide aptamers have been presented which specifically target Bfl-1 and were shown to sensitise malignant B-cells to treatments with chemotherapeutic agents [431]. Alternatively, a drug which targets Bfl-1 expression, i.e. the NFκB pathway, may lead to lower levels of Bfl-1 expression, but may also have off-target effects, as NFκB acts as a transcription factor for a range of targets.

These data highlight the point that in addition to its use in the treatment of metastatic melanoma, Bfl-1 could be a potential drug target in a range of cancers and other diseases. Large B-cell lymphomas, CLL and AML have all been shown to express high levels of Bfl-1 [373-375], as have long-lived mature B-cells [380], while malignant B-cells have been shown to be dependent on Bfl-1 for survival [385]. Bfl-1 has also been shown to play an important role in the survival of mast cells during an allergic reaction and a drug which inhibited its action or its upregulation in these cells could be used to treat a range of allergies [378,379]. Indeed, a drug targeted to Bfl-1 may be helpful in the prevention of inflammation as Bfl-1 is upregulated in response to inflammatory cytokines such as TNFα and IL-1β [370,379].

To define the physiological role of Bfl-1 outside of disease, transgenic and knock-out mice have been created. The murine version of Bfl-1, A1, has four different isoforms, making the creation of an A1 knock-out mouse a difficult and elusive goal, as detailed above [420]. However knock-out of one or more of these isoforms, as discussed in detail in section 1.6.5, suggests that Bfl-1 has an important role in the haematopoietic system, especially during lymphocyte maturation and differentiation [380,381]. Possibly due to the lack of knock down of all A1 murine isoforms, the phenotype of A1 knock-out mice is fairly mild compared to other pro-survival knock-out mice [324]. However, it has been established that Bfl-1 is expressed in endothelial cells, bone marrow, haematopoietic cells and in the lung [369,370]. Therefore toxicity and possible side effects may result from the use of a Bfl-1 inhibitor in patients according to the dependence of these cells of Bfl-1 for survival.

In conclusion, I have shown that Bfl-1 acts as a pro-survival protein in melanoma and that it plays a role in the resistance of these cells to current chemotherapeutic agents. I have confirmed that Bfl-1 is regulated by the NFκB pathway and localised to the mitochondria in melanoma and found that its regulation may also be influenced by the MEK/ERK and Akt pathways. I have demonstrated the degradation of Bfl-1 by the proteasome and shown that Bfl-1S represents 30-40% of the total Bfl-1 protein in melanocytes and melanoma cells, and that both these isoforms express the three common Bfl-1 SNPs. Importantly, I have shown that knock down of Bfl-1 in melanoma cell-lines can increase the effectiveness of some current therapies and our evidence suggests that Bfl-1 is a valid drug target in melanoma. In fact, its potential as a drug target could be expanded to include a range of other chemo resistant cancers and immune responses which rely on high levels of Bfl-1. Indeed, in the era of targeted therapies, tumour biopsies could be taken to establish the level of Bfl-1 expression and determine whether a Bfl-1 inhibitor could be used.

APPENDIX

APPENDIX A

A1: Creation of the TOPO vector containing Bfl-1

Bfl-1 cDNA from PBLs was extracted from the agarose gel using a QIAX II gel extraction kit to obtain purified Bfl-1 DNA (Figure A2). Bfl-1 was then ligated into the pCR 2.1 TOPO vector (Invitrogen) to create a stock DNA construct from which Bfl-1 could be isolated for further sub-cloning into other vectors. This work was carried out by Claire Harris, University of Southampton. Nine colonies were picked and grown up in LB broth (for recipe see section *2.3.5*) containing kanamycin for 6 hours. These colonies were checked for the Bfl-1 insert by purification of the plasmid DNA from the bacteria then restriction digest of the insert from the vector using the EcoR1 sites which flank the insert site in the TOPO vector (Figure A3). The colonies which appeared to be positive for Bfl-1, based on the correct band size, were sequenced using the T7 and sp6 promoters present in the TOPO vector (Figure A1; A). A clone confirmed as a positive for Bfl-1 by sequencing was grown up in 100ml LB broth overnight and the plasmid DNA was purified from the bacteria by maxiprep to obtain large quantities of the TOPO vector containing the Bfl-1 insert.

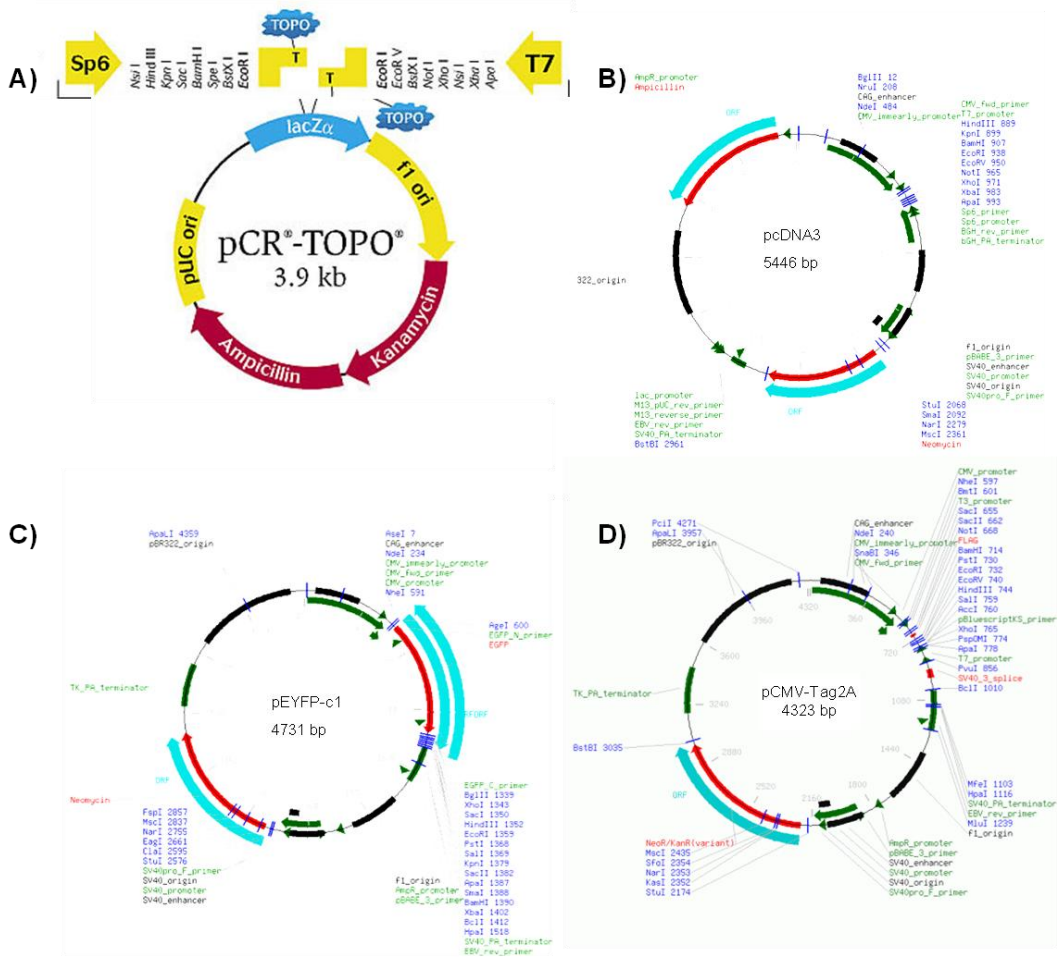

Figure A1: Vector maps of the plasmids used to create Bfl-1 fusion proteins. (Invitrogen and https://www.lablife.org/)

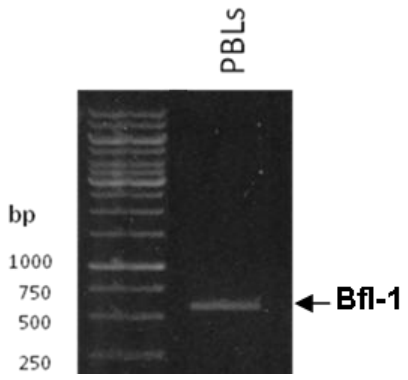

Figure A2: Extraction of Bfl-1 DNA from Peripheral Blood Leukocytes (PBLs).
Several cell-lines were explored for Bfl-1 expression by PCR and separation by electrophoreisis on an agarose gel. Bfl-1 was extracted using a QIAX II gel extraction kit (Qiagen) to obtain purified Bfl-1 DNA.

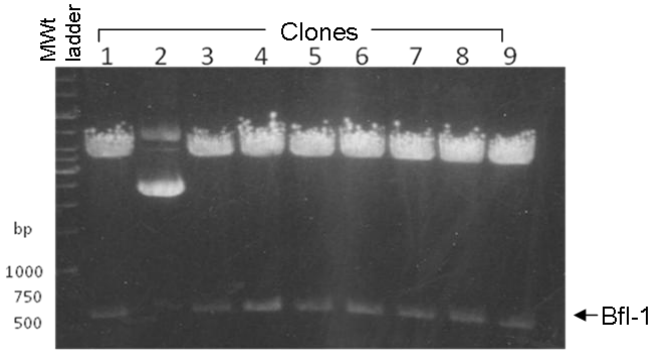

Figure A3: Amplification of Bfl-1 DNA shows Bfl-1 was successfully ligated into the TOPO plasmid vector.
The Bfl-1 isolated from PBLs was ligated into the TOPO vector and transformed into TOP10 E.coli. 9 separate clones were picked and grown up for 6 hours in 10ml LB broth containing kanamycin. DNA was purified by miniprep, cut with EcoRI, separated by electrophoreisis and run on a 0.7% agarose gel. All samples except sample 2 were sequenced to determine which clones had the correct DNA sequence. Clone 1 was shown to have the correct sequence and so was grown up overnight in 100ml LB broth containing kanamycin for maxiprep to obtain purified Bfl-1 in TOPO vector. A glycerol stock was also made.

A2: Creation of the Bfl-1pcDNA3 construct

The Bfl-1-TOPO vector was used for sub-cloning of Bfl-1 into the expression vector pcDNA3 (Figure A1 B). In brief, Bfl-1 was isolated from TOPO using the restriction digest enzymes BamHI and HindIII, separated on an agarose gel, the cut fragment was extracted and ligated into the vector pcDNA3 which was cut using BglII and HindIII to give complementary sites to the insert DNA (Figure A4). The Bfl-1 insert was ligated into the vector with T4 DNA ligase, isolated from the bacteriophage T4. T4 DNA ligase

catalyses the formation of phosphodiester bonds between the 5' phosphate and 3' hydroxyl groups in duplex DNA. The ligated DNA construct was transformed into the competent bacteria JM109 E.coli which were grown on an agar plate containing the selection agent ampicillin. Colonies were picked, grown in LB broth and the DNA was purified and cut by the restriction digest enzymes BamHI and HindIII to ensure the constructs contained the correct sized DNA insert (Figure A5). Clone 2 was grown up in 100ml LB broth containing ampicillin overnight and maxiprep was performed to yield large quantities of the expression vector Bfl-1pcDNA3.

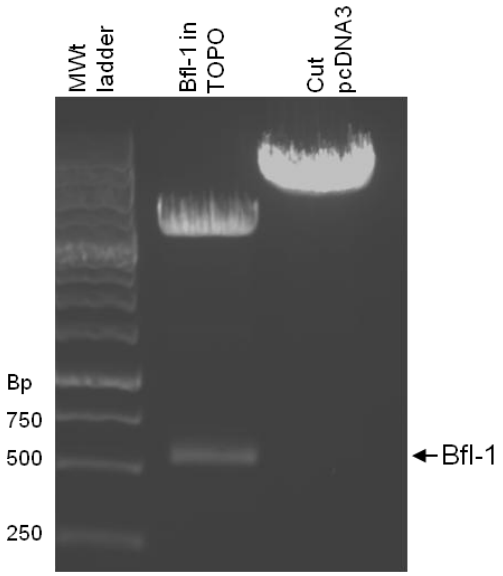

Figure A4: Bfl-1 DNA was cut from the TOPO plasmid vector by restriction digest and the pcDNA3 plasmid was cut with complementary restriction digest enzymes.
Bfl-1 in TOPO was cut with BamHI and HindIII, pcDNA3 was digested with BglII and HindIII and both were run on a 0.7% agarose gel. Bfl-1 and the cut pcDNA3 vector were extracted from the agarose gel and ligated using T4 DNA ligase. The new vector, Bfl-1pcDNA3, was transformed into JM109 E.coli.

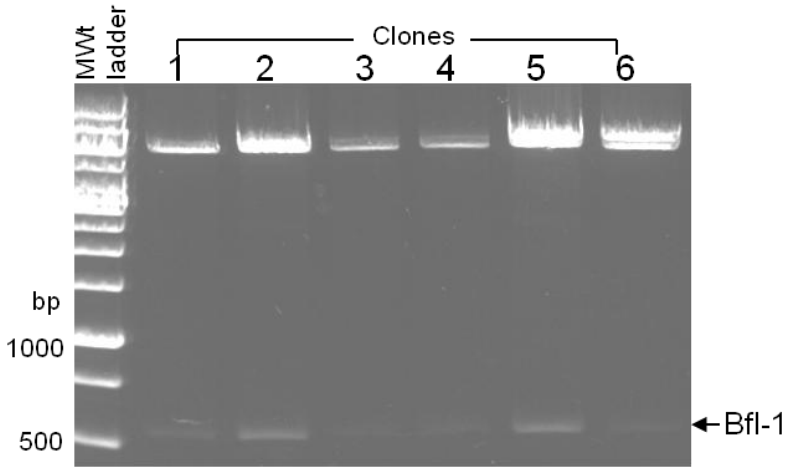

Figure A5: Plasmid analysis by restriction digests shows colonies of JM109 E.coli were transformed with the correct plasmid Bfl-1pcDNA3 containing Bfl-1 DNA.
6 clones were picked from the agar plate with the transformed JM109 E.coli. These were grown up in 10ml LB broth containing ampicillin for 6 hours and the DNA was extracted by miniprep. The DNA was digested overnight by BamHI and HindIII and run on a 0.7% agarose gel. Sample 2 was picked and grown up overnight in 100ml LB broth containing ampicillin. Bfl-1pcDNA3 DNA was purified by maxiprep and a glycerol stock was made.

A3: Creation of the Bfl-1YFP construct

Bfl-1 was sub-cloned from the TOPO vector into pEYFP-C1 (BD BioSciences) (performed by Claire Harris, University of Southampton, UK). The pEYFP-C1 vector contains an YFP coding sequence and a kanamycin resistance gene (Figure A1 C). Bfl-1 was isolated from TOPO by restriction digest with the enzymes BamHI and HindIII (Figure A6). The pEYFP-C1 vector was also cut with BglII and HindIII to give complementary sites for the Bfl-1 insert. The DNA was separated by gel electrophoreisis and the DNA of interest was isolated from the agarose gel. The Bfl-1 insert was ligated into the vector with T4 DNA ligase and the ligated DNA was transformed into JM109 E. Coli. The transformed bacteria were grown overnight on an agar plate containing the selection agent kanamycin and colonies were picked and grown up for 6 hours in LB broth containing kanamycin. Plasmid DNA was isolated from bacteria and the insert was cut out of the vector to determine which clones contained the correct sized insert (Figure A7). The restriction digest was performed with the enzymes HindIII and Pstl as the ligation destroyed the BglII site in the DNA construct producing two small bands by gel electrophoresis, the larger of the two representing the Bfl-1 insert. These two bands are observed because there were two Pstl sites present in the construct, one in the insert and one just inside the vector, so when the construct was cut with Pstl and HindIII, two small and a single large band were seen in the positive clones. A positive clone was chosen and grown up in LB broth before the plasmid

DNA was isolated from the bacteria by maxiprep giving large quantities of the expression construct for the protein Bfl-1YFP.

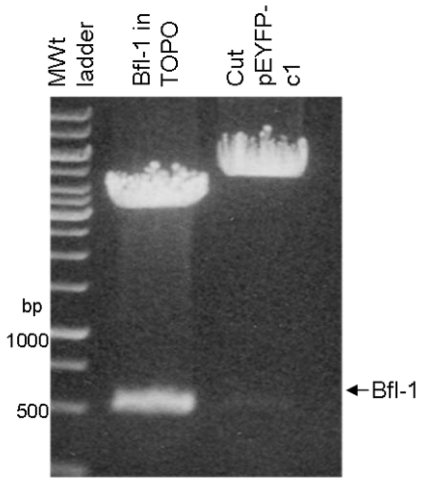

Figure A6: Bfl-1 DNA was cut from the TOPO plasmid vector by restriction digest and the eYFP-c1 plasmid was cut with complementary restriction digest enzymes.
Bfl-1 in TOPO was cut with BamHI and HindIII, pEYFP-c1 was digested with BgIII and HindIII (Promega) and both were separated by electrophoreisis on a 0.7% agarose gel. Bfl-1 and the cut vector were extracted from the gel and ligated using T4 DNA ligase. The new vector, Bfl-1YFP, was transformed into JM109 E.coli.

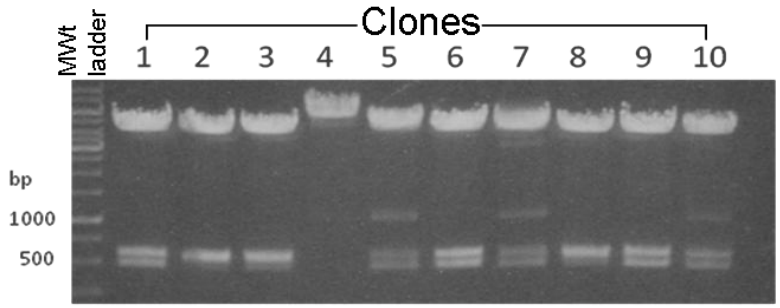

Figure A7: Plasmid analysis by restriction digest shows colonies of JM109 E.coli were transformed with the correct Bfl-1YFP plasmid containing Bfl-1 DNA.
Ten colonies of Bfl-1YFP transformed into JM109 E.coli were picked and grown up in 10ml LB broth containing kanamycin for 6 hours. DNA was purified by miniprep and cut by restriction digest with HindIII and Pstl as the ligation destroyed the BgIII site. This produced 2 small bands on the gel as there are Pstl sites inside the vector and just inside the insert which produces 3 fragments when Pstl and HindIII are used. Sample 1 was grown up overnight in 100ml LB broth containing kanamycin and maxiprep was performed to obtain purified Bfl-1YFP DNA.

A4: Creation of the Bfl-1FLAG construct

Bfl-1 was sub-cloned from the TOPO vector into the pCMV-Tag2A vector (performed by Claire Harris, University of Southampton). The pCMV-Tag2A vector contains the FLAG tag and a kanamycin resistance gene (Figure A1 D). Bfl-1 was isolated from TOPO by

restriction digest with the enzymes BamHI and HindIII (Figure A8). The pCMV-Tag2A vector was also cut with BamHI and HindIII to give complementary sites for the Bfl-1 insert. As before, the DNA was separated by gel electrophoreisis and the DNA of interest was isolated from the agarose gel. The Bfl-1 insert was ligated into the vector with T4 DNA ligase and the ligated DNA was transformed into JM109 E. Coli. The transformed bacteria were grown overnight on an agar plate containing the selection agent kanamycin and colonies were picked and grown for 6 hours in LB broth containing kanamycin. Plasmid DNA was isolated from bacteria and the insert was cut out of the vector using the restriction enzymes BamHI and HindIII to determine which clones contained the correct sized insert (Figure A9). A positive clone was chosen and grown up in LB broth before the plasmid DNA was isolated from the bacteria by maxiprep giving large quantities of the expression construct for the protein Bfl-1FLAG.

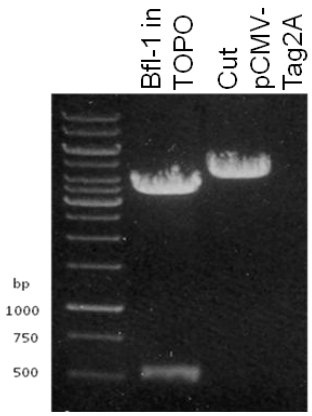

Figure A8: Bfl-1 DNA was cut from the TOPO plasmid vector by restriction digest and the pCMV-Tag2A plasmid was cut with complementary restriction digest enzymes.
Bfl-1 in TOPO was cut with BamHI and HindIII, pCMV-Tag2A was digested with BamHI and HindIII (Promega) and both were separated by electrophoreisis on a 0.7% agarose gel. Bfl-1 and the cut vector were extracted from the gel and ligated using T4 DNA ligase. The new vector, Bfl-1FLAG, was transformed into JM109 E.coli.

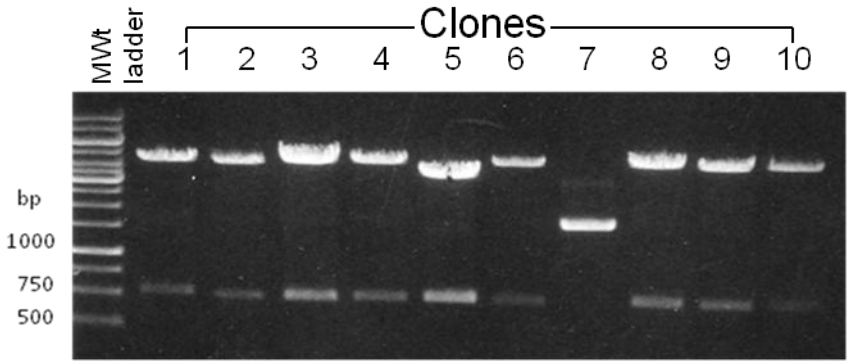

Figure A9: Plasmid analysis by restriction digest shows colonies of JM109 E.coli were transformed with the correct Bfl-1FLAG plasmid containing Bfl-1 DNA.
Ten colonies of Bfl-1FLAG transformed into JM109 E.coli were picked and grown up in 10ml LB broth containing kanamycin for 6 hours. DNA was purified by miniprep and cut by restriction digest with HindIII and BamHI. Sample 3 was grown up overnight in 100ml LB broth containing kanamycin and maxiprep was performed to obtain purified Bfl-1FLAG DNA.

APPENDIX B

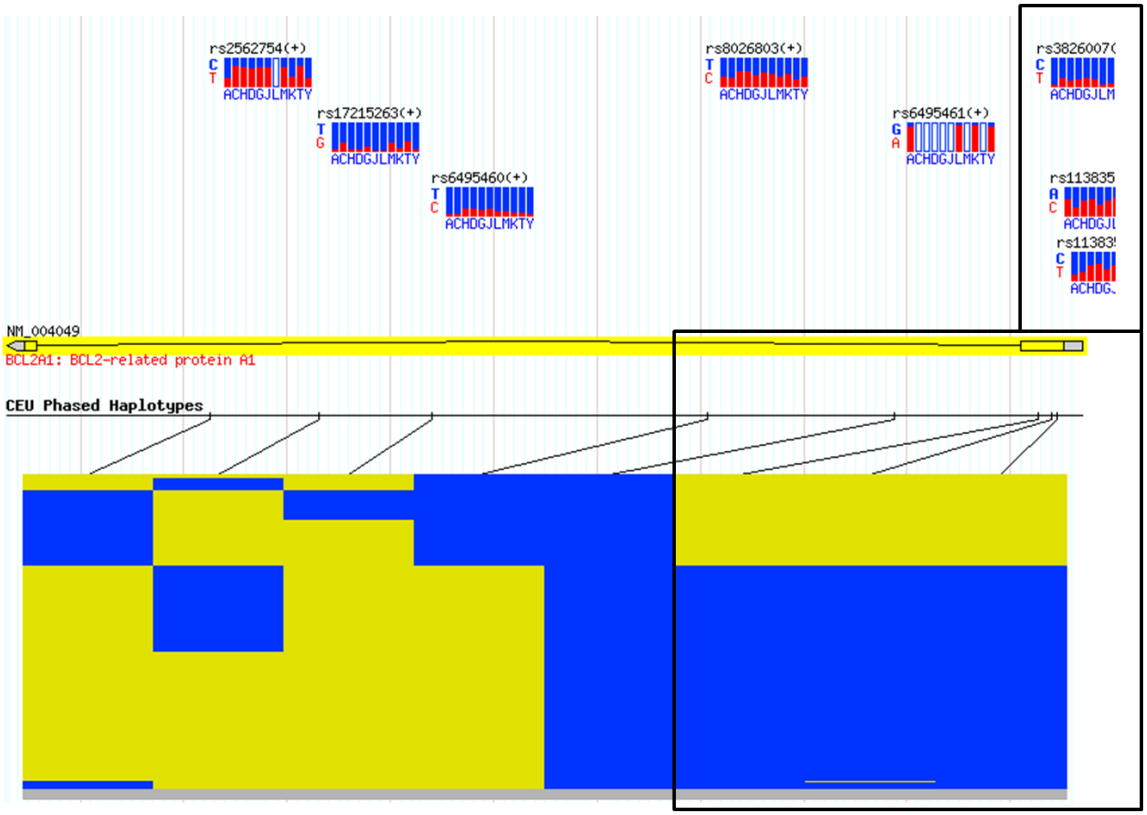

Figure B1: Sequence pictogram for polymorphisms in Bfl-1 in the Caucasian population.
The polymorphisms highlighted by black boxes are the three SNPs we sequenced in Bfl-1 from melanoma and melanocyte cells. The pictogram demonstrates that in the Caucasian population, 71% contain all three SNPs (blue), while 29% present wild-type Bfl-1 (yellow). The blue and red bars for each SNP represent the ratio of polymorphism to wild-type across several racial populations. (A; African, USA, C: Utah European, Caucasian, H; Han Chinese, China, D; Chinese, Denver, USA, G; Indians, Texas, J; Japanese, L; Luhya, Kenya, M; Mexican, California, K; Maasai, Kenya, T; Tuscan, Italy, Y; Yoruban, Nigeria). This figure was sourced from snp.cshl.org.

REFERENCES

1. Pott, P. Cancer Scroti. *Chirurgical Observations*, 63-68 (1775).
2. Kipling, M.D. & Waldron, H.A. Percivall Pott and cancer scroti. *Br J Ind Med* **32**, 244-246 (1975).
3. Rous, P. A Transmissible Avian Neoplasm. (Sarcoma of the Common Fowl.). *J Exp Med* **12**, 696-705 (1910).
4. Rous, P. A Sarcoma of the Fowl Transmissible by an Agent Separable from the Tumor Cells. *J Exp Med* **13**, 397-411 (1911).
5. Huebner, R.J. & Todaro, G.J. Oncogenes of RNA tumor viruses as determinants of cancer. *Proc Natl Acad Sci U S A* **64**, 1087-1094 (1969).
6. Duesberg, P.H. & Vogt, P.K. Differences between the ribonucleic acids of transforming and nontransforming avian tumor viruses. *Proc Natl Acad Sci U S A* **67**, 1673-1680 (1970).
7. Stehelin, D. The transforming gene of avian tumor viruses. *Pathol Biol (Paris)* **24**, 513-515 (1976).
8. Stehelin, D., Varmus, H.E., Bishop, J.M. & Vogt, P.K. DNA related to the transforming gene(s) of avian sarcoma viruses is present in normal avian DNA. *Nature* **260**, 170-173 (1976).
9. Iba, H., Takeya, T., Cross, F.R., Hanafusa, T. & Hanafusa, H. Rous sarcoma virus variants that carry the cellular src gene instead of the viral src gene cannot transform chicken embryo fibroblasts. *Proc Natl Acad Sci U S A* **81**, 4424-4428 (1984).
10. Knudson, A.G., Jr. Mutation and cancer: statistical study of retinoblastoma. *Proc Natl Acad Sci U S A* **68**, 820-823 (1971).
11. Comings, D.E. A general theory of carcinogenesis. *Proc Natl Acad Sci U S A* **70**, 3324-3328 (1973).
12. Lane, D.P. & Crawford, L.V. T antigen is bound to a host protein in SV40-transformed cells. *Nature* **278**, 261-263 (1979).
13. Pellegata, N.S., Antoniono, R.J., Redpath, J.L. & Stanbridge, E.J. DNA damage and p53-mediated cell cycle arrest: a reevaluation. *Proc Natl Acad Sci U S A* **93**, 15209-15214 (1996).
14. Shen, Y. & White, E. p53-dependent apoptosis pathways. *Adv Cancer Res* **82**, 55-84 (2001).
15. Hollstein, M., Sidransky, D., Vogelstein, B. & Harris, C.C. p53 mutations in human cancers. *Science* **253**, 49-53 (1991).
16. Hanahan, D. & Weinberg, R.A. The hallmarks of cancer. *Cell* **100**, 57-70 (2000).
17. Hanahan, D. & Weinberg, R.A. Hallmarks of cancer: the next generation. *Cell* **144**, 646-674 (2011).
18. Slamon, D.J., *et al.* Human breast cancer: correlation of relapse and survival with amplification of the HER-2/neu oncogene. *Science* **235**, 177-182 (1987).
19. Lukashev, M.E. & Werb, Z. ECM signalling: orchestrating cell behaviour and misbehaviour. *Trends Cell Biol* **8**, 437-441 (1998).
20. Fynan, T.M. & Reiss, M. Resistance to inhibition of cell growth by transforming growth factor-beta and its role in oncogenesis. *Crit Rev Oncog* **4**, 493-540 (1993).
21. Shay, J.W., Zou, Y., Hiyama, E. & Wright, W.E. Telomerase and cancer. *Hum Mol Genet* **10**, 677-685 (2001).
22. Hanahan, D. & Folkman, J. Patterns and emerging mechanisms of the angiogenic switch during tumorigenesis. *Cell* **86**, 353-364 (1996).
23. Fuller, B.B., Spaulding, D.T. & Smith, D.R. Regulation of the catalytic activity of preexisting tyrosinase in black and Caucasian human melanocyte cell cultures. *Exp Cell Res* **262**, 197-208 (2001).
24. Sparmann, A. & Bar-Sagi, D. Ras-induced interleukin-8 expression plays a critical role in tumor growth and angiogenesis. *Cancer Cell* **6**, 447-458 (2004).
25. Condeelis, J. & Pollard, J.W. Macrophages: obligate partners for tumor cell migration, invasion, and metastasis. *Cell* **124**, 263-266 (2006).

26. Qian, B.Z. & Pollard, J.W. Macrophage diversity enhances tumor progression and metastasis. *Cell* **141**, 39-51 (2010).
27. DeBerardinis, R.J., Lum, J.J., Hatzivassiliou, G. & Thompson, C.B. The biology of cancer: metabolic reprogramming fuels cell growth and proliferation. *Cell Metab* **7**, 11-20 (2008).
28. Shields, J.D., Kourtis, I.C., Tomei, A.A., Roberts, J.M. & Swartz, M.A. Induction of lymphoidlike stroma and immune escape by tumors that express the chemokine CCL21. *Science* **328**, 749-752 (2010).
29. Onder, T.T., *et al.* Loss of E-cadherin promotes metastasis via multiple downstream transcriptional pathways. *Cancer Res* **68**, 3645-3654 (2008).
30. Alam, M. & Ratner, D. Cutaneous squamous-cell carcinoma. *N Engl J Med* **344**, 975-983 (2001).
31. Fuchs, E. Keratins and the skin. *Annu Rev Cell Dev Biol* **11**, 123-153 (1995).
32. Dupin, E. & Le Douarin, N.M. Development of melanocyte precursors from the vertebrate neural crest. *Oncogene* **22**, 3016-3023 (2003).
33. Raper, H.S. & Wayne, E.J. A quantitative study of the oxidation of phenyl-fatty acids in the animal organism. *Biochem J* **22**, 188-197 (1928).
34. Patel, R.P., Okun, M.R., Edelstein, L.M. & Cariglia, N. Peroxidatic oxidation of tyrosine to melanin in supernatant of crude mouse melanoma homogenates. *Biochem J* **142**, 441-443 (1974).
35. Takeuchi, S., *et al.* Melanin acts as a potent UVB photosensitizer to cause an atypical mode of cell death in murine skin. *Proc Natl Acad Sci U S A* **101**, 15076-15081 (2004).
36. Geschwind, II. Change in hair color in mice induced by injection of alpha-MSH. *Endocrinology* **79**, 1165-1167 (1966).
37. Lu, D., *et al.* Agouti protein is an antagonist of the melanocyte-stimulating-hormone receptor. *Nature* **371**, 799-802 (1994).
38. Blanchard, S.G., *et al.* Agouti antagonism of melanocortin binding and action in the B16F10 murine melanoma cell line. *Biochemistry* **34**, 10406-10411 (1995).
39. Seiberg, M. Keratinocyte-melanocyte interactions during melanosome transfer. *Pigment Cell Res* **14**, 236-242 (2001).
40. Montagna, W. & Carlisle, K. The architecture of black and white facial skin. *J Am Acad Dermatol* **24**, 929-937 (1991).
41. Kobayashi, N., *et al.* Supranuclear melanin caps reduce ultraviolet induced DNA photoproducts in human epidermis. *J Invest Dermatol* **110**, 806-810 (1998).
42. Kipp, C. & Young, A.R. The soluble eumelanin precursor 5,6-dihydroxyindole-2-carboxylic acid enhances oxidative damage in human keratinocyte DNA after UVA irradiation. *Photochem Photobiol* **70**, 191-198 (1999).
43. Kvam, E. & Tyrrell, R.M. The role of melanin in the induction of oxidative DNA base damage by ultraviolet A irradiation of DNA or melanoma cells. *J Invest Dermatol* **113**, 209-213 (1999).
44. Korytowski, W., Pilas, B., Sarna, T. & Kalyanaraman, B. Photoinduced generation of hydrogen peroxide and hydroxyl radicals in melanins. *Photochem Photobiol* **45**, 185-190 (1987).
45. Felix, C.C., Hyde, J.S., Sarna, T. & Sealy, R.C. Melanin photoreactions in aerated media: electron spin resonance evidence for production of superoxide and hydrogen peroxide. *Biochem Biophys Res Commun* **84**, 335-341 (1978).
46. Streutker, C.J., McCready, D., Jimbow, K. & From, L. Malignant melanoma in a patient with oculocutaneous albinism. *J Cutan Med Surg* **4**, 149-152 (2000).
47. Jemal, A., Devesa, S.S., Hartge, P. & Tucker, M.A. Recent trends in cutaneous melanoma incidence among whites in the United States. *J Natl Cancer Inst* **93**, 678-683 (2001).
48. Breslow, A. The surgical treatment of stage I cutaneous melanoma. *Cancer Treat Rev* **5**, 195-198 (1978).

49. Buzzell, R.A. & Zitelli, J.A. Favorable prognostic factors in recurrent and metastatic melanoma. *J Am Acad Dermatol* **34**, 798-803 (1996).
50. Balch, C.M., *et al.* Final version of 2009 AJCC melanoma staging and classification. *J Clin Oncol* **27**, 6199-6206 (2009).
51. Korn, E.L., *et al.* Meta-analysis of phase II cooperative group trials in metastatic stage IV melanoma to determine progression-free and overall survival benchmarks for future phase II trials. *J Clin Oncol* **26**, 527-534 (2008).
52. Davies, H., *et al.* Mutations of the BRAF gene in human cancer. *Nature* **417**, 949-954 (2002).
53. Shinozaki, M., Fujimoto, A., Morton, D.L. & Hoon, D.S. Incidence of BRAF oncogene mutation and clinical relevance for primary cutaneous melanomas. *Clin Cancer Res* **10**, 1753-1757 (2004).
54. Karasarides, M., *et al.* B-RAF is a therapeutic target in melanoma. *Oncogene* **23**, 6292-6298 (2004).
55. Cartlidge, R.A., *et al.* Oncogenic BRAF(V600E) inhibits BIM expression to promote melanoma cell survival. *Pigment Cell Melanoma Res* **21**, 534-544 (2008).
56. Houben, R., *et al.* Constitutive activation of the Ras-Raf signaling pathway in metastatic melanoma is associated with poor prognosis. *J Carcinog* **3**, 6 (2004).
57. Curtin, J.A., *et al.* Distinct sets of genetic alterations in melanoma. *N Engl J Med* **353**, 2135-2147 (2005).
58. Manning, B.D. & Cantley, L.C. AKT/PKB signaling: navigating downstream. *Cell* **129**, 1261-1274 (2007).
59. Wang, C.Y., Guttridge, D.C., Mayo, M.W. & Baldwin, A.S., Jr. NF-kappaB induces expression of the Bcl-2 homologue A1/Bfl-1 to preferentially suppress chemotherapy-induced apoptosis. *Mol Cell Biol* **19**, 5923-5929 (1999).
60. Rajagopalan, H., *et al.* Tumorigenesis: RAF/RAS oncogenes and mismatch-repair status. *Nature* **418**, 934 (2002).
61. Yoshida, H., *et al.* Review: melanocyte migration and survival controlled by SCF/c-kit expression. *J Invest Dermatol* **6**, 1-5 (2001).
62. Curtin, J.A., Busam, K., Pinkel, D. & Bastian, B.C. Somatic activation of KIT in distinct subtypes of melanoma. *J Clin Oncol* **24**, 4340-4346 (2006).
63. Zhuang, D., *et al.* C-MYC overexpression is required for continuous suppression of oncogene-induced senescence in melanoma cells. *Oncogene* **27**, 6623-6634 (2008).
64. Khodadoust, M.S., *et al.* Melanoma proliferation and chemoresistance controlled by the DEK oncogene. *Cancer Res* **69**, 6405-6413 (2009).
65. Soengas, M.S., *et al.* Inactivation of the apoptosis effector Apaf-1 in malignant melanoma. *Nature* **409**, 207-211 (2001).
66. Tsao, H., Zhang, X., Fowlkes, K. & Haluska, F.G. Relative reciprocity of NRAS and PTEN/MMAC1 alterations in cutaneous melanoma cell lines. *Cancer Res* **60**, 1800-1804 (2000).
67. McGill, G.G., *et al.* Bcl2 regulation by the melanocyte master regulator Mitf modulates lineage survival and melanoma cell viability. *Cell* **109**, 707-718 (2002).
68. Irmler, M., *et al.* Inhibition of death receptor signals by cellular FLIP. *Nature* **388**, 190-195 (1997).
69. Takeuchi, H., Morton, D.L., Elashoff, D. & Hoon, D.S. Survivin expression by metastatic melanoma predicts poor disease outcome in patients receiving adjuvant polyvalent vaccine. *Int J Cancer* **117**, 1032-1038 (2005).
70. Zerp, S.F., van Elsas, A., Peltenburg, L.T. & Schrier, P.I. p53 mutations in human cutaneous melanoma correlate with sun exposure but are not always involved in melanomagenesis. *Br J Cancer* **79**, 921-926 (1999).
71. Castellano, M., *et al.* CDKN2A/p16 is inactivated in most melanoma cell lines. *Cancer Res* **57**, 4868-4875 (1997).

72. Quelle, D.E., Cheng, M., Ashmun, R.A. & Sherr, C.J. Cancer-associated mutations at the INK4a locus cancel cell cycle arrest by p16INK4a but not by the alternative reading frame protein p19ARF. *Proc Natl Acad Sci U S A* **94**, 669-673 (1997).
73. Scaini, M.C., *et al.* Functional impairment of p16(INK4A) due to CDKN2A p.Gly23Asp missense mutation. *Mutat Res* **671**, 26-32 (2009).
74. Zhang, Y., Xiong, Y. & Yarbrough, W.G. ARF promotes MDM2 degradation and stabilizes p53: ARF-INK4a locus deletion impairs both the Rb and p53 tumor suppression pathways. *Cell* **92**, 725-734 (1998).
75. Kamijo, T., *et al.* Functional and physical interactions of the ARF tumor suppressor with p53 and Mdm2. *Proc Natl Acad Sci U S A* **95**, 8292-8297 (1998).
76. Yang, G., Rajadurai, A. & Tsao, H. Recurrent patterns of dual RB and p53 pathway inactivation in melanoma. *J Invest Dermatol* **125**, 1242-1251 (2005).
77. Hersey, P. & Zhang, X.D. Adaptation to ER stress as a driver of malignancy and resistance to therapy in human melanoma. *Pigment Cell Melanoma Res* **21**, 358-367 (2008).
78. Atkins, M.B., *et al.* High-dose recombinant interleukin 2 therapy for patients with metastatic melanoma: analysis of 270 patients treated between 1985 and 1993. *J Clin Oncol* **17**, 2105-2116 (1999).
79. Flaherty, K.T., *et al.* Inhibition of mutated, activated BRAF in metastatic melanoma. *N Engl J Med* **363**, 809-819 (2010).
80. Chapman, P.B., *et al.* Improved survival with vemurafenib in melanoma with BRAF V600E mutation. *N Engl J Med* **364**, 2507-2516 (2011).
81. Long, G.V. & Kefford, R. Phase 1/2 Study Of GSK2118436, A Selective Inhibitor Of V600 Mutant (Mut) Braf Kinase: Evidence Of Activity In Melanoma Brain Metastases (Mets). in *Presented at 35th European Society for Medical Oncology ESMO Congress* Vol. 21 Suppl 8 (2010).
82. Hatzivassiliou, G., *et al.* RAF inhibitors prime wild-type RAF to activate the MAPK pathway and enhance growth. *Nature* **464**, 431-435 (2010).
83. Heidorn, S.J., *et al.* Kinase-dead BRAF and oncogenic RAS cooperate to drive tumor progression through CRAF. *Cell* **140**, 209-221 (2010).
84. Paraiso, K.H., *et al.* PTEN loss confers BRAF inhibitor resistance to melanoma cells through the suppression of BIM expression. *Cancer Res* **71**, 2750-2760 (2011).
85. Arkenau, H.T., Kefford, R. & Long, G.V. Targeting BRAF for patients with melanoma. *Br J Cancer* **104**, 392-398 (2011).
86. Guo, J., Si, L. & Kong, Y. A phase II study of imatinib for advanced melanoma patients with KIT aberrations. in *J Clin Oncol.* , Vol. 29:[abstr. 8527] (2010).
87. O'Day, S.J., Hamid, O. & Urba, W.J. Targeting cytotoxic T-lymphocyte antigen-4 (CTLA-4): a novel strategy for the treatment of melanoma and other malignancies. *Cancer* **110**, 2614-2627 (2007).
88. Eggermont, A.M., Testori, A., Maio, M. & Robert, C. Anti-CTLA-4 antibody adjuvant therapy in melanoma. *Semin Oncol* **37**, 455-459 (2010).
89. Brahmer, J.R., *et al.* Phase I study of single-agent anti-programmed death-1 (MDX-1106) in refractory solid tumors: safety, clinical activity, pharmacodynamics, and immunologic correlates. *J Clin Oncol* **28**, 3167-3175 (2010).
90. Molckovsky, A. & Siu, L.L. First-in-class, first-in-human phase I results of targeted agents: highlights of the 2008 American society of clinical oncology meeting. *J Hematol Oncol* **1**, 20 (2008).
91. Eggermont, A.M., *et al.* Adjuvant therapy with pegylated interferon alfa-2b versus observation alone in resected stage III melanoma: final results of EORTC 18991, a randomised phase III trial. *Lancet* **372**, 117-126 (2008).
92. Veronese, F.M. Peptide and protein PEGylation: a review of problems and solutions. *Biomaterials* **22**, 405-417 (2001).

93. Kroemer, G., *et al.* Classification of cell death: recommendations of the Nomenclature Committee on Cell Death 2009. *Cell Death Differ* **16**, 3-11 (2009).
94. Van Cruchten, S. & Van Den Broeck, W. Morphological and biochemical aspects of apoptosis, oncosis and necrosis. *Anat Histol Embryol* **31**, 214-223 (2002).
95. Kroemer, G. & Levine, B. Autophagic cell death: the story of a misnomer. *Nat Rev Mol Cell Biol* **9**, 1004-1010 (2008).
96. Dobos, K.M., Spotts, E.A., Quinn, F.D. & King, C.H. Necrosis of lung epithelial cells during infection with Mycobacterium tuberculosis is preceded by cell permeation. *Infect Immun* **68**, 6300-6310 (2000).
97. Cho, Y.S., *et al.* Phosphorylation-driven assembly of the RIP1-RIP3 complex regulates programmed necrosis and virus-induced inflammation. *Cell* **137**, 1112-1123 (2009).
98. Rello, S., *et al.* Morphological criteria to distinguish cell death induced by apoptotic and necrotic treatments. *Apoptosis* **10**, 201-208 (2005).
99. Trump, B.F., Berezesky, I.K., Chang, S.H. & Phelps, P.C. The pathways of cell death: oncosis, apoptosis, and necrosis. *Toxicol Pathol* **25**, 82-88 (1997).
100. Dumitriu, I.E., *et al.* Release of high mobility group box 1 by dendritic cells controls T cell activation via the receptor for advanced glycation end products. *J Immunol* **174**, 7506-7515 (2005).
101. Park, J.S., *et al.* Involvement of toll-like receptors 2 and 4 in cellular activation by high mobility group box 1 protein. *J Biol Chem* **279**, 7370-7377 (2004).
102. Scaffidi, P., Misteli, T. & Bianchi, M.E. Release of chromatin protein HMGB1 by necrotic cells triggers inflammation. *Nature* **418**, 191-195 (2002).
103. Vercammen, D., Vandenabeele, P., Beyaert, R., Declercq, W. & Fiers, W. Tumour necrosis factor-induced necrosis versus anti-Fas-induced apoptosis in L929 cells. *Cytokine* **9**, 801-808 (1997).
104. Holler, N., *et al.* Fas triggers an alternative, caspase-8-independent cell death pathway using the kinase RIP as effector molecule. *Nat Immunol* **1**, 489-495 (2000).
105. Morgan, M.J., Kim, Y.S. & Liu, Z.G. TNFalpha and reactive oxygen species in necrotic cell death. *Cell Res* **18**, 343-349 (2008).
106. Degterev, A., *et al.* Chemical inhibitor of nonapoptotic cell death with therapeutic potential for ischemic brain injury. *Nat Chem Biol* **1**, 112-119 (2005).
107. Degterev, A., *et al.* Identification of RIP1 kinase as a specific cellular target of necrostatins. *Nat Chem Biol* **4**, 313-321 (2008).
108. Vakkila, J. & Lotze, M.T. Inflammation and necrosis promote tumour growth. *Nat Rev Immunol* **4**, 641-648 (2004).
109. Sunderkotter, C., Steinbrink, K., Goebeler, M., Bhardwaj, R. & Sorg, C. Macrophages and angiogenesis. *J Leukoc Biol* **55**, 410-422 (1994).
110. Parajuli, P. & Singh, S.M. Alteration in IL-1 and arginase activity of tumor-associated macrophages: a role in the promotion of tumor growth. *Cancer Lett* **107**, 249-256 (1996).
111. Rovere-Querini, P., *et al.* HMGB1 is an endogenous immune adjuvant released by necrotic cells. *EMBO Rep* **5**, 825-830 (2004).
112. Degenhardt, K., *et al.* Autophagy promotes tumor cell survival and restricts necrosis, inflammation, and tumorigenesis. *Cancer Cell* **10**, 51-64 (2006).
113. Mizushima, N., *et al.* Dissection of autophagosome formation using Apg5-deficient mouse embryonic stem cells. *J Cell Biol* **152**, 657-668 (2001).
114. Lum, J.J., *et al.* Growth factor regulation of autophagy and cell survival in the absence of apoptosis. *Cell* **120**, 237-248 (2005).
115. Pandey, U.B., *et al.* HDAC6 rescues neurodegeneration and provides an essential link between autophagy and the UPS. *Nature* **447**, 859-863 (2007).
116. Hoyer-Hansen, M., *et al.* Control of macroautophagy by calcium, calmodulin-dependent kinase kinase-beta, and Bcl-2. *Mol Cell* **25**, 193-205 (2007).

117. Ogata, M., *et al.* Autophagy is activated for cell survival after endoplasmic reticulum stress. *Mol Cell Biol* **26**, 9220-9231 (2006).
118. Boya, P., *et al.* Inhibition of macroautophagy triggers apoptosis. *Mol Cell Biol* **25**, 1025-1040 (2005).
119. Kuma, A., *et al.* The role of autophagy during the early neonatal starvation period. *Nature* **432**, 1032-1036 (2004).
120. Mizushima, N., Yamamoto, A., Matsui, M., Yoshimori, T. & Ohsumi, Y. In vivo analysis of autophagy in response to nutrient starvation using transgenic mice expressing a fluorescent autophagosome marker. *Mol Biol Cell* **15**, 1101-1111 (2004).
121. Komatsu, M., *et al.* Impairment of starvation-induced and constitutive autophagy in Atg7-deficient mice. *J Cell Biol* **169**, 425-434 (2005).
122. Galluzzi, L., *et al.* To die or not to die: that is the autophagic question. *Curr Mol Med* **8**, 78-91 (2008).
123. Kegel, K.B., *et al.* Huntingtin expression stimulates endosomal-lysosomal activity, endosome tubulation, and autophagy. *J Neurosci* **20**, 7268-7278 (2000).
124. Tanaka, Y., *et al.* Accumulation of autophagic vacuoles and cardiomyopathy in LAMP-2-deficient mice. *Nature* **406**, 902-906 (2000).
125. Gutierrez, M.G., *et al.* Autophagy is a defense mechanism inhibiting BCG and Mycobacterium tuberculosis survival in infected macrophages. *Cell* **119**, 753-766 (2004).
126. Ling, D., Song, H.J., Garza, D., Neufeld, T.P. & Salvaterra, P.M. Abeta42-induced neurodegeneration via an age-dependent autophagic-lysosomal injury in Drosophila. *PLoS One* **4**, e4201 (2009).
127. Mathew, R., *et al.* Autophagy suppresses tumor progression by limiting chromosomal instability. *Genes Dev* **21**, 1367-1381 (2007).
128. Yu, L., *et al.* Regulation of an ATG7-beclin 1 program of autophagic cell death by caspase-8. *Science* **304**, 1500-1502 (2004).
129. Liang, X.H., *et al.* Induction of autophagy and inhibition of tumorigenesis by beclin 1. *Nature* **402**, 672-676 (1999).
130. Yue, Z., Jin, S., Yang, C., Levine, A.J. & Heintz, N. Beclin 1, an autophagy gene essential for early embryonic development, is a haploinsufficient tumor suppressor. *Proc Natl Acad Sci U S A* **100**, 15077-15082 (2003).
131. Qu, X., *et al.* Promotion of tumorigenesis by heterozygous disruption of the beclin 1 autophagy gene. *J Clin Invest* **112**, 1809-1820 (2003).
132. Aita, V.M., *et al.* Cloning and genomic organization of beclin 1, a candidate tumor suppressor gene on chromosome 17q21. *Genomics* **59**, 59-65 (1999).
133. Liang, X.H., *et al.* Protection against fatal Sindbis virus encephalitis by beclin, a novel Bcl-2-interacting protein. *J Virol* **72**, 8586-8596 (1998).
134. Pattingre, S., *et al.* Bcl-2 antiapoptotic proteins inhibit Beclin 1-dependent autophagy. *Cell* **122**, 927-939 (2005).
135. Ogier-Denis, E., Pattingre, S., El Benna, J. & Codogno, P. Erk1/2-dependent phosphorylation of Galpha-interacting protein stimulates its GTPase accelerating activity and autophagy in human colon cancer cells. *J Biol Chem* **275**, 39090-39095 (2000).
136. Corcelle, E., *et al.* Disruption of autophagy at the maturation step by the carcinogen lindane is associated with the sustained mitogen-activated protein kinase/extracellular signal-regulated kinase activity. *Cancer Res* **66**, 6861-6870 (2006).
137. Paglin, S., *et al.* A novel response of cancer cells to radiation involves autophagy and formation of acidic vesicles. *Cancer Res* **61**, 439-444 (2001).
138. Yao, K.C., *et al.* Molecular response of human glioblastoma multiforme cells to ionizing radiation: cell cycle arrest, modulation of the expression of cyclin-dependent kinase inhibitors, and autophagy. *J Neurosurg* **98**, 378-384 (2003).

139. Ertmer, A., *et al.* The anticancer drug imatinib induces cellular autophagy. *Leukemia* **21**, 936-942 (2007).
140. Takeuchi, H., Kanzawa, T., Kondo, Y. & Kondo, S. Inhibition of platelet-derived growth factor signalling induces autophagy in malignant glioma cells. *Br J Cancer* **90**, 1069-1075 (2004).
141. Rez, G., *et al.* Time course of vinblastine-induced autophagocytosis and changes in the endoplasmic reticulum in murine pancreatic acinar cells: a morphometric and biochemical study. *Eur J Cell Biol* **71**, 341-350 (1996).
142. Bursch, W., *et al.* Active cell death induced by the anti-estrogens tamoxifen and ICI 164 384 in human mammary carcinoma cells (MCF-7) in culture: the role of autophagy. *Carcinogenesis* **17**, 1595-1607 (1996).
143. Amaravadi. in *102nd Annual Meeting of the American Association for Cancer Research* (2011).
144. Kerr, J.F. A histochemical study of hypertrophy and ischaemic injury of rat liver with special reference to changes in lysosomes. *J Pathol Bacteriol* **90**, 419-435 (1965).
145. Kressel, M. & Groscurth, P. Distinction of apoptotic and necrotic cell death by in situ labelling of fragmented DNA. *Cell Tissue Res* **278**, 549-556 (1994).
146. Hengartner, M.O. Apoptosis: corralling the corpses. *Cell* **104**, 325-328 (2001).
147. Walsh, G.M., Sexton, D.W., Blaylock, M.G. & Convery, C.M. Resting and cytokine-stimulated human small airway epithelial cells recognize and engulf apoptotic eosinophils. *Blood* **94**, 2827-2835 (1999).
148. Lauber, K., *et al.* Apoptotic cells induce migration of phagocytes via caspase-3-mediated release of a lipid attraction signal. *Cell* **113**, 717-730 (2003).
149. Nagaosa, K., Shiratsuchi, A. & Nakanishi, Y. Concomitant induction of apoptosis and expression of monocyte chemoattractant protein-1 in cultured rat luteal cells by nuclear factor-kappaB and oxidative stress. *Dev Growth Differ* **45**, 351-359 (2003).
150. Fadok, V.A., *et al.* Exposure of phosphatidylserine on the surface of apoptotic lymphocytes triggers specific recognition and removal by macrophages. *J Immunol* **148**, 2207-2216 (1992).
151. Martin, S.J., *et al.* Early redistribution of plasma membrane phosphatidylserine is a general feature of apoptosis regardless of the initiating stimulus: inhibition by overexpression of Bcl-2 and Abl. *J Exp Med* **182**, 1545-1556 (1995).
152. Arur, S., *et al.* Annexin I is an endogenous ligand that mediates apoptotic cell engulfment. *Dev Cell* **4**, 587-598 (2003).
153. Hoffmann, P.R., *et al.* Phosphatidylserine (PS) induces PS receptor-mediated macropinocytosis and promotes clearance of apoptotic cells. *J Cell Biol* **155**, 649-659 (2001).
154. Askew, D.S., Ashmun, R.A., Simmons, B.C. & Cleveland, J.L. Constitutive c-myc expression in an IL-3-dependent myeloid cell line suppresses cell cycle arrest and accelerates apoptosis. *Oncogene* **6**, 1915-1922 (1991).
155. Dang, C.V. & Lewis, B.C. Role of Oncogenic Transcription Factor c-Myc in Cell Cycle Regulation, Apoptosis and Metabolism. *J Biomed Sci* **4**, 269-278 (1997).
156. Evan, G.I., *et al.* Induction of apoptosis in fibroblasts by c-myc protein. *Cell* **69**, 119-128 (1992).
157. Bissonnette, R.P., Echeverri, F., Mahboubi, A. & Green, D.R. Apoptotic cell death induced by c-myc is inhibited by bcl-2. *Nature* **359**, 552-554 (1992).
158. Strasser, A., Harris, A.W., Bath, M.L. & Cory, S. Novel primitive lymphoid tumours induced in transgenic mice by cooperation between myc and bcl-2. *Nature* **348**, 331-333 (1990).
159. Shi, Y. Mechanisms of caspase activation and inhibition during apoptosis. *Mol Cell* **9**, 459-470 (2002).
160. Enari, M., *et al.* A caspase-activated DNase that degrades DNA during apoptosis, and its inhibitor ICAD. *Nature* **391**, 43-50 (1998).

161. Slee, E.A., Adrain, C. & Martin, S.J. Executioner caspase-3, -6, and -7 perform distinct, non-redundant roles during the demolition phase of apoptosis. *J Biol Chem* **276**, 7320-7326 (2001).
162. Srinivasula, S.M., Ahmad, M., Fernandes-Alnemri, T. & Alnemri, E.S. Autoactivation of procaspase-9 by Apaf-1-mediated oligomerization. *Mol Cell* **1**, 949-957 (1998).
163. Deveraux, Q.L. & Reed, J.C. IAP family proteins--suppressors of apoptosis. *Genes Dev* **13**, 239-252 (1999).
164. Yamamura, K., *et al.* Accelerated disappearance of melanocytes in bcl-2-deficient mice. *Cancer Res* **56**, 3546-3550 (1996).
165. Sax, J.K., *et al.* BID regulation by p53 contributes to chemosensitivity. *Nat Cell Biol* **4**, 842-849 (2002).
166. Selvakumaran, M., *et al.* Immediate early up-regulation of bax expression by p53 but not TGF beta 1: a paradigm for distinct apoptotic pathways. *Oncogene* **9**, 1791-1798 (1994).
167. Cregan, S.P., *et al.* p53 activation domain 1 is essential for PUMA upregulation and p53-mediated neuronal cell death. *The Journal of neuroscience : the official journal of the Society for Neuroscience* **24**, 10003-10012 (2004).
168. Er, E., *et al.* Mitochondria as the target of the pro-apoptotic protein Bax. *Biochim Biophys Acta* **1757**, 1301-1311 (2006).
169. Adrain, C., Creagh, E.M. & Martin, S.J. Apoptosis-associated release of Smac/DIABLO from mitochondria requires active caspases and is blocked by Bcl-2. *Embo J* **20**, 6627-6636 (2001).
170. Yu, X., *et al.* A structure of the human apoptosome at 12.8 A resolution provides insights into this cell death platform. *Structure* **13**, 1725-1735 (2005).
171. Yoshida, H., *et al.* Apaf1 is required for mitochondrial pathways of apoptosis and brain development. *Cell* **94**, 739-750 (1998).
172. Cecconi, F., Alvarez-Bolado, G., Meyer, B.I., Roth, K.A. & Gruss, P. Apaf1 (CED-4 homolog) regulates programmed cell death in mammalian development. *Cell* **94**, 727-737 (1998).
173. Marsden, V.S., *et al.* Apoptosis initiated by Bcl-2-regulated caspase activation independently of the cytochrome c/Apaf-1/caspase-9 apoptosome. *Nature* **419**, 634-637 (2002).
174. Honarpour, N., Gilbert, S.L., Lahn, B.T., Wang, X. & Herz, J. Apaf-1 deficiency and neural tube closure defects are found in fog mice. *Proc Natl Acad Sci U S A* **98**, 9683-9687 (2001).
175. Du, C., Fang, M., Li, Y., Li, L. & Wang, X. Smac, a mitochondrial protein that promotes cytochrome c-dependent caspase activation by eliminating IAP inhibition. *Cell* **102**, 33-42 (2000).
176. Verhagen, A.M., *et al.* Identification of DIABLO, a mammalian protein that promotes apoptosis by binding to and antagonizing IAP proteins. *Cell* **102**, 43-53 (2000).
177. Rampino, N., *et al.* Somatic frameshift mutations in the BAX gene in colon cancers of the microsatellite mutator phenotype. *Science* **275**, 967-969 (1997).
178. Itoh, N. & Nagata, S. A novel protein domain required for apoptosis. Mutational analysis of human Fas antigen. *J Biol Chem* **268**, 10932-10937 (1993).
179. Chinnaiyan, A.M., O'Rourke, K., Tewari, M. & Dixit, V.M. FADD, a novel death domain-containing protein, interacts with the death domain of Fas and initiates apoptosis. *Cell* **81**, 505-512 (1995).
180. Park, A. & Baichwal, V.R. Systematic mutational analysis of the death domain of the tumor necrosis factor receptor 1-associated protein TRADD. *J Biol Chem* **271**, 9858-9862 (1996).
181. Fanzo, J.C., *et al.* CD95 rapidly clusters in cells of diverse origins. *Cancer Biol Ther* **2**, 392-395 (2003).

182. Wang, L., *et al.* The Fas-FADD death domain complex structure reveals the basis of DISC assembly and disease mutations. *Nat Struct Mol Biol* **17**, 1324-1329 (2010).
183. Kischkel, F.C., *et al.* Cytotoxicity-dependent APO-1 (Fas/CD95)-associated proteins form a death-inducing signaling complex (DISC) with the receptor. *Embo J* **14**, 5579-5588 (1995).
184. Kataoka, T., *et al.* The caspase-8 inhibitor FLIP promotes activation of NF-kappaB and Erk signaling pathways. *Curr Biol* **10**, 640-648 (2000).
185. Stanger, B.Z., Leder, P., Lee, T.H., Kim, E. & Seed, B. RIP: a novel protein containing a death domain that interacts with Fas/APO-1 (CD95) in yeast and causes cell death. *Cell* **81**, 513-523 (1995).
186. Harper, N., Hughes, M., MacFarlane, M. & Cohen, G.M. Fas-associated death domain protein and caspase-8 are not recruited to the tumor necrosis factor receptor 1 signaling complex during tumor necrosis factor-induced apoptosis. *J Biol Chem* **278**, 25534-25541 (2003).
187. Jackson-Bernitsas, D.G., *et al.* Evidence that TNF-TNFR1-TRADD-TRAF2-RIP-TAK1-IKK pathway mediates constitutive NF-kappaB activation and proliferation in human head and neck squamous cell carcinoma. *Oncogene* **26**, 1385-1397 (2007).
188. Micheau, O. & Tschopp, J. Induction of TNF receptor I-mediated apoptosis via two sequential signaling complexes. *Cell* **114**, 181-190 (2003).
189. Legler, D.F., Micheau, O., Doucey, M.A., Tschopp, J. & Bron, C. Recruitment of TNF receptor 1 to lipid rafts is essential for TNFalpha-mediated NF-kappaB activation. *Immunity* **18**, 655-664 (2003).
190. Krueger, A., Schmitz, I., Baumann, S., Krammer, P.H. & Kirchhoff, S. Cellular FLICE-inhibitory protein splice variants inhibit different steps of caspase-8 activation at the CD95 death-inducing signaling complex. *J Biol Chem* **276**, 20633-20640 (2001).
191. Strasser, A., Jost, P.J. & Nagata, S. The many roles of FAS receptor signaling in the immune system. *Immunity* **30**, 180-192 (2009).
192. Scaffidi, C., *et al.* Two CD95 (APO-1/Fas) signaling pathways. *Embo J* **17**, 1675-1687 (1998).
193. Ward, M.W., *et al.* Real time single cell analysis of Bid cleavage and Bid translocation during caspase-dependent and neuronal caspase-independent apoptosis. *J Biol Chem* **281**, 5837-5844 (2006).
194. Roucou, X., Montessuit, S., Antonsson, B. & Martinou, J.C. Bax oligomerization in mitochondrial membranes requires tBid (caspase-8-cleaved Bid) and a mitochondrial protein. *Biochem J* **368**, 915-921 (2002).
195. Kaufmann, T., *et al.* Fatal hepatitis mediated by tumor necrosis factor TNFalpha requires caspase-8 and involves the BH3-only proteins Bid and Bim. *Immunity* **30**, 56-66 (2009).
196. Yin, X.M., *et al.* Bid-deficient mice are resistant to Fas-induced hepatocellular apoptosis. *Nature* **400**, 886-891 (1999).
197. Kaufmann, T., *et al.* The BH3-only protein bid is dispensable for DNA damage- and replicative stress-induced apoptosis or cell-cycle arrest. *Cell* **129**, 423-433 (2007).
198. Debatin, K.M., Stahnke, K. & Fulda, S. Apoptosis in hematological disorders. *Semin Cancer Biol* **13**, 149-158 (2003).
199. Pitti, R.M., *et al.* Genomic amplification of a decoy receptor for Fas ligand in lung and colon cancer. *Nature* **396**, 699-703 (1998).
200. Gliniak, B. & Le, T. Tumor necrosis factor-related apoptosis-inducing ligand's antitumor activity in vivo is enhanced by the chemotherapeutic agent CPT-11. *Cancer Res* **59**, 6153-6158 (1999).

201. Shalin, S.C., Hernandez, C.M., Dougherty, M.K., Morrison, D.K. & Sweatt, J.D. Kinase suppressor of Ras1 compartmentalizes hippocampal signal transduction and subserves synaptic plasticity and memory formation. *Neuron* **50**, 765-779 (2006).
202. Yu, W., Fantl, W.J., Harrowe, G. & Williams, L.T. Regulation of the MAP kinase pathway by mammalian Ksr through direct interaction with MEK and ERK. *Curr Biol* **8**, 56-64 (1998).
203. Kornfeld, K., Hom, D.B. & Horvitz, H.R. The ksr-1 gene encodes a novel protein kinase involved in Ras-mediated signaling in C. elegans. *Cell* **83**, 903-913 (1995).
204. Calipel, A., *et al.* Mutation of B-Raf in human choroidal melanoma cells mediates cell proliferation and transformation through the MEK/ERK pathway. *J Biol Chem* **278**, 42409-42418 (2003).
205. Govindarajan, B., *et al.* Malignant transformation of melanocytes to melanoma by constitutive activation of mitogen-activated protein kinase kinase (MAPKK) signaling. *J Biol Chem* **278**, 9790-9795 (2003).
206. Sheridan, C., Brumatti, G. & Martin, S.J. Oncogenic B-RafV600E inhibits apoptosis and promotes ERK-dependent inactivation of Bad and Bim. *J Biol Chem* **283**, 22128-22135 (2008).
207. Schmelzle, T., *et al.* Functional role and oncogene-regulated expression of the BH3-only factor Bmf in mammary epithelial anoikis and morphogenesis. *PNAS* **104**, 3787-3792 (2007).
208. Allan, L.A., *et al.* Inhibition of caspase-9 through phosphorylation at Thr 125 by ERK MAPK. *Nat Cell Biol* **5**, 647-654 (2003).
209. Lavoie, J.N., L'Allemain, G., Brunet, A., Muller, R. & Pouyssegur, J. Cyclin D1 expression is regulated positively by the p42/p44MAPK and negatively by the p38/HOGMAPK pathway. *J Biol Chem* **271**, 20608-20616 (1996).
210. Reszka, A.A., Seger, R., Diltz, C.D., Krebs, E.G. & Fischer, E.H. Association of mitogen-activated protein kinase with the microtubule cytoskeleton. *Proc Natl Acad Sci U S A* **92**, 8881-8885 (1995).
211. Tsuruta, F., *et al.* JNK promotes Bax translocation to mitochondria through phosphorylation of 14-3-3 proteins. *Embo J* **23**, 1889-1899 (2004).
212. Mehta, P.B., *et al.* MEK5 overexpression is associated with metastatic prostate cancer, and stimulates proliferation, MMP-9 expression and invasion. *Oncogene* **22**, 1381-1389 (2003).
213. Drew, B.A., Burow, M.E. & Beckman, B.S. MEK5/ERK5 pathway: The first fifteen years. *Biochimica et biophysica acta* **1825**, 37-48 (2012).
214. Staal, S.P., Hartley, J.W. & Rowe, W.P. Isolation of transforming murine leukemia viruses from mice with a high incidence of spontaneous lymphoma. *Proc Natl Acad Sci U S A* **74**, 3065-3067 (1977).
215. Chen, W.S., *et al.* Growth retardation and increased apoptosis in mice with homozygous disruption of the Akt1 gene. *Genes Dev* **15**, 2203-2208 (2001).
216. Cho, H., *et al.* Insulin resistance and a diabetes mellitus-like syndrome in mice lacking the protein kinase Akt2 (PKB beta). *Science* **292**, 1728-1731 (2001).
217. Peng, X.D., *et al.* Dwarfism, impaired skin development, skeletal muscle atrophy, delayed bone development, and impeded adipogenesis in mice lacking Akt1 and Akt2. *Genes Dev* **17**, 1352-1365 (2003).
218. Jones, R.G., *et al.* Protein kinase B regulates T lymphocyte survival, nuclear factor kappaB activation, and Bcl-X(L) levels in vivo. *J Exp Med* **191**, 1721-1734 (2000).
219. Franke, T.F., Kaplan, D.R., Cantley, L.C. & Toker, A. Direct regulation of the Akt proto-oncogene product by phosphatidylinositol-3,4-bisphosphate. *Science* **275**, 665-668 (1997).
220. Alessi, D.R., *et al.* Mechanism of activation of protein kinase B by insulin and IGF-1. *Embo J* **15**, 6541-6551 (1996).

221. Maehama, T. & Dixon, J.E. The tumor suppressor, PTEN/MMAC1, dephosphorylates the lipid second messenger, phosphatidylinositol 3,4,5-trisphosphate. *J Biol Chem* **273**, 13375-13378 (1998).
222. Diehl, J.A., Cheng, M., Roussel, M.F. & Sherr, C.J. Glycogen synthase kinase-3beta regulates cyclin D1 proteolysis and subcellular localization. *Genes Dev* **12**, 3499-3511 (1998).
223. Qi, X.J., Wildey, G.M. & Howe, P.H. Evidence that Ser87 of BimEL is phosphorylated by Akt and regulates BimEL apoptotic function. *J Biol Chem* **281**, 813-823 (2006).
224. Reginato, M.J., *et al.* Integrins and EGFR coordinately regulate the pro-apoptotic protein Bim to prevent anoikis. *Nat Cell Biol* **5**, 733-740 (2003).
225. Dijkers, P.F., Medema, R.H., Lammers, J.W., Koenderman, L. & Coffer, P.J. Expression of the pro-apoptotic Bcl-2 family member Bim is regulated by the forkhead transcription factor FKHR-L1. *Curr Biol* **10**, 1201-1204 (2000).
226. Tran, H., Brunet, A., Griffith, E.C. & Greenberg, M.E. The many forks in FOXO's road. *Sci STKE* **2003**, RE5 (2003).
227. Zha, J., Harada, H., Yang, E., Jockel, J. & Korsmeyer, S.J. Serine phosphorylation of death agonist BAD in response to survival factor results in binding to 14-3-3 not BCL-X(L). *Cell* **87**, 619-628 (1996).
228. Hyun, T., *et al.* Loss of PTEN expression leading to high Akt activation in human multiple myelomas. *Blood* **96**, 3560-3568 (2000).
229. Coffer, P.J. & Woodgett, J.R. Molecular cloning and characterisation of a novel putative protein-serine kinase related to the cAMP-dependent and protein kinase C families. *Eur J Biochem* **205**, 1217 (1992).
230. Sen, R. & Baltimore, D. Multiple nuclear factors interact with the immunoglobulin enhancer sequences. *Cell* **46**, 705-716 (1986).
231. Rayet, B. & Gelinas, C. Aberrant rel/nfkb genes and activity in human cancer. *Oncogene* **18**, 6938-6947 (1999).
232. Ravi, R., *et al.* Regulation of death receptor expression and TRAIL/Apo2L-induced apoptosis by NF-kappaB. *Nat Cell Biol* **3**, 409-416 (2001).
233. Chan, H., Bartos, D.P. & Owen-Schaub, L.B. Activation-dependent transcriptional regulation of the human Fas promoter requires NF-kappaB p50-p65 recruitment. *Mol Cell Biol* **19**, 2098-2108 (1999).
234. Bernard, D., Quatannens, B., Vandenbunder, B. & Abbadie, C. Rel/NF-kappaB transcription factors protect against tumor necrosis factor (TNF)-related apoptosis-inducing ligand (TRAIL)-induced apoptosis by up-regulating the TRAIL decoy receptor DcR1. *J Biol Chem* **276**, 27322-27328 (2001).
235. Zong, W.X., Edelstein, L.C., Chen, C., Bash, J. & Gelinas, C. The prosurvival Bcl-2 homolog Bfl-1/A1 is a direct transcriptional target of NF-kappaB that blocks TNFalpha-induced apoptosis. *Genes Dev* **13**, 382-387 (1999).
236. Rangamani, P. & Sirovich, L. Survival and apoptotic pathways initiated by TNF-alpha: modeling and predictions. *Biotechnol Bioeng* **97**, 1216-1229 (2007).
237. Singh, R.K., Varney, M.L., Bucana, C.D. & Johansson, S.L. Expression of interleukin-8 in primary and metastatic malignant melanoma of the skin. *Melanoma Res* **9**, 383-387 (1999).
238. Richmond, A., Lawson, D.H., Nixon, D.W. & Chawla, R.K. Characterization of autostimulatory and transforming growth factors from human melanoma cells. *Cancer Res* **45**, 6390-6394 (1985).
239. Haussler, U., von Wichert, G., Schmid, R.M., Keller, F. & Schneider, G. Epidermal growth factor activates nuclear factor-kappaB in human proximal tubule cells. *Am J Physiol Renal Physiol* **289**, F808-815 (2005).
240. Grilli, M., Chiu, J.J. & Lenardo, M.J. NF-kappa B and Rel: participants in a multiform transcriptional regulatory system. *Int Rev Cytol* **143**, 1-62 (1993).

241. Kopp, E.B. & Ghosh, S. NF-kappa B and rel proteins in innate immunity. *Adv Immunol* **58**, 1-27 (1995).
242. Lin, L. & Ghosh, S. A glycine-rich region in NF-kappaB p105 functions as a processing signal for the generation of the p50 subunit. *Mol Cell Biol* **16**, 2248-2254 (1996).
243. Palombella, V.J., Rando, O.J., Goldberg, A.L. & Maniatis, T. The ubiquitin-proteasome pathway is required for processing the NF-kappa B1 precursor protein and the activation of NF-kappa B. *Cell* **78**, 773-785 (1994).
244. Brown, A.M., *et al.* Function of NF-kappa B/Rel binding sites in the major histocompatibility complex class II invariant chain promoter is dependent on cell-specific binding of different NF-kappa B/Rel subunits. *Mol Cell Biol* **14**, 2926-2935 (1994).
245. Grundstrom, S., Anderson, P., Scheipers, P. & Sundstedt, A. Bcl-3 and NFkappaB p50-p50 homodimers act as transcriptional repressors in tolerant CD4+ T cells. *J Biol Chem* **279**, 8460-8468 (2004).
246. Baeuerle, P.A. & Baltimore, D. A 65-kappaD subunit of active NF-kappaB is required for inhibition of NF-kappaB by I kappaB. *Genes Dev* **3**, 1689-1698 (1989).
247. Zandi, E., Rothwarf, D.M., Delhase, M., Hayakawa, M. & Karin, M. The IkappaB kinase complex (IKK) contains two kinase subunits, IKKalpha and IKKbeta, necessary for IkappaB phosphorylation and NF-kappaB activation. *Cell* **91**, 243-252 (1997).
248. Brown, K., Park, S., Kanno, T., Franzoso, G. & Siebenlist, U. Mutual regulation of the transcriptional activator NF-kappa B and its inhibitor, I kappa B-alpha. *Proc Natl Acad Sci U S A* **90**, 2532-2536 (1993).
249. Yamaoka, S., *et al.* Complementation cloning of NEMO, a component of the IkappaB kinase complex essential for NF-kappaB activation. *Cell* **93**, 1231-1240 (1998).
250. Nolan, G.P., Ghosh, S., Liou, H.C., Tempst, P. & Baltimore, D. DNA binding and I kappa B inhibition of the cloned p65 subunit of NF-kappa B, a rel-related polypeptide. *Cell* **64**, 961-969 (1991).
251. Ling, L., Cao, Z. & Goeddel, D.V. NF-kappaB-inducing kinase activates IKK-alpha by phosphorylation of Ser-176. *Proc Natl Acad Sci U S A* **95**, 3792-3797 (1998).
252. Homig-Holzel, C., *et al.* Constitutive CD40 signaling in B cells selectively activates the noncanonical NF-kappaB pathway and promotes lymphomagenesis. *The Journal of experimental medicine* **205**, 1317-1329 (2008).
253. Gu, L., Zhu, N., Findley, H.W., Woods, W.G. & Zhou, M. Identification and characterization of the IKKalpha promoter: positive and negative regulation by ETS-1 and p53, respectively. *J Biol Chem* **279**, 52141-52149 (2004).
254. Becker, T.M., *et al.* Impaired inhibition of NF-kappaB activity by melanoma-associated p16INK4a mutations. *Biochem Biophys Res Commun* **332**, 873-879 (2005).
255. Castelli, C., *et al.* Expression of interleukin 1 alpha, interleukin 6, and tumor necrosis factor alpha genes in human melanoma clones is associated with that of mutated N-RAS oncogene. *Cancer Res* **54**, 4785-4790 (1994).
256. Koul, D., Yao, Y., Abbruzzese, J.L., Yung, W.K. & Reddy, S.A. Tumor suppressor MMAC/PTEN inhibits cytokine-induced NFkappaB activation without interfering with the IkappaB degradation pathway. *J Biol Chem* **276**, 11402-11408 (2001).
257. Tsujimoto, Y. & Croce, C.M. Molecular cloning of a human immunoglobulin lambda chain variable sequence. *Nucleic Acids Res* **12**, 8407-8414 (1984).
258. Vaux, D.L., Cory, S. & Adams, J.M. Bcl-2 gene promotes haemopoietic cell survival and cooperates with c-myc to immortalize pre-B cells. *Nature* **335**, 440-442 (1988).

259. McDonnell, T.J., *et al.* bcl-2-immunoglobulin transgenic mice demonstrate extended B cell survival and follicular lymphoproliferation. *Cell* **57**, 79-88 (1989).
260. Chen, L., *et al.* Differential targeting of prosurvival Bcl-2 proteins by their BH3-only ligands allows complementary apoptotic function. *Mol Cell* **17**, 393-403 (2005).
261. Opferman, J.T., *et al.* Development and maintenance of B and T lymphocytes requires antiapoptotic MCL-1. *Nature* **426**, 671-676 (2003).
262. Certo, M., *et al.* Mitochondria primed by death signals determine cellular addiction to antiapoptotic BCL-2 family members. *Cancer Cell* **9**, 351-365 (2006).
263. Leo, C.P., Hsu, S.Y., Chun, S.Y., Bae, H.W. & Hsueh, A.J. Characterization of the antiapoptotic Bcl-2 family member myeloid cell leukemia-1 (Mcl-1) and the stimulation of its message by gonadotropins in the rat ovary. *Endocrinology* **140**, 5469-5477 (1999).
264. Willis, S.N., *et al.* Apoptosis initiated when BH3 ligands engage multiple Bcl-2 homologs, not Bax or Bak. *Science* **315**, 856-859 (2007).
265. Uren, R.T., *et al.* Mitochondrial permeabilization relies on BH3 ligands engaging multiple prosurvival Bcl-2 relatives, not Bak. *J Cell Biol* **177**, 277-287 (2007).
266. Letai, A., *et al.* Distinct BH3 domains either sensitize or activate mitochondrial apoptosis, serving as prototype cancer therapeutics. *Cancer Cell* **2**, 183-192 (2002).
267. Wei, M.C., *et al.* tBID, a membrane-targeted death ligand, oligomerizes BAK to release cytochrome c. *Genes Dev* **14**, 2060-2071 (2000).
268. Lindsten, T., *et al.* The combined functions of proapoptotic Bcl-2 family members bak and bax are essential for normal development of multiple tissues. *Mol Cell* **6**, 1389-1399 (2000).
269. Willis, S.N., *et al.* Proapoptotic Bak is sequestered by Mcl-1 and Bcl-xL, but not Bcl-2, until displaced by BH3-only proteins. *Genes Dev* **19**, 1294-1305 (2005).
270. Cartron, P.F., *et al.* The first alpha helix of Bax plays a necessary role in its ligand-induced activation by the BH3-only proteins Bid and PUMA. *Mol Cell* **16**, 807-818 (2004).
271. Jabbour, A.M., *et al.* Puma indirectly activates Bax to cause apoptosis in the absence of Bid or Bim. *Cell Death Differ* **16**, 555-563 (2009).
272. Du, H., *et al.* BH3 domains other than Bim and Bid can directly activate Bax/Bak. *J Biol Chem* **286**, 491-501 (2011).
273. Chipuk, J.E., Maurer, U., Green, D.R. & Schuler, M. Pharmacologic activation of p53 elicits Bax-dependent apoptosis in the absence of transcription. *Cancer Cell* **4**, 371-381 (2003).
274. Chipuk, J.E., *et al.* Direct activation of Bax by p53 mediates mitochondrial membrane permeabilization and apoptosis. *Science* **303**, 1010-1014 (2004).
275. Leber, B., Lin, J. & Andrews, D.W. Embedded together: the life and death consequences of interaction of the Bcl-2 family with membranes. *Apoptosis* **12**, 897-911 (2007).
276. Leber, B., Lin, J. & Andrews, D.W. Still embedded together binding to membranes regulates Bcl-2 protein interactions. *Oncogene* **29**, 5221-5230 (2010).
277. Bogner, C., Leber, B. & Andrews, D.W. Apoptosis: embedded in membranes. *Curr Opin Cell Biol* **22**, 845-851 (2010).
278. Chittenden, T., *et al.* A conserved domain in Bak, distinct from BH1 and BH2, mediates cell death and protein binding functions. *Embo J* **14**, 5589-5596 (1995).
279. Aouacheria, A., Brunet, F. & Gouy, M. Phylogenomics of life-or-death switches in multicellular animals: Bcl-2, BH3-only, and BNip families of apoptotic regulators. *Molecular Biology and Evolution* **22**, 2395-2416 (2005).
280. McDonnell, J.M., Fushman, D., Milliman, C.L., Korsmeyer, S.J. & Cowburn, D. Solution structure of the proapoptotic molecule BID: a structural basis for apoptotic agonists and antagonists. *Cell* **96**, 625-634 (1999).

281. Bouillet, P., *et al.* Proapoptotic Bcl-2 relative Bim required for certain apoptotic responses, leukocyte homeostasis, and to preclude autoimmunity. *Science* **286**, 1735-1738 (1999).
282. Villunger, A., *et al.* p53- and drug-induced apoptotic responses mediated by BH3-only proteins puma and noxa. *Science* **302**, 1036-1038 (2003).
283. Oda, E., *et al.* Nora, a BH3-only member of the Bcl-2 family and candidate mediator of p53-induced apoptosis. *Science* **288**, 1053-1058 (2000).
284. Nakano, K. & Vousden, K.H. PUMA, a novel proapoptotic gene, is induced by p53. *Molecular Cell* **7**, 683-694 (2001).
285. Kim, J.Y., Ahn, H.J., Ryu, J.H., Suk, K. & Park, J.H. BH3-only protein Noxa is a mediator of hypoxic cell death induced by hypoxia-inducible factor 1alpha. *J Exp Med* **199**, 113-124 (2004).
286. Jeffers, J.R., *et al.* Puma is an essential mediator of p53-dependent and -independent apoptotic pathways. *Cancer Cell* **4**, 321-328 (2003).
287. Dijkers, P.F., Medema, R.H., Lammers, J.W.J., Koenderman, L. & Coffer, P.J. Expression of the pro-apoptotic Bcl-2 family member Bim is regulated by the forkhead transcription factor FKHR-L1. *Current Biology* **10**, 1201-1204 (2000).
288. Puthalakath, H., *et al.* ER stress triggers apoptosis by activating BH3-only protein Bim. *Cell* **129**, 1337-1349 (2007).
289. Puthalakath, H., Huang, D.C., O'Reilly, L.A., King, S.M. & Strasser, A. The proapoptotic activity of the Bcl-2 family member Bim is regulated by interaction with the dynein motor complex. *Mol Cell* **3**, 287-296 (1999).
290. Luciano, F., *et al.* Phosphorylation of Bim-EL by Erk1/2 on serine 69 promotes its degradation via the proteasome pathway and regulates its proapoptotic function. *Oncogene* **22**, 6785-6793 (2003).
291. Puthalakath, H., *et al.* Bmf: a proapoptotic BH3-only protein regulated by interaction with the myosin V actin motor complex, activated by anoikis. *Science* **293**, 1829-1832 (2001).
292. Tan, Y., Ruan, H., Demeter, M.R. & Comb, M.J. p90(RSK) blocks bad-mediated cell death via a protein kinase C-dependent pathway. *The Journal of biological chemistry* **274**, 34859-34867 (1999).
293. del Peso, L., Gonzalez-Garcia, M., Page, C., Herrera, R. & Nunez, G. Interleukin-3-induced phosphorylation of BAD through the protein kinase Akt. *Science* **278**, 687-689 (1997).
294. Tan, Y., Demeter, M.R., Ruan, H. & Comb, M.J. BAD Ser-155 phosphorylation regulates BAD/Bcl-XL interaction and cell survival. *The Journal of biological chemistry* **275**, 25865-25869 (2000).
295. Li, H., Zhu, H., Xu, C.J. & Yuan, J. Cleavage of BID by caspase 8 mediates the mitochondrial damage in the Fas pathway of apoptosis. *Cell* **94**, 491-501 (1998).
296. Chen, M., *et al.* Bid is cleaved by calpain to an active fragment in vitro and during myocardial ischemia/reperfusion. *J Biol Chem* **276**, 30724-30728 (2001).
297. Stoka, V., *et al.* Lysosomal protease pathways to apoptosis. Cleavage of bid, not pro-caspases, is the most likely route. *J Biol Chem* **276**, 3149-3157 (2001).
298. Mathai, J.P., Germain, M., Marcellus, R.C. & Shore, G.C. Induction and endoplasmic reticulum location of BIK/NBK in response to apoptotic signaling by E1A and p53. *Oncogene* **21**, 2534-2544 (2002).
299. Karst, A.M., Dai, D.L., Martinka, M. & Li, G. PUMA expression is significantly reduced in human cutaneous melanomas. *Oncogene* **24**, 1111-1116 (2005).
300. Hemann, M.T., *et al.* Suppression of tumorigenesis by the p53 target PUMA. *Proc Natl Acad Sci U S A* **101**, 9333-9338 (2004).
301. Qin, J.Z., *et al.* Proteasome inhibitors trigger NOXA-mediated apoptosis in melanoma and myeloma cells. *Cancer Res* **65**, 6282-6293 (2005).

302. Mandic, A., *et al.* Calpain-mediated Bid cleavage and calpain-independent Bak modulation: two separate pathways in cisplatin-induced apoptosis. *Mol Cell Biol* **22**, 3003-3013 (2002).
303. Krajewska, M., *et al.* Expression of Bcl-2 family member Bid in normal and malignant tissues. *Neoplasia* **4**, 129-140 (2002).
304. Tan, T.T., *et al.* Key roles of BIM-driven apoptosis in epithelial tumors and rational chemotherapy. *Cancer Cell* **7**, 227-238 (2005).
305. Zhang, X.D., Wu, J.J., Gillespie, S., Borrow, J. & Hersey, P. Human melanoma cells selected for resistance to apoptosis by prolonged exposure to tumor necrosis factor-related apoptosis-inducing ligand are more vulnerable to necrotic cell death induced by cisplatin. *Clin Cancer Res* **12**, 1355-1364 (2006).
306. Eisenmann, K.M., VanBrocklin, M.W., Staffend, N.A., Kitchen, S.M. & Koo, H.M. Mitogen-activated protein kinase pathway-dependent tumor-specific survival signaling in melanoma cells through inactivation of the proapoptotic protein bad. *Cancer Res* **63**, 8330-8337 (2003).
307. Wang, H.T., Choi, B. & Tang, M.S. Melanocytes are deficient in repair of oxidative DNA damage and UV-induced photoproducts. *Proc Natl Acad Sci U S A* **107**, 12180-12185 (2010).
308. Oppermann, M., *et al.* Caspase-independent induction of apoptosis in human melanoma cells by the proapoptotic Bcl-2-related protein Nbk / Bik. *Oncogene* **24**, 7369-7380 (2005).
309. Chauhan, D., *et al.* A novel Bcl-2/Bcl-X(L)/Bcl-w inhibitor ABT-737 as therapy in multiple myeloma. *Oncogene* **26**, 2374-2380 (2007).
310. Petros, A.M., *et al.* Solution structure of the antiapoptotic protein bcl-2. *Proc Natl Acad Sci U S A* **98**, 3012-3017 (2001).
311. Muchmore, S.W., *et al.* X-ray and NMR structure of human Bcl-xL, an inhibitor of programmed cell death. *Nature* **381**, 335-341 (1996).
312. Denisov, A.Y., *et al.* Solution structure of human BCL-w: modulation of ligand binding by the C-terminal helix. *J Biol Chem* **278**, 21124-21128 (2003).
313. Sattler, M., *et al.* Structure of Bcl-xL-Bak peptide complex: recognition between regulators of apoptosis. *Science* **275**, 983-986 (1997).
314. Wang, K., Gross, A., Waksman, G. & Korsmeyer, S.J. Mutagenesis of the BH3 domain of BAX identifies residues critical for dimerization and killing. *Mol Cell Biol* **18**, 6083-6089 (1998).
315. Fletcher, J.I., *et al.* Apoptosis is triggered when prosurvival Bcl-2 proteins cannot restrain Bax. *Proc Natl Acad Sci U S A* **105**, 18081-18087 (2008).
316. Day, C.L., *et al.* Solution structure of prosurvival Mcl-1 and characterization of its binding by proapoptotic BH3-only ligands. *J Biol Chem* **280**, 4738-4744 (2005).
317. Minn, A.J., *et al.* Bcl-x(L) forms an ion channel in synthetic lipid membranes. *Nature* **385**, 353-357 (1997).
318. Schendel, S.L., *et al.* Channel formation by antiapoptotic protein Bcl-2. *Proc Natl Acad Sci U S A* **94**, 5113-5118 (1997).
319. Maiuri, M.C., *et al.* Functional and physical interaction between Bcl-X(L) and a BH3-like domain in Beclin-1. *Embo J* **26**, 2527-2539 (2007).
320. Rinkenberger, J.L., Horning, S., Klocke, B., Roth, K. & Korsmeyer, S.J. Mcl-1 deficiency results in peri-implantation embryonic lethality. *Genes Dev* **14**, 23-27 (2000).
321. Wagner, K.U., *et al.* Conditional deletion of the Bcl-x gene from erythroid cells results in hemolytic anemia and profound splenomegaly. *Development* **127**, 4949-4958 (2000).
322. Kamada, S., *et al.* bcl-2 deficiency in mice leads to pleiotropic abnormalities: accelerated lymphoid cell death in thymus and spleen, polycystic kidney, hair hypopigmentation, and distorted small intestine. *Cancer Res* **55**, 354-359 (1995).

323. Russell, L.D., *et al.* Spermatogenesis in Bclw-deficient mice. *Biol Reprod* **65**, 318-332 (2001).
324. Hamasaki, A., *et al.* Accelerated neutrophil apoptosis in mice lacking A1-a, a subtype of the bcl-2-related A1 gene. *J Exp Med* **188**, 1985-1992 (1998).
325. Catz, S.D. & Johnson, J.L. Transcriptional regulation of bcl-2 by nuclear factor kappa B and its significance in prostate cancer. *Oncogene* **20**, 7342-7351 (2001).
326. Chen, C., Edelstein, L.C. & Gelinas, C. The Rel/NF-kappaB family directly activates expression of the apoptosis inhibitor Bcl-x(L). *Mol Cell Biol* **20**, 2687-2695 (2000).
327. Pidgeon, G.P., Barr, M.P., Harmey, J.H., Foley, D.A. & Bouchier-Hayes, D.J. Vascular endothelial growth factor (VEGF) upregulates BCL-2 and inhibits apoptosis in human and murine mammary adenocarcinoma cells. *Br J Cancer* **85**, 273-278 (2001).
328. Pike, C.J. Estrogen modulates neuronal Bcl-xL expression and beta-amyloid-induced apoptosis: relevance to Alzheimer's disease. *J Neurochem* **72**, 1552-1563 (1999).
329. Puthier, D., *et al.* Mcl-1 and Bcl-xL are co-regulated by IL-6 in human myeloma cells. *Br J Haematol* **107**, 392-395 (1999).
330. Miyashita, T., *et al.* Tumor suppressor p53 is a regulator of bcl-2 and bax gene expression in vitro and in vivo. *Oncogene* **9**, 1799-1805 (1994).
331. Wu, Y., Mehew, J.W., Heckman, C.A., Arcinas, M. & Boxer, L.M. Negative regulation of bcl-2 expression by p53 in hematopoietic cells. *Oncogene* **20**, 240-251 (2001).
332. van Delft, M.F., *et al.* The BH3 mimetic ABT-737 targets selective Bcl-2 proteins and efficiently induces apoptosis via Bak/Bax if Mcl-1 is neutralized. *Cancer Cell* **10**, 389-399 (2006).
333. Pervin, S., *et al.* Reduced association of anti-apoptotic protein Mcl-1 with E3 ligase Mule increases the stability of Mcl-1 in breast cancer cells. *Br J Cancer* **105**, 428-437 (2011).
334. Ding, Q., *et al.* Degradation of Mcl-1 by beta-TrCP mediates glycogen synthase kinase 3-induced tumor suppression and chemosensitization. *Mol Cell Biol* **27**, 4006-4017 (2007).
335. Schwickart, M., *et al.* Deubiquitinase USP9X stabilizes MCL1 and promotes tumour cell survival. *Nature* **463**, 103-107 (2010).
336. Tang, L., *et al.* Expression of apoptosis regulators in cutaneous malignant melanoma. *Clin Cancer Res* **4**, 1865-1871 (1998).
337. Cerroni, L., Soyer, H.P. & Kerl, H. bcl-2 protein expression in cutaneous malignant melanoma and benign melanocytic nevi. *Am J Dermatopathol* **17**, 7-11 (1995).
338. Selzer, E., *et al.* Expression of Bcl-2 family members in human melanocytes, in melanoma metastases and in melanoma cell lines. *Melanoma Res* **8**, 197-203 (1998).
339. Mooy, C.M., *et al.* Immunohistochemical and prognostic analysis of apoptosis and proliferation in uveal melanoma. *Am J Pathol* **147**, 1097-1104 (1995).
340. Jiang, G., *et al.* Enhanced anti-tumor activity by the combination of a conditionally replicating adenovirus mediated interleukin-24 and dacarbazine against melanoma cells via induction of apoptosis. *Cancer Lett* **294**, 220-228 (2010).
341. Weber, A., Kirejczyk, Z., Potthoff, S., Ploner, C. & Hacker, G. Endogenous Noxa Determines the Strong Proapoptotic Synergism of the BH3-Mimetic ABT-737 with Chemotherapeutic Agents in Human Melanoma Cells. *Transl Oncol* **2**, 73-83 (2009).
342. Jansen, B., *et al.* bcl-2 antisense therapy chemosensitizes human melanoma in SCID mice. *Nat Med* **4**, 232-234 (1998).

343. Cragg, M.S., *et al.* Treatment of B-RAF mutant human tumor cells with a MEK inhibitor requires Bim and is enhanced by a BH3 mimetic. *J Clin Invest* **118**, 3651-3659 (2008).
344. Keuling, A.M., Andrew, S.E. & Tron, V.A. Inhibition of p38 MAPK enhances ABT-737-induced cell death in melanoma cell lines: novel regulation of PUMA. *Pigment Cell Melanoma Res* **23**, 430-440.
345. Konopleva, M., *et al.* Mechanisms of apoptosis sensitivity and resistance to the BH3 mimetic ABT-737 in acute myeloid leukemia. *Cancer Cell* **10**, 375-388 (2006).
346. Verhaegen, M., *et al.* A novel BH3 mimetic reveals a mitogen-activated protein kinase-dependent mechanism of melanoma cell death controlled by p53 and reactive oxygen species. *Cancer Res* **66**, 11348-11359 (2006).
347. Karbowski, M., Norris, K.L., Cleland, M.M., Jeong, S.Y. & Youle, R.J. Role of Bax and Bak in mitochondrial morphogenesis. *Nature* **443**, 658-662 (2006).
348. Chan, D.C. Mitochondria: dynamic organelles in disease, aging, and development. *Cell* **125**, 1241-1252 (2006).
349. Sheridan, C., Delivani, P., Cullen, S.P. & Martin, S.J. Bax- or Bak-induced mitochondrial fission can be uncoupled from cytochrome C release. *Mol Cell* **31**, 570-585 (2008).
350. Suzuki, M., Youle, R.J. & Tjandra, N. Structure of Bax: coregulation of dimer formation and intracellular localization. *Cell* **103**, 645-654 (2000).
351. Wolter, K.G., *et al.* Movement of Bax from the cytosol to mitochondria during apoptosis. *J Cell Biol* **139**, 1281-1292 (1997).
352. Zong, W.X., *et al.* Bax and Bak can localize to the endoplasmic reticulum to initiate apoptosis. *J Cell Biol* **162**, 59-69 (2003).
353. Hsu, Y.T. & Youle, R.J. Nonionic detergents induce dimerization among members of the Bcl-2 family. *J Biol Chem* **272**, 13829-13834 (1997).
354. Moldoveanu, T., *et al.* The X-ray structure of a BAK homodimer reveals an inhibitory zinc binding site. *Mol Cell* **24**, 677-688 (2006).
355. Yethon, J.A., Epand, R.F., Leber, B., Epand, R.M. & Andrews, D.W. Interaction with a membrane surface triggers a reversible conformational change in Bax normally associated with induction of apoptosis. *J Biol Chem* **278**, 48935-48941 (2003).
356. Khaled, A.R., *et al.* Interleukin-3 withdrawal induces an early increase in mitochondrial membrane potential unrelated to the Bcl-2 family. Roles of intracellular pH, ADP transport, and F(0)F(1)-ATPase. *J Biol Chem* **276**, 6453-6462 (2001).
357. Pagliari, L.J., *et al.* The multidomain proapoptotic molecules Bax and Bak are directly activated by heat. *Proc Natl Acad Sci U S A* **102**, 17975-17980 (2005).
358. Gavathiotis, E., *et al.* BAX activation is initiated at a novel interaction site. *Nature* **455**, 1076-1081 (2008).
359. Reed, J.C. Proapoptotic multidomain Bcl-2/Bax-family proteins: mechanisms, physiological roles, and therapeutic opportunities. *Cell Death Differ* **13**, 1378-1386 (2006).
360. Westphal, D., Dewson, G., Czabotar, P.E. & Kluck, R.M. Molecular biology of Bax and Bak activation and action. *Biochim Biophys Acta* **1813**, 521-531 (2011).
361. Dewson, G., *et al.* Bax dimerizes via a symmetric BH3:groove interface during apoptosis. *Cell death and differentiation* **19**, 661-670 (2012).
362. Vander Heiden, M.G., Chandel, N.S., Williamson, E.K., Schumacker, P.T. & Thompson, C.B. Bcl-xL regulates the membrane potential and volume homeostasis of mitochondria. *Cell* **91**, 627-637 (1997).
363. Nakagawa, T., *et al.* Cyclophilin D-dependent mitochondrial permeability transition regulates some necrotic but not apoptotic cell death. *Nature* **434**, 652-658 (2005).

364. Dejean, L.M., *et al.* Oligomeric Bax is a component of the putative cytochrome c release channel MAC, mitochondrial apoptosis-induced channel. *Mol Biol Cell* **16**, 2424-2432 (2005).
365. Sedlak, T.W., *et al.* Multiple Bcl-2 family members demonstrate selective dimerizations with Bax. *Proc Natl Acad Sci U S A* **92**, 7834-7838 (1995).
366. Edlich, F., *et al.* Bcl-x(L) retrotranslocates Bax from the mitochondria into the cytosol. *Cell* **145**, 104-116 (2011).
367. Fecker, L.F., *et al.* Loss of proapoptotic Bcl-2-related multidomain proteins in primary melanomas is associated with poor prognosis. *J Invest Dermatol* **126**, 1366-1371 (2006).
368. Riker, A.I., *et al.* The gene expression profiles of primary and metastatic melanoma yields a transition point of tumor progression and metastasis. *BMC Med Genomics* **1**, 13 (2008).
369. Choi, S.S., *et al.* A novel Bcl-2 related gene, Bfl-1, is overexpressed in stomach cancer and preferentially expressed in bone marrow. *Oncogene* **11**, 1693-1698 (1995).
370. Karsan, A., Yee, E., Kaushansky, K. & Harlan, J.M. Cloning of human Bcl-2 homologue: inflammatory cytokines induce human A1 in cultured endothelial cells. *Blood* **87**, 3089-3096 (1996).
371. Simmons, M.J., *et al.* Bfl-1/A1 functions, similar to Mcl-1, as a selective tBid and Bak antagonist. *Oncogene* **27**, 1421-1428 (2008).
372. Hsu, S.Y., Kaipia, A., McGee, E., Lomeli, M. & Hsueh, A.J. Bok is a pro-apoptotic Bcl-2 protein with restricted expression in reproductive tissues and heterodimerizes with selective anti-apoptotic Bcl-2 family members. *Proc Natl Acad Sci U S A* **94**, 12401-12406 (1997).
373. Morales, A.A., *et al.* High expression of bfl-1 contributes to the apoptosis resistant phenotype in B-cell chronic lymphocytic leukemia. *Int J Cancer* **113**, 730-737 (2005).
374. Feuerhake, F., *et al.* NFkappaB activity, function, and target-gene signatures in primary mediastinal large B-cell lymphoma and diffuse large B-cell lymphoma subtypes. *Blood* **106**, 1392-1399 (2005).
375. Xia, L., Wurmbach, E., Waxman, S. & Jing, Y. Upregulation of Bfl-1/A1 in leukemia cells undergoing differentiation by all-trans retinoic acid treatment attenuates chemotherapeutic agent-induced apoptosis. *Leukemia* **20**, 1009-1016 (2006).
376. Lin, E.Y., Orlofsky, A., Berger, M.S. & Prystowsky, M.B. Characterization of A1, a novel hemopoietic-specific early-response gene with sequence similarity to bcl-2. *J Immunol* **151**, 1979-1988 (1993).
377. Kenny, J.J., *et al.* GRS, a novel member of the Bcl-2 gene family, is highly expressed in multiple cancer cell lines and in normal leukocytes. *Oncogene* **14**, 997-1001 (1997).
378. Xiang, Z., Moller, C. & Nilsson, G. IgE-receptor activation induces survival and Bfl-1 expression in human mast cells but not basophils. *Allergy* **61**, 1040-1046 (2006).
379. Xiang, Z., *et al.* Essential role of the prosurvival bcl-2 homologue A1 in mast cell survival after allergic activation. *J Exp Med* **194**, 1561-1569 (2001).
380. Tomayko, M.M. & Cancro, M.P. Long-lived B cells are distinguished by elevated expression of A1. *J Immunol* **160**, 107-111 (1998).
381. Tomayko, M.M., *et al.* Expression of the Bcl-2 family member A1 is developmentally regulated in T cells. *Int Immunol* **11**, 1753-1761 (1999).
382. Verschelde, C., *et al.* A1/Bfl-1 expression is restricted to TCR engagement in T lymphocytes. *Cell Death Differ* **10**, 1059-1067 (2003).

383. Sakuma, H., *et al.* High glucose inhibits apoptosis in human coronary artery smooth muscle cells by increasing bcl-xL and bfl-1/A1. *Am J Physiol Cell Physiol* **283**, C422-428 (2002).
384. Kathania, M., Raje, C.I., Raje, M., Dutta, R.K. & Majumdar, S. Bfl-1/A1 acts as a negative regulator of autophagy in mycobacteria infected macrophages. *Int J Biochem Cell Biol* **43**, 573-585.
385. Brien, G., Trescol-Biemont, M.C. & Bonnefoy-Berard, N. Downregulation of Bfl-1 protein expression sensitizes malignant B cells to apoptosis. *Oncogene* **26**, 5828-5832 (2007).
386. Nagy, B., *et al.* Abnormal expression of apoptosis-related genes in haematological malignancies: overexpression of MYC is poor prognostic sign in mantle cell lymphoma. *Br J Haematol* **120**, 434-441 (2003).
387. Piva, R., *et al.* Functional validation of the anaplastic lymphoma kinase signature identifies CEBPB and BCL2A1 as critical target genes. *J Clin Invest* **116**, 3171-3182 (2006).
388. Lin, E.Y., Orlofsky, A., Wang, H.G., Reed, J.C. & Prystowsky, M.B. A1, a Bcl-2 family member, prolongs cell survival and permits myeloid differentiation. *Blood* **87**, 983-992 (1996).
389. Yoon, H.S., *et al.* Bfl-1 gene expression in breast cancer: its relationship with other prognostic factors. *J Korean Med Sci* **18**, 225-230 (2003).
390. He, C.H., *et al.* Bcl-2-related protein A1 is an endogenous and cytokine-stimulated mediator of cytoprotection in hyperoxic acute lung injury. *J Clin Invest* **115**, 1039-1048 (2005).
391. Chuang, P.I., *et al.* Perturbation of B-cell development in mice overexpressing the Bcl-2 homolog A1. *Blood* **99**, 3350-3359 (2002).
392. D'Sa-Eipper, C., Subramanian, T. & Chinnadurai, G. bfl-1, a bcl-2 homologue, suppresses p53-induced apoptosis and exhibits potent cooperative transforming activity. *Cancer Res* **56**, 3879-3882 (1996).
393. Beverly, L.J. & Varmus, H.E. MYC-induced myeloid leukemogenesis is accelerated by all six members of the antiapoptotic BCL family. *Oncogene* **28**, 1274-1279 (2009).
394. Mandal, M., *et al.* The BCL2A1 gene as a pre-T cell receptor-induced regulator of thymocyte survival. *J Exp Med* **201**, 603-614 (2005).
395. Cheng, Q., Lee, H.H., Li, Y., Parks, T.P. & Cheng, G. Upregulation of Bcl-x and Bfl-1 as a potential mechanism of chemoresistance, which can be overcome by NF-kappaB inhibition. *Oncogene* **19**, 4936-4940 (2000).
396. Shim, Y.H., Byun, E.K., Lee, M.J., Huh, J. & Kim, C.W. Anti-apoptotic role of Bfl-1 in staurosporine-treated B-lymphoblastic cells. *Int J Hematol* **72**, 484-490 (2000).
397. Olsson, A., *et al.* Upregulation of bfl-1 is a potential mechanism of chemoresistance in B-cell chronic lymphocytic leukaemia. *Br J Cancer* **97**, 769-777 (2007).
398. Kim, J.K., *et al.* Up-regulation of Bfl-1/A1 via NF-kappaB activation in cisplatin-resistant human bladder cancer cell line. *Cancer Lett* **212**, 61-70 (2004).
399. Lee, H.H., Dadgostar, H., Cheng, Q., Shu, J. & Cheng, G. NF-kappaB-mediated up-regulation of Bcl-x and Bfl-1/A1 is required for CD40 survival signaling in B lymphocytes. *Proc Natl Acad Sci U S A* **96**, 9136-9141 (1999).
400. Chen, F., *et al.* Involvement of 5'-flanking kappaB-like sites within bcl-x gene in silica-induced Bcl-x expression. *J Biol Chem* **274**, 35591-35595 (1999).
401. Jing, Y., *et al.* Combined effect of all-trans retinoic acid and arsenic trioxide in acute promyelocytic leukemia cells in vitro and in vivo. *Blood* **97**, 264-269 (2001).
402. Rasooly, R., *et al.* Retinoid x receptor agonists increase bcl2a1 expression and decrease apoptosis of naive T lymphocytes. *J Immunol* **175**, 7916-7929 (2005).

403. Simpson, L.A., *et al.* The antiapoptotic gene A1/BFL1 is a WT1 target gene that mediates granulocytic differentiation and resistance to chemotherapy. *Blood* **107**, 4695-4702 (2006).
404. Jenal, M., *et al.* The anti-apoptotic gene BCL2A1 is a novel transcriptional target of PU.1. *Leukemia* **24**, 1073-1076.
405. Shaffer, A.L., *et al.* Blimp-1 orchestrates plasma cell differentiation by extinguishing the mature B cell gene expression program. *Immunity* **17**, 51-62 (2002).
406. Kucharczak, J.F., Simmons, M.J., Duckett, C.S. & Gelinas, C. Constitutive proteasome-mediated turnover of Bfl-1/A1 and its processing in response to TNF receptor activation in FL5.12 pro-B cells convert it into a prodeath factor. *Cell Death Differ* **12**, 1225-1239 (2005).
407. Herold, M.J., *et al.* The stability and anti-apoptotic function of A1 are controlled by its C terminus. *J Biol Chem* **281**, 13663-13671 (2006).
408. Zhang, H., *et al.* Structural basis of BFL-1 for its interaction with BAX and its anti-apoptotic action in mammalian and yeast cells. *J Biol Chem* **275**, 11092-11099 (2000).
409. Tao, W., Kurschner, C. & Morgan, J.I. Modulation of cell death in yeast by the Bcl-2 family of proteins. *J Biol Chem* **272**, 15547-15552 (1997).
410. Holmgreen, S.P., Huang, D.C., Adams, J.M. & Cory, S. Survival activity of Bcl-2 homologs Bcl-w and A1 only partially correlates with their ability to bind pro-apoptotic family members. *Cell Death Differ* **6**, 525-532 (1999).
411. Werner, A.B., de Vries, E., Tait, S.W., Bontjer, I. & Borst, J. Bcl-2 family member Bfl-1/A1 sequesters truncated bid to inhibit is collaboration with pro-apoptotic Bak or Bax. *J Biol Chem* **277**, 22781-22788 (2002).
412. Tse, C., *et al.* ABT-263: a potent and orally bioavailable Bcl-2 family inhibitor. *Cancer Res* **68**, 3421-3428 (2008).
413. Choi, S.S., Park, S.H., Kim, U.J. & Shin, H.S. Bfl-1, a Bcl-2-related gene, is the human homolog of the murine A1, and maps to chromosome 15q24.3. *Mamm Genome* **8**, 781-782 (1997).
414. Herman, M.D., *et al.* Completing the family portrait of the anti-apoptotic Bcl-2 proteins: crystal structure of human Bfl-1 in complex with Bim. *FEBS Lett* **582**, 3590-3594 (2008).
415. Sattler, M., *et al.* Structure of Bcl-x(L)-Bak peptide complex: Recognition between regulators of apoptosis. *Science* **275**, 983-986 (1997).
416. Smits, C., Czabotar, P.E., Hinds, M.G. & Day, C.L. Structural plasticity underpins promiscuous binding of the prosurvival protein A1. *Structure* **16**, 818-829 (2008).
417. Brien, G., *et al.* C-terminal residues regulate localization and function of the antiapoptotic protein Bfl-1. *J Biol Chem* **284**, 30257-30263 (2009).
418. Vance, B.A., Zacharchuk, C.M. & Segal, D.M. Recombinant mouse Bcl-2(1-203). Two domains connected by a long protease-sensitive linker. *J Biol Chem* **271**, 30811-30815 (1996).
419. Chang, B.S., Minn, A.J., Muchmore, S.W., Fesik, S.W. & Thompson, C.B. Identification of a novel regulatory domain in Bcl-X(L) and Bcl-2. *Embo J* **16**, 968-977 (1997).
420. Hatakeyama, S., *et al.* Multiple gene duplication and expression of mouse bcl-2-related genes, A1. *Int Immunol* **10**, 631-637 (1998).
421. Oberdoerffer, P., *et al.* Efficiency of RNA interference in the mouse hematopoietic system varies between cell types and developmental stages. *Mol Cell Biol* **25**, 3896-3905 (2005).
422. Ko, J.K., *et al.* Bfl-1S, a novel alternative splice variant of Bfl-1, localizes in the nucleus via its C-terminus and prevents cell death. *Oncogene* **22**, 2457-2465 (2003).

423. Wang, L., Miura, M., Bergeron, L., Zhu, H. & Yuan, J. Ich-1, an Ice/ced-3-related gene, encodes both positive and negative regulators of programmed cell death. *Cell* **78**, 739-750 (1994).
424. Duriez, P.J., Wong, F., Dorovini-Zis, K., Shahidi, R. & Karsan, A. A1 functions at the mitochondria to delay endothelial apoptosis in response to tumor necrosis factor. *J Biol Chem* **275**, 18099-18107 (2000).
425. Orlofsky, A., Somogyi, R.D., Weiss, L.M. & Prystowsky, M.B. The murine antiapoptotic protein A1 is induced in inflammatory macrophages and constitutively expressed in neutrophils. *J Immunol* **163**, 412-419 (1999).
426. Yang, W.S., *et al.* C-terminal region of Bfl-1 induces cell death that accompanies caspase activation when fused with GFP. *J Cell Biochem* **94**, 1234-1247 (2005).
427. Fan, G., *et al.* Defective ubiquitin-mediated degradation of antiapoptotic Bfl-1 predisposes to lymphoma. *Blood* **115**, 3559-3569 (2010).
428. Zhai, D., *et al.* Gambogic acid is an antagonist of antiapoptotic Bcl-2 family proteins. *Mol Cancer Ther* **7**, 1639-1646 (2008).
429. Cashman, J.R., *et al.* Inhibition of Bfl-1 with N-aryl maleimides. *Bioorg Med Chem Lett* **20**, 6560-6564 (2010).
430. Wei, J., *et al.* Apogossypol derivatives as antagonists of antiapoptotic Bcl-2 family proteins. *Mol Cancer Ther* **8**, 904-913 (2009).
431. Brien, G., *et al.* Characterization of peptide aptamers targeting Bfl-1 anti-apoptotic protein. *Biochemistry* **50**, 5120-5129 (2011).
432. Munshi, A., *et al.* Inhibition of constitutively activated nuclear factor-kappaB radiosensitizes human melanoma cells. *Mol Cancer Ther* **3**, 985-992 (2004).
433. Shishodia, S. & Aggarwal, B.B. Guggulsterone inhibits NF-kappaB and IkappaBalpha kinase activation, suppresses expression of anti-apoptotic gene products, and enhances apoptosis. *J Biol Chem* **279**, 47148-47158 (2004).
434. Nicoletti, I., Migliorati, G., Pagliacci, M.C., Grignani, F. & Riccardi, C. A rapid and simple method for measuring thymocyte apoptosis by propidium iodide staining and flow cytometry. *J Immunol Methods* **139**, 271-279 (1991).
435. Liu, R., Page, C., Beidler, D.R., Wicha, M.S. & Nunez, G. Overexpression of Bcl-x(L) promotes chemotherapy resistance of mammary tumors in a syngeneic mouse model. *Am J Pathol* **155**, 1861-1867 (1999).
436. Buchholz, T.A., *et al.* Chemotherapy-induced apoptosis and Bcl-2 levels correlate with breast cancer response to chemotherapy. *Cancer* **9**, 33-41 (2003).
437. Ross, D.T., *et al.* Systematic variation in gene expression patterns in human cancer cell lines. *Nat Genet* **24**, 227-235 (2000).
438. Blower, P.E., *et al.* MicroRNA expression profiles for the NCI-60 cancer cell panel. *Mol Cancer Ther* **6**, 1483-1491 (2007).
439. Amundson, S.A., *et al.* An informatics approach identifying markers of chemosensitivity in human cancer cell lines. *Cancer Res* **60**, 6101-6110 (2000).
440. van Schanke, A., *et al.* Single UVB overexposure stimulates melanocyte proliferation in murine skin, in contrast to fractionated or UVA-1 exposure. *J Invest Dermatol* **124**, 241-247 (2005).
441. Coffer, P.J. & Woodgett, J.R. Molecular cloning and characterisation of a novel putative protein-serine kinase related to the cAMP-dependent and protein kinase C families. *Eur J Biochem* **201**, 475-481 (1991).
442. Gray, A., *et al.* Polymorphisms of the Bcl-2 family member bfl-1 in children with atopic dermatitis. *Pediatr Allergy Immunol* **17**, 578-582 (2006).
443. Laurell, G., Ekborn, A., Viberg, A. & Canlon, B. Effects of a single high dose of cisplatin on the melanocytes of the stria vascularis in the guinea pig. *Audiol Neurootol* **12**, 170-178 (2007).
444. Akasaka, K., *et al.* Loss of class III beta-tubulin induced by histone deacetylation is associated with chemosensitivity to paclitaxel in malignant melanoma cells. *J Invest Dermatol* **129**, 1516-1526 (2009).

445. VanBrocklin, M.W., Verhaegen, M., Soengas, M.S. & Holmen, S.L. Mitogen-activated protein kinase inhibition induces translocation of Bmf to promote apoptosis in melanoma. *Cancer Res* **69**, 1985-1994 (2009).
446. Bowen, A.R., *et al.* Apoptosis regulators and responses in human melanocytic and keratinocytic cells. *J Invest Dermatol* **120**, 48-55 (2003).
447. Celli, A., Que, F.G., Gores, G.J. & LaRusso, N.F. Glutathione depletion is associated with decreased Bcl-2 expression and increased apoptosis in cholangiocytes. *Am J Physiol* **275**, G749-757 (1998).
448. Reed, J.C. A day in the life of the Bcl-2 protein: does the turnover rate of Bcl-2 serve as a biological clock for cellular lifespan regulation? *Leukemia* **20**, 109-111 (1996).
449. Kvam, E. & Dahle, J. Pigmented melanocytes are protected against ultraviolet-A-induced membrane damage. *J Invest Dermatol* **121**, 564-569 (2003).
450. O'Reilly, L.A., *et al.* Tissue expression and subcellular localization of the pro-survival molecule Bcl-w. *Cell Death Differ* **8**, 486-494 (2001).
451. Legha, S.S., *et al.* Treatment of metastatic melanoma with combined chemotherapy containing cisplatin, vinblastine and dacarbazine (CVD) and biotherapy using interleukin-2 and interferon-alpha. *Ann Oncol* **7**, 827-835 (1996).
452. Rao, R.D., *et al.* Combination of paclitaxel and carboplatin as second-line therapy for patients with metastatic melanoma. *Cancer* **106**, 375-382 (2006).
453. Nathan, F.E., Berd, D., Sato, T. & Mastrangelo, M.J. Paclitaxel and tamoxifen: An active regimen for patients with metastatic melanoma. *Cancer* **88**, 79-87 (2000).
454. Franciosi, V., *et al.* Front-line chemotherapy with cisplatin and etoposide for patients with brain metastases from breast carcinoma, nonsmall cell lung carcinoma, or malignant melanoma: a prospective study. *Cancer* **85**, 1599-1605 (1999).
455. Burden, D.A., *et al.* Topoisomerase II.etoposide interactions direct the formation of drug-induced enzyme-DNA cleavage complexes. *J Biol Chem* **271**, 29238-29244 (1996).
456. Ferlini, C., *et al.* Paclitaxel directly binds to Bcl-2 and functionally mimics activity of Nur77. *Cancer Res* **69**, 6906-6914 (2009).
457. Wang, X., *et al.* MAD2-induced sensitization to vincristine is associated with mitotic arrest and Raf/Bcl-2 phosphorylation in nasopharyngeal carcinoma cells. *Oncogene* **22**, 109-116 (2003).
458. Dhiman, R., Kathania, M., Raje, M. & Majumdar, S. Inhibition of bfl-1/A1 by siRNA inhibits mycobacterial growth in THP-1 cells by enhancing phagosomal acidification. *Biochim Biophys Acta* **1780**, 733-742 (2008).
459. Happo, L., *et al.* Maximal killing of lymphoma cells by DNA damage-inducing therapy requires not only the p53 targets Puma and Noxa, but also Bim. *Blood* **116**, 5256-5267 (2010).
460. Blajeski, A.L., Phan, V.A., Kottke, T.J. & Kaufmann, S.H. G(1) and G(2) cell-cycle arrest following microtubule depolymerization in human breast cancer cells. *J Clin Invest* **110**, 91-99 (2002).
461. Meng, X., Martinez, M.A., Raymond-Stintz, M.A., Winter, S.S. & Wilson, B.S. IKK inhibitor bay 11-7082 induces necroptotic cell death in precursor-B acute lymphoblastic leukaemic blasts. *British journal of haematology* **148**, 487-490 (2010).
462. Groth-Pedersen, L., Ostenfeld, M.S., Hoyer-Hansen, M., Nylandsted, J. & Jaattela, M. Vincristine induces dramatic lysosomal changes and sensitizes cancer cells to lysosome-destabilizing siramesine. *Cancer Res* **67**, 2217-2225 (2007).
463. Simonian, P.L., Grillot, D.A. & Nunez, G. Bcl-2 and Bcl-XL can differentially block chemotherapy-induced cell death. *Blood* **90**, 1208-1216 (1997).
464. Milross, C.G., *et al.* Relationship of mitotic arrest and apoptosis to antitumor effect of paclitaxel. *J Natl Cancer Inst* **88**, 1308-1314 (1996).

465. Gonzalez, V.M., Fuertes, M.A., Alonso, C. & Perez, J.M. Is cisplatin-induced cell death always produced by apoptosis? *Mol Pharmacol* **59**, 657-663 (2001).
466. Facompre, M., Wattez, N., Kluza, J., Lansiaux, A. & Bailly, C. Relationship between cell cycle changes and variations of the mitochondrial membrane potential induced by etoposide. *Mol Cell Biol Res Commun* **4**, 37-42 (2000).
467. Sorenson, C.M., Barry, M.A. & Eastman, A. Analysis of events associated with cell cycle arrest at G2 phase and cell death induced by cisplatin. *J Natl Cancer Inst* **82**, 749-755 (1990).
468. Hoshino, R., Tanimura, S., Watanabe, K., Kataoka, T. & Kohno, M. Blockade of the extracellular signal-regulated kinase pathway induces marked G1 cell cycle arrest and apoptosis in tumor cells in which the pathway is constitutively activated: up-regulation of p27(Kip1). *J Biol Chem* **276**, 2686-2692 (2001).
469. Schonn, I., Hennesen, J. & Dartsch, D.C. Cellular responses to etoposide: cell death despite cell cycle arrest and repair of DNA damage. *Apoptosis* **15**, 162-172 (2010).
470. Smith, P.J., *et al.* Etoposide-induced cell cycle delay and arrest-dependent modulation of DNA topoisomerase II in small-cell lung cancer cells. *Br J Cancer* **70**, 914-921 (1994).
471. Larsen, A.K., Escargueil, A.E. & Skladanowski, A. From DNA damage to G2 arrest: the many roles of topoisomerase II. *Prog Cell Cycle Res* **5**, 295-300 (2003).
472. Sekiguchi, I., *et al.* Effects of cisplatin on cell cycle kinetics, morphological change, and cleavage pattern of DNA in two human ovarian carcinoma cell lines. *Oncology* **53**, 19-26 (1996).
473. Mueller, S., *et al.* Cell-cycle progression and response of germ cell tumors to cisplatin in vitro. *Int J Oncol* **29**, 471-479 (2006).
474. Woessmann, W., Chen, X. & Borkhardt, A. Ras-mediated activation of ERK by cisplatin induces cell death independently of p53 in osteosarcoma and neuroblastoma cell lines. *Cancer Chemother Pharmacol* **50**, 397-404 (2002).
475. Cardinali, G. Studies on the Antimitotic Activity of Leurocristine (Vincristine). *Blood* **21**, 102-110 (1963).
476. Mujagic, H., *et al.* Effects of vincristine on cell survival, cell cycle progression, and mitotic accumulation in asynchronously growing Sarcoma 180 cells. *Cancer Res* **43**, 3591-3597 (1983).
477. Al-Katib, A., *et al.* I-kappa-kinase-2 (IKK-2) inhibition potentiates vincristine cytotoxicity in non-Hodgkin's lymphoma. *Mol Cancer* **9**, 228 (2010).
478. Horwitz, S.B. Taxol (paclitaxel): mechanisms of action. *Ann Oncol* **5 Suppl 6**, S3-6 (1994).
479. Poruchynsky, M.S., *et al.* Accompanying protein alterations in malignant cells with a microtubule-polymerizing drug-resistance phenotype and a primary resistance mechanism. *Biochem Pharmacol* **62**, 1469-1480 (2001).
480. Brichese, L., Barboule, N., Heliez, C. & Valette, A. Bcl-2 phosphorylation and proteasome-dependent degradation induced by paclitaxel treatment: consequences on sensitivity of isolated mitochondria to Bid. *Exp Cell Res* **278**, 101-111 (2002).
481. Ibrado, A.M., Liu, L. & Bhalla, K. Bcl-xL overexpression inhibits progression of molecular events leading to paclitaxel-induced apoptosis of human acute myeloid leukemia HL-60 cells. *Cancer Res* **57**, 1109-1115 (1997).
482. Chen, Y., *et al.* Aberrant subcellular localization of BRCA1 in breast cancer. *Science* **270**, 789-791 (1995).
483. Chou, K.C. & Shen, H.B. Recent progress in protein subcellular location prediction. *Anal Biochem* **370**, 1-16 (2007).
484. Akao, Y., Otsuki, Y., Kataoka, S., Ito, Y. & Tsujimoto, Y. Multiple subcellular localization of bcl-2: detection in nuclear outer membrane, endoplasmic reticulum membrane, and mitochondrial membranes. *Cancer Res* **54**, 2468-2471 (1994).
485. Herrant, M., *et al.* Cleavage of Mcl-1 by caspases impaired its ability to counteract Bim-induced apoptosis. *Oncogene* **23**, 7863-7873 (2004).

486. Hsu, Y.T., Wolter, K.G. & Youle, R.J. Cytosol-to-membrane redistribution of Bax and Bcl-X(L) during apoptosis. *Proc Natl Acad Sci U S A* **94**, 3668-3672 (1997).
487. Ostermeier, C., Iwata, S. & Michel, H. Cytochrome c oxidase. *Curr Opin Struct Biol* **6**, 460-466 (1996).
488. Chaturvedi, A., Martz, R., Dorward, D., Waisberg, M. & Pierce, S.K. Endocytosed BCRs sequentially regulate MAPK and Akt signaling pathways from intracellular compartments. *Nat Immunol* **12**, 1119-1126 (2011).
489. Ko, J.K., *et al.* Conversion of Bfl-1, an anti-apoptotic Bcl-2 family protein, to a potent pro-apoptotic protein by fusion with green fluorescent protein (GFP). *FEBS letts* **551**, 29-36 (2003).
490. Cui, R., *et al.* Central role of p53 in the suntan response and pathologic hyperpigmentation. *Cell* **128**, 853-864 (2007).
491. Gambichler, T., *et al.* Significant downregulation of transforming growth factor-beta signal transducers in human skin following ultraviolet-A1 irradiation. *British journal of dermatology* **156**, 951-956 (2007).
492. Rodeck, U., *et al.* Transforming growth factor beta production and responsiveness in normal human melanocytes and melanoma cells. *Cancer Res* **54**, 575-581 (1994).
493. Martinez-Esparza, M., Solano, F. & Garcia-Borron, J.C. Independent regulation of tyrosinase by the hypopigmenting cytokines TGF beta1 and TNF alpha and the melanogenic hormone alpha-MSH in B16 mouse melanocytes. *Cell Mol Biol (Noisy-le-grand)* **45**, 991-1000 (1999).
494. Yang, G., *et al.* Inhibition of PAX3 by TGF-beta modulates melanocyte viability. *Mol Cell* **32**, 554-563 (2008).
495. Kawaguchi, Y., Mori, N. & Nakayama, A. Kit(+) melanocytes seem to contribute to melanocyte proliferation after UV exposure as precursor cells. *J Invest Dermatol* **116**, 920-925 (2001).
496. Walter, S.D., *et al.* The association of cutaneous malignant melanoma with the use of sunbeds and sunlamps. *Am J Epidemiol* **131**, 232-243 (1990).
497. Tsao, H., Mihm, M.C., Jr. & Sheehan, C. PTEN expression in normal skin, acquired melanocytic nevi, and cutaneous melanoma. *J Am Acad Dermatol* **49**, 865-872 (2003).
498. Wang, Y.F., *et al.* Apoptosis induction in human melanoma cells by inhibition of MEK is caspase-independent and mediated by the Bcl-2 family members PUMA, Bim, and Mcl-1. *Clin Cancer Res* **13**, 4934-4942 (2007).
499. Konopleva, M., *et al.* MEK inhibition enhances ABT-737-induced leukemia cell apoptosis via prevention of ERK-activated MCL-1 induction and modulation of MCL-1/BIM complex. *Leukemia* **26**, 778-787 (2012).
500. Hodi, F.S. Well-defined melanoma antigens as progression markers for melanoma: insights into differential expression and host response based on stage. *Clin Cancer Res* **12**, 673-678 (2006).